doi.org/10.26434/chemrxiv.14291644.v2

How Reproducible Are Surface Areas Calculated from the BET Equation?

Johannes Osterrieth, James Rampersad, David G. Madden, Nakul Rampal, Luka Skoric, Bethany Connolly, Mark Allendorf, Vitalie Stavila, JONATHAN SNIDER, Rob Ameloot, Joao Marreiros, Conchi O. Ania, Diana C. S. Azevedo, Enrique Vilarrasa-García, Bianca F Santos, Xian-He Bu, Xe Zang, Hana Bunzen, Neil Champness, Sarah L. Griffin, Banglin Chen, Rui-Biao Lin, Benoit Coasne, Seth M. Cohen, Jessica C. Moreton, Yamil J. Colon, Linjiang Chen, Rob Clowes, François-Xavier Coudert, Yong Cui, Bang Hou, Deanna D'Alessandro, Patrick W. Doheny, Mircea Dinca, Chenyue Sun, Christian Doonan, Michael Huxley, Jack D. Evans, paolo falcaro, Raffaele Riccò, Omar K. Farha, Karam B. Idrees, Timur Islamoglu, Pingyun Feng, Huajun Yang, Ross Forgan, Dominic Bara, Shuhei Furukawa, Elisabeth Sanchez, Jorge Gascon, Selvedin Telalovic, Sujit K. Ghosha, SOUMYA MUKHERJEE, Matthew R. Hill, Muhammad Munir Sadiq, Patricia Horcajada, Pablo Salcedo-Abraira, Katsumi Kaneko, Radovan Kukobat, Jeffrey Kenvin, Seda Keskin, Susumu Kitagawa, Kenichi Otake, Ryan P. Lively, Stephen J. A. DeWitt, Philip L. Llewellyn, Bettina Lotsch, Sebastian T. Emmerling, Alexander Pütz, Carlos Martí-Gastaldo, Natalia Muñoz, Javier Garcia-Martinez, Noemi Linares, Daniel Maspoch, Jose Antonio Suarez, Peyman Moghadam, Rama Oktavian, Russell Morris, Paul Wheatley, Jorge Navarro, Camille Petit, David Danaci, Matthew Rosseinsky, Alexandros Katsoulidis, Martin Schroder, Xue Han, Sihai Yang, Christian Serre, Georges Mouchaham, David Sholl, Raghuram Thyagarajan, Daniel Siderius, Randall Q. Snurr, Rebecca B. Goncalves, Shane G. Telfer, Seok J. Lee, Valeska Ting, Jemma Rowlandson, Takeshi Uemura, Tomoya Iiyuka, Monique van der Veen, Davide Rega, Veronique Vanspeybroeck, Aran Lamaire, Sven Rogge, Krista Walton, Lukas W. Bingel, Stefan Wuttke, Jacopo Andreo, Omar Yaghi, Bing Zhang, Cafer Yavuz, Thien Nguyen, Felix Zamora, Carmen Montoro, Hong-Cai Zhou, Kirchon Angelo, David Fairen-Jimenez

Submitted date: 25/05/2021 • Posted date: 26/05/2021

Citation information: Osterrieth, Johannes; Rampersad, James; Madden, David G.; Rampal, Nakul; Skoric, Luka; Connolly, Bethany; et al. (2021): How Reproducible Are Surface Areas Calculated from the BET Equation?. ChemRxiv. Preprint. https://doi.org/10.26434/chemrxiv.14291644.v2

Porosity and surface area analysis play a prominent role in modern materials science, where 123 their determination spans the fields of natural sciences, engineering, geology and medical 124 research. At the heart of this sits the Brunauer-Emmett-Teller (BET) theory,[1] which has been 125 a remarkably successful contribution to the field of materials science. The BET method was 126 developed in the 1930s and is now the most widely used metric for the estimation of surface 127 areas of porous materials.[2] Since the BET method was first developed, there has been an 128 explosion in the field of nanoporous materials with the discovery of synthetic zeolites,[3] 129 nanostructured silicas,[4–6] metal-organic frameworks (MOFs),[7] and others.

Despite its 130 widespread use, the manual calculation of BET surface areas causes a significant spread in 131 reported areas, resulting in reproducibility problems in both academia and industry. To probe 132 this, we have brought together 60 labs with strong track records in the study of nanoporous 133 materials. We provided eighteen adsorption isotherms and asked these researchers to 134 calculate the corresponding BET areas, resulting in a wide range of values for each one. We 135 show here that the reproducibility of BET area determination from identical isotherms is a 136 largely ignored issue, raising critical concerns over the reliability of reported BET areas in 137 the literature. To solve this major issue, we have developed a new computational approach 138 to accurately and systematically determine the BET area of nanoporous materials. Our 139 software, called BET Surface Identification (BETSI), expands on the well-known Rouquerol 140 criteria and makes, for the first time, an unambiguous BET area assignment possible.

File list (2)

Osterrieth - 2021 - Manuscript.pdf (490.94 KiB)	view on ChemRxiv • download file
Osterrieth - 2021 - SI.pdf (16.70 MiB)	view on ChemRxiv • download file

How reproducible are surface areas calculated from the BET equation?

Johannes W. M. Osterrieth[a], James Rampersad[a], David Madden[a], Nakul Rampal[a], Luka Skoric[b], Bethany Connolly[a]; Mark D. Allendorf[c], Vitalie Stavila[c], Jonathan L. Snider[c]; Rob Ameloot[d], João Marreiros[d]; Conchi Ania[e]; Diana Azevedo[f], Enrique Vilarrasa-Garcia[f], Bianca F. Santos[f]; Xian-He Bu[g], Xe Zang[g]; Hana Bunzen[h]; Neil R. Champness[i], Sarah L. Griffin[i]; Banglin Chen[j], Rui-Biao Lin[j]; Benoit Coasne[k]; Seth Cohen[l], Jessica C. Moreton[l]; Yamil J. Colon[m]; Linjiang Chen[n], Rob Clowes[n]; François-Xavier Coudert[o]; Yong Cui[p], Bang Hou[p]; Deanna M. D'Alessandro[q], Patrick W. Doheny[q]; Mircea Dincă[r], Chenyue Sun[r]; Christian Doonan[s], Michael Thomas Huxley[s]; Jack D. Evans[t]; Paolo Falcaro[u], Raffaele Ricco[u]; Omar Farha[v], Karam B. Idrees[v], Timur Islamoglu[v]; Pingyun Feng[w], Huajun Yang[w]; Ross S. Forgan[x], Dominic Bara[x]; Shuhei Furukawa[y], Eli Sanchez[y]; Jorge Gascon[z], Selvedin Telalovic[z]; Sujit K. Ghosh[aa], Soumya Mukherjee[aa]; Matthew R. Hill[ab], Muhammad Munir Sadiq[ab]; Patricia Horcajada[ac], Pablo Salcedo-Abraira[ac]; Katsumi Kaneko[ad], Radovan Kukobat[ad]; Jeff Kenvin[ae]; Seda Keskin[af]; Susumu Kitagawa[ag], Kenichi Otake[ag]; Ryan P. Lively[ah], Stephen J. A. DeWitt[ah]; Phillip Llewellyn[aj]; Bettina V. Lotsch[aj,ak], Sebastian T. Emmerling[aj,ak], Alexander M. Pütz[aj,ak]; Carlos Martí-Gastaldo[al], Natalia M. Padial[al]; Javier García-Martínez[am], Noemi Linares[am]; Daniel Maspoch[an,ao], Jose A. Suárez del Pino[ao]; Peyman Moghadam[ap], Rama Oktavian[ap]; Russel E. Morris[aq], Paul S. Wheatley[aq]; Jorge Navarro[ar]; Camille Petit[as], David Danaci[as]; Matthew J. Rosseinsky[at], Alexandros P. Katsoulidis[at]; Martin Schröder[au], Xue Han[au], Sihai Yang[au]; Christian Serre[av], Georges Mouchaham[av]; David S. Sholl[ah], Raghuram Thyagarajan[ah]; Daniel Siderius[ψ,φ,aw]; Randall Q. Snurr[ax], Rebecca B. Goncalves[ay]; Shane G. Telfer[az], Seok J. Lee[az]; Valeska P. Tin[ba], Jemma L. Rowlandson[ba]; Takashi Uemura[bb], Tomoya Iiyuka[bb]; Monique A. van der Veen[bc], Davide Rega[bc]; Veronique Van Speybroeck[bd], Sven M. J. Rogge[bd], Aran Lamaire[bd]; Krista S. Walton[ah], Lukas W. Bingel[ah]; Stefan Wuttke[be,bf], Jacopo Andreo[be,bf]; Omar Yaghi[bg,bh], Bing Zhang[bg]; Cafer T. Yavuz[bi], Thien S. Nguyen[bi]; Felix Zamora[bj], Carmen Montoro[bj]; Hongcai Zhou[bk], Angelo Kirchon[bk]; and David Fairen-Jimenez[a,]*

[a] Adsorption & Advanced Materials Laboratory (A²ML), Department of Chemical Engineering & Biotechnology, University of Cambridge, Philippa Fawcett Drive, Cambridge CB3 0AS, UK

[b] Cavendish Laboratory, University of Cambridge, JJ Thomson Avenue, CB3 0HE, Cambridge, United Kingdom

[c] Sandia National Laboratories, 7011 East Avenue, Livermore, California 94550, United States

[d] cMACS, Department of Microbial and Molecular Systems (M²S), KU Leuven, 3001 Leuven, Belgium

[e] CEMHTI, CNRS (UPR 3079), Université d'Orléans, 45071 Orléans, France

[f] LPACO2/GPSA, Department of Chemical Engineering, Federal University of Ceará, 60455-760 Fortaleza (CE), Brazil

[g] School of Materials Science and Engineering, National Institute for Advanced Materials, Nankai University, Tianjin 300350, China

[h] Chair of Solid State and Materials Chemistry, Institute of Physics, University of Augsburg, Universitaetsstrasse 1, Augsburg 86159, Germany
[l] School of Chemistry, University of Nottingham, University Park, Nottingham, NG7 2RD UK
[j] Department of Chemistry, University of Texas at San Antonio, One UTSA Circle, San Antonio, TX 78249-0698, USA
[k] Univ. Grenoble Alpes, CNRS, LIPhy, 38000 Grenoble, France
[l] Department of Chemistry and Biochemistry, University of California, San Diego, La Jolla, California, 92093 USA
[m] Department of Chemical and Biomolecular Engineering, University of Notre Dame, Notre Dame, IN, 46556, USA
[n] Leverhulme Research Centre for Functional Materials Design, Materials Innovation Factory and Department of Chemistry, University of Liverpool, Liverpool, UK
[o] Chimie ParisTech, PSL University, CNRS, Institut de Recherche de Chimie Paris, 75005 Paris, France
[p] School of Chemistry and Chemical Engineering, Shanghai Jiaotong University, 800 Dongchuan Road, Minhang District, Shanghai
[q] School of Chemistry, The University of Sydney, New South Wales, 2006, Australia
[r] Department of Chemistry, Massachusetts Institute of Technology, Cambridge, Massachusetts 02139, USA
[s] Centre for Advanced Nanomaterials and Department of Chemistry, The University of Adelaide, North Terrace, Adelaide, SA 5000, Australia
[t] Department of Inorganic Chemistry, Technische Universität Dresden, Bergstrasse 66, 01062, Dresden, Germany
[u] Institute of Physical and Theoretical Chemistry, Graz University of Technology, Graz, Austria
[v] Department of Chemistry and International Institute of Nanotechnology, Northwestern University, 2145 Sheridan Road, Evanston, Illinois 60208, United States
[w] Department of Chemistry, University of California, Riverside, California 92521, USA
[x] WestCHEM School of Chemistry, University of Glasgow, Glasgow, UK
[y] Institute for Integrated Cell-Material Sciences, Kyoto University, Yoshida, Sakyo-ku, Kyoto 606-8501, Japan
[z] KAUST Catalysis Center (KCC), King Abdullah University of Science and Technology, P.O.Box 4700, 23955-6900, Thuwal-Jeddah, Kingdom od Saudi Arabia
[aa] Department of Chemistry, Indian Institute of Science Education and Research (IISER), Pune, Dr. Homi Bhabha Road, Pashan, Pune 411008, India
[ab] CSIRO, Private Bag 33, Clayton South MDC, VIC 3169, Australia and Department of Chemical Engineering, Monash University, Clayton, VIC 3168, Australia
[ac] Advanced Porous Materials Unit (APMU), IMDEA Energy, Avda. Ramón de la Sagra 3, E-28935 Móstoles, Madrid, Spain
[ad] Research Initiative for Supra-Materials, Shinshu University, Nagano, Japan
[ae] Micromeritics Instrument Corporation, Norcross, GA 30093, USA
[af] Department of Chemical and Biological Engineering, Koc University, Rumelifeneri Yolu 34450 Sariyer, Istanbul, Turkey
[ag] Institute for Integrated Cell-Material Sciences (WPI-iCeMS), Kyoto University Institute for Advanced Study (KUIAS), Kyoto University, Yoshida Ushinomiya-cho, Sakyo-ku, Kyoto 606-8501, Japan
[ah] School of Chemical & Biomolecular Engineering, Georgia Institute of Technology, Atlanta, GA 30332, USA

[ai] CNRS / Aix-Marseille Univ. / TOTAL
[aj] Max Planck Institute for Solid State Research, Heisenbergstrasse 1, 70569 Stuttgart, Germany
[ak] Department of Chemistry, University of Munich (LMU), Butenandtstrasse 5-13, 81377 Munich, Germany
[al] Instituto de Ciencia Molecular (ICMol), Universitat de València, Paterna 46980, València, Spain
[am] Laboratorio de Nanotecnología Molecular, Departamento de Química Inorgánica, Universidad de Alicante, Ctra. San Vicente-Alicante s/n, E-03690 San Vicente del Raspeig, Spain
[an] ICREA, Pg. Lluís Companys 23, Barcelona, 08010, Spain
[ao] Catalan Institute of Nanoscience and Nanotechnology (ICN2), CSIC and the Barcelona Institute of Science and Technology. Campus UAB, Bellaterra, 08193 Barcelona, Spain
[ap] Department of Chemical and Biological Engineering, University of Sheffield, Sheffield S1 3JD, UK
[aq] School of Chemistry, University of St Andrews, North Haugh, St Andrews, KY16 9ST, UK
[ar] Departamento de Química Inorgánica, Universidad de Granada, 18071 Granada, Spain
[as] Barrer Centre, Department of Chemical Engineering, Imperial College London, London, U.K., SW7 2AZ
[at] Materials Innovation Factory, Department of Chemistry, University of Liverpool, Liverpool, L7 3NY, UK
[au] School of Chemistry, The University of Manchester, Manchester, U.K. M13 9PL
[av] Institut des Matériaux Poreux de Paris, Ecole Normale Supérieure, ESPCI Paris, CNRS, PSL University, 75005 Paris, France
[aw] Chemical Sciences Division, National Institute of Standards and Technology, Gaithersburg, Maryland USA 20899-8320
[ax] Departments of Chemical & Biological Engineering, Northwestern University, 2145 Sheridan Road, Evanston, Illinois 60208, USA
[ay] Department of Chemistry, Northwestern University, 2145 Sheridan Road, Evanston, Illinois 60208, USA
[az] MacDiarmid Institute of Advanced Materials and Nanotechnology, School of Fundamental Sciences, Massey University, Palmerston North, New Zealand
[ba] Department of Mechanical Engineering, University of Bristol, Bristol BS8 1TR, U.K.
[bb] Department of Advanced Materials Science, Graduate School of Frontier Sciences, The University of Tokyo, 5-1-5 Kashiwanoha, Kashiwa, Chiba 277-8561, Japan
[bc] Department of Chemical Engineering, Delft University of Technology, van der Maasweg 9, 2629HZ Delft, the Netherlands
[bd] Center for Molecular Modeling (CMM), Ghent University, Technologiepark 46, B-9052 Zwijnaarde, Belgium
[be] BCMaterials, Basque Center for Materials, Applications and Nanostructures, UPV/EHU Science Park, 48940, Leioa, Spain
[bf] IKERBASQUE, Basque Foundation for Science, 48009, Bilbao, Spain
[bg] Department of Chemistry, University of California—Berkeley; Kavli Energy Nanoscience Institute at UC Berkeley
[bh] Berkeley Global Science Institute, Berkeley, California 94720, United States
[bi] Department of Chemical and Biomolecular Engineering, Korea Advanced Institute of Science and Technology (KAIST), Yuseong-gu, 34141 Daejeon, Korea
[bj] Departamento de Química Inorgánica, Universidad Autónoma de Madrid, 28049 Madrid, Spain
[bk] Chemistry Department -Texas A&M University

φ Certain commercially available items may be identified in this paper. This identification does not imply recommendation by NIST, nor does it imply that it is the best available for the purposes described
* E-mail: df334@cam.ac.uk

To the editor:

The Brunauer-Emmett-Teller (BET) equation is arguably one of the most used equations in physical chemistry and porosimetry. Since its conception in the 1930s[1] to estimate open surfaces whilst working with adsorbents of the time such as Fe/Cu catalysts, silica gel, and charcoal, it has found widespread use in the characterisation of synthetic zeolites.[2] Furthermore, it gained considerable momentum following the discovery of more complex porous materials such as mesoporous silicas,[3] porous coordination polymers (PCPs),[4] metal-organic frameworks (MOFs),[5] and covalent organic frameworks (COFs).[6] Novel porous materials are of significant academic and industrial interest due to their applications in gas storage and separation,[7–10] catalysis,[11] and drug delivery,[12] and the BET area is their *de facto* standard for the characterisation. It has been recognized by the International Union of Pure and Applied Chemistry (IUPAC) as "the most widely used procedure for evaluating the surface area of porous and finely-divided materials",[13,14] and it has been an International Organization for Standardization (ISO) standard for surface area determination since 1995.[15] Whilst concerns over the applicability of the BET theory for microporous materials are important, it remains, arguably, the most important figure of merit for porous materials. Given the broad use of the BET equation, it is not surprising to see that much has been written on the *applicability* and the *accuracy* of the BET theory – that is, its model of the adsorption process – and on the reproducibility of the raw data, *i.e.* the adsorption isotherm.[16–20]

The advent of materials with more complex pore networks and dynamic frameworks through material design strategies such as reticular chemistry has boosted interest in BET theory (**Figure S1**) and given rise to reported BET areas in excess of 8,000 m^2 g^{-1}.[8,21,22] Often, these modern materials have complex adsorption isotherms that are more problematic or ambiguous to fit to the BET model, *e.g.* several steps can occur due to different pore types and/or flexibility being present in the material.[23] Whilst adsorption rigs capable of ultra-low pressure (<10^{-5} mbar) recordings have been developed, reliance on manual calculations of BET areas remains commonplace. In this context, 'manual' refers to the judicious selection of the *optimal pressure range* by a scientist, be it through a self-developed spreadsheet or commercial software. This raises the question of the *reproducibility* of BET calculations *from the same measured isotherm* but from different assessors.

The eponymously named Rouquerol criteria (**Section S2**, Supplementary Information) aim to ensure good practice in identifying a valid fitting range, and, as such, they have found widespread acceptance in the literature and have been adopted in both IUPAC and ISO standards.[13–15,17,18,24,25] Despite this safeguard, we herein propose that current BET area calculations are many times irreproducible for two reasons: first, the Rouquerol criteria are indeterminate in identifying the correct

fitting region, as they apply to multiple regions simultaneously. Second, even if they were determinate, they are too cumbersome and lengthy to be systematically implemented and are therefore often neglected in practice.

To prove our hypothesis and to assess the current spread of BET calculation results, we have shared a set of 18 experimental isotherms representing four classes of porous materials (zeolites, mesoporous silicas, MOFs, and COFs) with 60 laboratories with expertise in adsorption science and synthesis of porous materials. In this round-robin exercise, we asked the researchers to calculate the BET areas in the way they saw most fit. More details about the specific materials and the adsorption isotherms, sampled both from our laboratory and from the NIST/ARPA-E database,[26] are included in the Supplementary Information, **Section S12**. To avoid any recognition bias, all isotherms were anonymised and scaled off arbitrarily.

In parallel, we have developed a computational approach to calculating BET areas that only requires the adsorption isotherm as input data. The BET Surface Identification (BETSI) algorithm, steps through *all* possible fitting regions and outputs a full distribution of BET areas that are consistent under the Rouquerol criteria. We further propose an addition to the criteria that makes, for the first time, an unambiguous assignment of BET areas from an adsorption isotherm possible: the ideal fitting range ends on the highest permissible pressure point under all criteria, representing the end of the bulk adsorptive activity of the material, *i.e.* the isotherm knee. Further, it is chosen as having the lowest percentage error under the last Rouquerol criterion. Further details on the BETSI algorithm and the extension of the Rouquerol criteria can be found in **Section S3**, and a more detailed description in **Section S14**. The source code is fully published under GitHub https://github.com/fairen-group/betsi-gui.

Figure 1 shows the comparison between BET areas calculated by researchers in the round-robin evaluation and using BETSI. Bar a few exceptions, virtually no two groups of experts reported identical BET areas for any given isotherm. The results are fully tabulated and graphically represented in **Section S4** and **Section S5** respectively. We observed a spread of at least 300 m^2 g^{-1} for each isotherm; however, that number was significantly higher for some individual isotherms. For NU-1104, a modern MOF with substantial porosity[22] the highest estimate of 9,341 m^2 g^{-1} and the lowest estimate of 1,757 m^2 g^{-1} differed by an astonishing 7,584 m^2 g^{-1}, making the highest estimate more than five times higher than the lowest one. Most groups (90%) reported using the Rouquerol criteria in their manual calculation, 23% used a commercial software package, and 6% used a self-developed code. Full details on each individual group's methods can be found in **Section S13**.

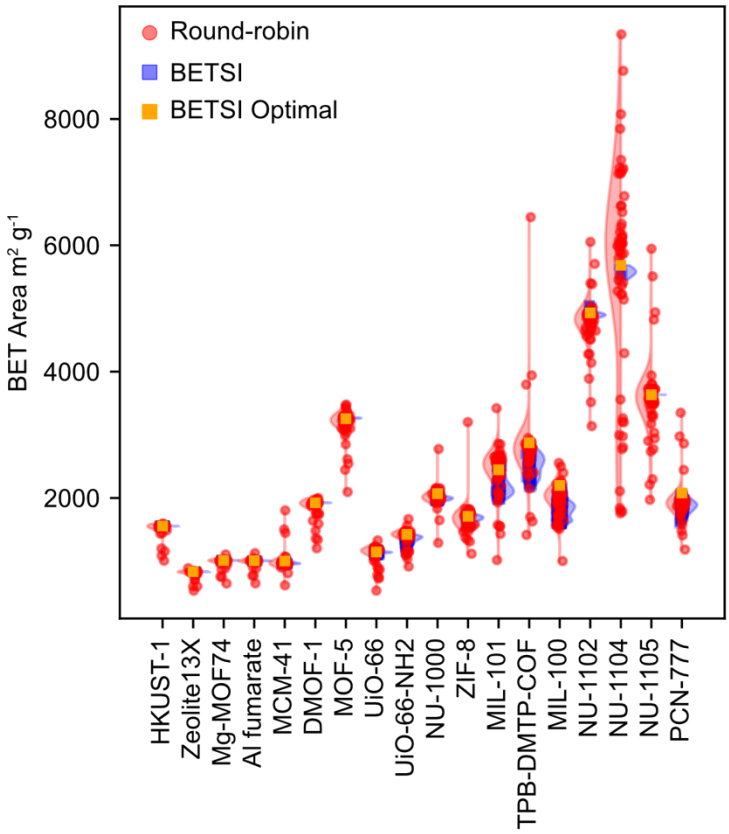

Figure 1 | Round-robin results and BETSI results. Distribution of BET areas from identical isotherms as calculated by 60 laboratories with expertise in adsorption science and synthesis of porous materials in red. Superimposed are normalised probability distribution functions obtained by kernel density estimation. Predictions under BETSI are shown in blue alongside, and the 'optimal' BET area in yellow.

Under BETSI, on the other hand, whilst multiple BET areas are passed as valid, the spread of values was considerably narrower than that obtained by manual calculation (**Figure 1**; for full BETSI results, see **Section S6** and further comparative data **Section S7**, **Section S8, and Section S9**). From this, both our first and second hypotheses are substantiated: since BETSI calculates *all* valid BET areas, it proves that the Rouquerol criteria by themselves are indeterminate and that even full compliance does not guarantee an unambiguous answer. Besides, since the spread of all valid BET areas is narrower than that obtained in the round-robin exercise, it demonstrates how the manual and systematic implementation of the Rouquerol criteria is difficult and often neglected in practice. For instance, in the case of NU-1104, the range of estimates decreases from 7,500 $m^2\ g^{-1}$ in the social study to 235 $m^2\ g^{-1}$ under BETSI.

Interestingly, some isotherms returned under BETSI much larger spreads of results than others, suggesting that they BET model does not describe them as naturally and thus they were more susceptible to problems associated with the Rouquerol criteria; a trend that was mirrored in the round-robin evaluation. To further investigate the goodness of the isotherm fittings, we define the *BETSI Variation Coefficient* as the relative standard deviation of BETSI results, and the *Pass Rate* as the number of BET fits that pass under the Rouquerol criteria as a fraction of all potential fits.

Further, the *Hit Rate* expresses the fractional number of BET areas calculated in the round-robin exercise that lie within the BETSI range. **Figure 2** demonstrates the correlation between the *Pass Rate*, the *BETSI Variation Coefficient*, and the *Hit Rate*. Simply put, the more BET fits are valid, the greater the spread of possible BET areas is, and the more likely researchers are to satisfy the Rouquerol criteria in manual calculations; an alternative representation can be found in **Section S10**. From **Figure 2**, we classify adsorption isotherms into three broad categories, types A, B and C. Whilst it is difficult to generalise about the shape of these isotherms, we offer some discussion about common features in **Section S11**. Type A isotherms fit the BET model 'best'. Under BETSI, they have a relatively high Pass Rate and return a fairly narrow spread of results. Examples include materials such as Al fumarate, NU-1000, Zeolite-13X and MCM-41. Hit Rates greater than 70% are generally observed for these materials, suggesting that the majority of researchers did not struggle with the fittings. Type B isotherms only fit the BET model over a very limited range. These have extremely low Pass Rates, meaning that only a few BET fits are valid, which in turn will be spread narrowly. Examples include MOF-5, DMOF-1, NU-1104, HKUST-1, and NU-1105. For the latter, out of 9,409 hypothetical 10-point fits (the minimum point requirement for BET fits), only one is permissible under the Rouquerol criteria. Such prohibitively low Pass Rates make the correct BET assignment by hand virtually impossible and demonstrate the need for computational support. Type C isotherm fittings are arguably the most problematic. They have high Pass Rates and, concomitantly, they return large spreads of BET results. Typical materials that fit into this category are MIL-101, MIL-100, TPB-DMTP-COF and PCN-777. It is for these materials that the necessity to extend the Rouquerol criteria is demonstrated and the BETSI algorithm makes an unambiguous BET assignment possible.

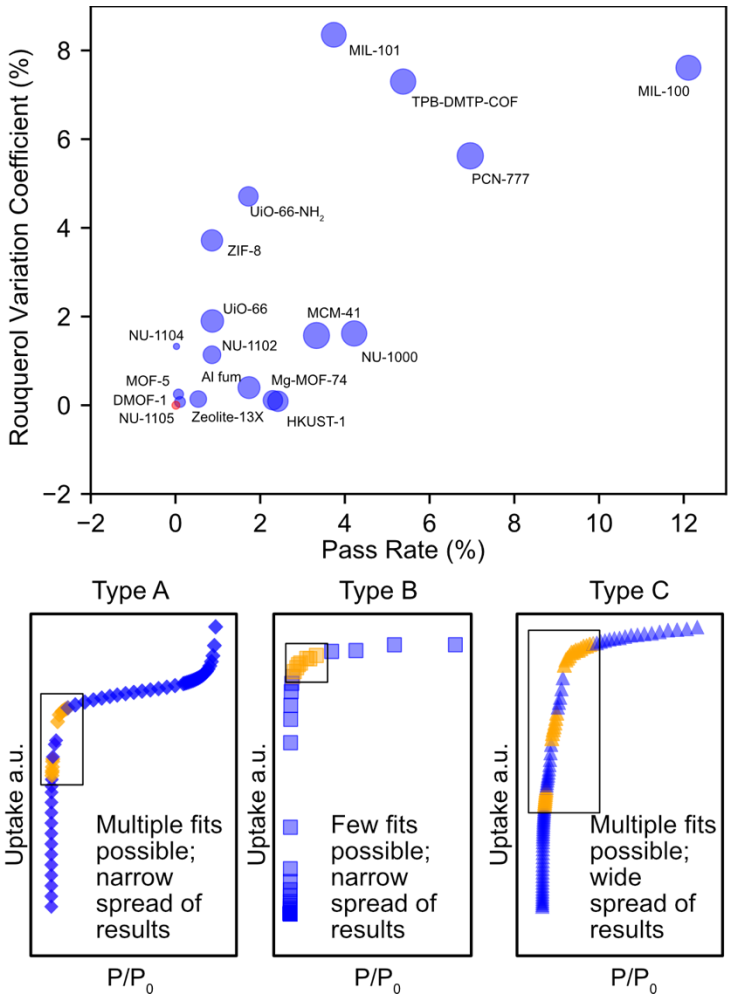

Figure 2 | Isotherm classifications. Plot of the BETSI Variation Coefficient (relative standard deviation of BETSI results) against the Pass Rate (fraction of valid fits against all hypothetical ones). Bubble size scales with the Hit Rate, the fraction of results from the social study that lie within the BETSI range. Red symbols have a Hit Rate of zero. Note the positive correlation between all three parameters. Isotherm fit classifications. Type A fits have a relatively wide fitting window, within which multiple fits are possible, but return a relatively narrow spread of BET results. Type B fits have a narrow fitting window and concomitantly return a narrow set of spread of results. Type C fits have wide fitting windows, which translates to multiple passable fits and a wide spread of permissible BET areas.

In conclusion, BET theory is a great success story. Developed in the 1930s for open surfaces, it continues to be applied to modern adsorbents with complex porosities. Despite the advances from classical density functional theory (DFT) methods, the BET area will likely continue playing a crucial role in porosimetry for decades to come, with impacts in energy research, transport, medical applications and climate-change mitigation. In light of these future developments, it will become increasingly important to share critical scientific metrics reliably to find a common language to report both academic and industrial progress.

Here, we have demonstrated the difficulties in unambiguously determining BET areas from adsorption isotherms, which in turn affect the assessment of material quality and reproducibility. These problems arise from imperfect and insufficient manual calculations and can only be met using modern computational methods. BETSI is a step towards greater transparency and critical

assessment in reporting BET areas. We stress here that it is neither the function nor the purpose of BETSI to eliminate doubt and treat a particular BET area as 'true'. Researchers should remain aware of the limitations of BET theory when applied to microporous adsorbents in general and when BET areas are reported, the pressure range and number of points used should always be stated. We further recommend here that isotherms must be reported transparently and in detail, *i.e*. semi-log representation to show the low-pressure regions. The 'experiment' is the adsorption isotherm – not the BET area.

Online Content

Any methods, additional references, source data, extended data, supplementary information, acknowledgements, peer review information; details of author contributions and competing interests are available at request.

Isotherm data reported with this paper are included in the NIST/ARPA-E Database of Novel and Emerging Adsorbent Materials, https://adsorption.nist.gov, and may be accessed directly at https://adsorption.nist.gov/isodb/index.php?DOI=10.XXXX/YYYYY#biblio.

Bibliography

1. Brunauer, S., Emmett, P. H. & Teller, E. Adsorption of Gases in Multimolecular Layers. *J. Am. Chem. Soc.* **60**, 309–319 (1938).
2. Cid, R., Arriagada, R. & Orellana, F. Zeolites surface area calculation from nitrogen adsorption data. *J. Catal.* **80**, 228–230 (1983).
3. Beck, J. S. *et al.* A New Family of Mesoporous Molecular Sieves Prepared with Liquid Crystal Templates. *J. Am. Chem. Soc.* **114**, 10834–10843 (1992).
4. Kitagawa, S., Kitaura, R. & Noro, S. I. Functional porous coordination polymers. *Angew. Chemie - Int. Ed.* **43**, 2334–2375 (2004).
5. Zhou, H. C., Long, J. R. & Yaghi, O. M. Introduction to metal-organic frameworks. *Chemical Reviews* vol. 112 673–674 (2012).
6. Diercks, C. S. & Yaghi, O. M. The atom, the molecule, and the covalent organic framework. *Science* **355**, (2017).
7. Li, J., Sculley, J. & Zhou, H. Metal-Organic Frameworks for Separations. *Chem. Rev.* **112**, 869–932 (2012).
8. Farha, O. K. *et al.* De novo synthesis of a metal-organic framework material featuring ultrahigh surface area and gas storage capacities. *Nat. Chem.* **2**, 944–948 (2010).
9. Li, B., Wen, H.-M., Zhou, W. & Chen, B. Porous Metal–Organic Frameworks for Gas Storage and Separation: What, How, and Why? *J. Phys. Chem. Lett.* **5**, 3468–3479 (2014).
10. Moghadam, P. Z. *et al.* Computer-aided discovery of a metal-organic framework with superior oxygen uptake. *Nat. Commun.* **9**, 1378–1385 (2018).
11. Corma, A., García, H. & Llabrés i Xamena, F. X. Engineering Metal Organic Frameworks for Heterogeneous Catalysis. *Chem. Rev.* **110**, 4606–4655 (2010).
12. Horcajada, P. *et al.* Metal-organic frameworks in biomedicine. *Chem. Rev.* **112**, 1232–1268 (2012).
13. Thommes, M. *et al.* Physisorption of gases, with special reference to the evaluation of

surface area and pore size distribution (IUPAC Technical Report). *Pure Appl. Chem.* **87**, 1051–1069 (2015).

14. Sing, K. S. W. *et al.* Reporting Physisorption Data for Gas/Solid Systems with Special Reference to the Determination of Surface Area and Porosity. *Pure Appl. Chem.* **57**, 603–619 (1985).
15. ISO [International Organization for Standardization]. Determination of the specific surface area of solids by gas adsorption - BET method (ISO 9277:2010(E)). (2010) doi:10.1007/s11367-011-0297-3.
16. Ambroz, F., Macdonald, T. J., Martis, V. & Parkin, I. P. Evaluation of the BET Theory for the Characterization of Meso and Microporous MOFs. *Small Methods* **2**, 1800173 (2018).
17. Gómez-Gualdrón, D. A., Moghadam, P. Z., Hupp, J. T., Farha, O. K. & Snurr, R. Q. Application of Consistency Criteria To Calculate BET Areas of Micro- And Mesoporous Metal-Organic Frameworks. *J. Am. Chem. Soc.* **138**, 215–24 (2016).
18. Walton, K. S. & Snurr, R. Q. Applicability of the BET method for determining surface areas of microporous metal-organic frameworks. *J. Am. Chem. Soc.* **129**, 8552–8556 (2007).
19. Park, J., Howe, J. D. & Sholl, D. S. How Reproducible Are Isotherm Measurements in Metal-Organic Frameworks? *Chem. Mater.* **29**, 10487–10495 (2017).
20. Sinha, P. *et al.* Surface Area Determination of Porous Materials Using the Brunauer-Emmett-Teller (BET) Method: Limitations and Improvements. *J. Phys. Chem. C* **123**, 20195–20209 (2019).
21. Furukawa, H., Cordova, K. E., O'Keeffe, M. & Yaghi, O. M. The Chemistry and Applications of Metal-Organic Frameworks. *Science* **341**, 1230444–1230444 (2013).
22. Wang, T. C. *et al.* Ultrahigh Surface Area Zirconium MOFs and Insights into the Applicability of the BET Theory. *J. Am. Chem. Soc.* **137**, 3585–3591 (2015).
23. Fairen-Jimenez, D. *et al.* Opening the gate: Framework flexibility in ZIF-8 explored by experiments and simulations. *J. Am. Chem. Soc.* **133**, 8900–8902 (2011).
24. Rouquerol, J., Llewellyn, P. & Rouquerol, F. Is the BET equation applicable to microporous adsorbents? *Stud. Surf. Sci. Catal.* **160**, 49–56 (2007).
25. Rouquerol, J., Rouquerol, F., Llewellyn, P., Maurin, G. & Sing, K. S. W. *Adsorption by Powders and Porous Solids: Principles, Methodology and Applications: Second Edition*. *Adsorption by Powders and Porous Solids: Principles, Methodology and Applications: Second Edition* (Academic Press, 2013). doi:10.1016/C2010-0-66232-8.
26. D.W. Siderius, V.K. Shen, R.D. Johnson III, and R.d. van Zee, Eds., NIST/ARPA-E Database of Novel and Emerging Adsorbent Materials, National Institute of Standards and Technology, Gaithersburg MD, 20899, https://dx.doi.org/10.18434/T43882, (retrieved Augu. vol. 91.

Acknowledgements

This project has received funding from the European Research Council (ERC) under the European Union's Horizon 2020 research and innovation programme (NanoMOFdeli), ERC-2016-COG 726380. D.F.-J. thanks the Royal Society for funding through a University Research Fellowship. Mark Carrington is acknowledged for his contribution to the COF isotherm.

O.K.F. and R.Q.S. acknowledge funding from the U.S. Department of Energy (DE-FG02-08ER15967).

R.S.F. and D.B. acknowledge funding from the European Research Council (ERC) under the European Union's Horizon 2020 research and innovation programme (SCoTMOF), ERC-2015-StG 677289.

Sandia National Laboratories is a multimission laboratory managed and operated by National Technology and Engineering Solutions of Sandia, LLC., a wholly owned subsidiary of Honeywell International, Inc., for the U.S. Department of Energy's National Nuclear Security Administration under contract DE-NA-0003525. The authors gratefully acknowledge funding from the U.S. Department of Energy, Office of Energy Efficiency and Renewable Energy, Hydrogen and Fuel Cell Technologies Office, through the Hydrogen Storage Materials Advanced Research Consortium (HyMARC). This paper describes objective technical results and analysis. Any subjective views or opinions that might be expressed in the paper do not necessarily represent the views of the U.S. Department of Energy or the United States Government.

J.D.E acknowledges the support of the Alexander von Humboldt Foundation and the Center for Information Services and High-Performance Computing (ZIH) at TU Dresden.

S.K.G. and S.M. acknowledge SERB (Project No. CRG/2019/000906), India for financial support.

K.K. and R.K. acknowledge Active Co. Research Grant for funding.

S.K. acknowledge funding from the European Research Council (ERC) under the European Union's Horizon 2020 research and innovation programme (COSMOS), ERC-2017-StG 756489.

N.L. and J.G.M acknowledge funding from the European Commission through the H2020-MSCA-RISE-2019 program (ZEOBIOCHEM – 872102) and the Spanish MICINN and AEI/FEDER (RTI2018-099504-B-C21). N.L. thanks the University of Alicante for funding (UATALENTO17-05).

ICN2 is supported by the Severo Ochoa program from the Spanish MINECO (Grant No. SEV-2017-0706)

S.M.J.R. and A.L wish to thank the Fund for Scientific Research Flanders (FWO), under grant nos. 12T3519N and 11D2220N. V.V.S. acknowledges the Research Board of the Ghent University and funding from the European Union's Horizon 2020 research and innovation programme (consolidator ERC grant agreement No. 647755 – DYNPOR (2015-2020)).

L.S. was supported by the EPSRC Cambridge NanoDTC EP/L015978/1

C.T.Y. and T.S.N. acknowledge funds from the National Research Foundation of Korea, NRF-2017M3A7B4042140 and NRF-2017M3A7B4042235

P.F. and H. Y. acknowledge US Department of Energy, Office of Basic Energy Sciences, Materials Sciences and Engineering Division under Award No. DE-SC0010596 (P.F.).

R.O would like to acknowledge funding support during his Ph.D study from Indonesian Endowment Fund for Education-LPDP with the contract No. 202002220216006

S.W. and J.A. acknowledge funding from the Basque Government Industry Department under the ELKARTEK and HAZITEK programs.

B.V.L, S.T.E and A.M.P acknowledge funding from the European Research Council (ERC) under the European Union's Horizon 2020 Research and Innovation Program (Grant agreement no.

639233, COFLeaf), and the Deutsche Forschungsgemeinschaft (DFG) via the cluster of excellence e-conversion (project number EXC2089/1-390776260).

VPT and JLR would like to acknowledge funding from the EPSRC (EP/R01650X/1).

M.A.v.d.V and D.R. are grateful for funding from the European Research Council (ERC) under the European Union's Horizon 2020 research and innovation programme (grant agreement n° 759212)

Supplementary Information for:

How reproducible are surface areas calculated from the BET equation?

Johannes W. M. Osterrieth[a], James Rampersad[a], David Madden[a], Nakul Rampal[a], Luka Skoric[b], Bethany Connolly[a]; Mark D. Allendorf[c], Vitalie Stavila[c], Jonathan L. Snider[c]; Rob Ameloot[d], João Marreiros[d]; Conchi Ania[e]; Diana Azevedo[f], Enrique Vilarrasa-Garcia[f], Bianca F. Santos[f]; Xian-He Bu[g], Xe Zang[g]; Hana Bunzen[h]; Neil R. Champness[i], Sarah L. Griffin[i]; Banglin Chen[j], Rui-Biao Lin[j]; Benoit Coasne[k]; Seth Cohen[l], Jessica C. Moreton[l]; Yamil J. Colon[m]; Linjiang Chen[n], Rob Clowes[n]; François-Xavier Coudert[o]; Yong Cui[p], Bang Hou[p]; Deanna M. D'Alessandro[q], Patrick W. Doheny[q]; Mircea Dincă[r], Chenyue Sun[r]; Christian Doonan[s], Michael Thomas Huxley[s]; Jack D. Evans[t]; Paolo Falcaro[u], Raffaele Ricco[u]; Omar Farha[v], Karam B. Idrees[v], Timur Islamoglu[v]; Pingyun Feng[w], Huajun Yang[w]; Ross S. Forgan[x], Dominic Bara[x]; Shuhei Furukawa[y], Eli Sanchez[y]; Jorge Gascon[z], Selvedin Telalovic[z]; Sujit K. Ghosh[aa], Soumya Mukherjee[aa]; Matthew R. Hill[ab], Muhammad Munir Sadiq[ab]; Patricia Horcajada[ac], Pablo Salcedo-Abraira[ac]; Katsumi Kaneko[ad], Radovan Kukobat[ad]; Jeff Kenvin[ae]; Seda Keskin[af]; Susumu Kitagawa[ag], Kenichi Otake[ag]; Ryan P. Lively[ah], Stephen J. A. DeWitt[ah]; Phillip Llewellyn[aj]; Bettina V. Lotsch[aj,ak], Sebastian T. Emmerling[aj,ak], Alexander M. Pütz[aj,ak]; Carlos Martí-Gastaldo[al], Natalia M. Padial[al]; Javier García-Martínez[am], Noemi Linares[am]; Daniel Maspoch[an,ao], Jose A. Suárez del Pino[ao]; Peyman Moghadam[ap], Rama Oktavian[ap]; Russel E. Morris[aq], Paul S. Wheatley[aq]; Jorge Navarro[ar]; Camille Petit[as], David Danaci[as]; Matthew J. Rosseinsky[at], Alexandros P. Katsoulidis[at]; Martin Schröder[au], Xue Han[au], Sihai Yang[au]; Christian Serre[av], Georges Mouchaham[av]; David S. Sholl[ah], Raghuram Thyagarajan[ah]; Daniel Siderius[ψ,φ,aw]; Randall Q. Snurr[ax], Rebecca B. Goncalves[ay]; Shane G. Telfer[az], Seok J. Lee[az]; Valeska P. Tin[ba], Jemma L. Rowlandson[ba]; Takashi Uemura[bb], Tomoya Iiyuka[bb]; Monique A. van der Veen[bc], Davide Rega[bc]; Veronique Van Speybroeck[bd], Sven M. J. Rogge[bd], Aran Lamaire[bd]; Krista S. Walton[ah], Lukas W. Bingel[ah]; Stefan Wuttke[be,bf], Jacopo Andreo[be,bf]; Omar Yaghi[bg,bh], Bing Zhang[bg]; Cafer T. Yavuz[bi], Thien S. Nguyen[bi]; Felix Zamora[bj], Carmen Montoro[bj]; Hongcai Zhou[bk], Angelo Kirchon[bk]; and David Fairen-Jimenez[a,]*

[a] The Adsorption & Advanced Materials Laboratory (A²ML), Department of Chemical Engineering & Biotechnology, University of Cambridge, Philippa Fawcett Drive, Cambridge CB3 0AS, UK

[b] Cavendish Laboratory, University of Cambridge, JJ Thomson Avenue, CB3 0HE, Cambridge, United Kingdom

[c] Sandia National Laboratories, 7011 East Avenue, Livermore, California 94550, United States

[d] cMACS, Department of Microbial and Molecular Systems (M²S), KU Leuven, 3001 Leuven, Belgium

[e] CEMHTI, CNRS (UPR 3079), Université d'Orléans, 45071 Orléans, France

[f] LPACO2/GPSA, Department of Chemical Engineering, Federal University of Ceará, 60455-760 Fortaleza (CE), Brazil

[g] School of Materials Science and Engineering, National Institute for Advanced Materials, Nankai University, Tianjin 300350, China

[h] Chair of Solid State and Materials Chemistry, Institute of Physics, University of Augsburg, Universitaetsstrasse 1, Augsburg 86159, Germany

[l] School of Chemistry, University of Nottingham, University Park, Nottingham, NG7 2RD UK

[j] Department of Chemistry, University of Texas at San Antonio, One UTSA Circle, San Antonio, TX 78249-0698, USA

[k] Univ. Grenoble Alpes, CNRS, LIPhy, 38000 Grenoble, France

[l] Department of Chemistry and Biochemistry, University of California, San Diego, La Jolla, California, 92093 USA

[m] Department of Chemical and Biomolecular Engineering, University of Notre Dame, Notre Dame, IN, 46556, USA

[n] Leverhulme Research Centre for Functional Materials Design, Materials Innovation Factory and Department of Chemistry, University of Liverpool, Liverpool, UK

[o] Chimie ParisTech, PSL University, CNRS, Institut de Recherche de Chimie Paris, 75005 Paris, France

[p] School of Chemistry and Chemical Engineering, Shanghai Jiaotong University, 800 Dongchuan Road, Minhang District, Shanghai
[q] School of Chemistry, The University of Sydney, New South Wales, 2006, Australia
[r] Department of Chemistry, Massachusetts Institute of Technology, Cambridge, Massachusetts 02139, USA
[s] Centre for Advanced Nanomaterials and Department of Chemistry, The University of Adelaide, North Terrace, Adelaide, SA 5000, Australia
[t] Department of Inorganic Chemistry, Technische Universität Dresden, Bergstrasse 66, 01062, Dresden, Germany
[u] Institute of Physical and Theoretical Chemistry, Graz University of Technology, Graz, Austria
[v] Department of Chemistry and International Institute of Nanotechnology, Northwestern University, 2145 Sheridan Road, Evanston, Illinois 60208, United States
[w] Department of Chemistry, University of California, Riverside, California 92521, USA
[x] WestCHEM School of Chemistry, University of Glasgow, Glasgow, UK
[y] Institute for Integrated Cell-Material Sciences, Kyoto University, Yoshida, Sakyo-ku, Kyoto 606-8501, Japan
[z] KAUST Catalysis Center (KCC), King Abdullah University of Science and Technology, P.O.Box 4700, 23955-6900, Thuwal-Jeddah, Kingdom od Saudi Arabia
[aa] Department of Chemistry, Indian Institute of Science Education and Research (IISER), Pune, Dr. Homi Bhabha Road, Pashan, Pune 411008, India
[ab] CSIRO, Private Bag 33, Clayton South MDC, VIC 3169, Australia and Department of Chemical Engineering, Monash University, Clayton, VIC 3168, Australia
[ac] Advanced Porous Materials Unit (APMU), IMDEA Energy, Avda. Ramón de la Sagra 3, E-28935 Móstoles, Madrid, Spain
[ad] Research Initiative for Supra-Materials, Shinshu University, Nagano, Japan
[ae] Micromeritics Instrument Corporation, Norcross, GA 30093, USA
[af] Department of Chemical and Biological Engineering, Koc University, Rumelifeneri Yolu 34450 Sariyer, Istanbul, Turkey
[ag] Institute for Integrated Cell-Material Sciences (WPI-iCeMS), Kyoto University Institute for Advanced Study (KUIAS), Kyoto University, Yoshida Ushinomiya-cho, Sakyo-ku, Kyoto 606-8501, Japan
[ah] School of Chemical & Biomolecular Engineering, Georgia Institute of Technology, Atlanta, GA 30332, USA
[ai] CNRS / Aix-Marseille Univ. / TOTAL
[aj] Max Planck Institute for Solid State Research, Heisenbergstrasse 1, 70569 Stuttgart, Germany
[ak] Department of Chemistry, University of Munich (LMU), Butenandtstrasse 5-13, 81377 Munich, Germany
[al] Instituto de Ciencia Molecular (ICMol), Universitat de València, Paterna 46980, València, Spain
[am] Laboratorio de Nanotecnología Molecular, Departamento de Química Inorgánica, Universidad de Alicante, Ctra. San Vicente-Alicante s/n, E-03690 San Vicente del Raspeig, Spain
[an] ICREA, Pg. Lluís Companys 23, Barcelona, 08010, Spain
[ao] Catalan Institute of Nanoscience and Nanotechnology (ICN2), CSIC and the Barcelona Institute of Science and Technology. Campus UAB, Bellaterra, 08193 Barcelona, Spain
[ap] Department of Chemical and Biological Engineering, University of Sheffield, Sheffield S1 3JD, UK
[aq] School of Chemistry, University of St Andrews, North Haugh, St Andrews, KY16 9ST, UK
[ar] Departamento de Química Inorgánica, Universidad de Granada, 18071 Granada, Spain
[as] Barrer Centre, Department of Chemical Engineering, Imperial College London, London, U.K., SW7 2AZ
[at] Materials Innovation Factory, Department of Chemistry, University of Liverpool, Liverpool, L7 3NY, UK
[au] School of Chemistry, The University of Manchester, Manchester, U.K. M13 9PL
[av] Institut des Matériaux Poreux de Paris, Ecole Normale Supérieure, ESPCI Paris, CNRS, PSL University, 75005 Paris, France
[aw] Chemical Sciences Division, National Institute of Standards and Technology, Gaithersburg, Maryland USA 20899-8320
[ax] Departments of Chemical & Biological Engineering, Northwestern University, 2145 Sheridan Road, Evanston, Illinois 60208, USA
[ay] Department of Chemistry, Northwestern University, 2145 Sheridan Road, Evanston, Illinois 60208, USA
[az] MacDiarmid Institute of Advanced Materials and Nanotechnology, School of Fundamental Sciences, Massey University, Palmerston North, New Zealand
[ba] Department of Mechanical Engineering, University of Bristol, Bristol BS8 1TR, U.K.

[bb] Department of Advanced Materials Science, Graduate School of Frontier Sciences, The University of Tokyo, 5-1-5 Kashiwanoha, Kashiwa, Chiba 277-8561, Japan
[bc] Department of Chemical Engineering, Delft University of Technology, van der Maasweg 9, 2629HZ Delft, the Netherlands
[bd] Center for Molecular Modeling (CMM), Ghent University, Technologiepark 46, B-9052 Zwijnaarde, Belgium
[be] BCMaterials, Basque Center for Materials, Applications and Nanostructures, UPV/EHU Science Park, 48940, Leioa, Spain
[bf] IKERBASQUE, Basque Foundation for Science, 48009, Bilbao, Spain
[bg] Department of Chemistry, University of California—Berkeley; Kavli Energy Nanoscience Institute at UC Berkeley
[bh] Berkeley Global Science Institute, Berkeley, California 94720, United States
[bi] Department of Chemical and Biomolecular Engineering, Korea Advanced Institute of Science and Technology (KAIST), Yuseong-gu, 34141 Daejeon, Korea
[bj] Departamento de Química Inorgánica, Universidad Autónoma de Madrid, 28049 Madrid, Spain
[bk] Chemistry Department -Texas A&M University

[φ] Certain commercially available items may be identified in this paper. This identification does not imply recommendation by NIST, nor does it imply that it is the best available for the purposes described
* E-mail: df334@cam.ac.uk

Table of Contents

Section S1 – Citation Report for original BET paper

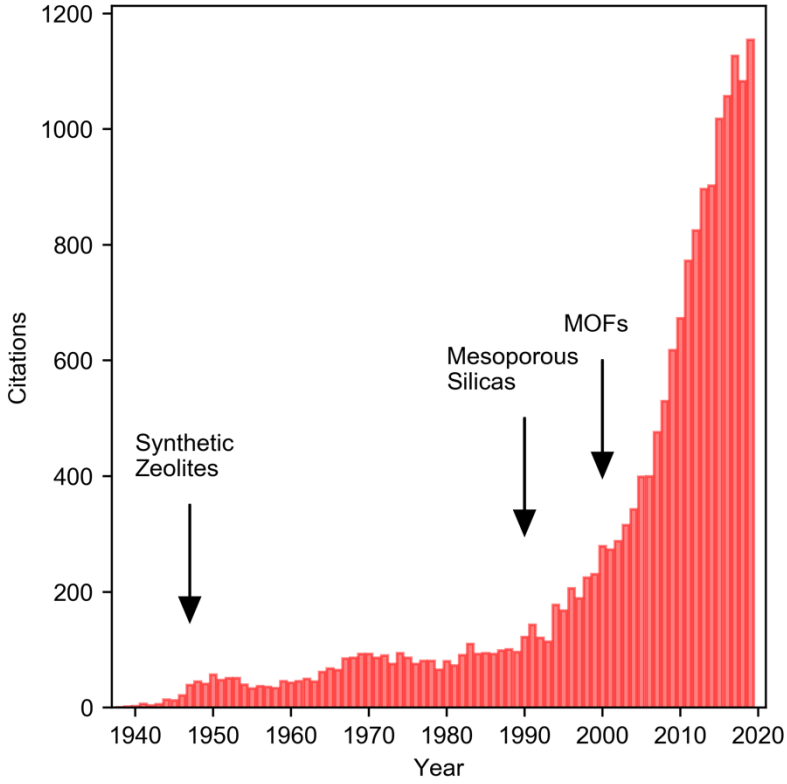

Figure S1 | Number of annual citations of the original BET publication "Adsorption of Gases in Multimolecular Layers", S. Brunauer, P. H. Emmett, E. Teller, *J. Am. Chem. Soc*. **1938**, 60, 309–319. Source: Web of Science

Section S2 – The Rouquerol Criteria

Regression criteria:

- The linear range should span at least 10 points
- The R^2 should be greater or equal to 0.995

Validity criteria:

1) Over the entire fitting range $N(1-P/P_0)$ must increase monotonically with P/P_0
2) The value of C obtained by linear regression must be positive

Self-consistency criteria:

3) The monolayer loading, when reported on the isotherm, N_m (Read), must correspond to a pressure that lies in the linear region
4) The relative pressure corresponding to the monolayer loading as obtained from BET theory, P/P_0 (N_m BET), must be equal to the pressure determined in criterion 3. A 20% error tolerance is accepted.

Section S3 – BET Surface Identification (BETSI)

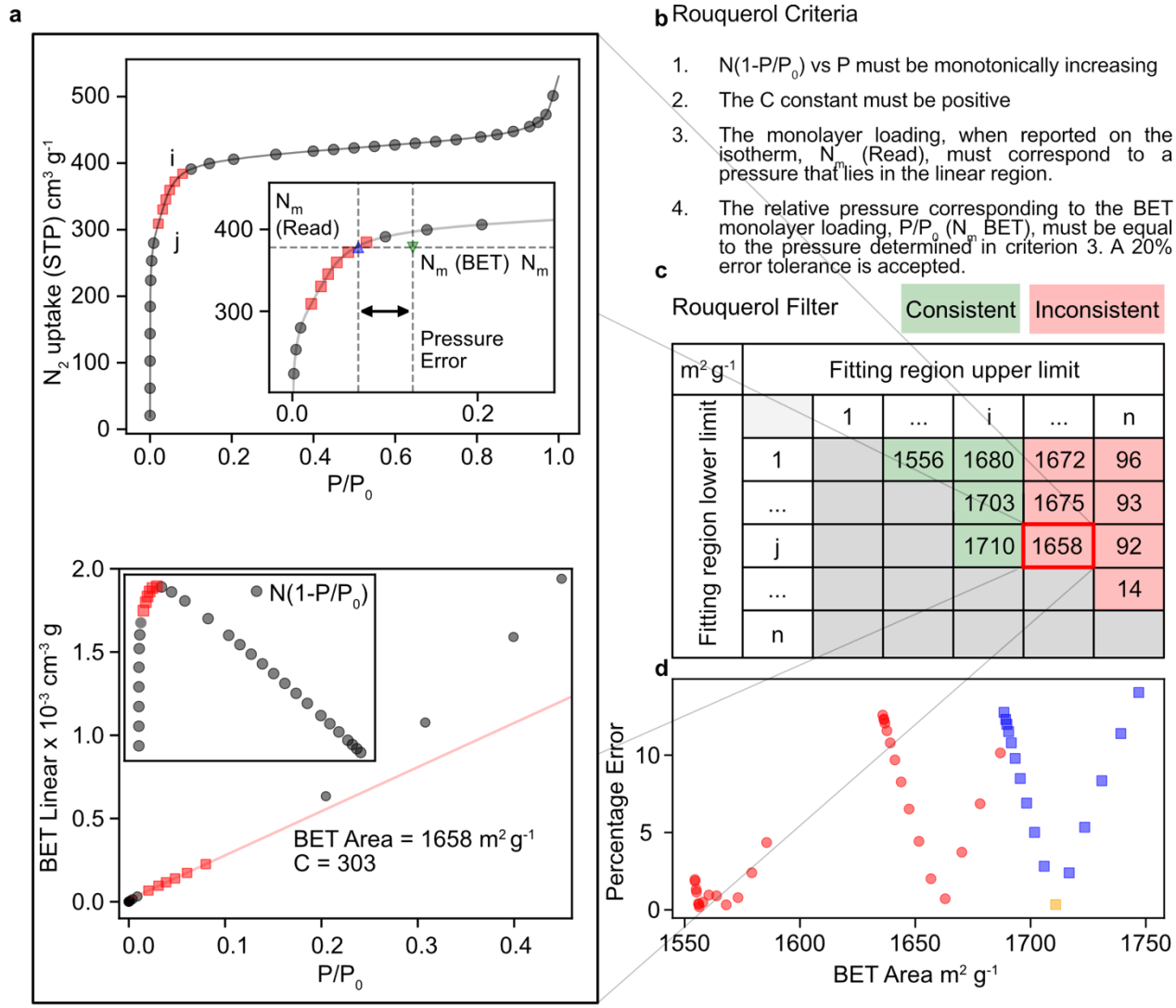

Figure S3 | Working principle for BETSI algorithm. a, The isotherm is shown with a particular fitting region highlighted in red. The linear BET equation is applied, and an ordinary least squares regression is applied to the fitting region. **b**, Subsequent checks against the Rouquerol criteria are performed (insets) and **c**, valid fits are passed**.** The analysis shown in **a** is repeated for all consecutive combinations of points on the isotherm. A results matrix with n x n dimensionality stores all acceptable and rejected fits. **d,** All acceptable BET areas are output and plotted against the percentage error under the 4th Rouquerol criterion (**a**, top inset). All BET areas ending on the highest permissible point under the 1st Rouquerol criterion (**a**, bottom inset, maximum in N(1-P/P$_0$) function) are labelled as the isotherm knee and shown in blue. The BETSI Optimal BET area (yellow) belongs to the isotherm knee group and has the lowest percentage error under the 4th Rouquerol criterion.

Figure S3 shows the working principle of the BETSI algorithm on a simplified N_2 adsorption isotherm at 77 K for ZIF-8. First, the linearized BET equation is fitted to a particular region of the isotherm using an ordinary least-squares (OLS) regression (**Figure S3a**). The top panel shows the isotherm with a fitting region highlighted in red, and the OLS regression is shown below. The plot insets show the checks against the Rouquerol criteria (**Figure S3b**). If all criteria are met, the fitting is passed. This calculation is looped over all data intervals of at least 10 points on the isotherm. The resulting BET fits are stored in a large n x n matrix, where the (j,i)-matrix element corresponds to a fitting region starting at the jth-point and ending on the ith-point (**Figure S3c**). All valid fitting results

are output and plotted against the percentage error under the 4th Rouquerol criterion (**Figure S3d**). Alongside, BETSI outputs all other BET parameters, such as monolayer capacity and the C constant, as well as full regression diagnostics (**Section S5**).

Since multiple fittings comply with the Rouquerol criteria (**Figure 2c-d**), BETSI demonstrates that an unambiguous assignment of the BET area is impossible under the Rouquerol criteria alone. BETSI assigns special relevance to fitting ranges that end on the highest permissible pressure point, which are usually dictated by the 1st Rouquerol criterion, and labels these as the isotherm knee. Beyond the isotherm knee, adsorptive activity decreases rapidly as the pores are mostly filled and the internal surfaces are saturated. Within this subset of BET areas, the BETSI optimum is chosen as the one with the smallest percentage error under the 4th Rouquerol criterion, thus making the BET assignment unambiguous.

Section S4 – Tabulated results from the 60 different laboratories in the round-robin evaluation

Lab Number	HKUST-1	Zeolite-13X	Mg-MOF-74	Al fumarate	MCM-41	DMOF-1	MOF-5	UiO-66	UiO-66-NH2
1	1560	833	1013	1007	970	1913	3218	1171	1464
2	1536	823	1000	996	970	1906	3210	1167	1452
3	1551	833	1014	1012	984	1926	3375	1212	1433
4	1556	832	1010	1005	984	1922	3286	1158	1416
5	1200	603	756	774	985	1359	2544	915	1141
6	1556	833	1012	1007	969	1924	3275	1179	1473
7	1558	831	1009	1009	984	1922	3246	1180	1438
8	1556	833	1011	1007	972	1913	3206	1165	1446
9	1555	831	1010	993	971	1753	3226	780	1152
10	1558	832	1012	1005	970	1950	3251	1168	1452
11	1553	834	1013	1008	932	1946	3257	1190	1415
12	1558	833	1010	1009	973	1915	3223	1172	1468
13	1155	601	750	770	1064	1339	2446	743	1104
14	1557	834	1013	1009	976	1933	3242	1180	1469
15	1555	828	1004	1014	981	1895	3123	1146	1385
16	1555	834	1011	1009	984	1918	3246	1179	1469
17	1533	825	1000	1000	971	1898	3040	1120	1426
18	1558	833	1012	1006	970	1926	3311	1135	1378
19	1444	713	882	903	968	1591	2850	1074	1412
20	1559	834	1014	1008	987	1919	3240	1190	1441
21	1007	533	646	649	618	1203	2095	533	915
22	1552	827	1005	1002	970	1907	3115	1183	1417
23	1555	838	1013	1007	971	1927	3264	1176	1455
24	1559	831	1014	1012	975	1924	3287	1192	1150
25	1488	782	960	1001	951	1748	3102	1159	1468
26	1558	833	1013	1002	972	1937	3250	1179	1406
27	1552	827	997	1006	973	1881	3160	1131	1441
28	1589	827	1008	993	957	1870	3477	1124	1390
29	1556	833	1015	1009	970	1999	3222	1188	1430
30	1557	827	1004	995	984	1925	3166	1161	1386
31	1551	830	1004	1004	968	1918	3218	1179	1445
32	1590	840	1008	1025	985	1870	3162	1200	1407
33	1566	837	1018	1013	971	1970	3361	1208	1419
34	1556	699	865	884	960	1483	2614	993	1261
35	1088	888	1105	1126	1447	1984	3460	1329	1666
36	1562	838	1013	1000	958	1905	3240	1120	1455
37	1556	839	1011	1006	966	1917	3225	1157	1433
38	1572	847	1033	1047	1073	1977	3425	1234	1561
39	1556	833	1013	1007	952	1923	3238	1109	1322
40	1552	832	1011	1005	981	1925	3286	866	1412
41	1555	833	1014	1002	975	1927	3247	1186	1474
42	1555	825	1013	985	971	1891	3088	726	1389
43	1561	835	1015	1014	971	1918	3224	1175	1463
44	1551	834	1011	1009	976	1938	3222	1176	1474
45	1557	835	1011	1005	970	1925	3279	1167	1406
46	1555	832	1011	1005	982	1923	3265	1136	1377
47	1559	830	1013	1014	968	1916	3236	1217	1427
48	1518	801	964	987	810	1766	3074	1128	1341
49	1535	821	998	978	952	1898	3232	1050	1129
50	1436	771	948	964	964	1640	2990	1010	1444
51	1557	834	1014	1009	966	1923	3248	1190	1435
52	1558	833	1014	1002	1502	1926	3165	1149	1375
53	1529	831	999	995	969	1903	3243	1083	1359
54	1556	829	1009	1003	968		3259	1153	1394
55	1556	826	1009	1004	963	1892	3146	1159	1419
56	1557	831	1010	1002	898	1737	3265	1188	1089
57	1556	833	1012	1008	968	1931	3275	1180	1434
58	1555	834	1011	1009	960	1913	3275	1180	1424
59	1536	823	998	996	1803	1893	3204	1164	1406
60	1534	820	1000	991	950	1904	3104	1130	1370
61	1556	829	1006	995	971	1927	3306	871	1039

Lab Number	NU-1000	ZIF-8	MIL-101	TPB-DMTP-COF	MIL-100	NU-1102	NU-1104	NU-1105	PCN-777
1	2153	1601	2387	2836	2043	4607	7218	3527	1973
2	2099	1734	2550	2839	2256	4913	7845	3574	1990
3	2061	1788	2509	2859	1936	4564	6163	3695	2036
4	1979	1558	2499	2800	1584	4889	3210	3722	2028
5	2152	1341	2363	2792	1784	3889	5999	3667	1952
6	1987	1573	2546	2815	1620	4883	7353	3722	1848
7	2054	1768	2548	2815	2224	4691	7151	3612	2444
8	1961	1601	2445	2754	2129	4278	3559	3635	1898
9	1961	1373	1432	2800	1995	4701	5223	3554	1893
10	2009	1466	2612	2805	2130	4928	6017	3651	1928
11	1968	1574	2578	2658	1711	4893	5914	3808	1916
12	1973	1720	2577	2816	1949	4753	5223	3489	1866
13	2066	1310	2187	6446	1510	3517	4291	4940	1870
14	1971	1760	2646	2754	2226	4814	3263	2942	1893
15	2129	1740	2376	2894	1948	4859	6119	3585	1968
16	2058	1766	2567	2800	2129	4926	6036	3712	1898
17	1963	1623	2749	2825	1999	5400	6080	3724	1950
18	1988	1687	2319	2601	1915	4854	6039	3175	1936
19	1986	1623	2680	2659	2133	5385	6130	2737	1780
20	2076	1774	2467	2791	2111	4762	5361	3528	1948
21	1289	1117	1017	1415	1001	3138	1757	2297	1183
22	2044	1729	2058	2725	1721	4928	5799	3591	1908
23	2100	1756	2573	2800	2279	4896	7197	3564	1900
24	2149	1567	2606	2880	2082	5015	6780	3939	1974
25	1996	1731	2342	2401	1711	4514	5874	3731	1864
26	2041	1720	2652	2804	2129	4926	5983	3688	1930
27	2006	1720	2572	2858	2113	4842	6039	3688	1898
28	2009	1702	2444	2568	1934	4907	7225	3310	1973
29	2090	1764	2567	2855	2114	4874	6291	3535	1929
30	1968	1732	2642	2895	2032	4693	5409	3614	1911
31	2045	1818	2589	2856	2129	4839	6035	3659	1884
32	2070	1607	2624	2792	2099	4646	5999	3738	1635
33	2005	1782	2850	2818	2054	4876	5653	3798	1995
34	2005	1523	2445	2500	1879	4142	6208	3659	1897
35	2775	3201	3421	3941	2499	5706	9341	4823	2863
36	2000	1822	2646	2800	1735	4896	3197	3032	1725
37	2014	1579	2588	2800	2046	4831	7136	3528	1914
38	2125	1506	2433	3796	2555	6053	8763	5508	2975
39	1961	1579	2277	2800	1648	4884	6342	3640	1575
40	1992	1579	2526	2779	2068	4889	5507	3645	2028
41	2149	1762	2856	2844	2039	4730	5720	3538	1946
42	2013	1716	1573	2750	1544	4816	2774	3551	1988
43	1966	1600	2697	2950	2042	4762	5275	3578	1983
44	2049	1540	2565	2855	2030	4604	8077	3527	1970
45	2007	1580	2501	2573	1979	4851	7136	3592	1824
46	2018	1712	2321	2600	1917	4856	2806	3400	1935
47	1647	1599	2681	2906	1763	4510	2975	3493	1926
48	1918	1828	2092	1699	1861	4277	2108	2210	1409
49	1951	1536	1932	2151	1566	4820	6524	3479	1972
50	2039	1732	2515	2348	2073	4823	5851	3725	1865
51	1971	1586	2633	2817	2006	4856	5451	3724	1897
52	1994	1731	2050	2842	2006	4649	5142	3508	1970
53	2056	1665	1973	2648	1830	4883	6003	3482	1978
54	1979	1560	2361	2662		4889	6625	3278	1873
55	2024	1757	2561	2810	2033	4823	5891	3719	1900
56	1832	1819	1549	1629	1531	4778	1840	1971	1480
57	2021	1752	2554	2830	2031	5024	6043	3733	1909
58	2008	1604	2503	2728	1982	4819	1804	2903	1865
59	1933	1580	2533	2764	2397	4648	6623	5945	3350
60	2008	1720	2386	2394	2064	4777	1783	2776	1756
61	2045	1466	1555	2779	1718	4925	2996	3318	1835

Section S5 – Insets of round-robin evaluation results

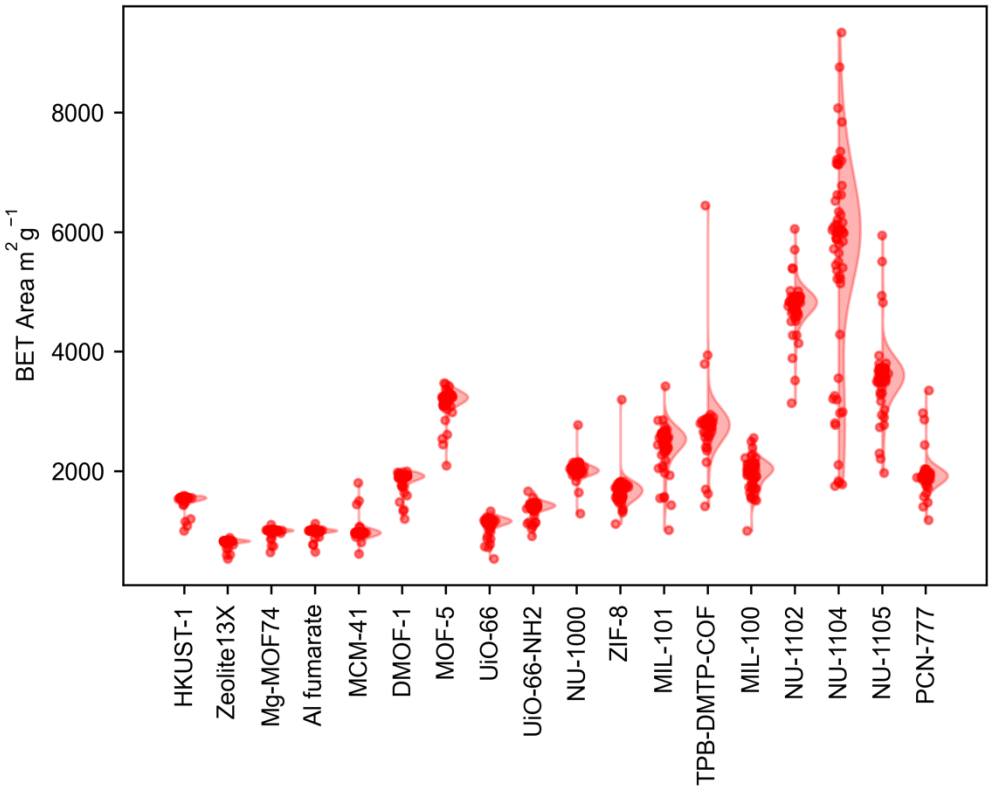

Figure S5 | Distribution of BET areas for set of 18 isotherms shared with international experts in adsorption science.

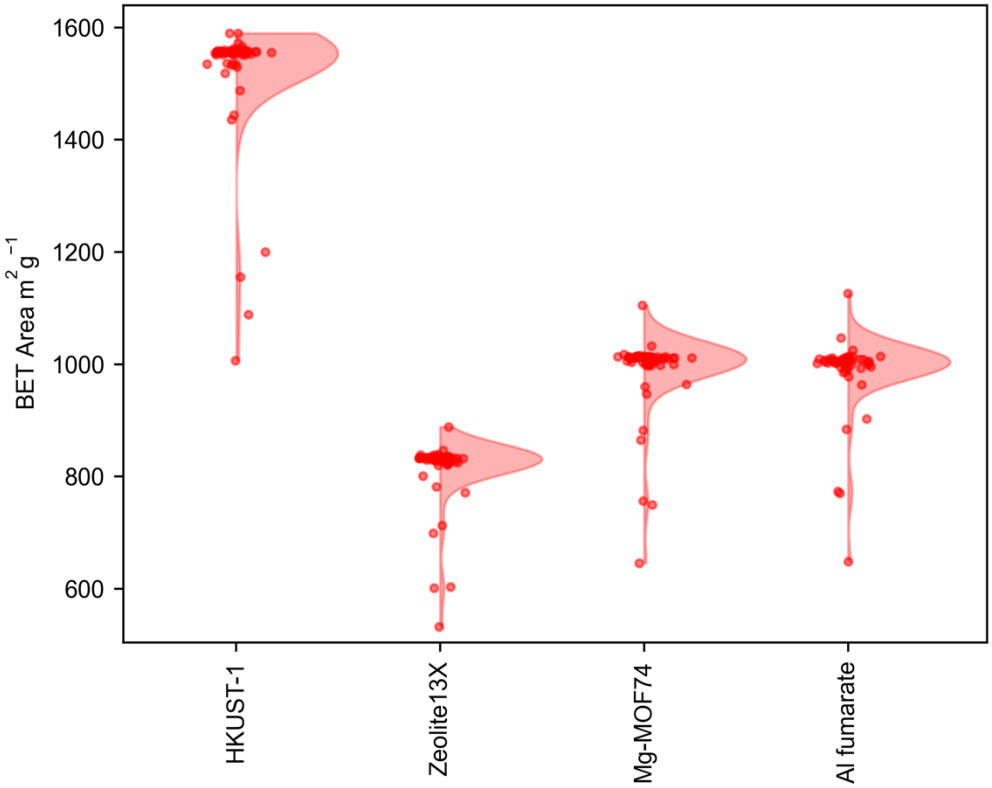

Figure S5-I | Inset of **Figure S5**: HKUST-1, Zeolite13X, Mg-MOF-74, Al fumarate

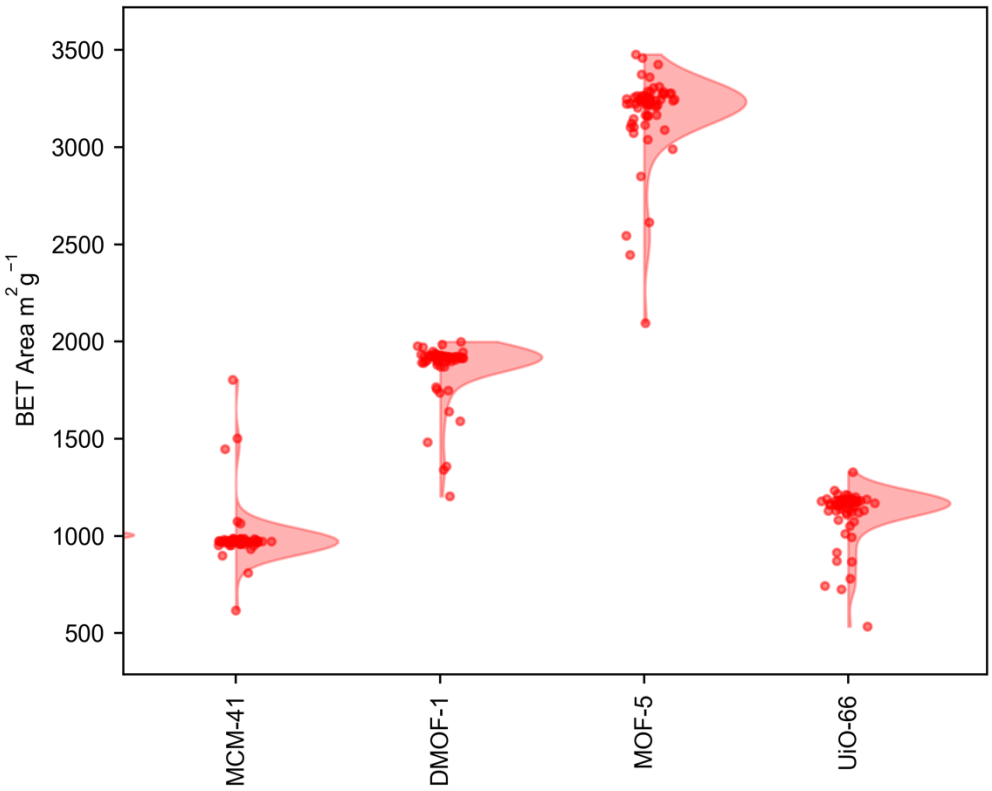

Figure S5-II | Inset of **Figure S5**: MCM-41, DMOF-1, MOF-5, UiO-66

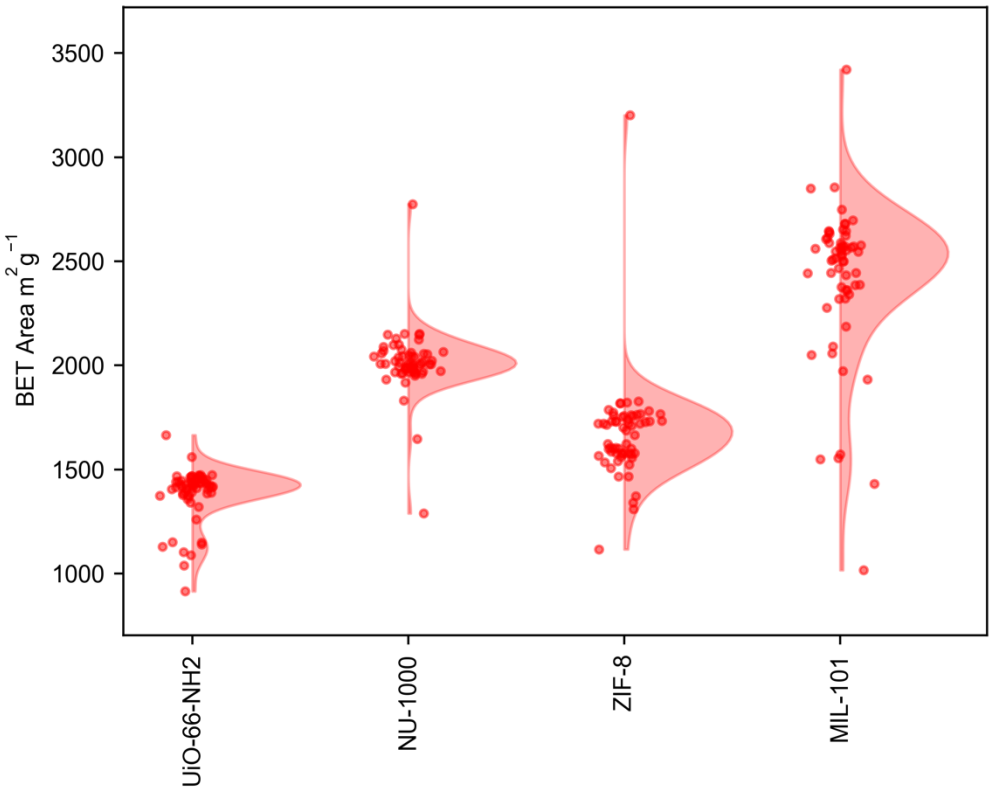

Figure S5-III | Inset of **Figure S5**: UiO-66-NH2, NU-1000, ZIF-8, MIL-101

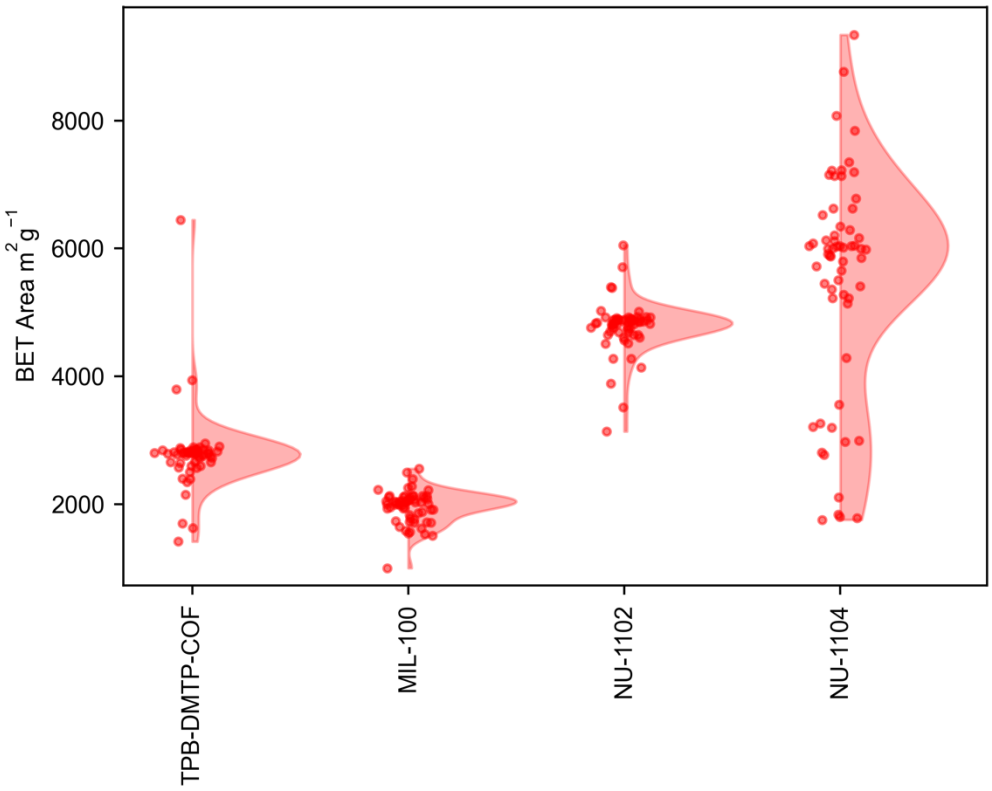

Figure S5-IV | Inset of **Figure S5**: TPB-COF, MIL-100, NU-1102, NU-1104

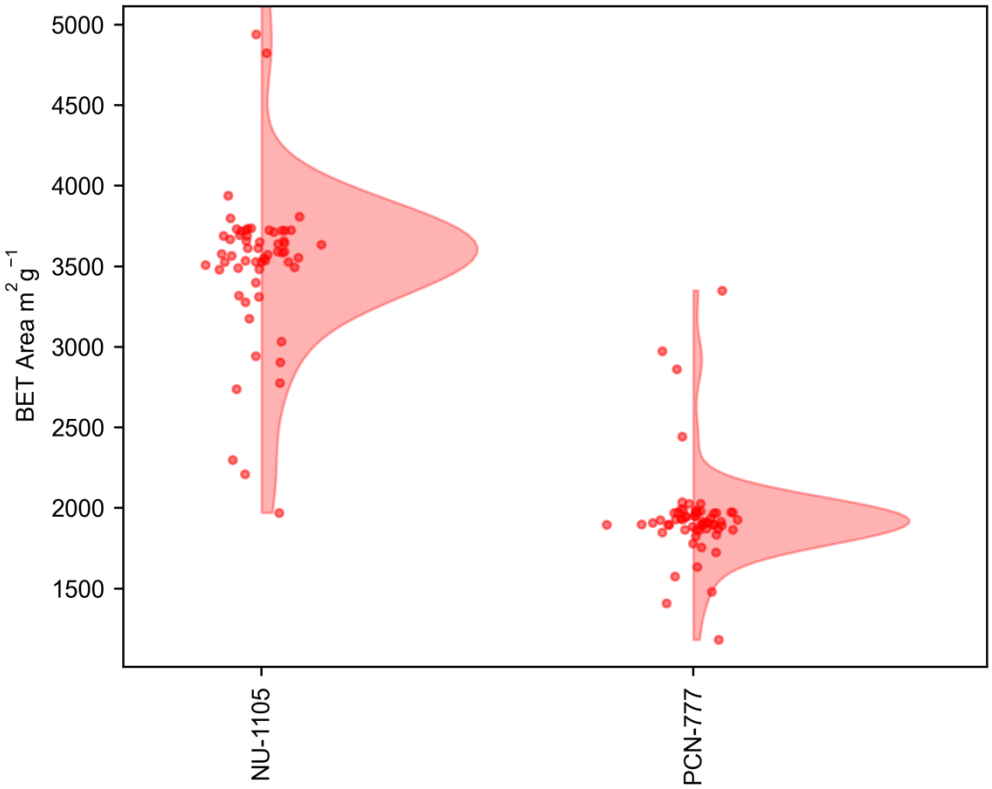

Figure S5-V | Inset of **Figure S5**: NU-1105 and PCN-777

Section S6 – BETSI results of isotherms distributed in round-robin evaluation

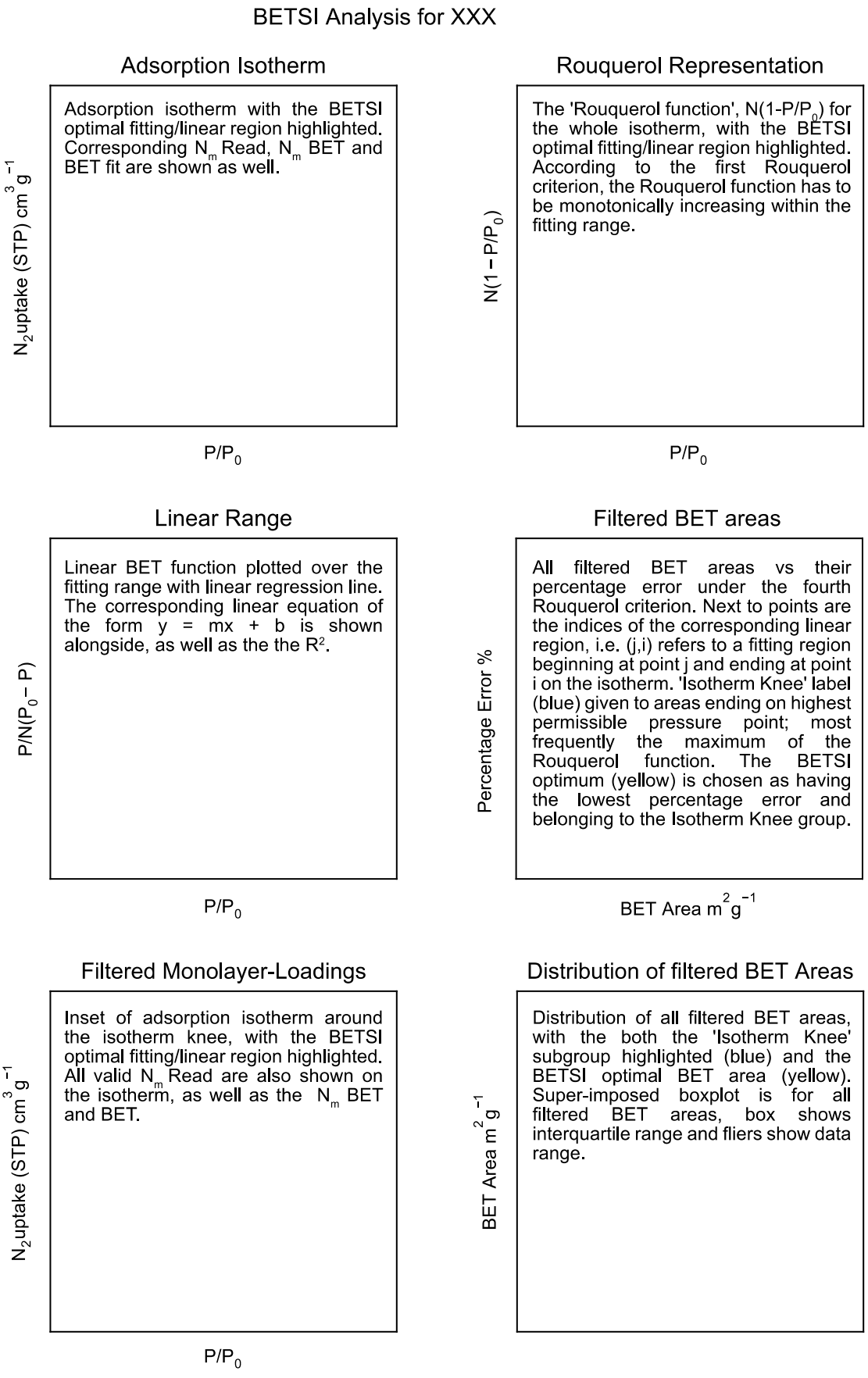

Figure S6 – A | BETSI results of isotherms distributed in round-robin evaluation

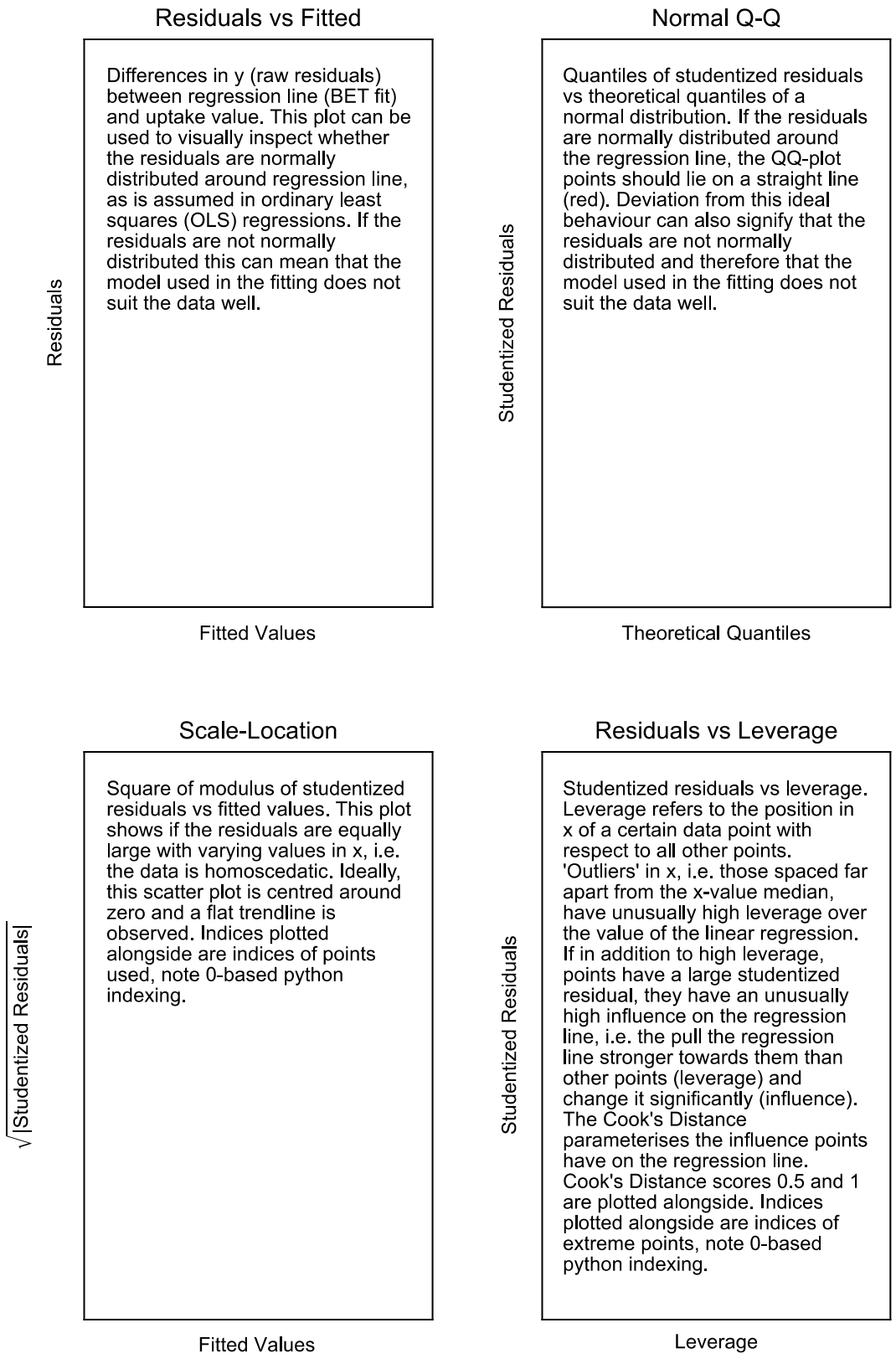

Figure S6 – B | Regression Diagnostics of optimal BETSI fits

HKUST-1

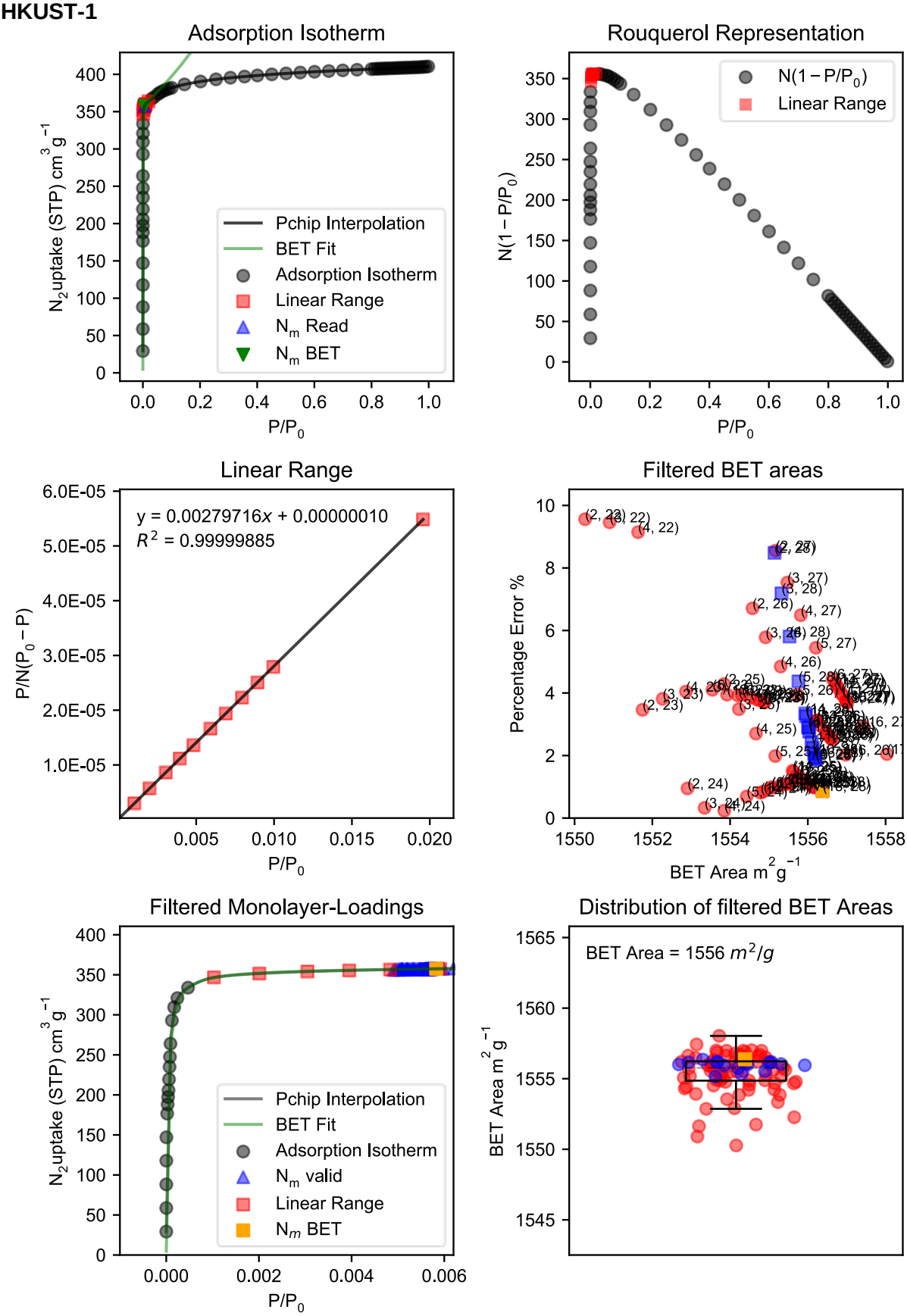

Figure S6 – I A | BETSI analysis of HKUST-1

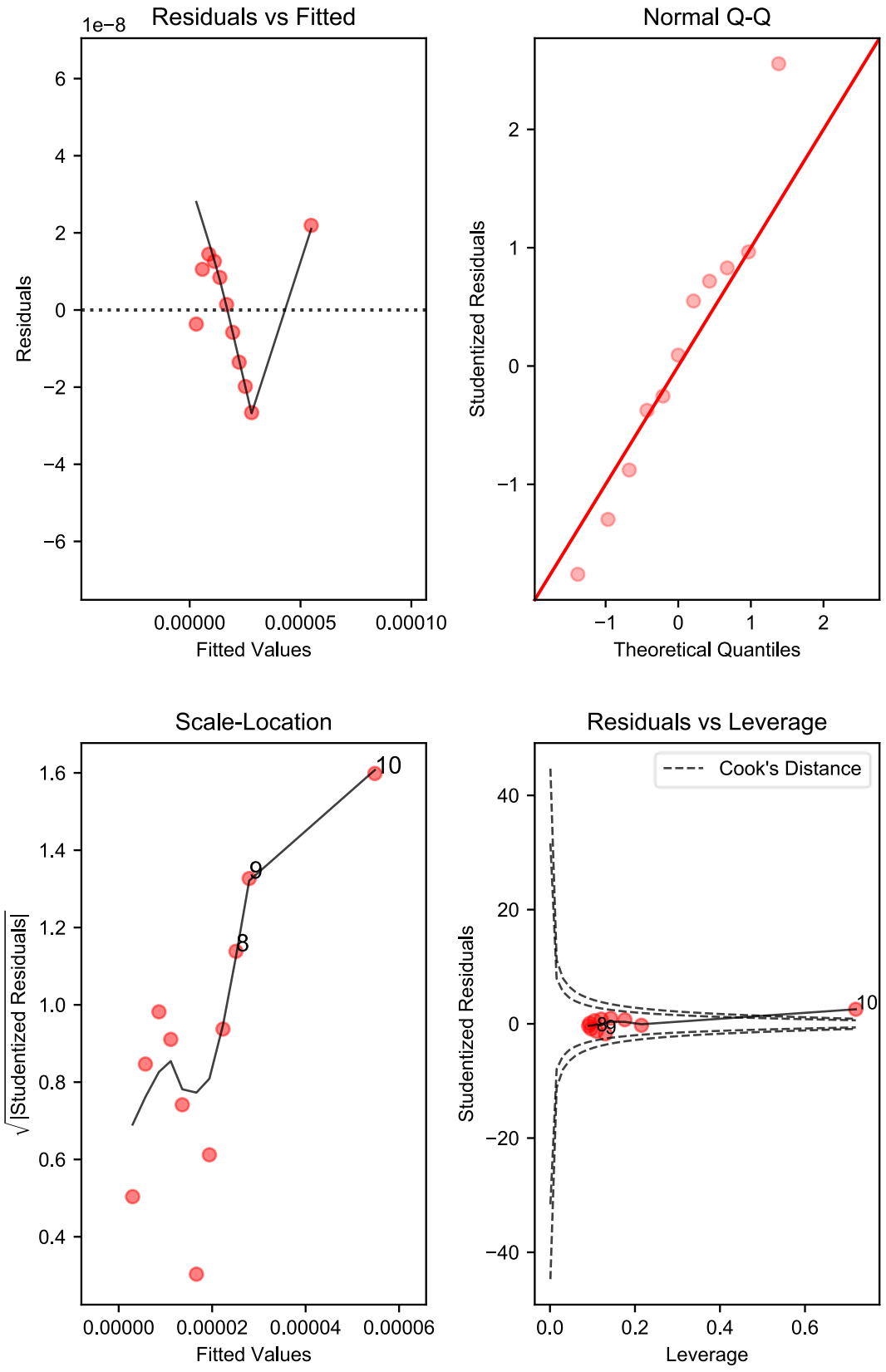

Figure S6 – I B | BETSI regression diagnostics for HKUST-1

Zeolite-13X

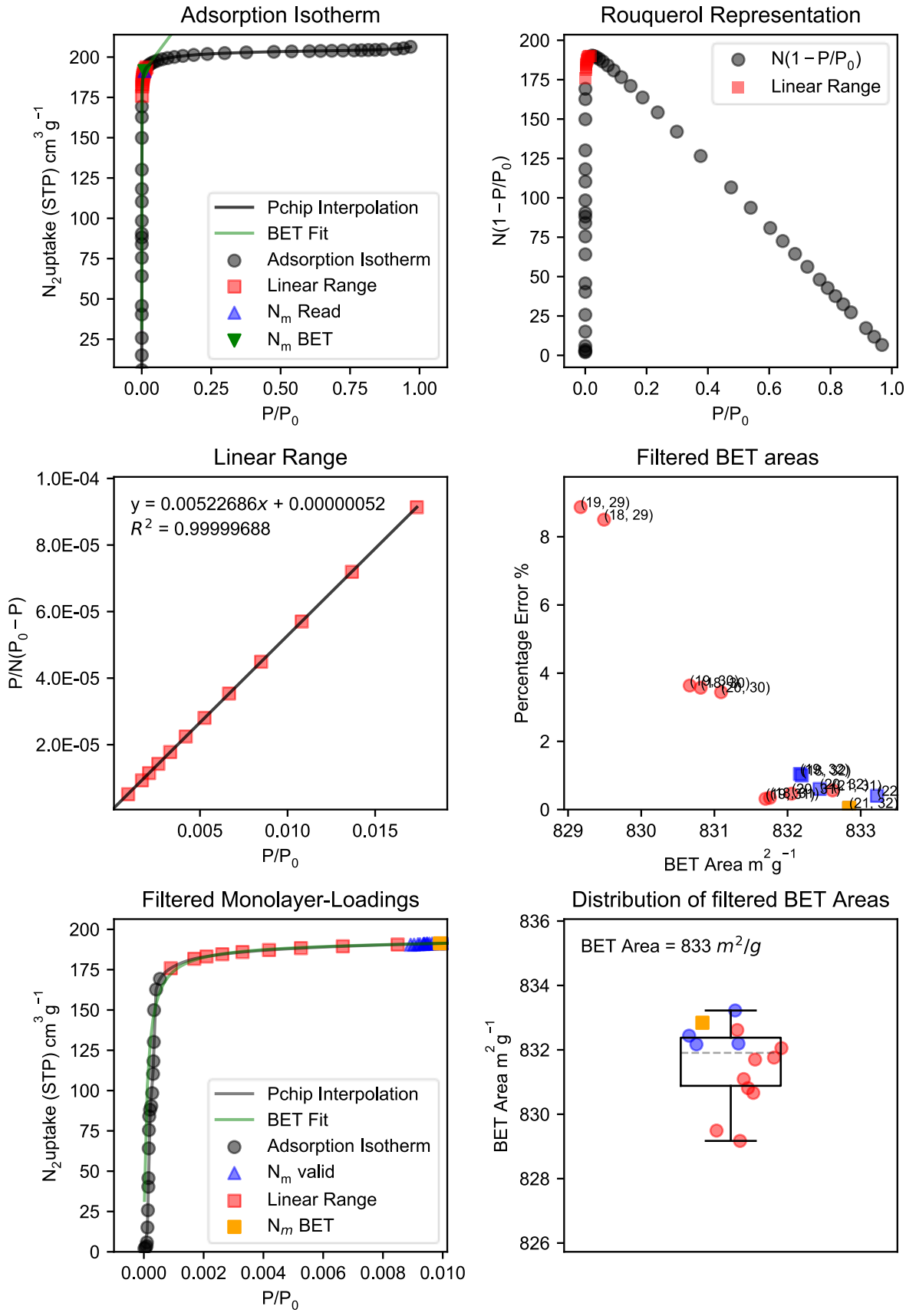

Figure S6 – II A | BETSI analysis of Zeolite-13X

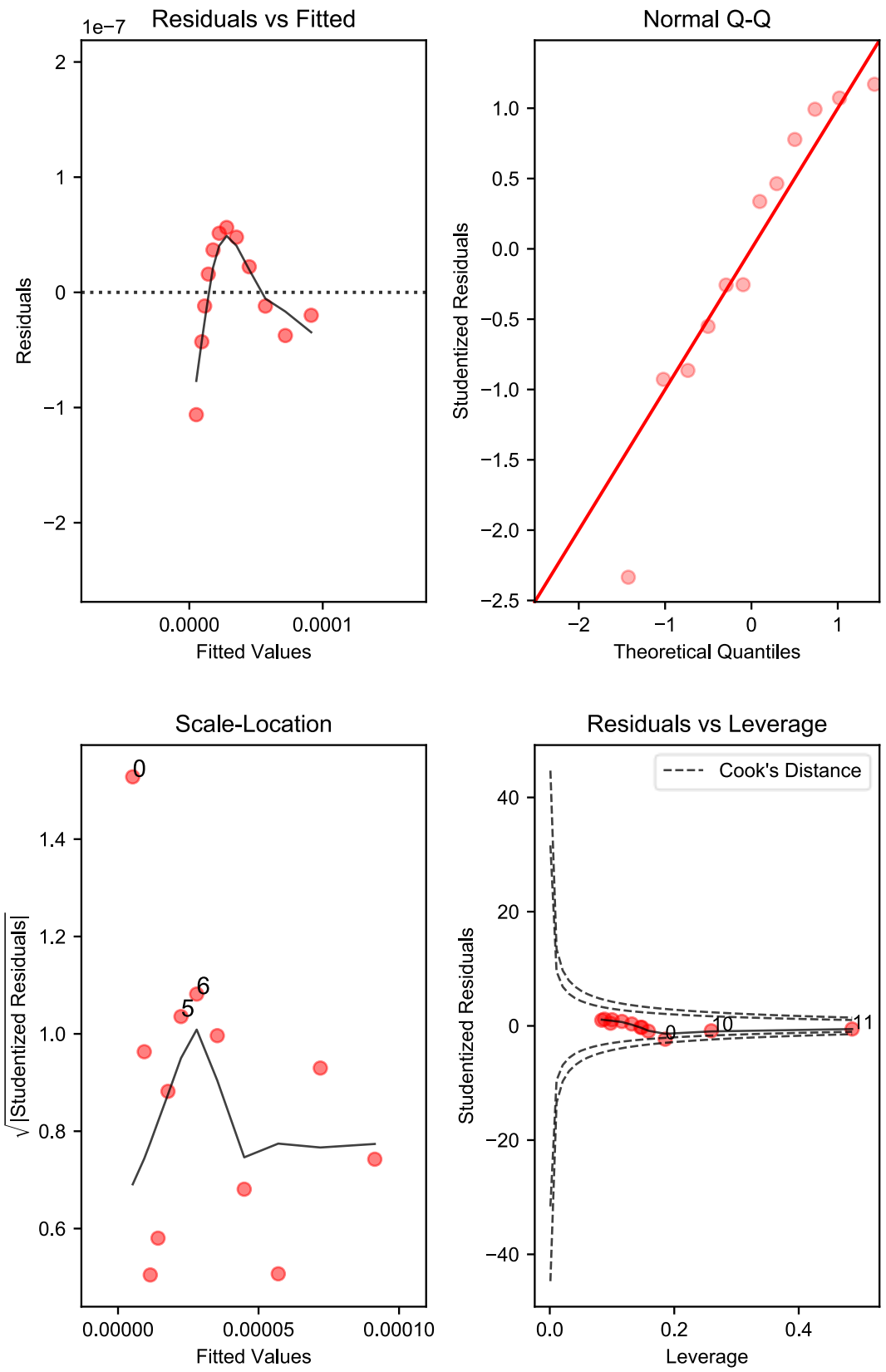

Figure S6 – II B | BETSI regression diagnostics for Zeolite-13X

Mg-MOF-74

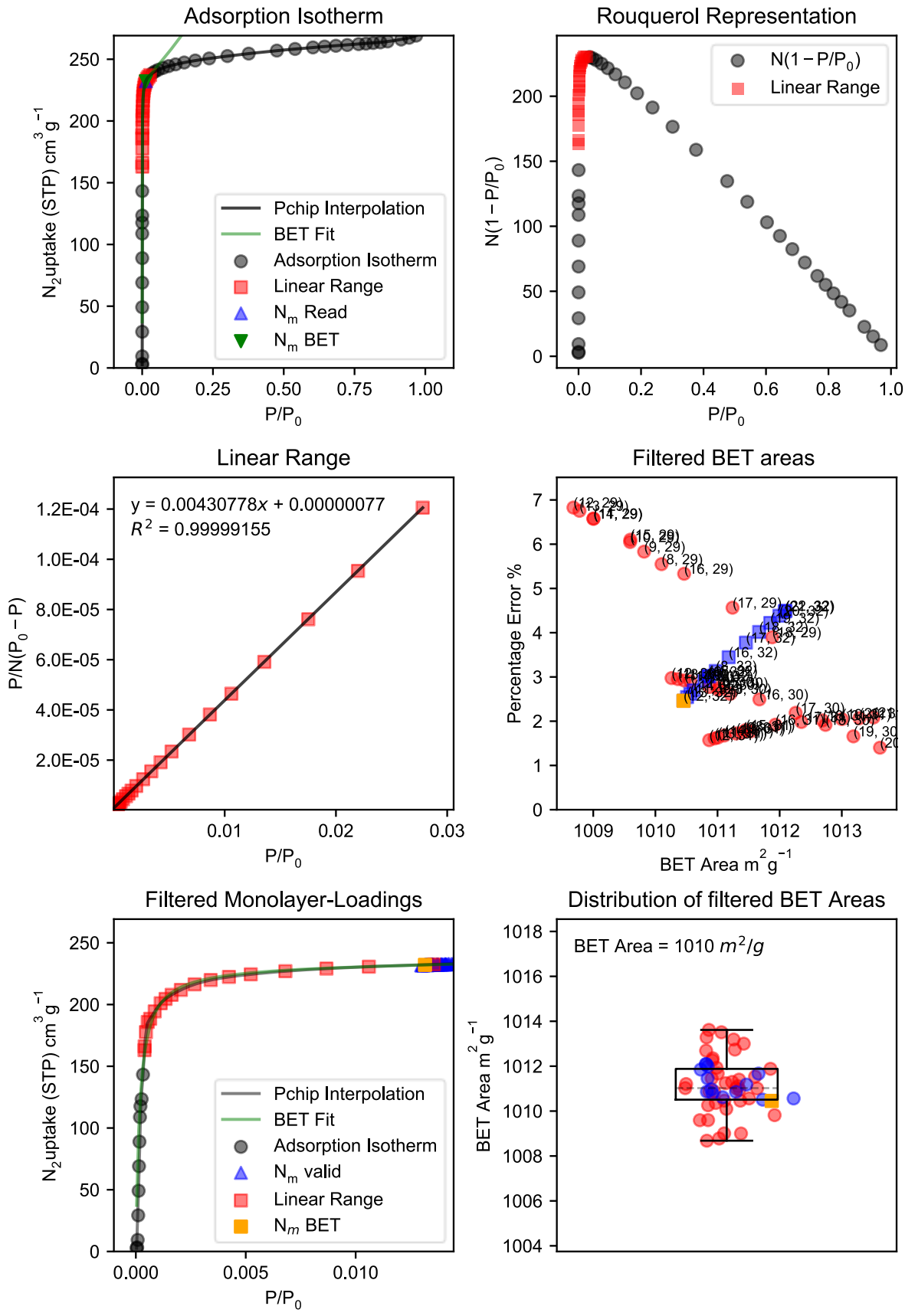

Figure S6 – III A | BETSI analysis of Mg-MOF-74

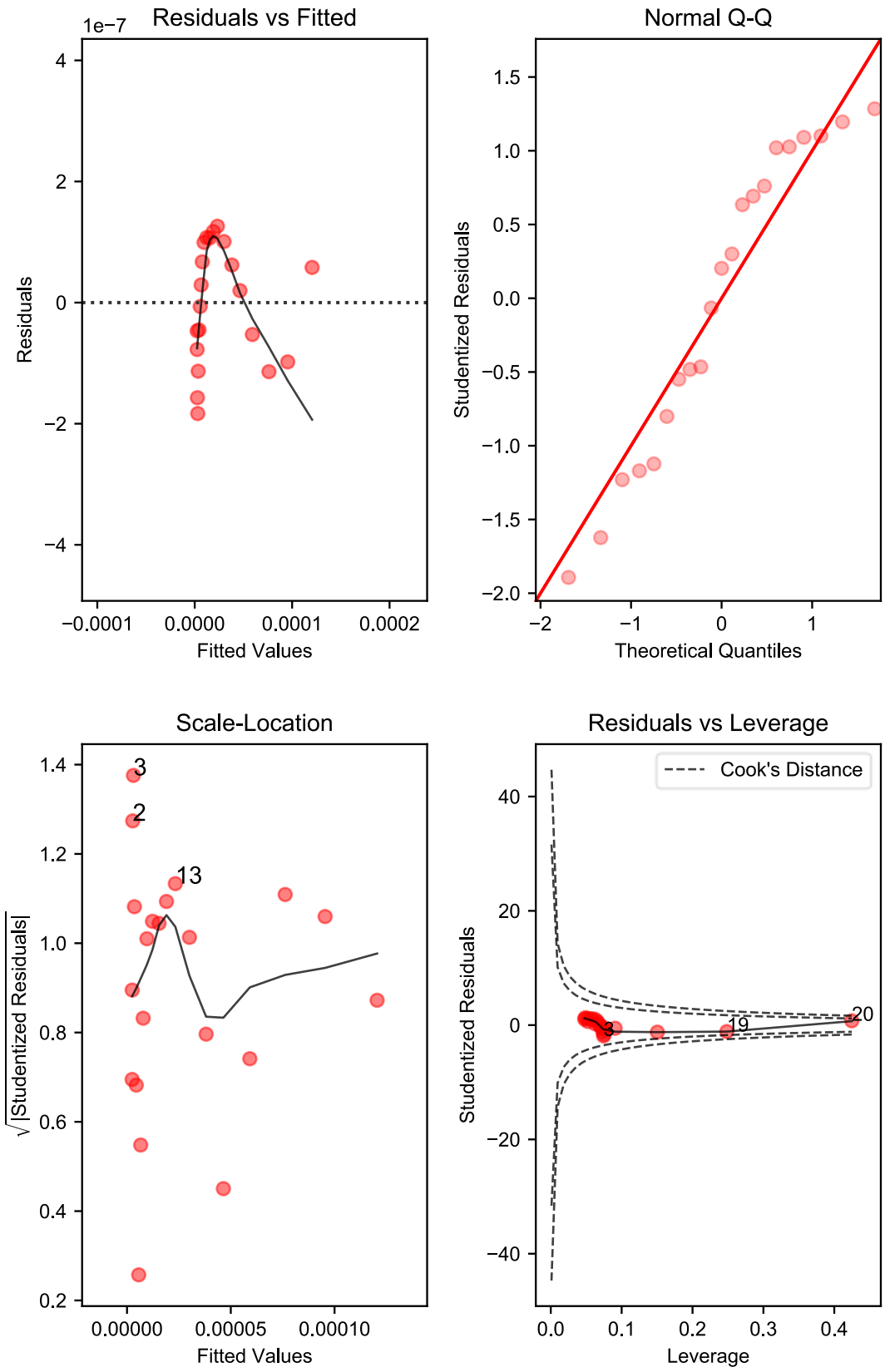

Figure S6 – III B | BETSI regression diagnostics for Mg-MOF-74

Al fumarate

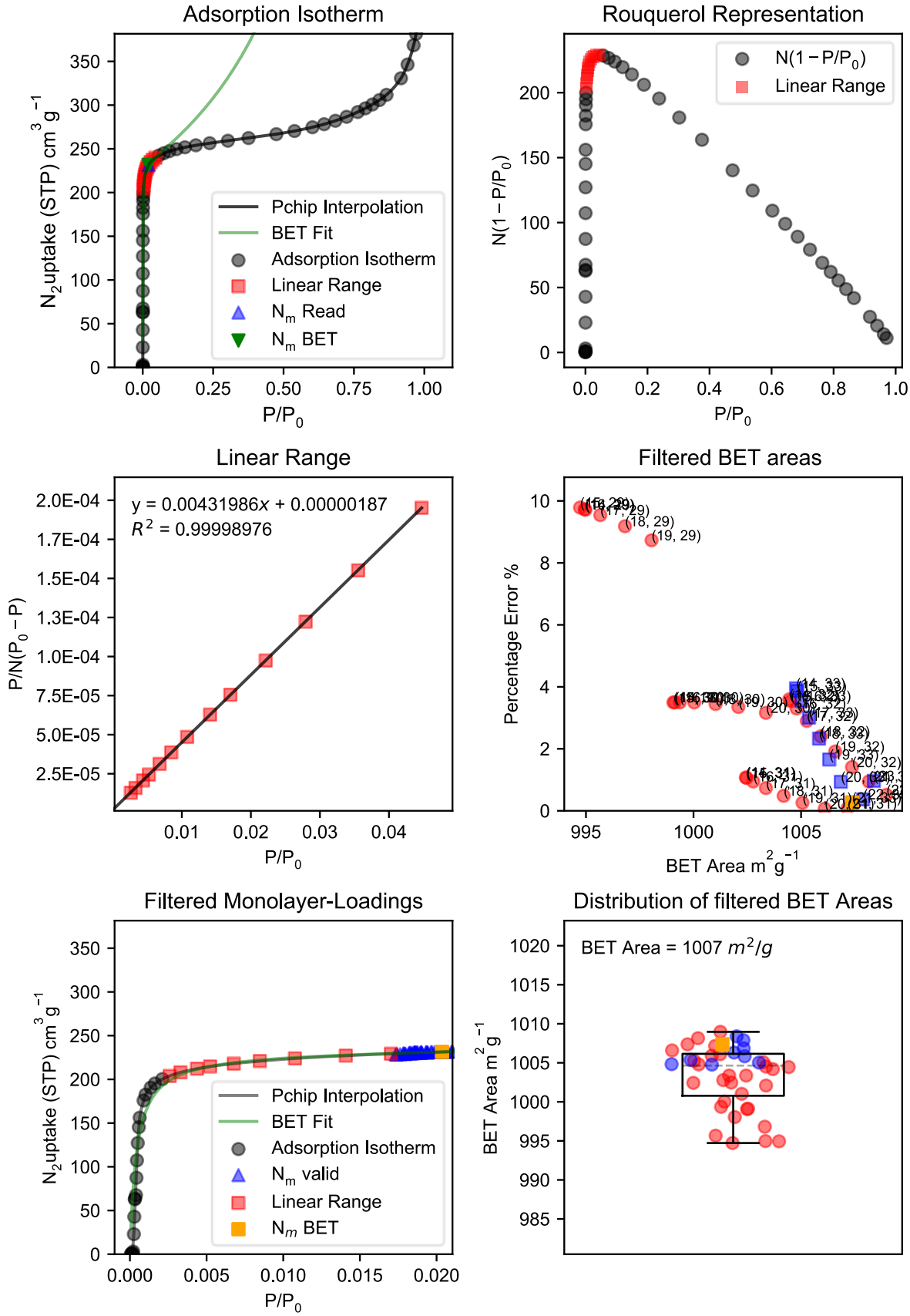

Figure S6 – IV A | BETSI analysis of Al fumarate

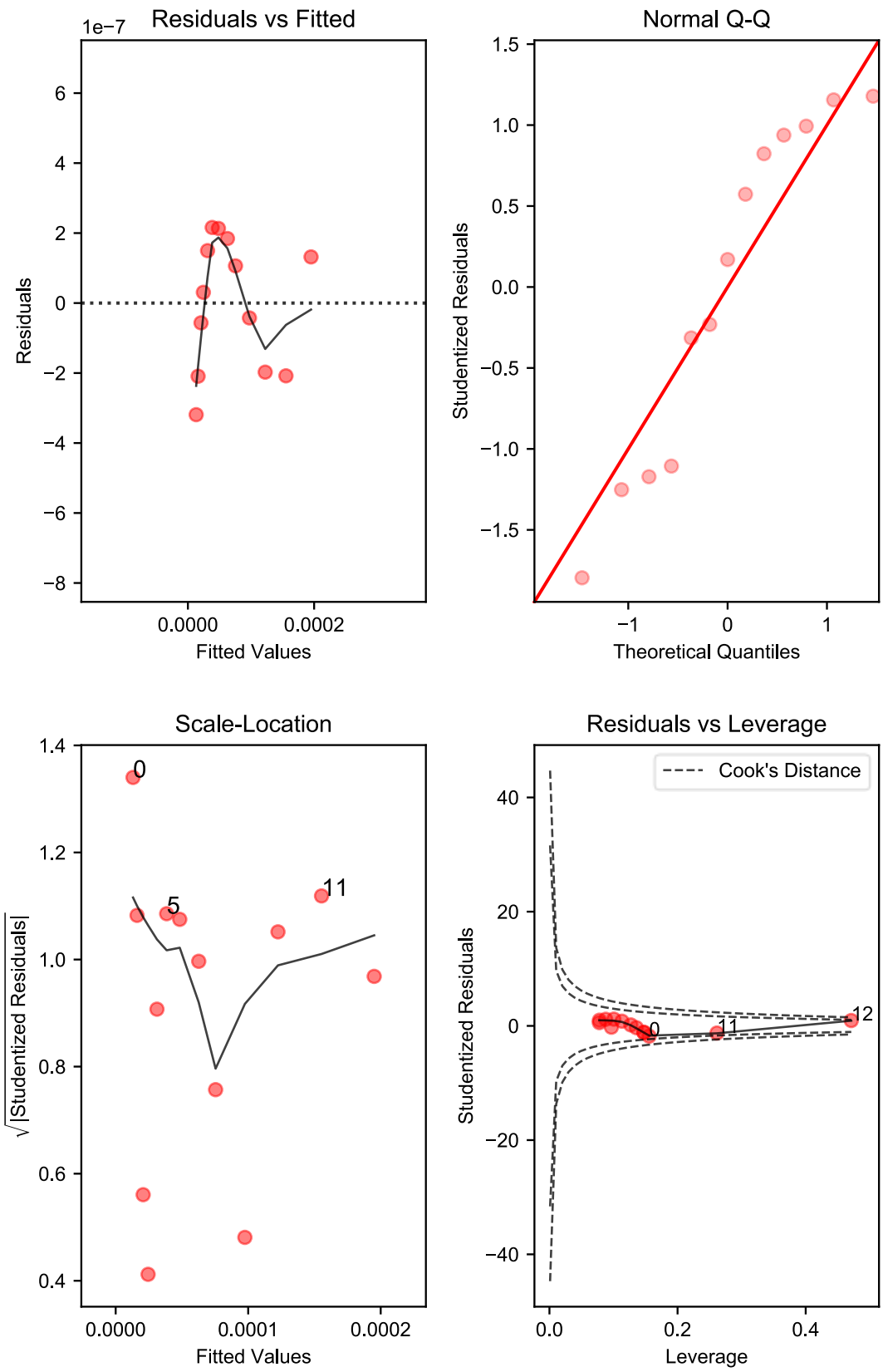

Figure S6 – IV B | BETSI regression diagnostics for Al fumarate

MCM-41

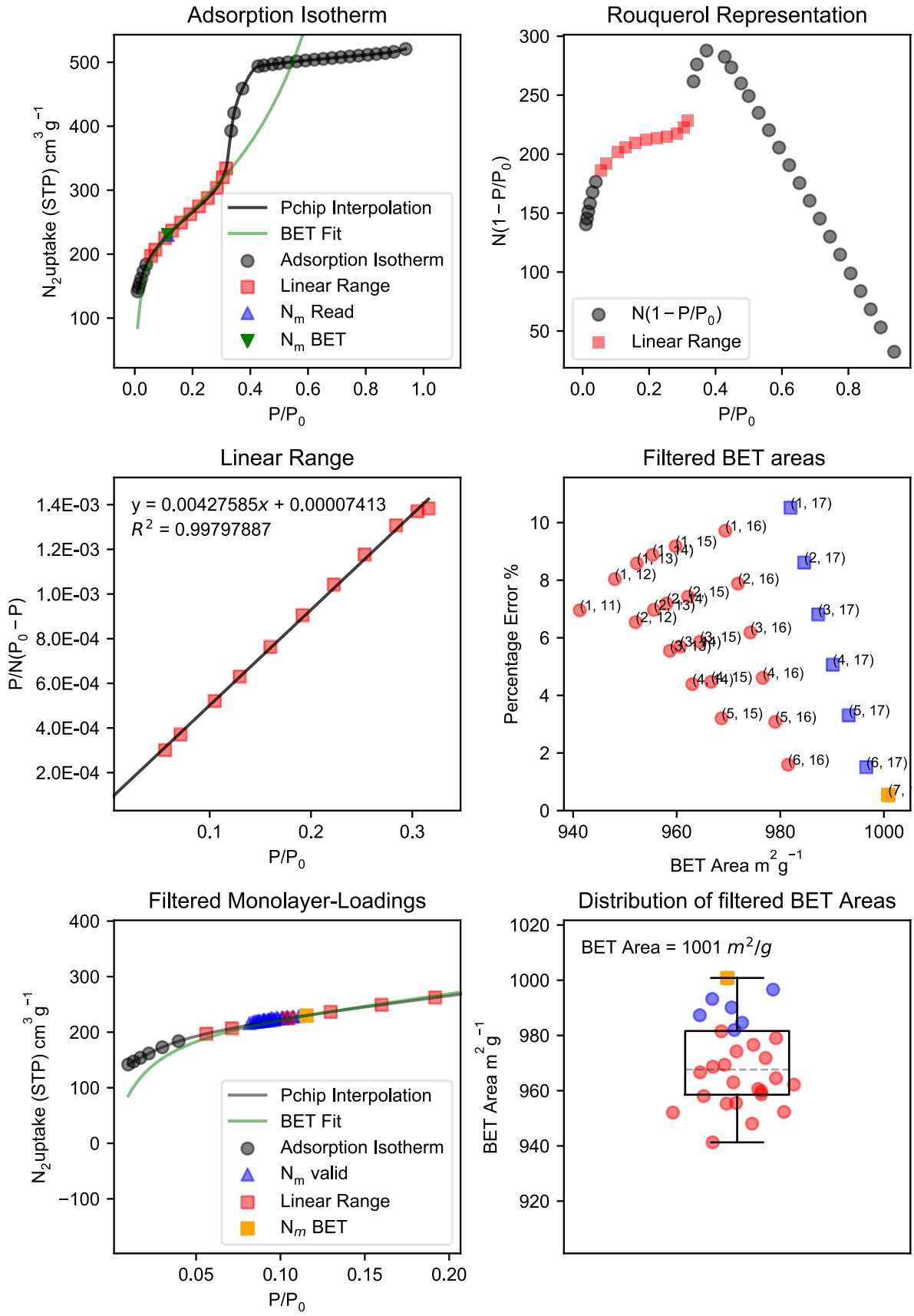

Figure S6 – V A | BETSI analysis of MCM-41

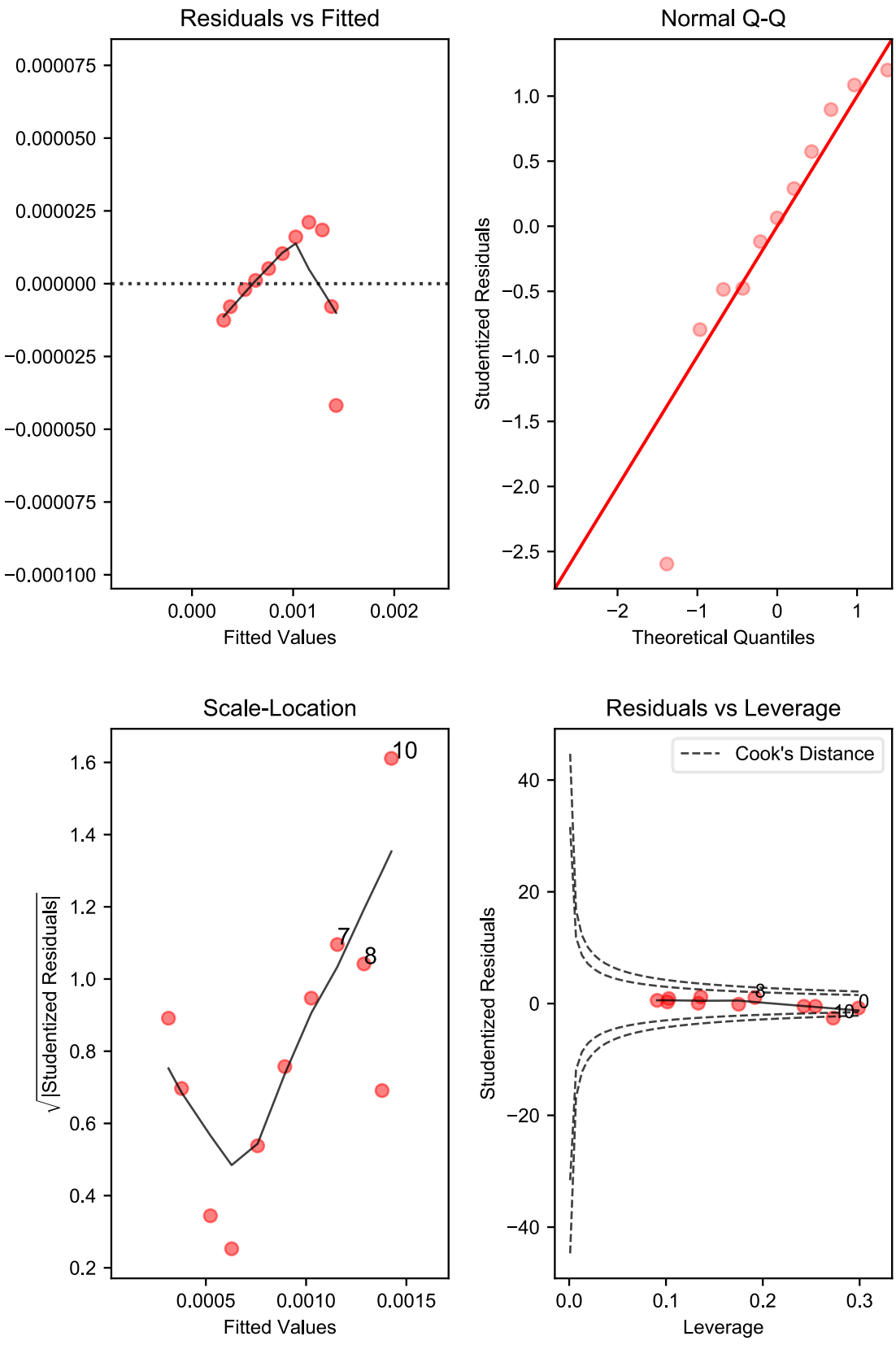

Figure S6 – V B | BETSI regression diagnostics for MCM-41

DMOF-1

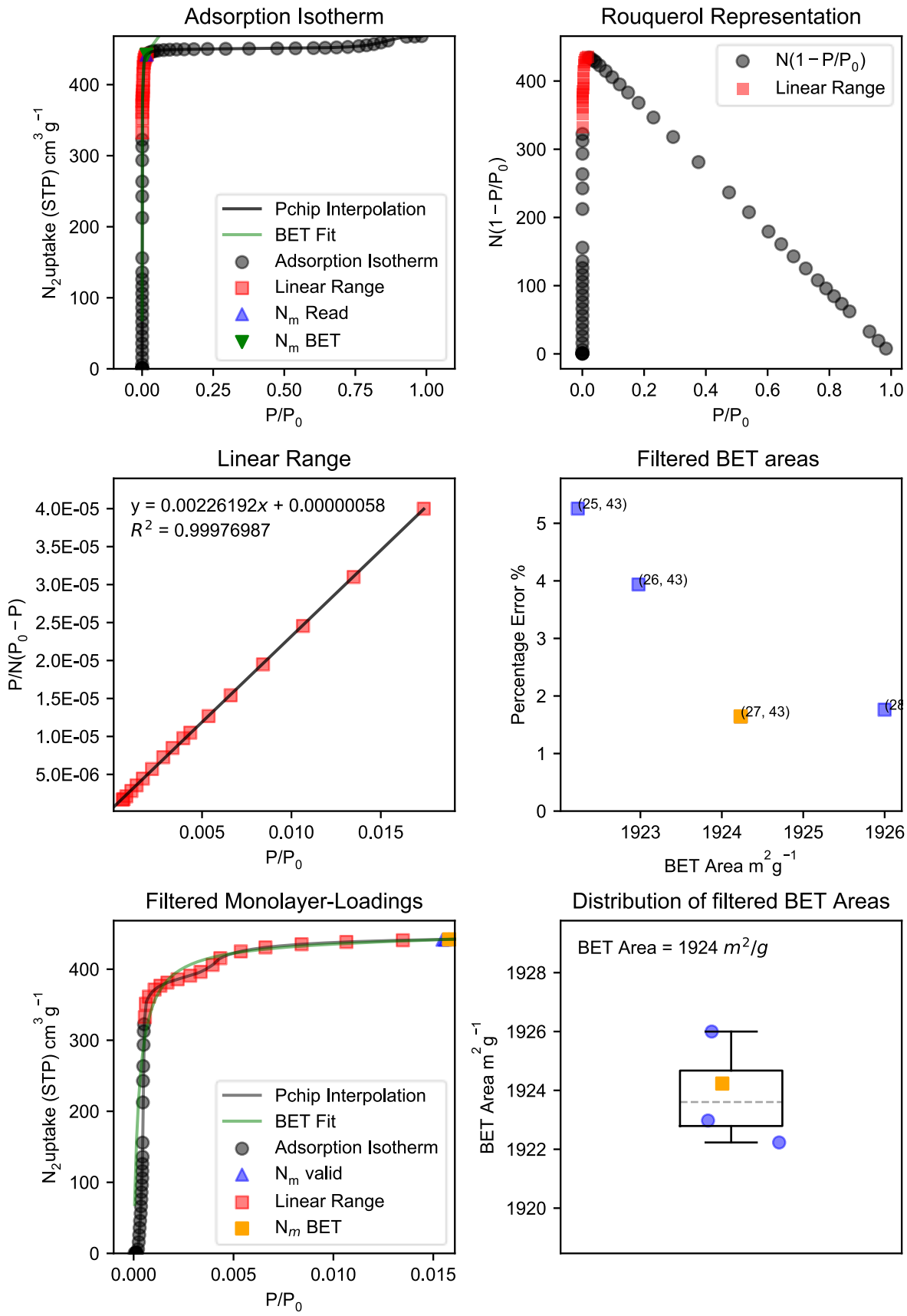

Figure S6 – VI A | BETSI analysis of DMOF-1

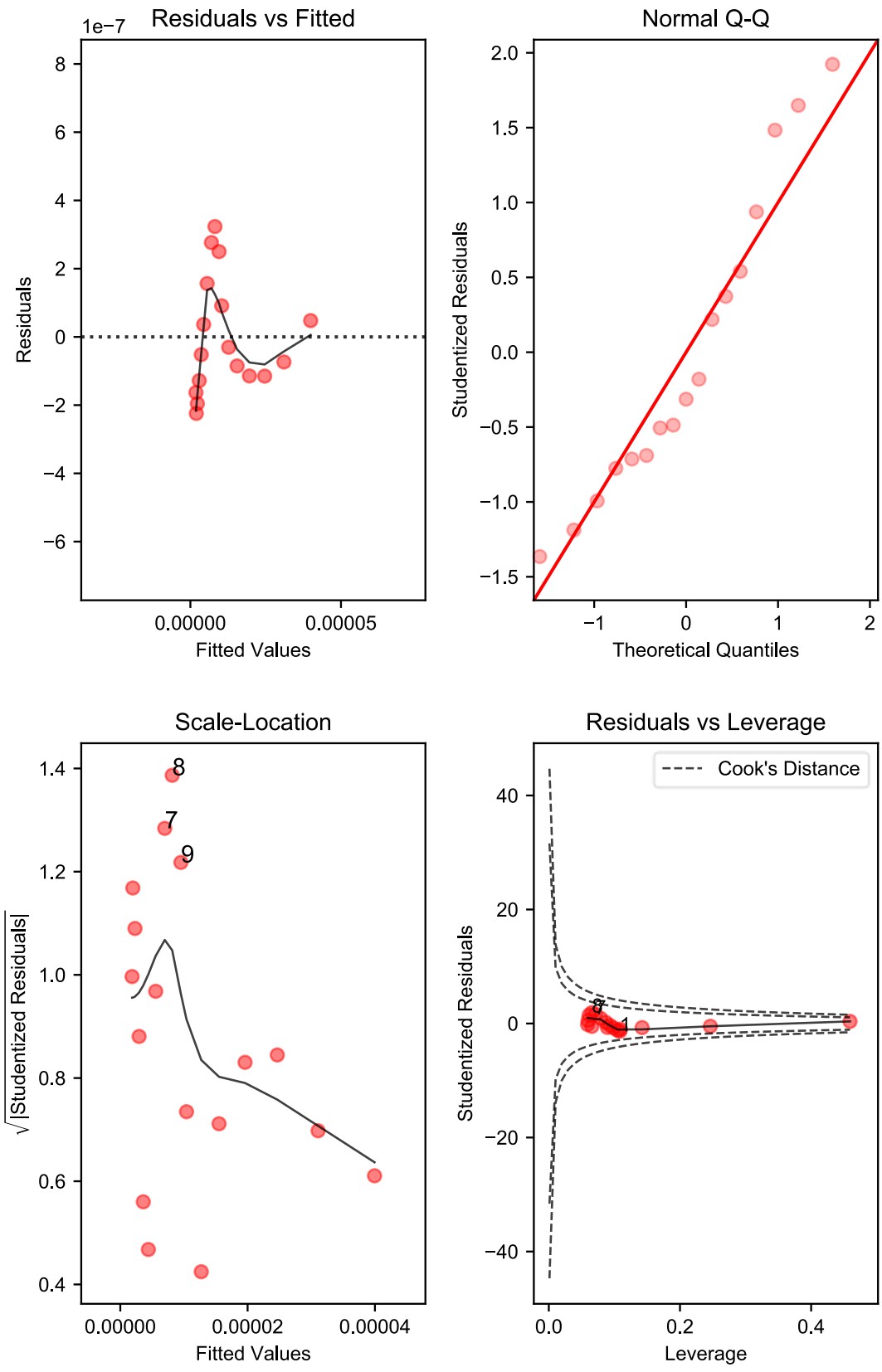

Figure S6 – VI B | BETSI regression diagnostics for DMOF-1

MOF-5

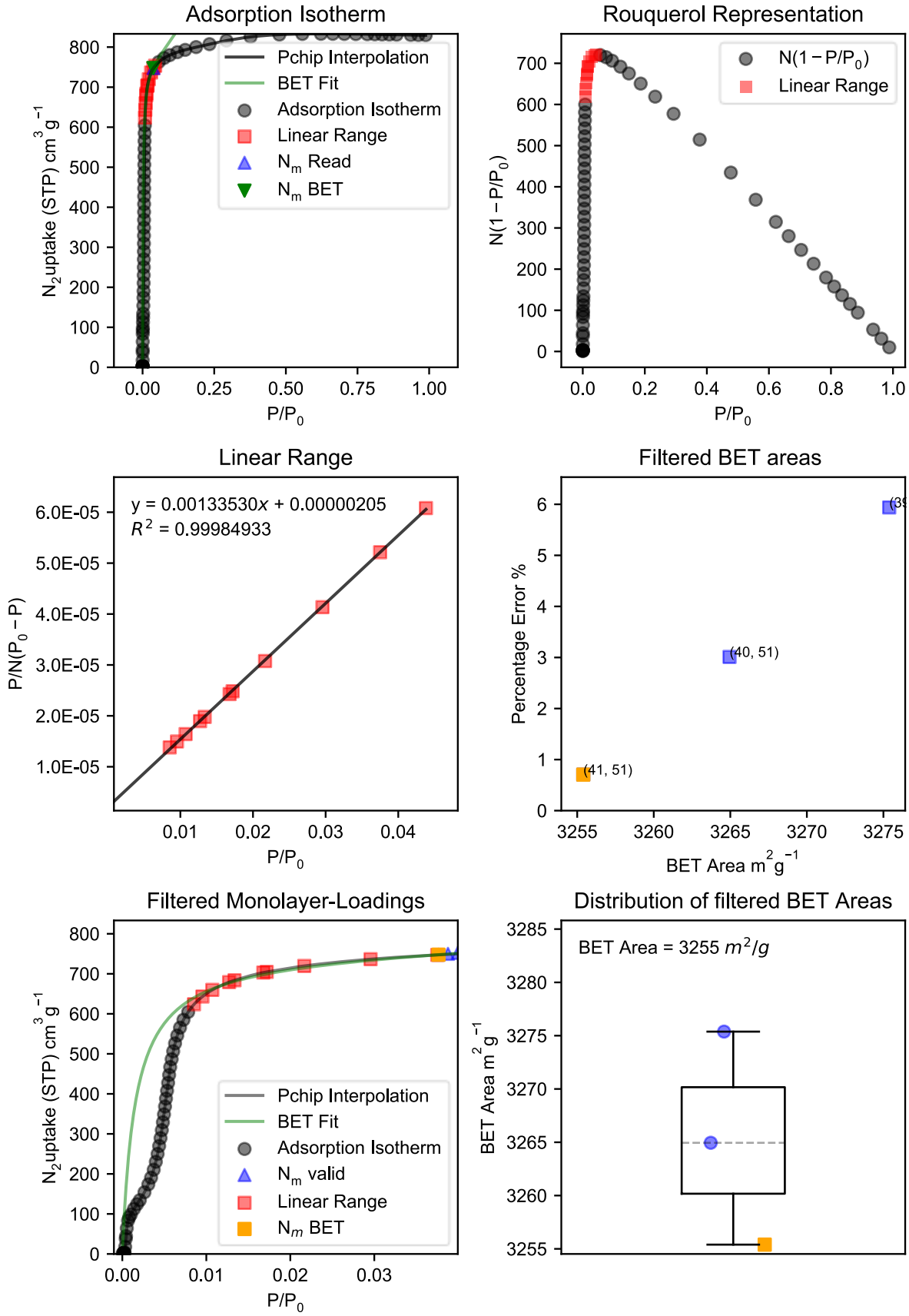

Figure S6 – VII A | BETSI analysis of MOF-5

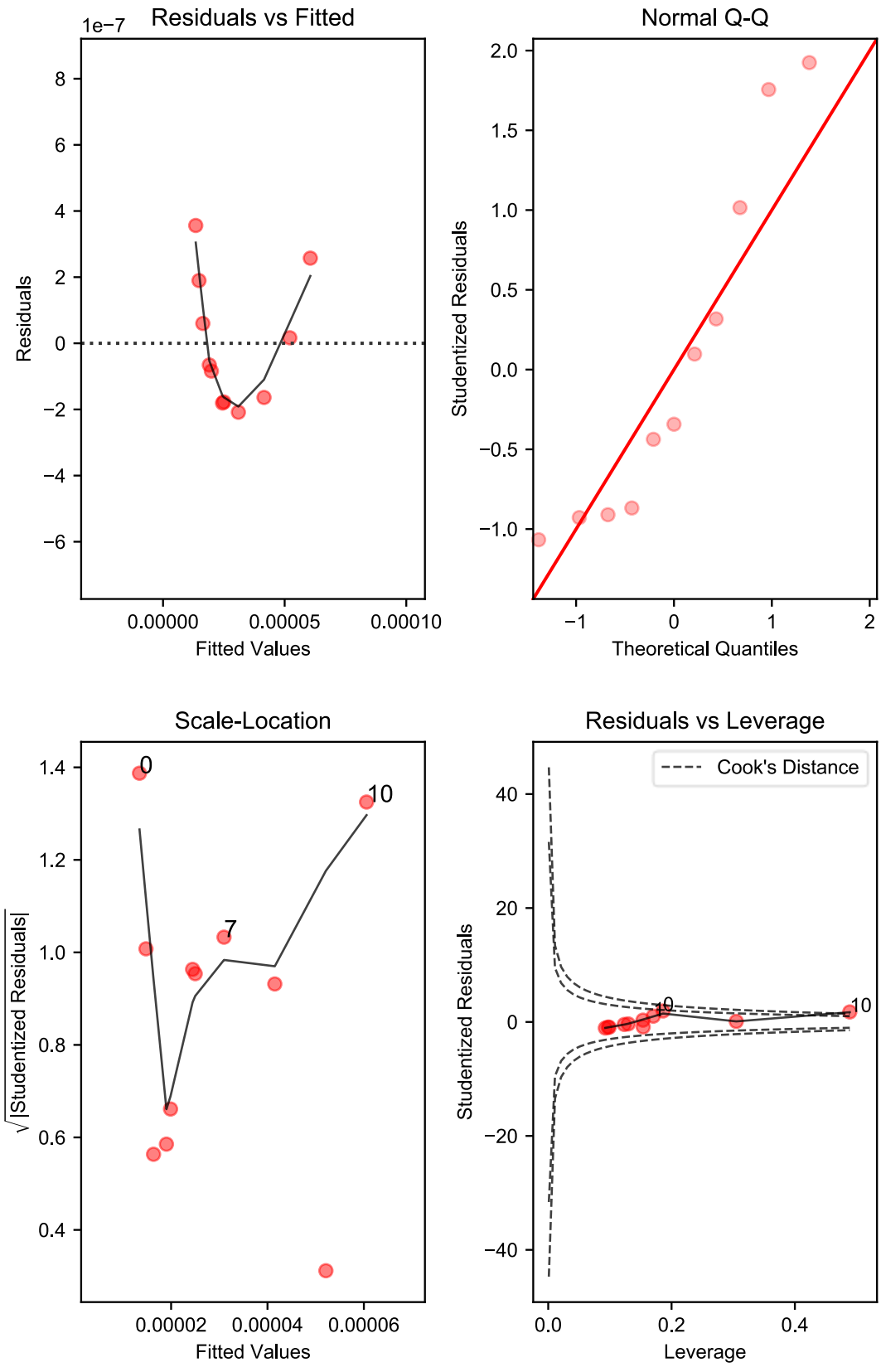

Figure S6 – VII B | BETSI regression diagnostics for MOF-5

UiO-66

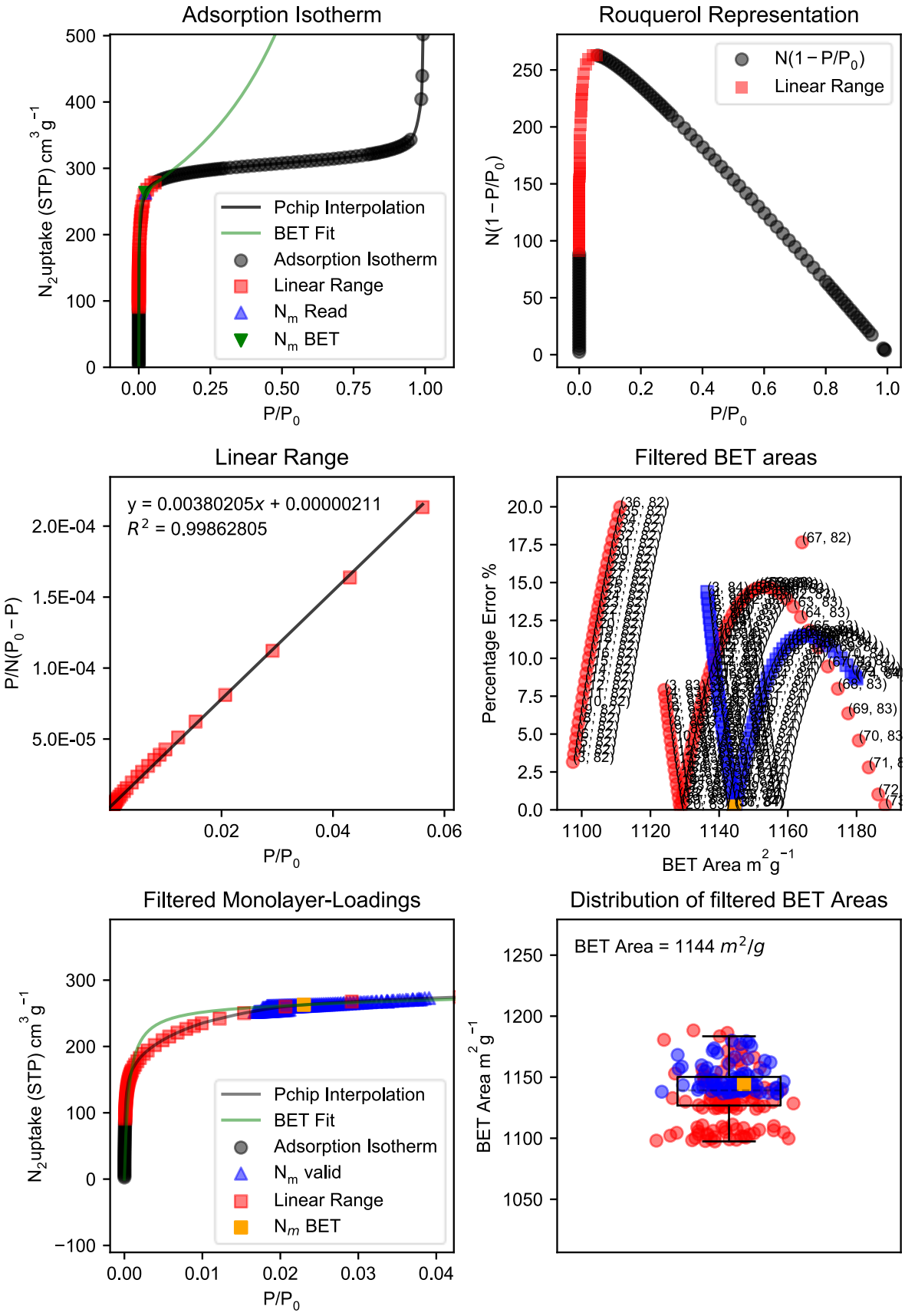

Figure S6 – VIII A | BETSI analysis of UiO-66

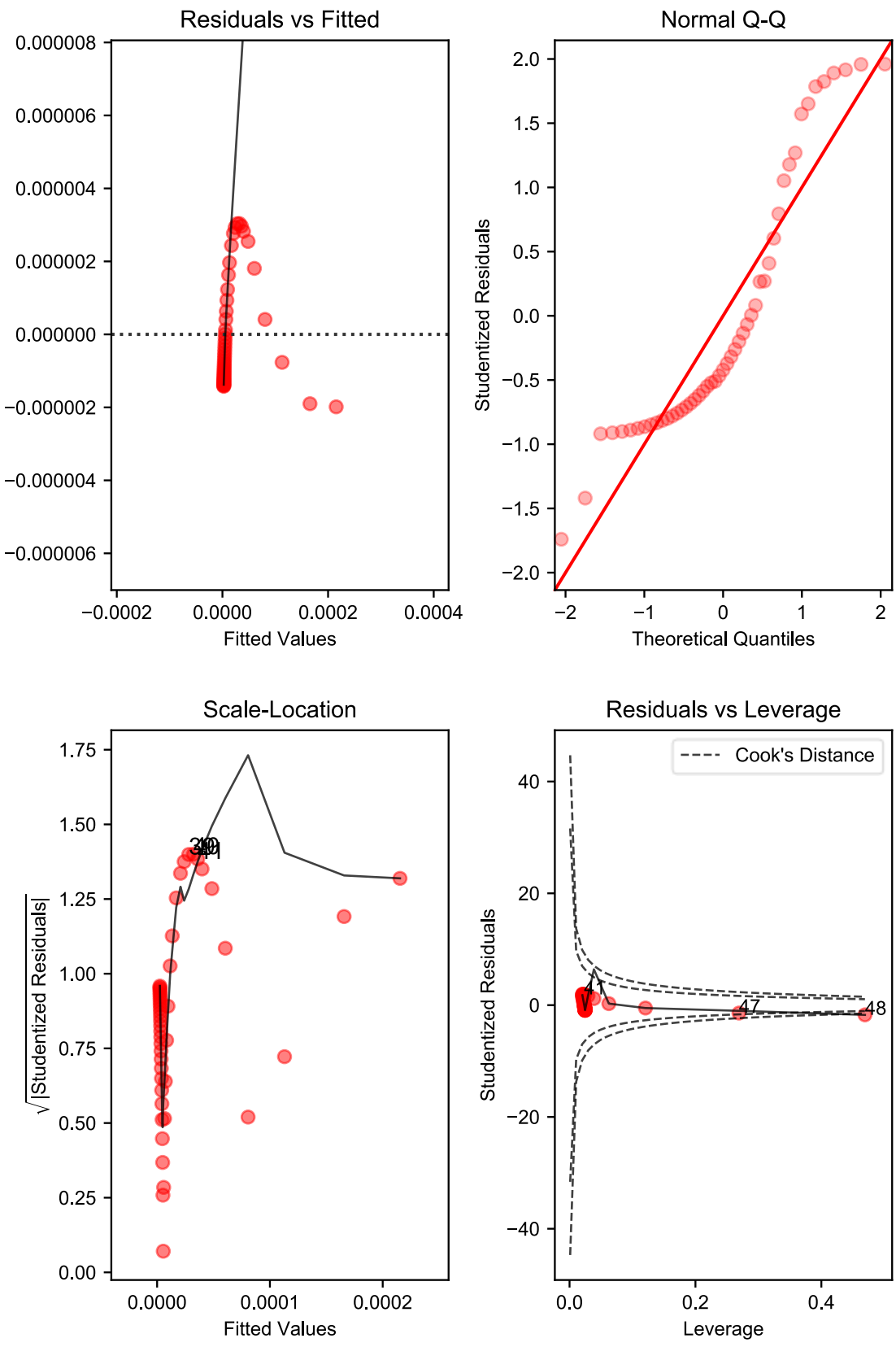

Figure S6 – VIII B | BETSI regression diagnostics for UiO-66

UiO-66-NH2

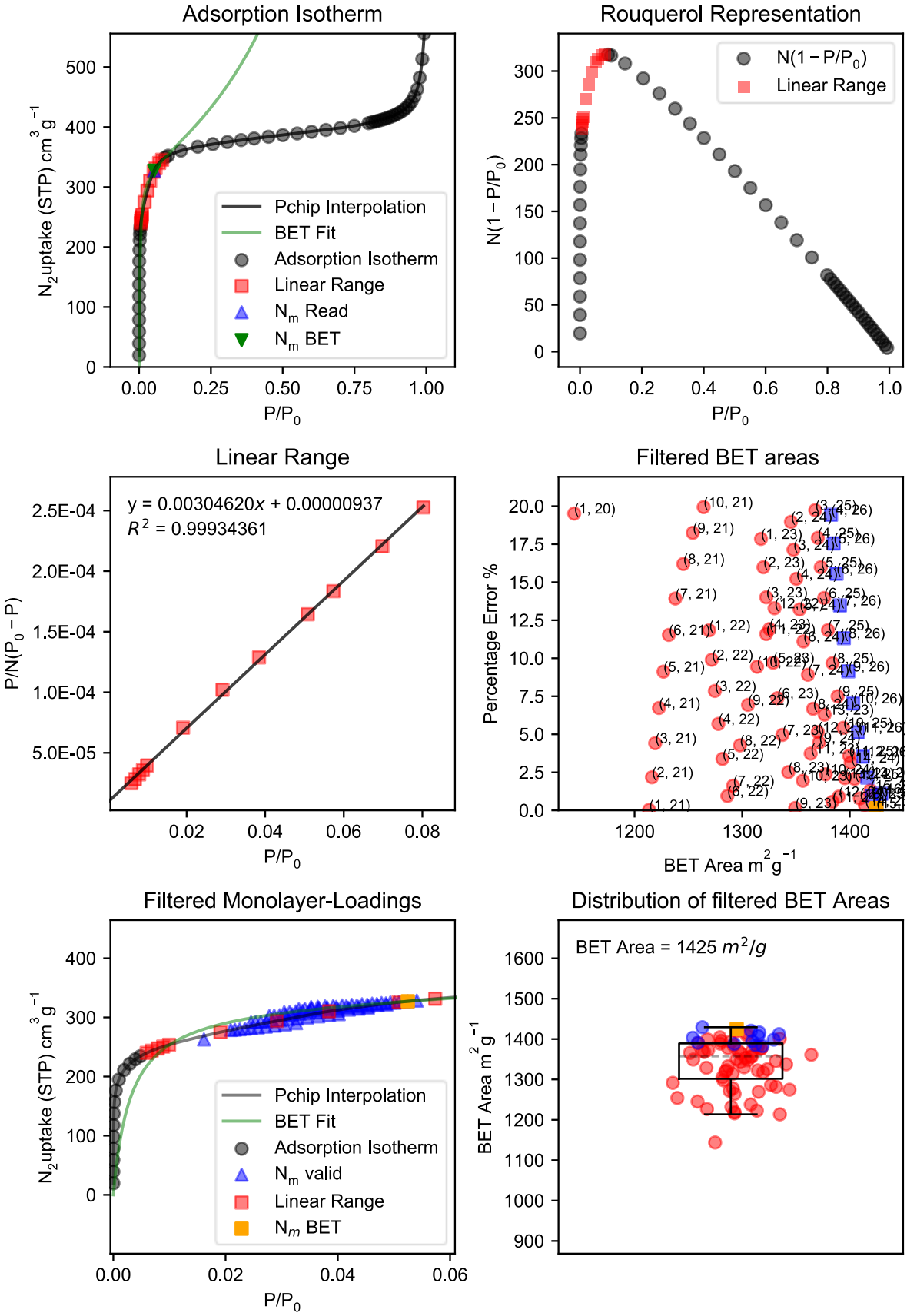

Figure S6 – IX A | BETSI analysis of UiO66-NH2

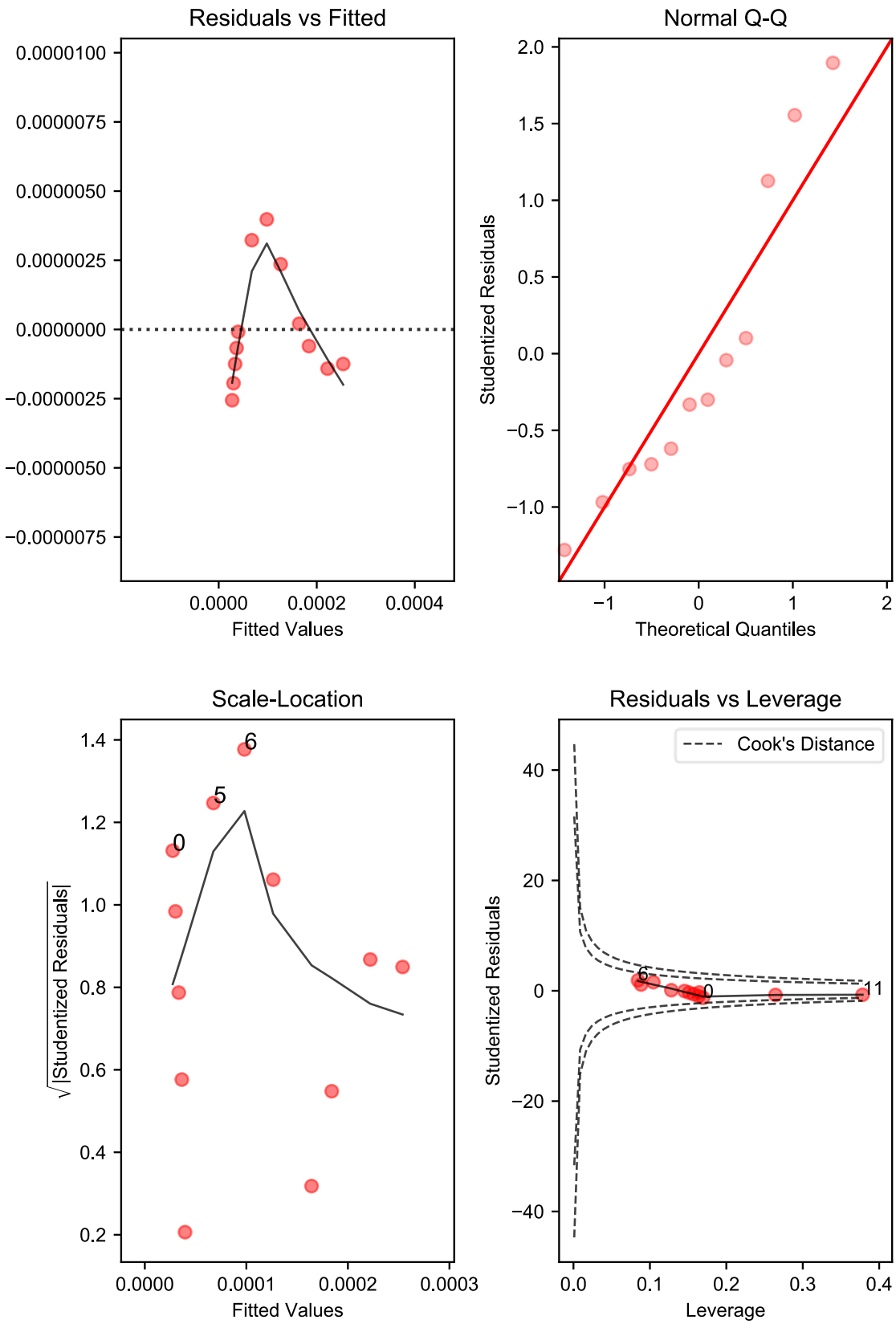

Figure S6 – IX B | BETSI regression diagnostics for UiO-66-NH2

NU-1000

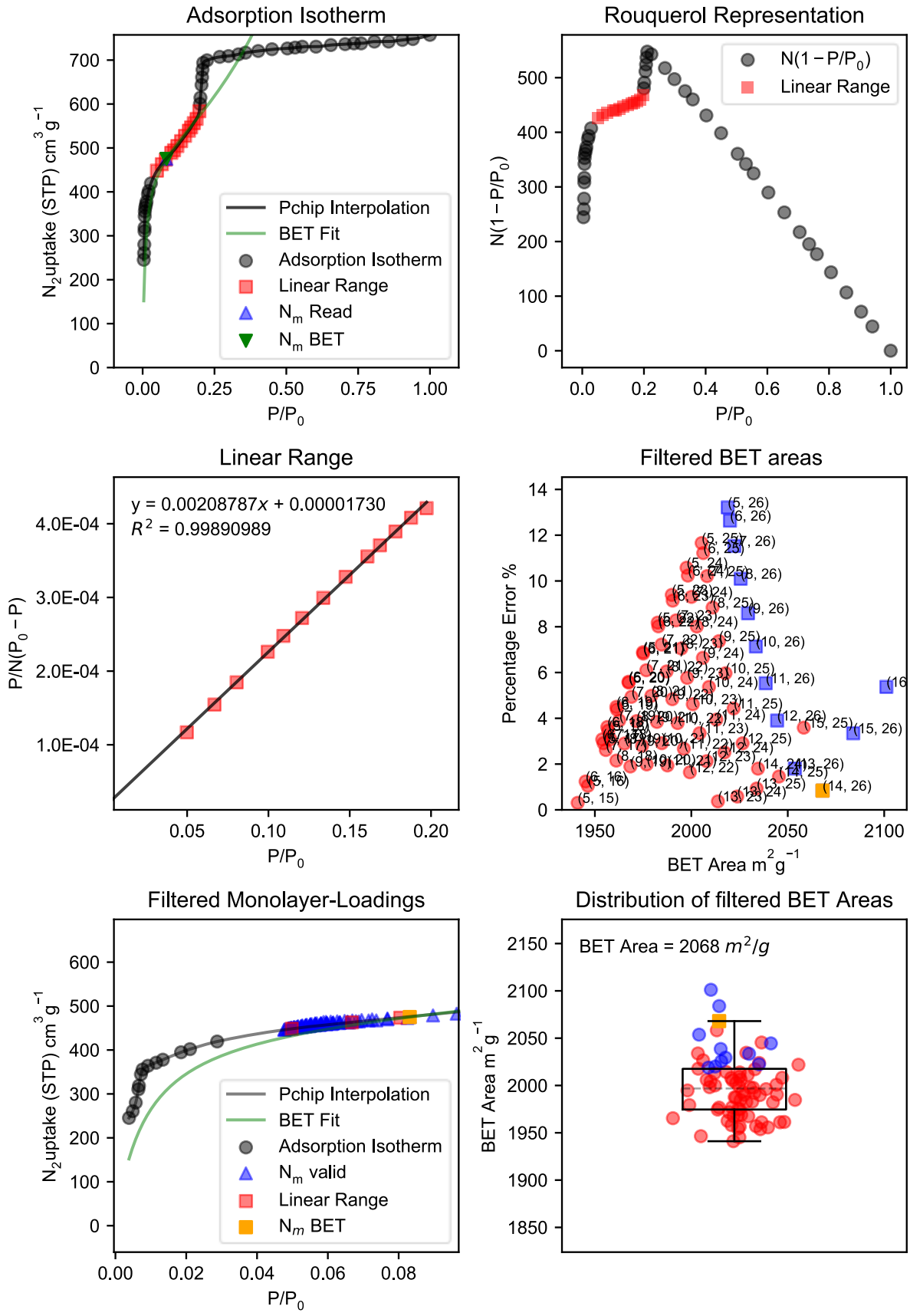

Figure S6 – X A | BETSI analysis of NU-1000

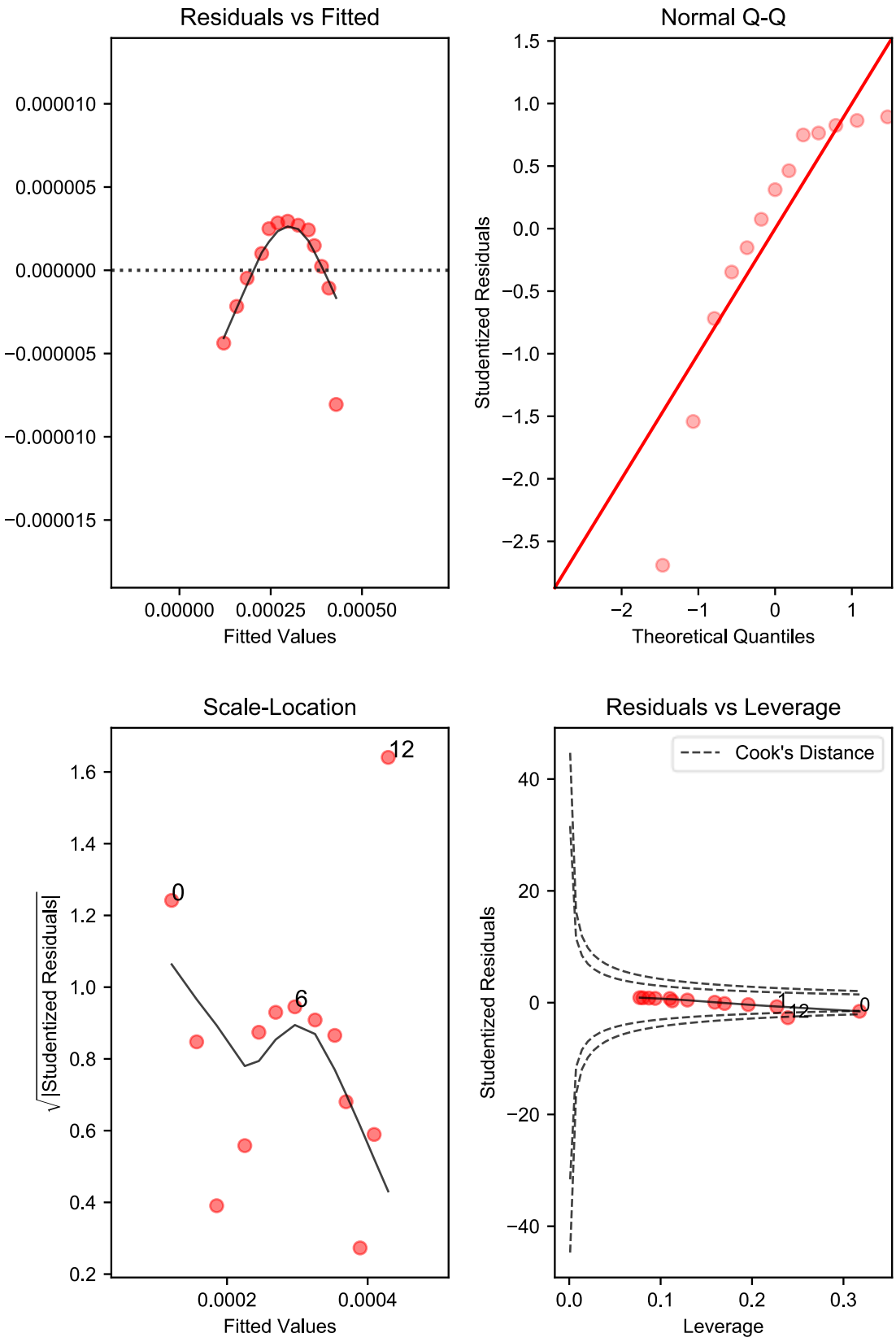

Figure S6 – X B | BETSI regression diagnostics for NU-1000

ZIF-8

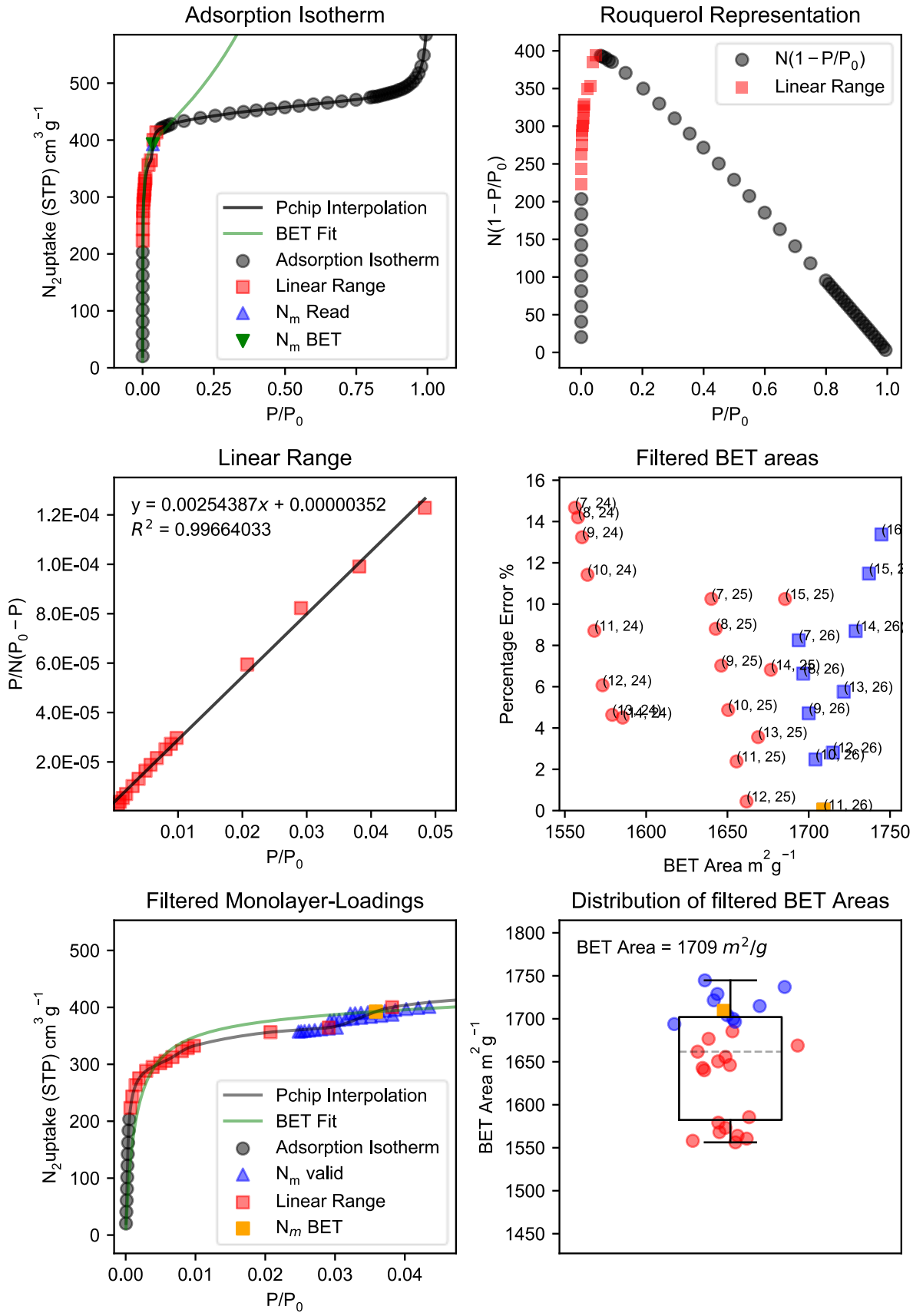

Figure S6 – XI A | BETSI analysis of ZIF-8

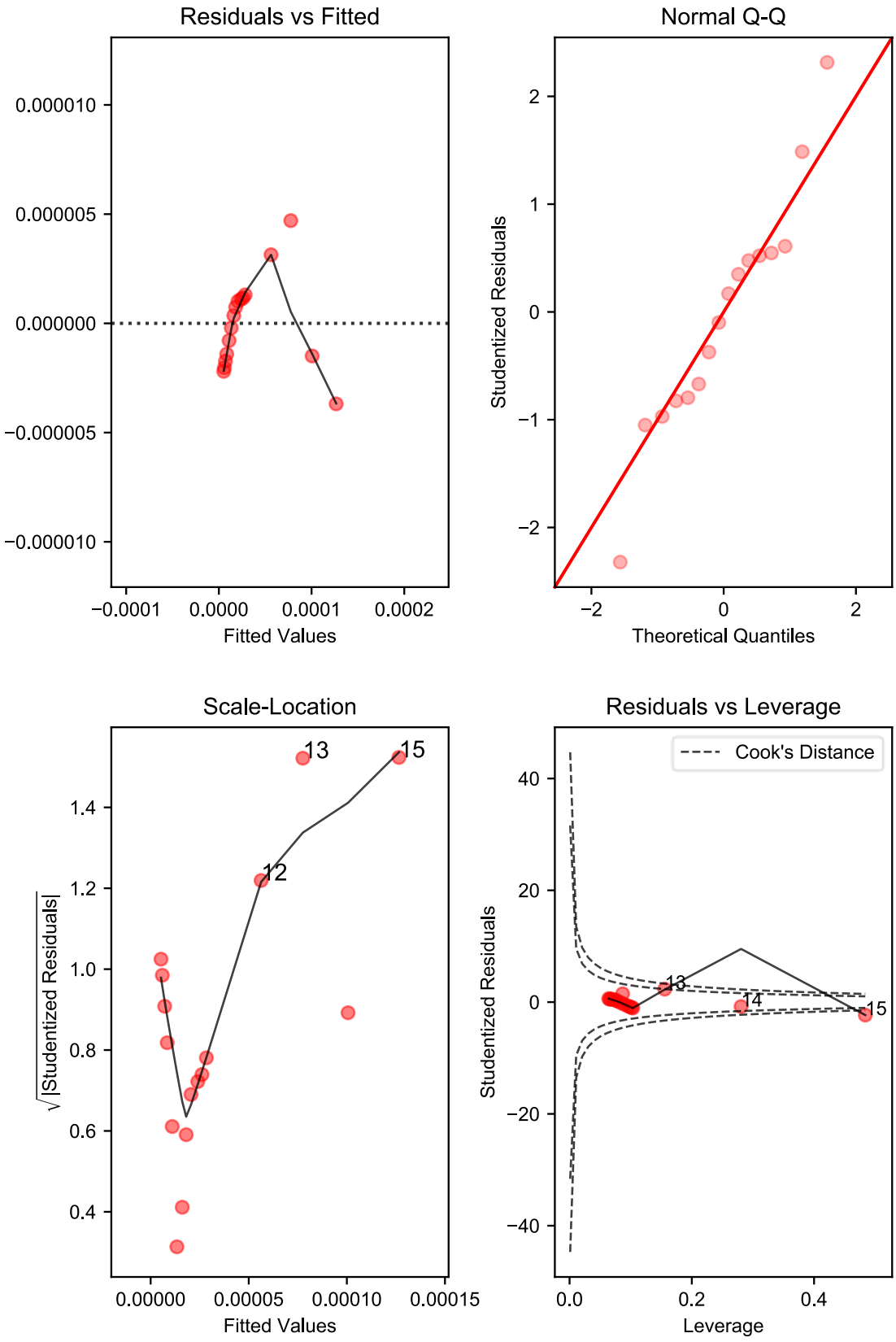

Figure S6 – XI B | BETSI regression diagnostics for ZIF-8

MIL-101

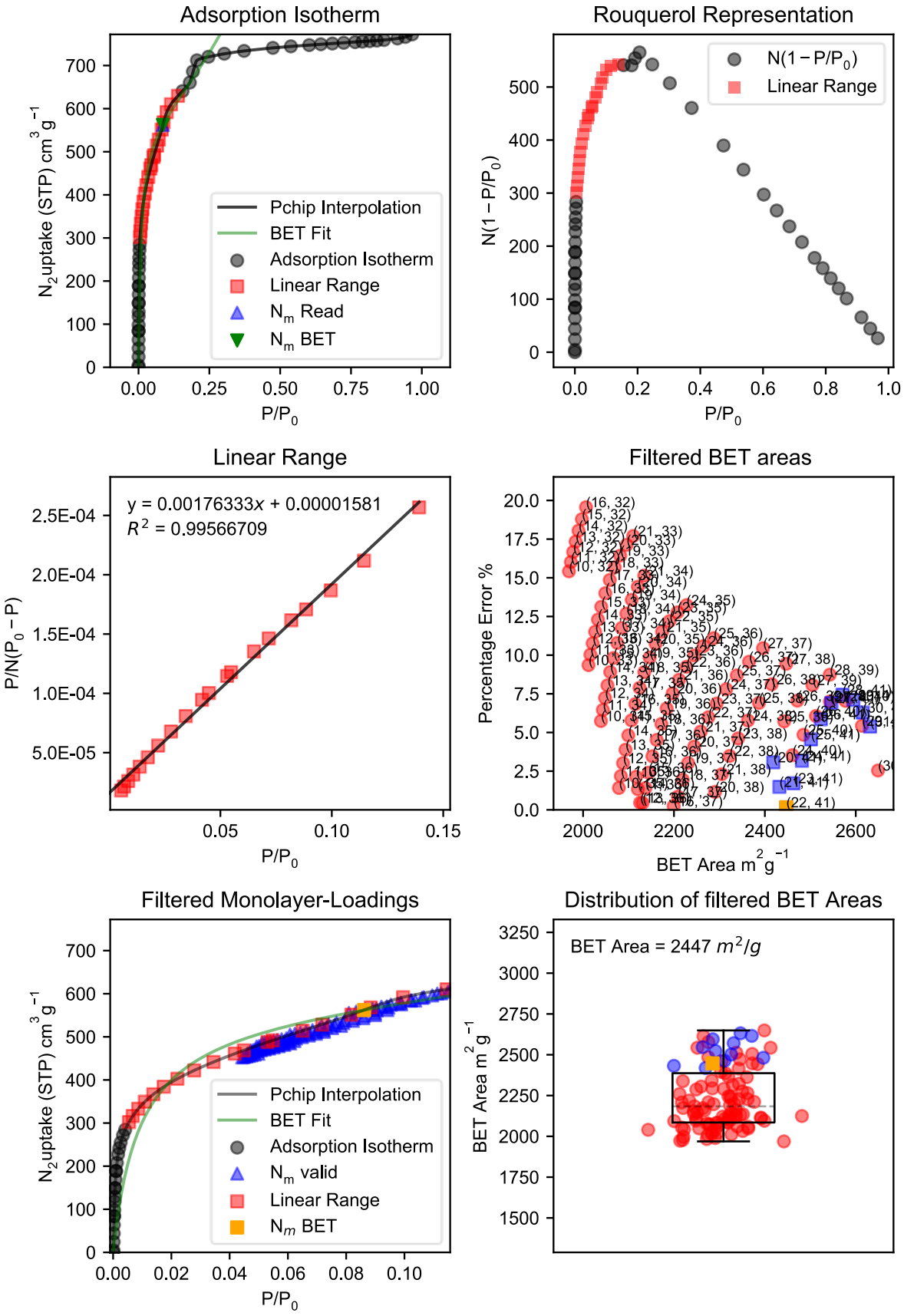

Figure S6 – XII A | BETSI analysis of MIL-101

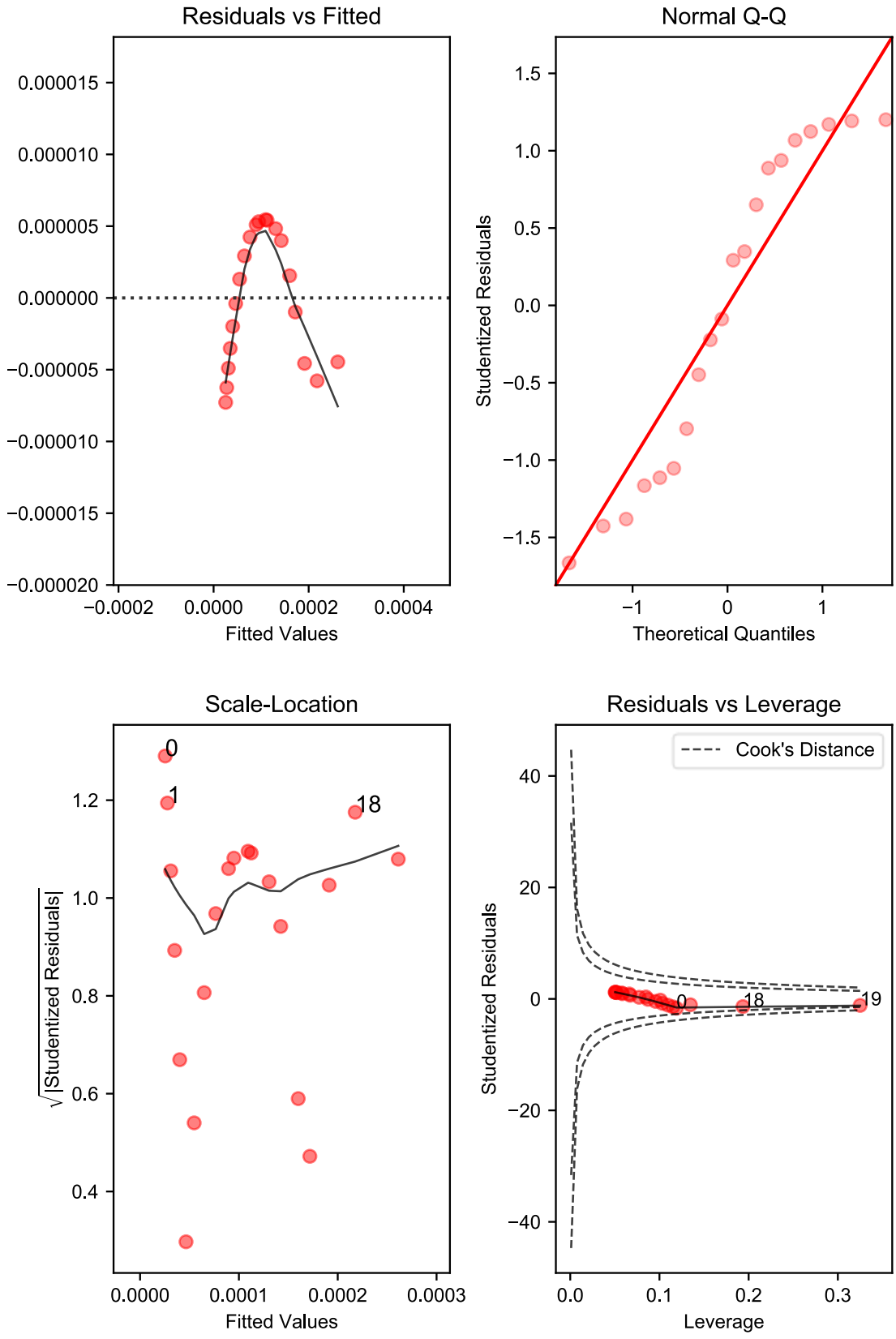

Figure S6 – XII B | BETSI regression diagnostics for MIL-101

TPB-DMTP-COF

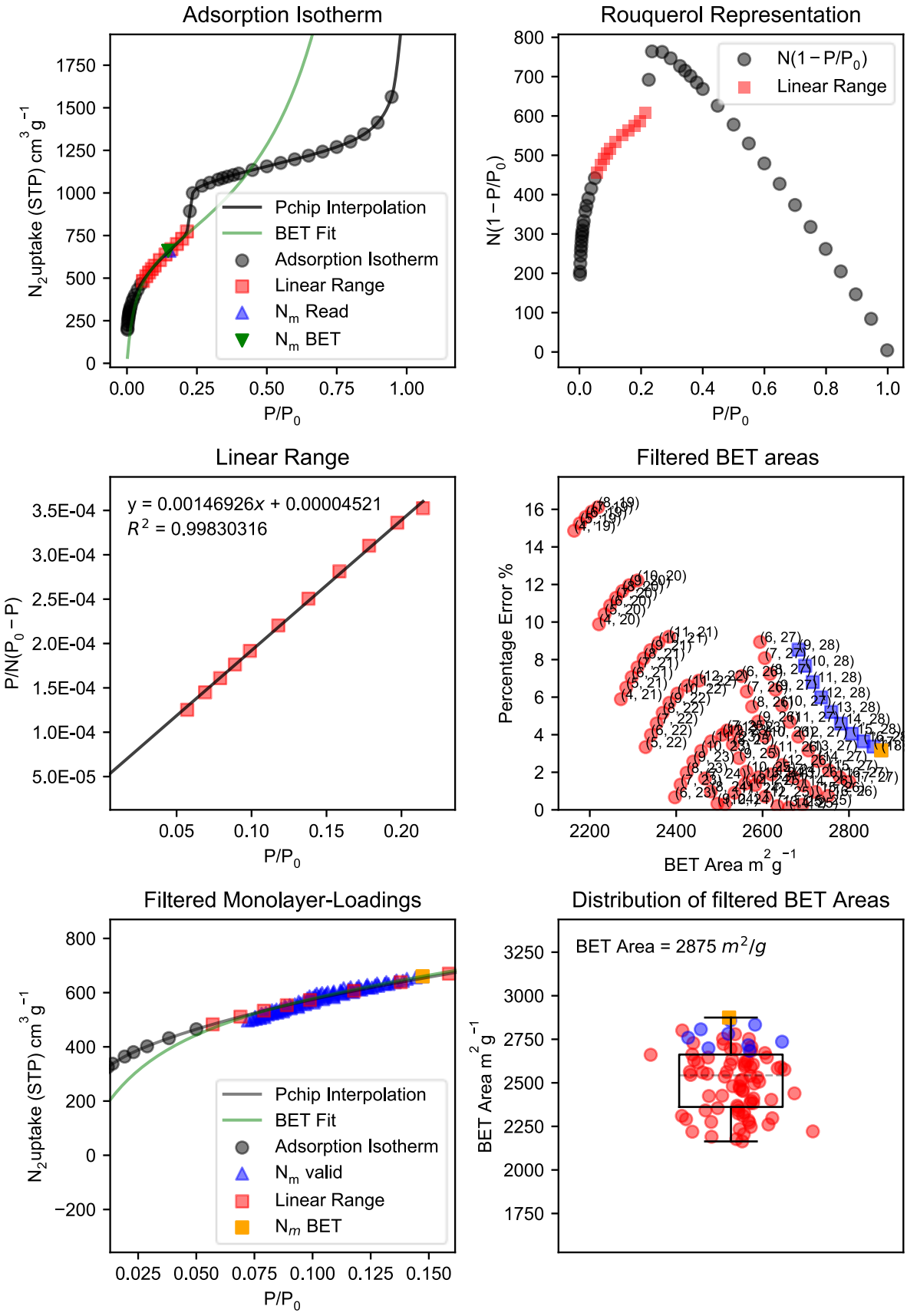

Figure S6 – XIII A | BETSI analysis of TPB-DMTP-COF

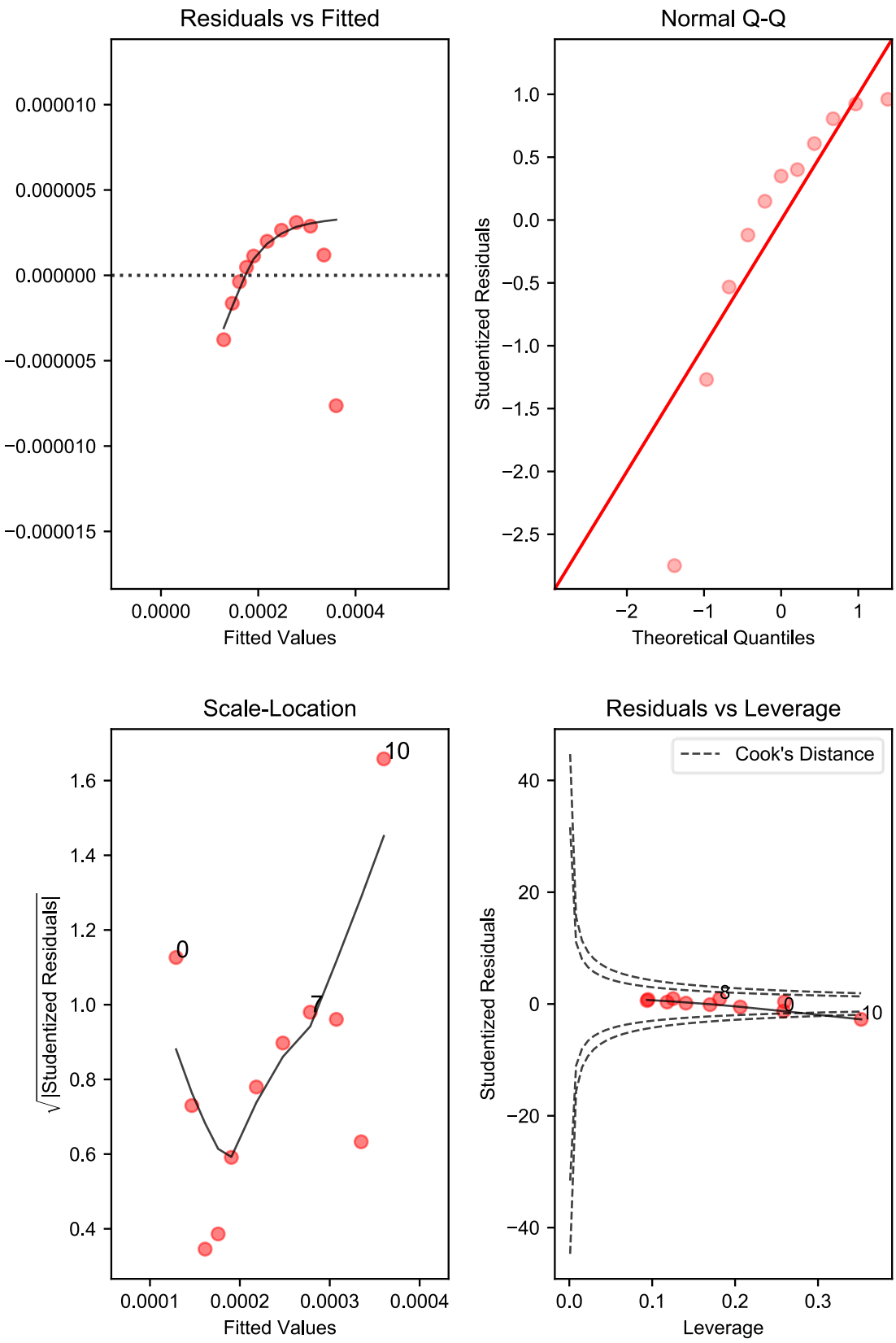

Figure S6 – XIII B | BETSI regression diagnostics for COF

MIL-100

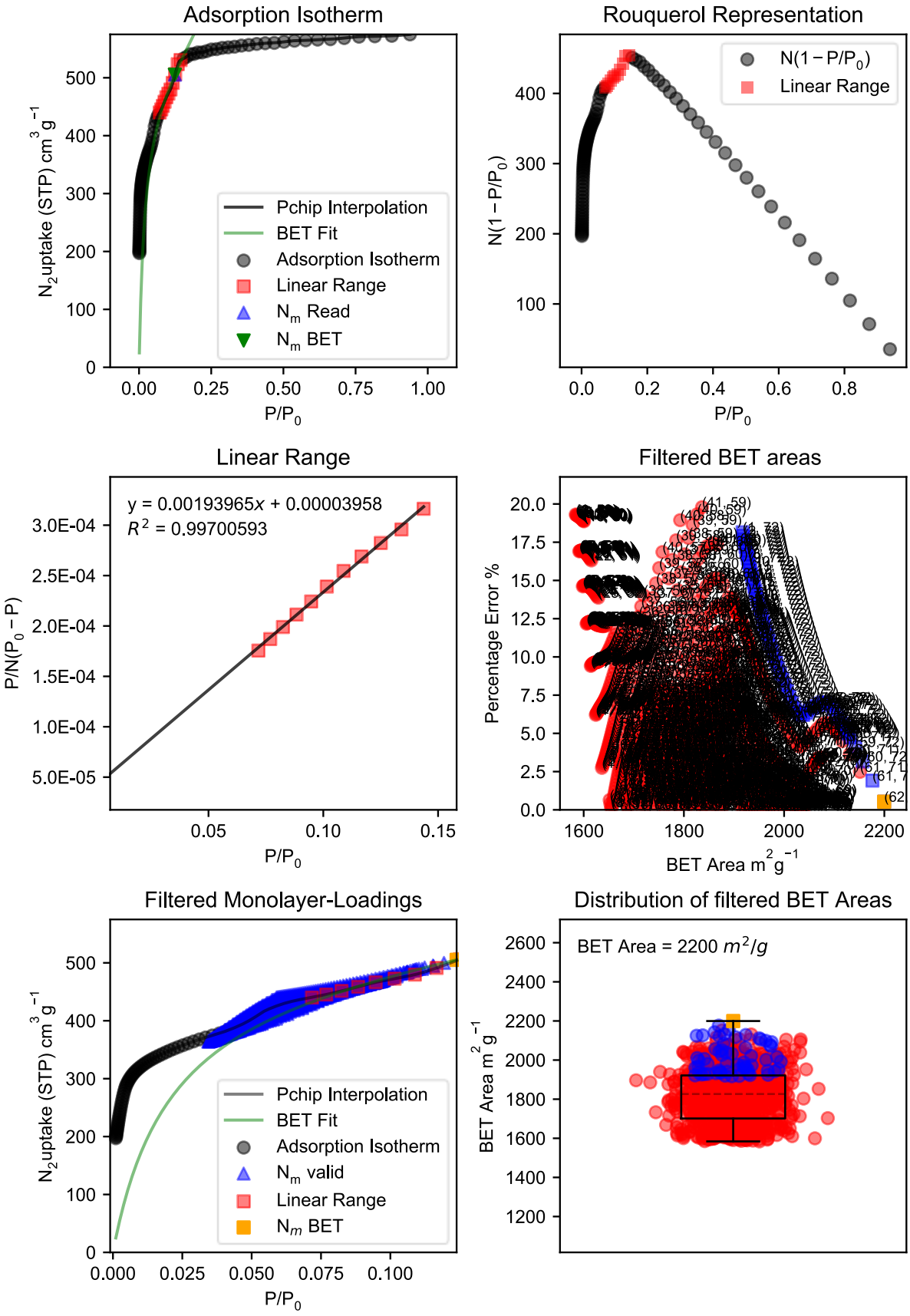

Figure S6 – XIV A | BETSI analysis of MIL-100

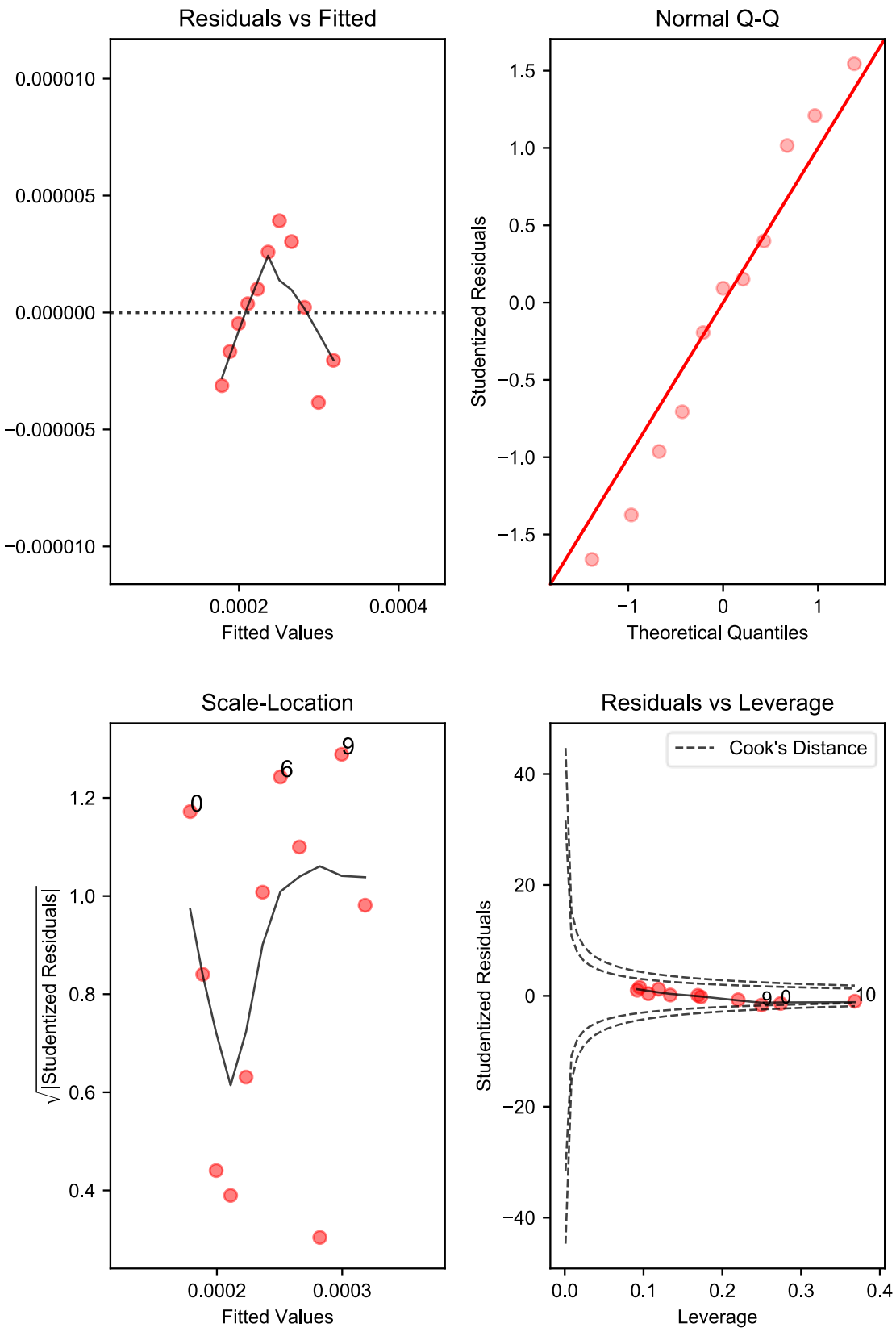

Figure S6 – XIV B | BETSI regression diagnostics for MIL-100

NU-1102

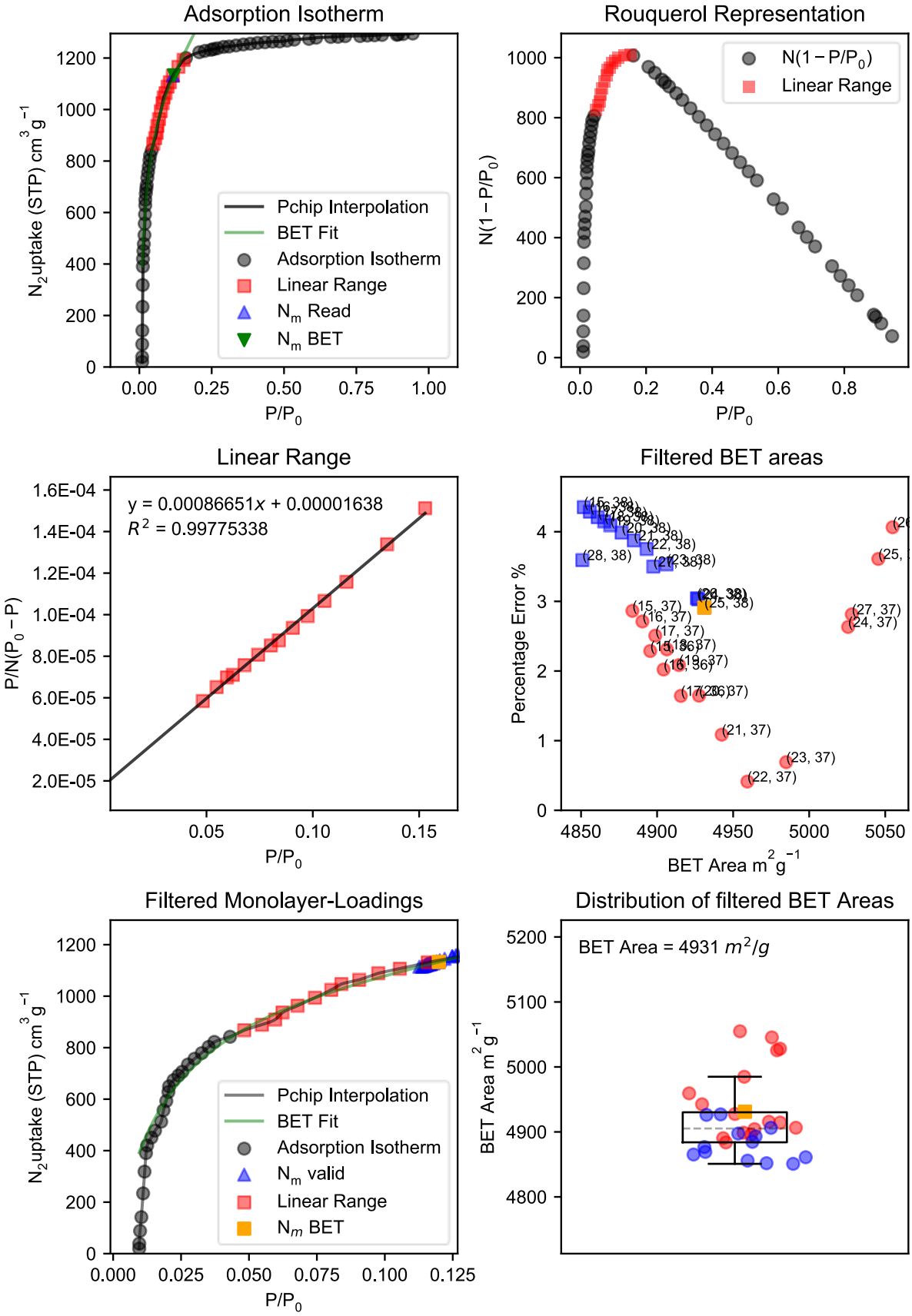

Figure S6 – XV A | BETSI analysis of NU-1102

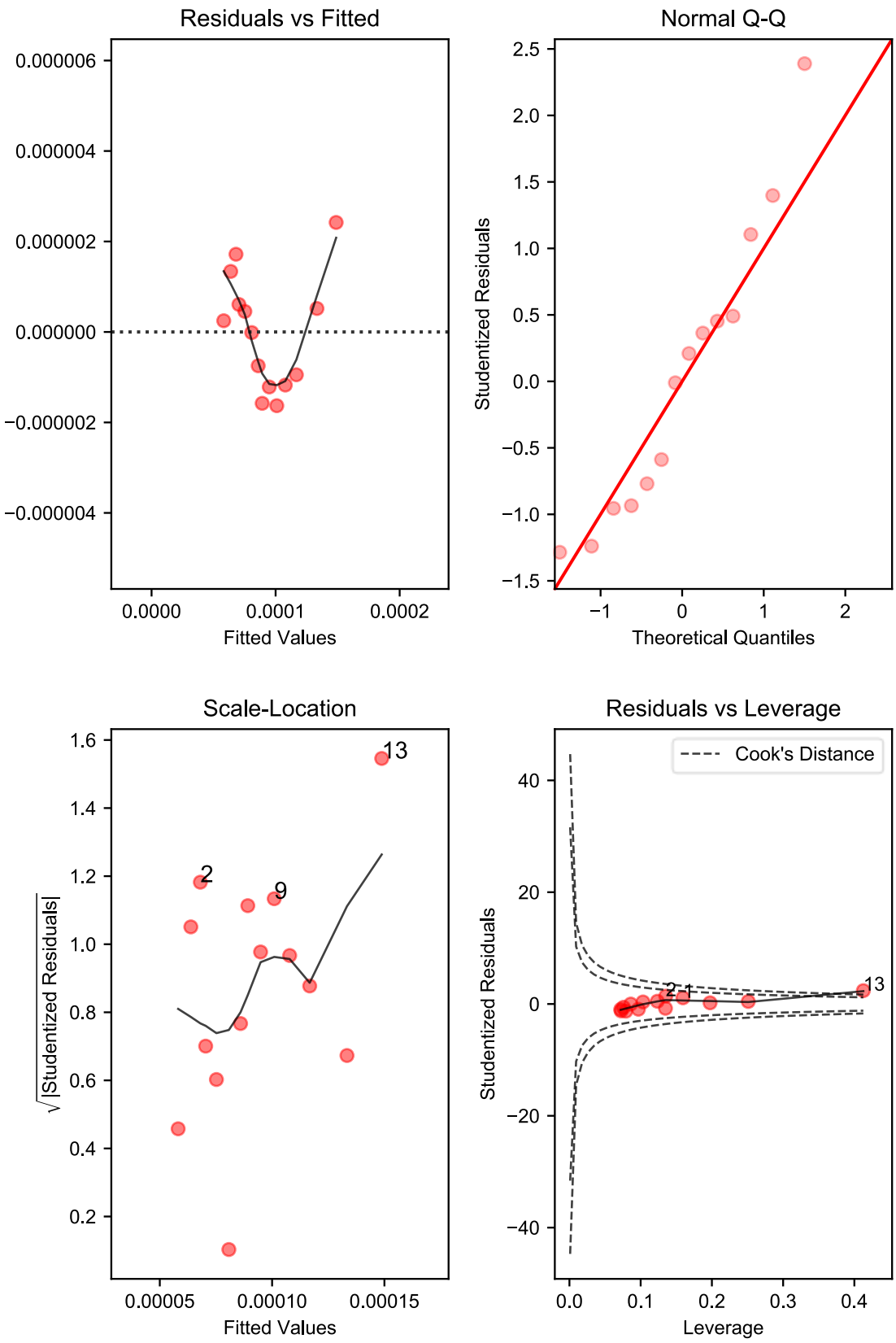

Figure S6 – XV B | BETSI regression diagnostics for NU-1102

NU-1104

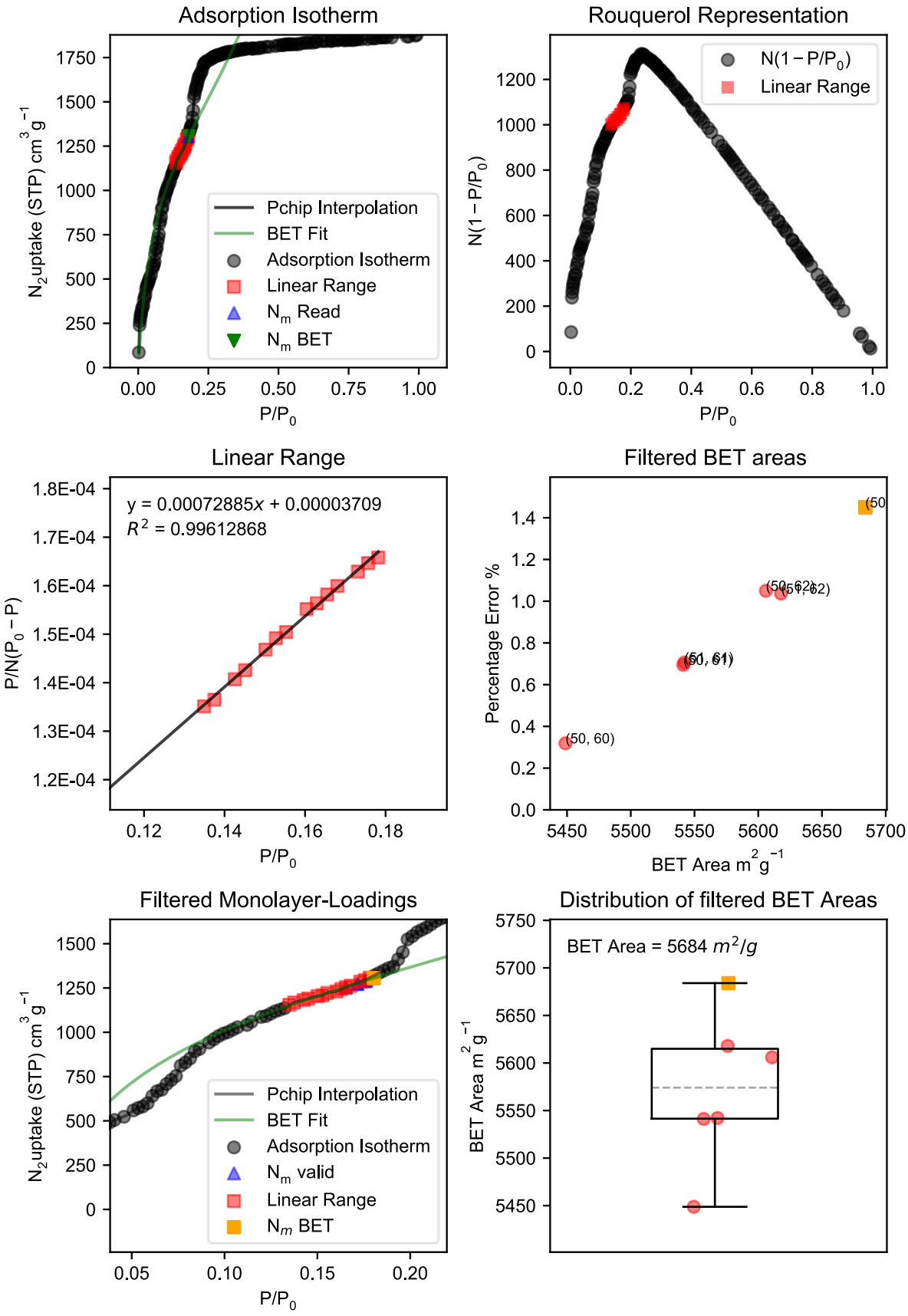

Figure S6 – XVI A | BETSI analysis of NU-1104

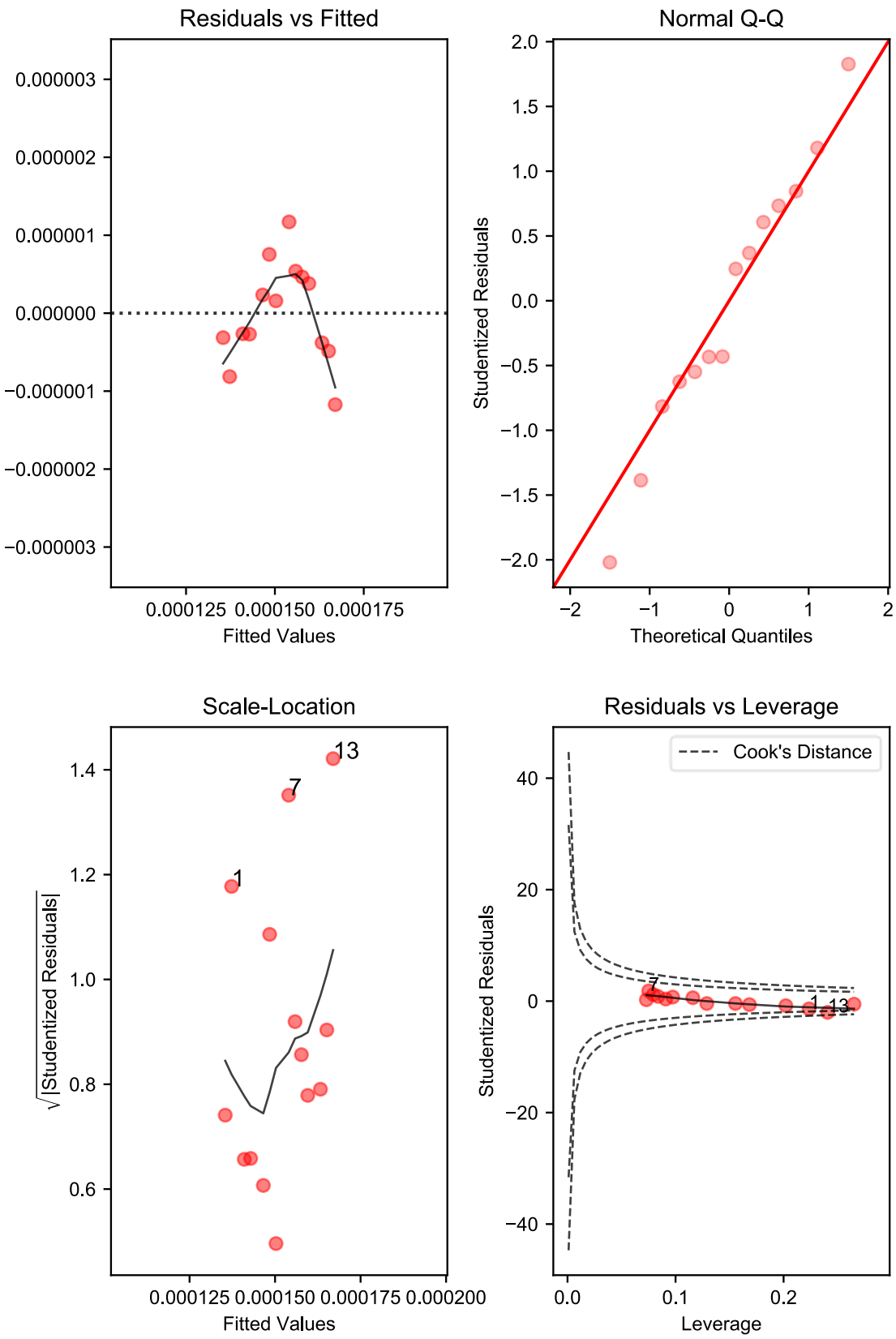

Figure S6 – XVI B | BETSI regression diagnostics for NU-1104

NU-1105

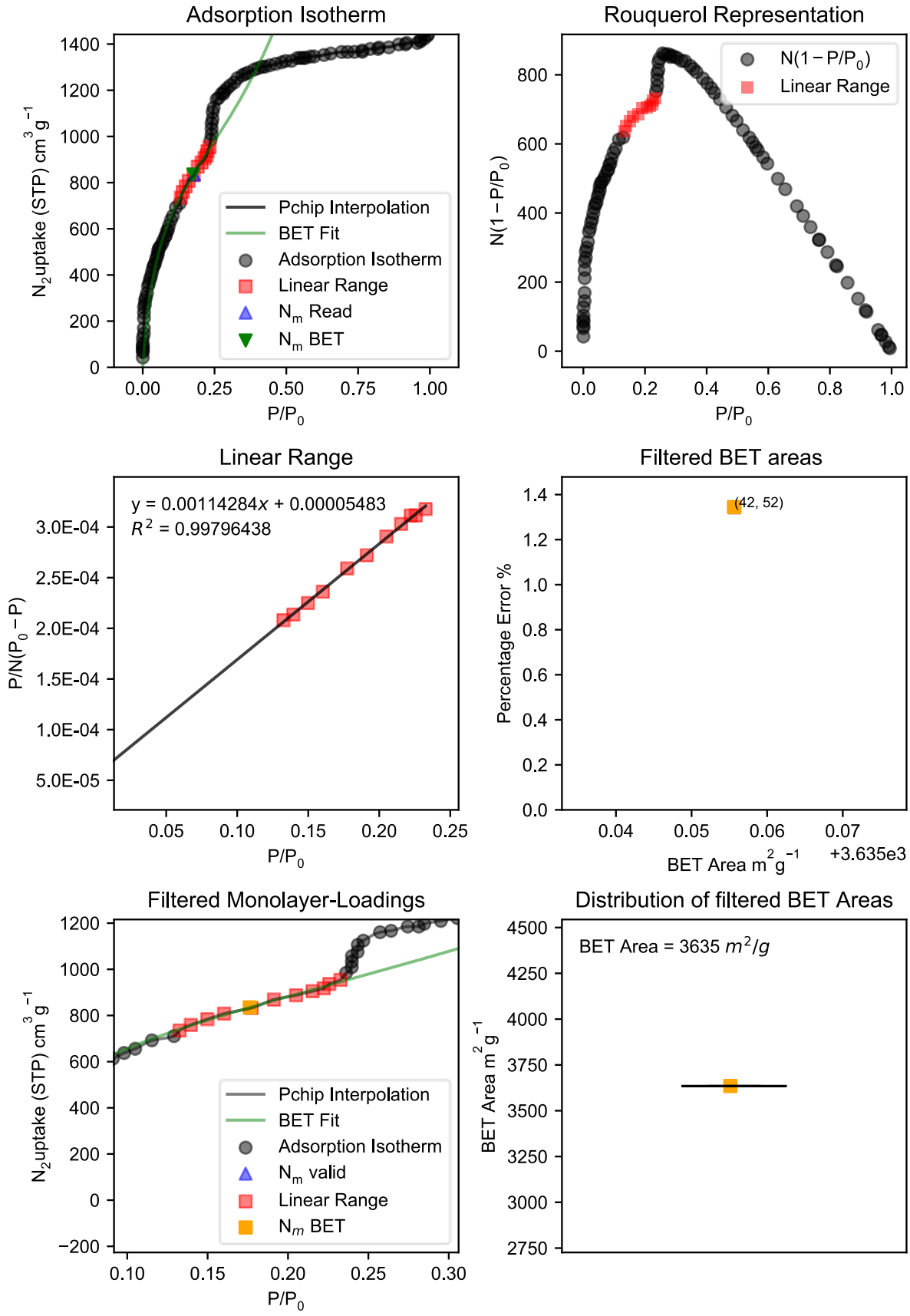

Figure S6 – XVII A | BETSI analysis of NU-1105

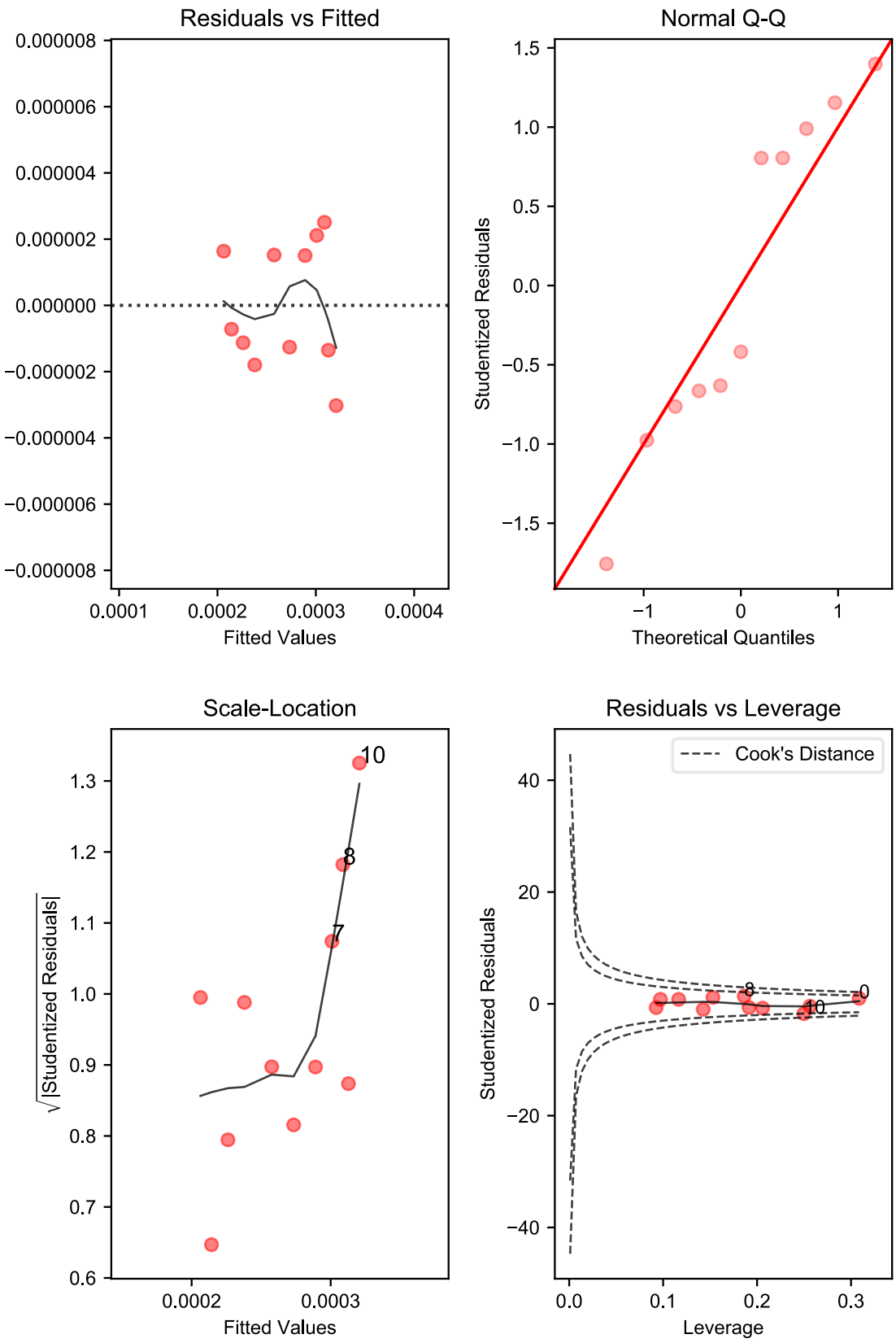

Figure S6 – XVII B | BETSI regression diagnostics for NU-1105

PCN-777

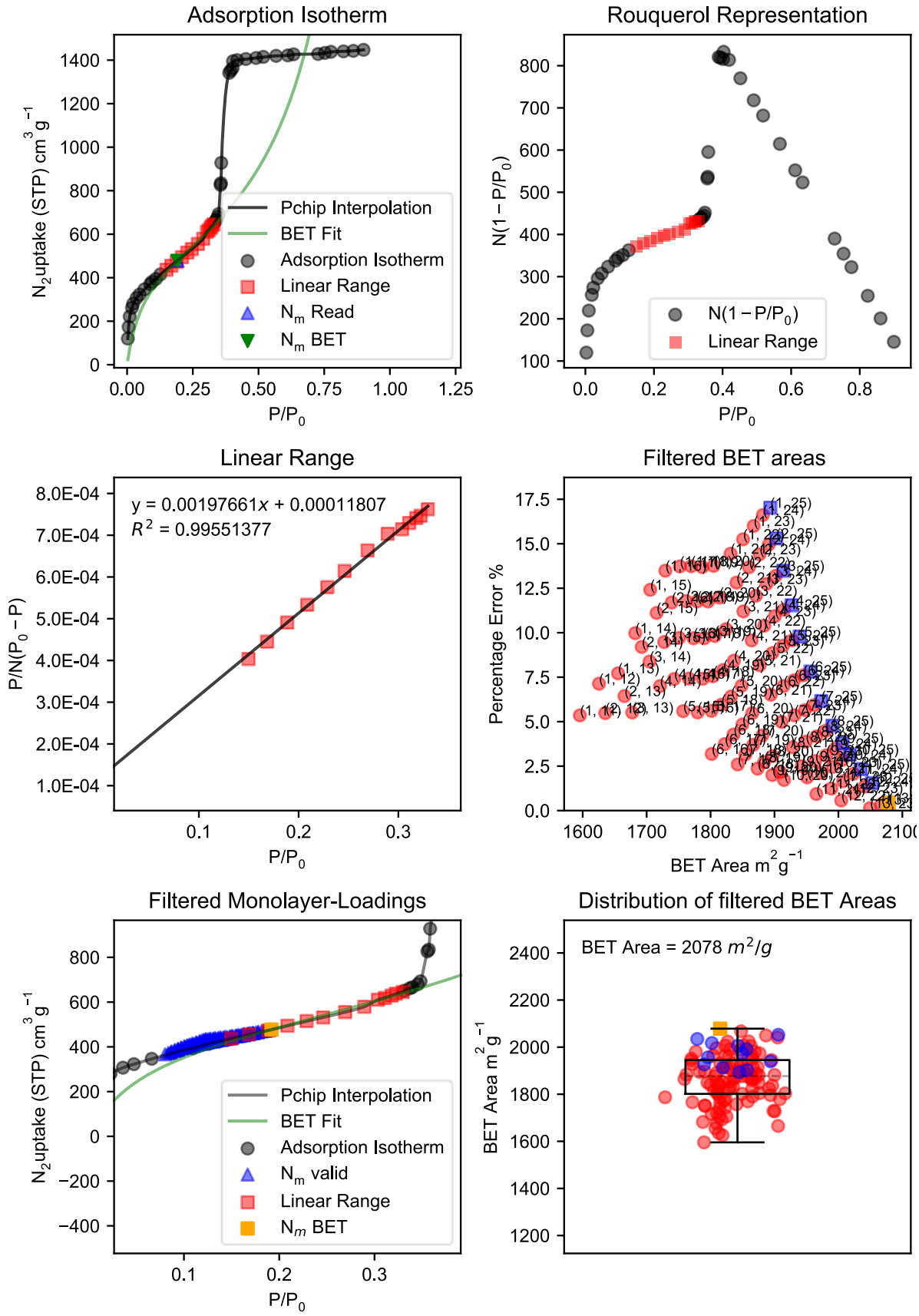

Figure S6 – XVIII A | BETSI analysis of PCN-777

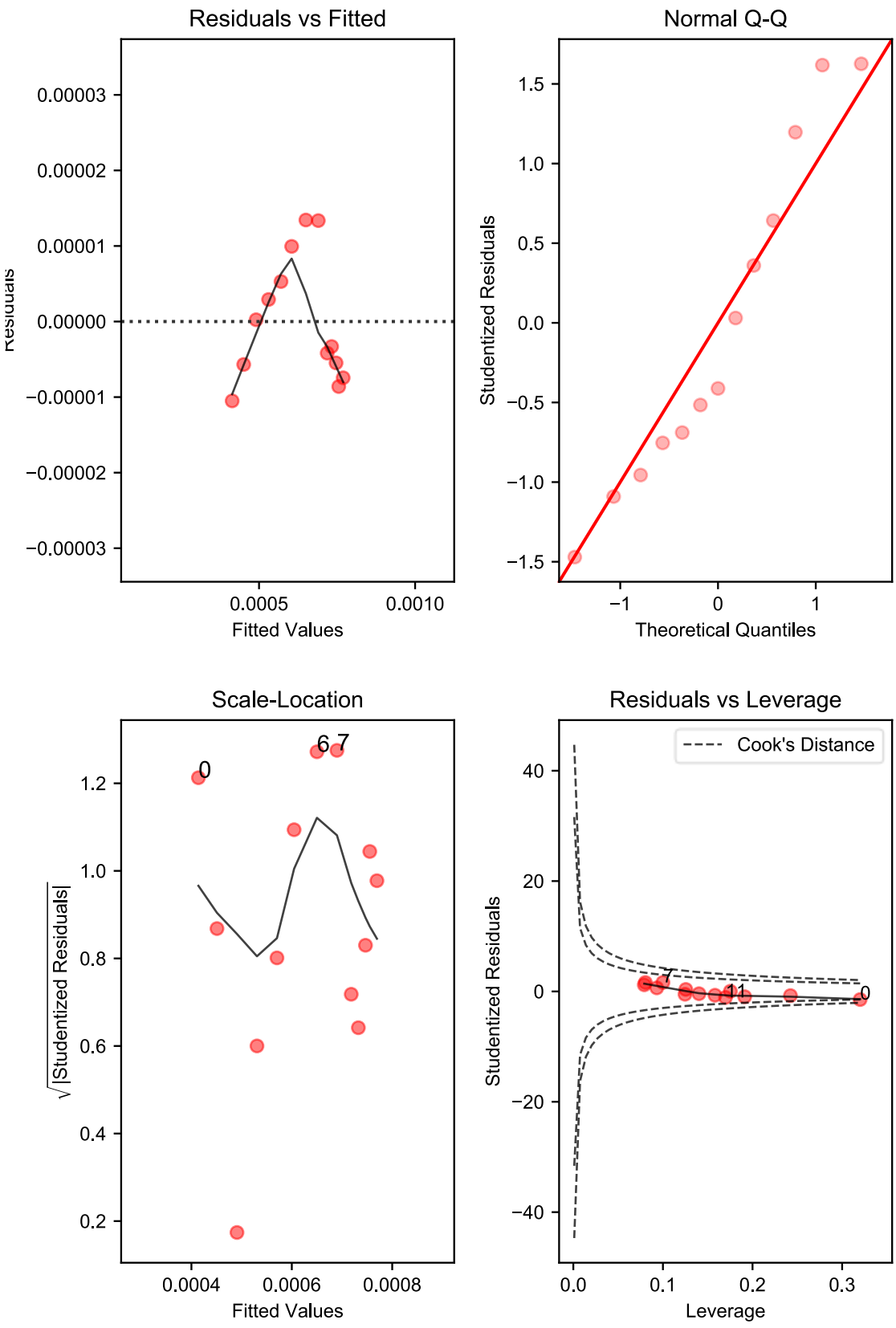

Figure S6 – XVIII B | BETSI regression diagnostics for PCN-777

Section S7 – Tabulated Results of BETSI analysis and round-robin evaluation

Material	BETSI $m^2 g^{-1}$	BETSI Range $m^2 g^{-1}$	BETSI Variation Coefficient %	Pass Rate %	Round-robin Average $m^2 g^{-1}$	Round-robin Range $m^2 g^{-1}$	Round-robin Variation Coefficient %	Hit Rate %
HKUST-1	1556	8	0.090	2.419	1521	583	7.393	52
Zeolite13X	833	4	0.140	0.538	814	356	7.345	34
Mg-MOF-74	1010	5	0.114	2.300	990	459	7.044	48
Al fumarate	1007	14	0.398	1.736	989	478	6.684	61
MCM-41	1001	60	1.573	3.329	994	1186	14.974	85
DMOF-1	1924	4	0.074	0.107	1861	795	8.437	15
MOF-5	3255	20	0.250	0.071	3173	1382	7.160	13
UiO-66	1145	91	1.901	0.870	1116	796	12.319	64
UiO-66-NH_2	1424	285	4.710	1.722	1383	750	9.263	48
NU-1000	2068	160	1.619	4.218	2015	1486	7.689	80
ZIF-8	1709	188	3.718	0.861	1668	2085	14.392	57
MIL-101	2446	680	8.353	3.738	2415	2404	15.479	77
TPB-DMTP-COF	2875	711	7.298	5.375	2787	5031	21.296	80
MIL-100	2199	616	7.611	12.111	1959	1554	13.059	78
NU-1102	4931	204	1.139	0.862	4772	2915	8.477	39
NU-1104	5684	235	1.327	0.024	5511	7584	31.580	5
NU-1105	3635	0	0.000	0.011	3581	3974	16.899	0
PCN-777	2079	483	5.624	6.960	1944	2168	15.715	87

Table 1 | Results of BETSI analysis and round-robin evaluation for the isotherms used in the study. *Material*, isotherm of material under investigation; *BETSI*, optimal BET area predicted by BETSI; *BETSI Range*, full spread of BET areas that pass under BETSI; *BETSI Variation Coefficient*, relative standard deviation of BET areas that pass under BETSI; *Pass Rate*, number of BET areas that pass under BETSI expressed as a fraction of all hypothetical fittings; *Round-robin Average*, mean of BET areas calculated in round-robin evaluation; *Round-robin Range*, full spread of BET areas determined in round-robin evaluation; *Round-robin Variation Coefficient*, relative standard deviation of BET areas calculated in round-robin evaluation; *Hit Rate*, fraction of BET areas calculated in the round-robin evaluation that lie within the BETSI range (Details **S14**).

Section S8 – Comparison of coefficients of variation of BET areas calculated in the round-robin evaluation and BETSI

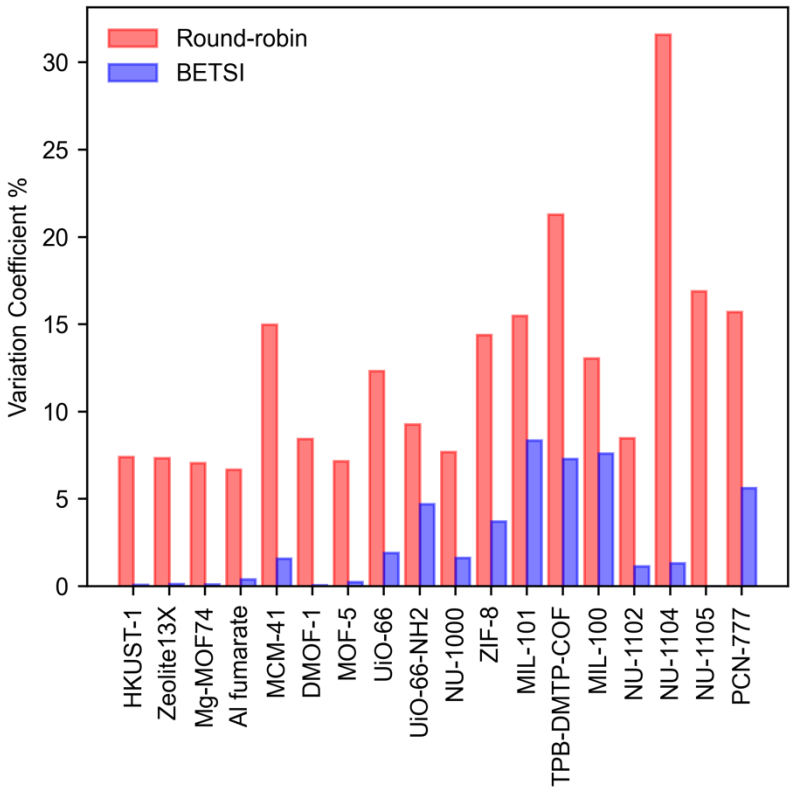

Figure S8 | Comparison of coefficients of variation of BET areas calculated in the round-robin evaluation and BETSI

Section S9 – Normalised BET areas calculated in round-robin evaluation

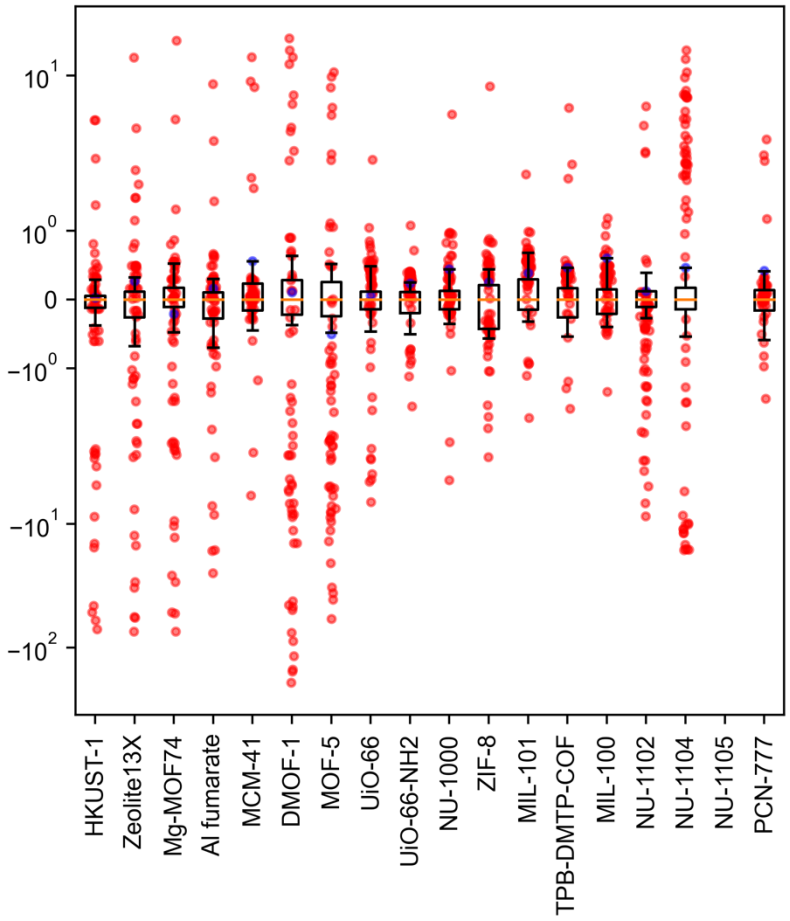

Figure S9 | BET areas calculated in round-robin evaluation normalised against the BETSI range. Normalisation done by dividing BET areas by the BETSI range and subtracting the median. Box represents the normalised BETSI interquartile range, and whiskers represent the normalised range. Note that for NU-1105 this analysis does not apply since only one BET area passes under BETSI, i.e. the BETSI range is zero. Blue dots are the BETSI optimal result.

Section S10 – Correlation between the BETSI Variation Coefficient and the Pressure Adjusted Pass rate

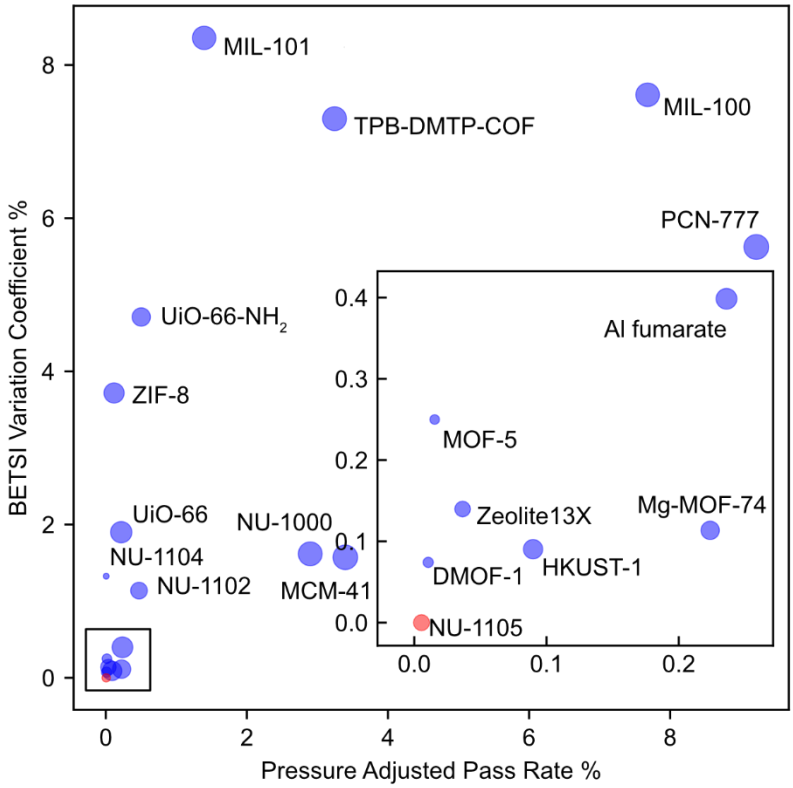

Figure S10 | Correlation between the BETSI Variation Coefficient, the relative standard deviation of BETSI results, and the Pressure Adjusted Pass Rate, the sum of pressure ranges that pass the Rouquerol criteria over all the hypothetical pressure intervals (Details **S14**). Bubble-size correlates with the Hit Rate, the fraction of manually calculated BET areas that lie within the BETSI range. Red symbols correspond to isotherms with a Hit Rate of zero.

Section S11 – A,B and C isotherm fittings

Whilst it is difficult to generalise about the shape of type A, B, and C isotherms, we nevertheless present here some discussion about common shape features of the isotherms. Type A isotherms – Al-fumarate, NU-1000, Zeolite-13X, MCM-41, HKUST-1, Mg-MOF-74 – do not have strongly pronounced knees and some have mesoporous steps indicating gas condensation in mesoporous cavities. In contrast, type B isotherms – MOF-5, DMOF-1 – often have sharp isotherm knees following strong adsorptive interactions at low relative pressures. Additionally, type B isotherms – NU-1105, and NU-1104 – are highly porous and have complex adsorption isotherms at low pressure. Finally, Type C isotherms – MIL-101, MIL-100, TPB-DMTP-COF, and PCN-777 – have, like type A, rounded isotherm knees, which appear at higher relative pressures.

Section S12 – Isotherms used in round-robin evaluation and BETSI case study

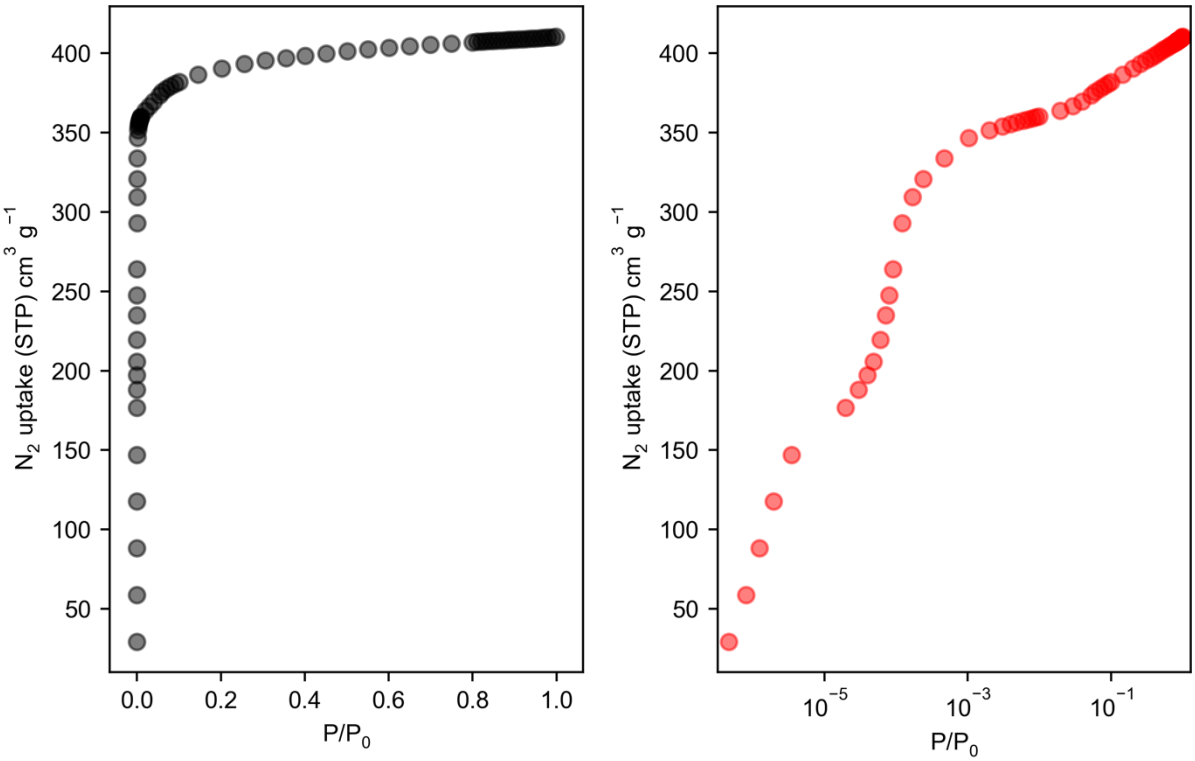

Figure S12 – I | HKUST-1 isotherm in linear representation (black) and semilog (red)

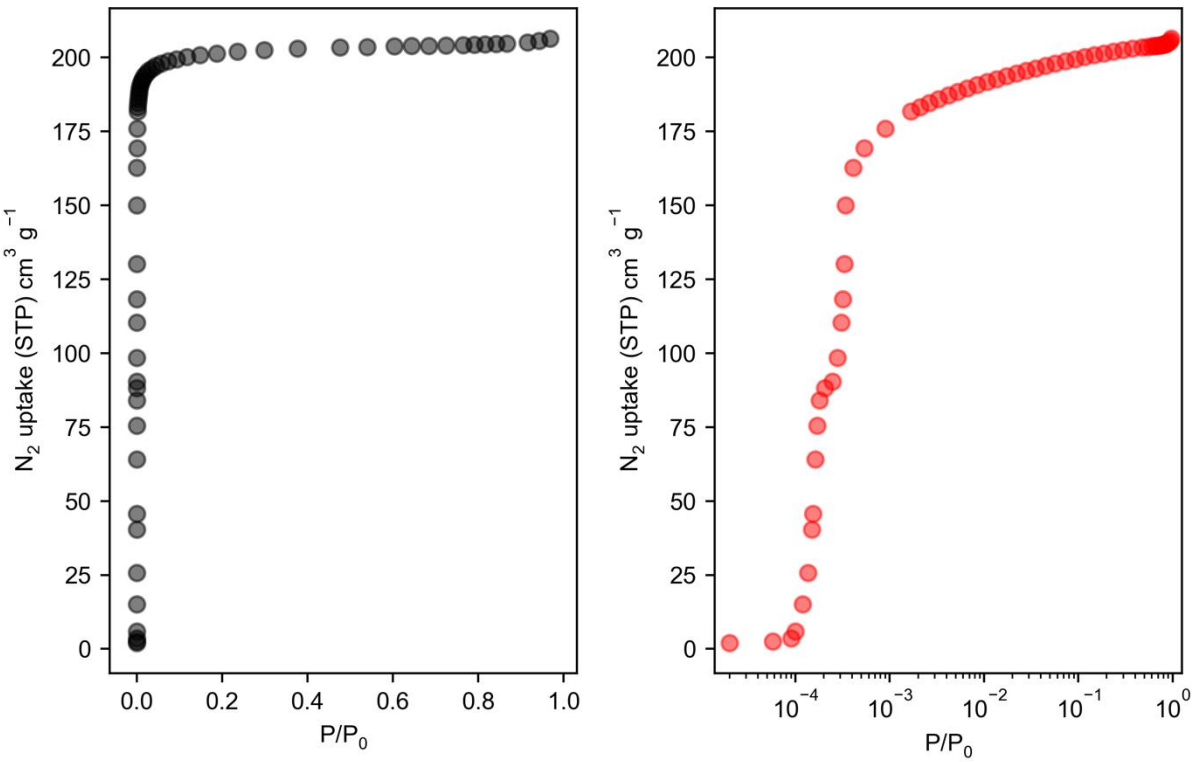

Figure S12 – II | Zeolite-13X isotherm in linear representation (black) and semilog (red)

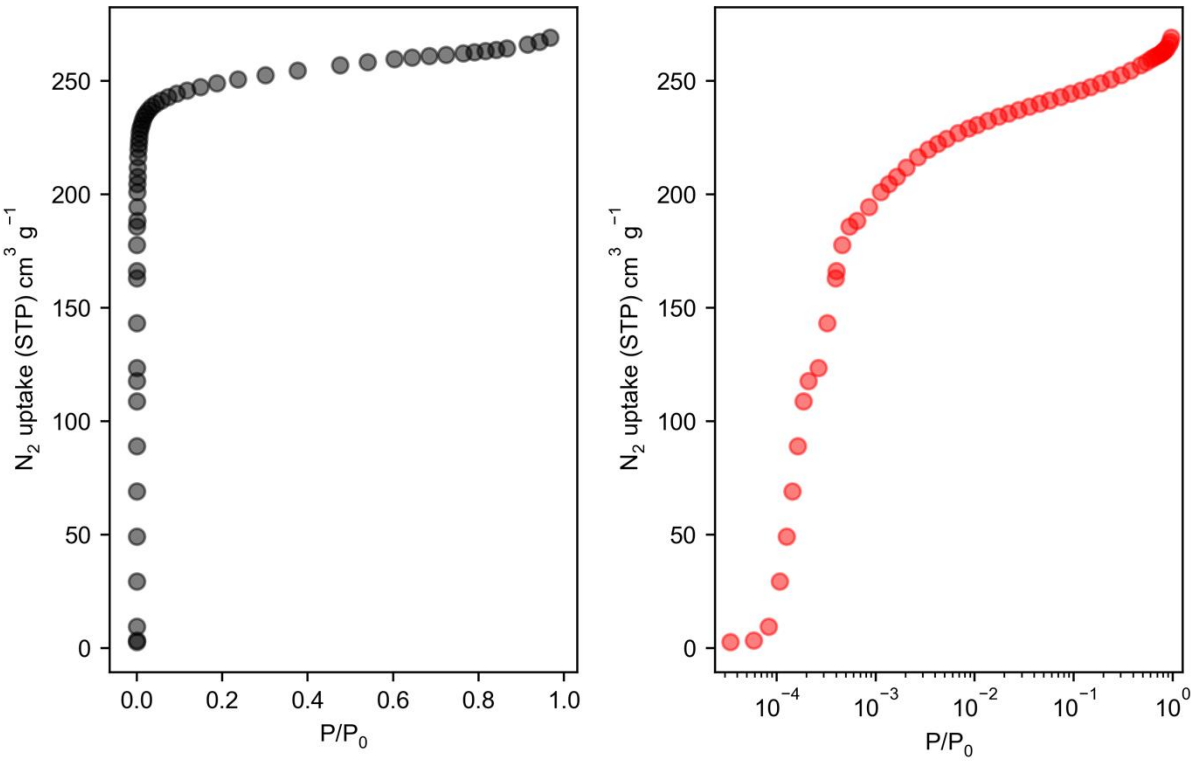

Figure S12 – III | Mg-MOF-74 isotherm in linear representation (black) and semilog (red)

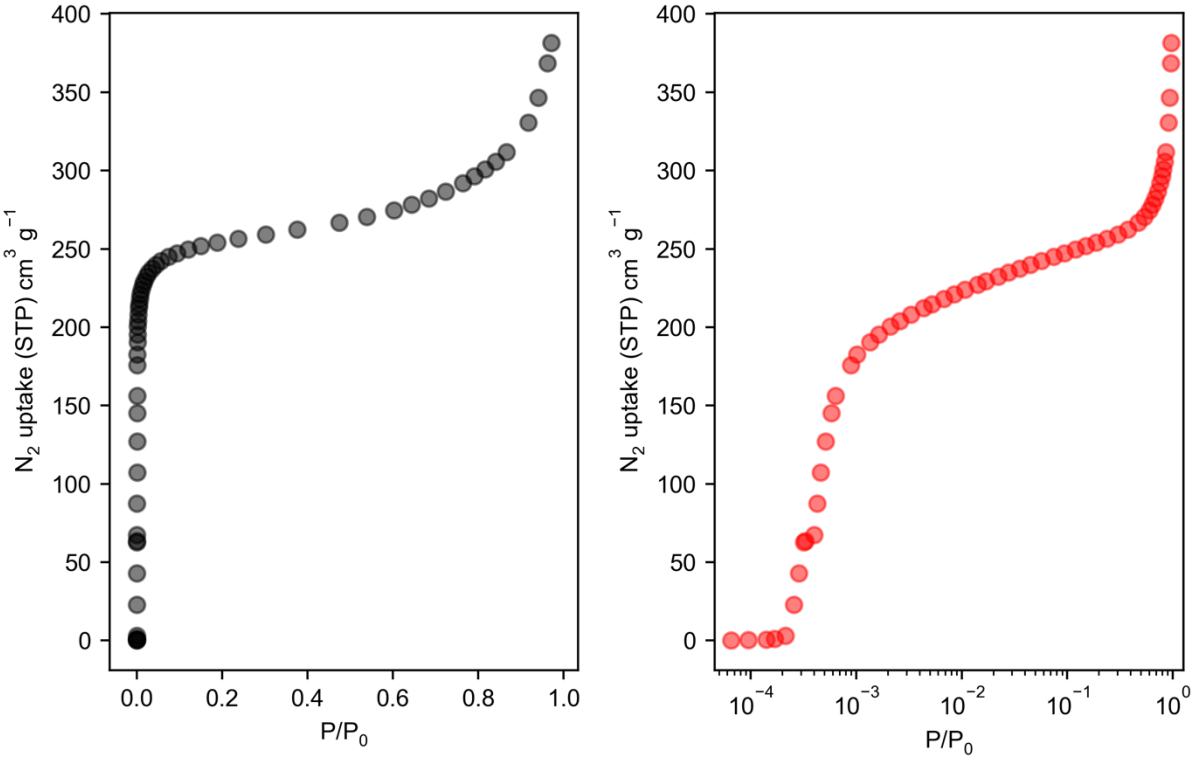

Figure S12 – IV | Al fumarate isotherm in linear representation (black) and semilog (red)

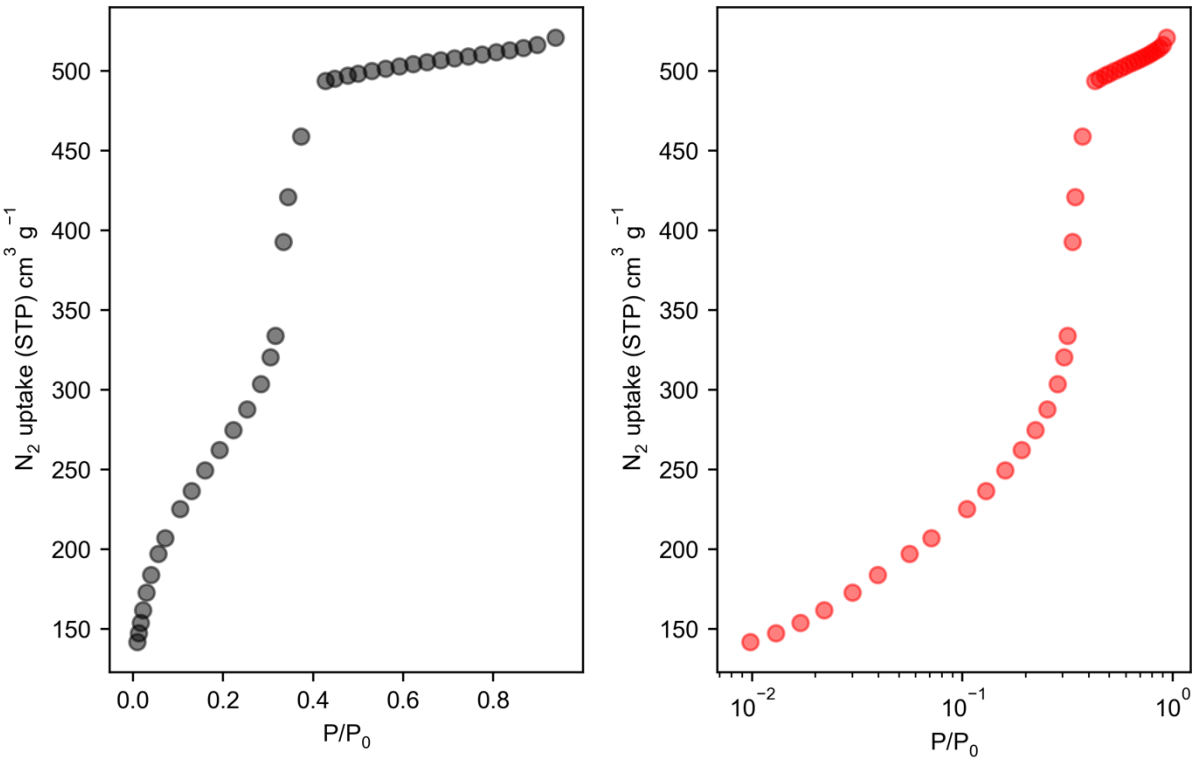

Figure S12 – V | MCM-41 isotherm in linear representation (black) and semilog (red)

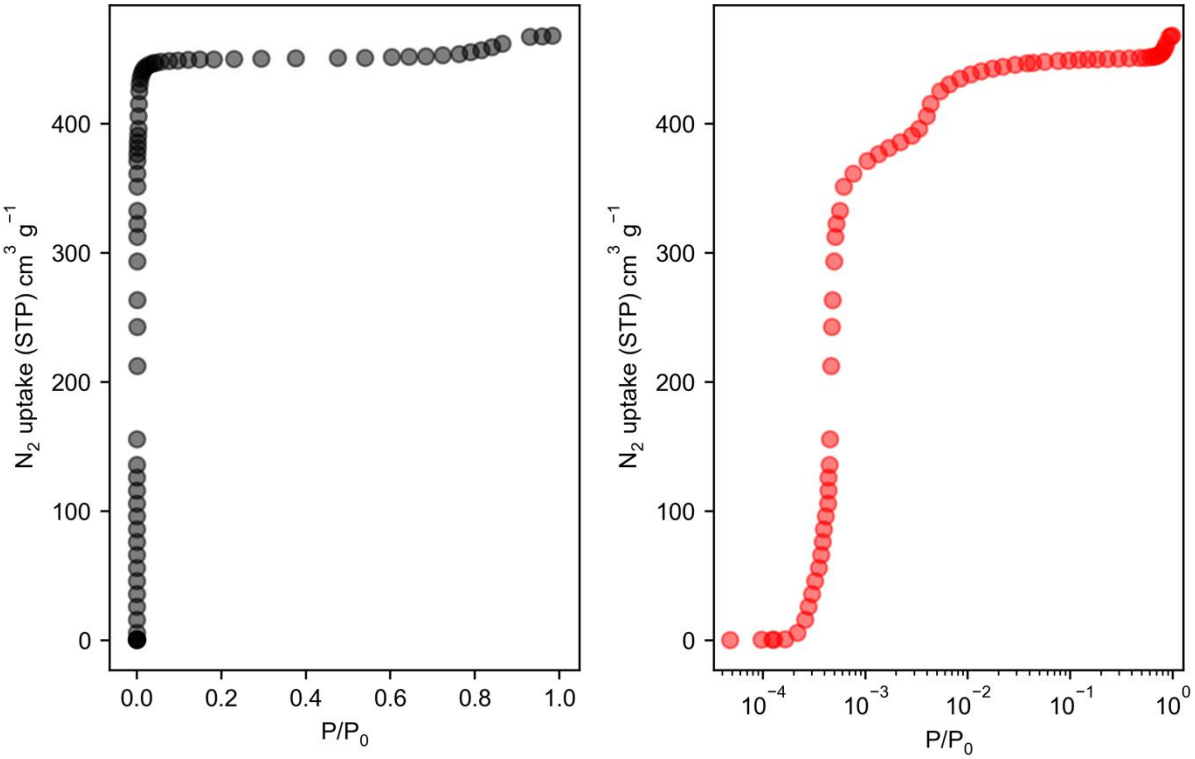

Figure S12 – VI | DMOF-1 isotherm in linear representation (black) and semilog (red)

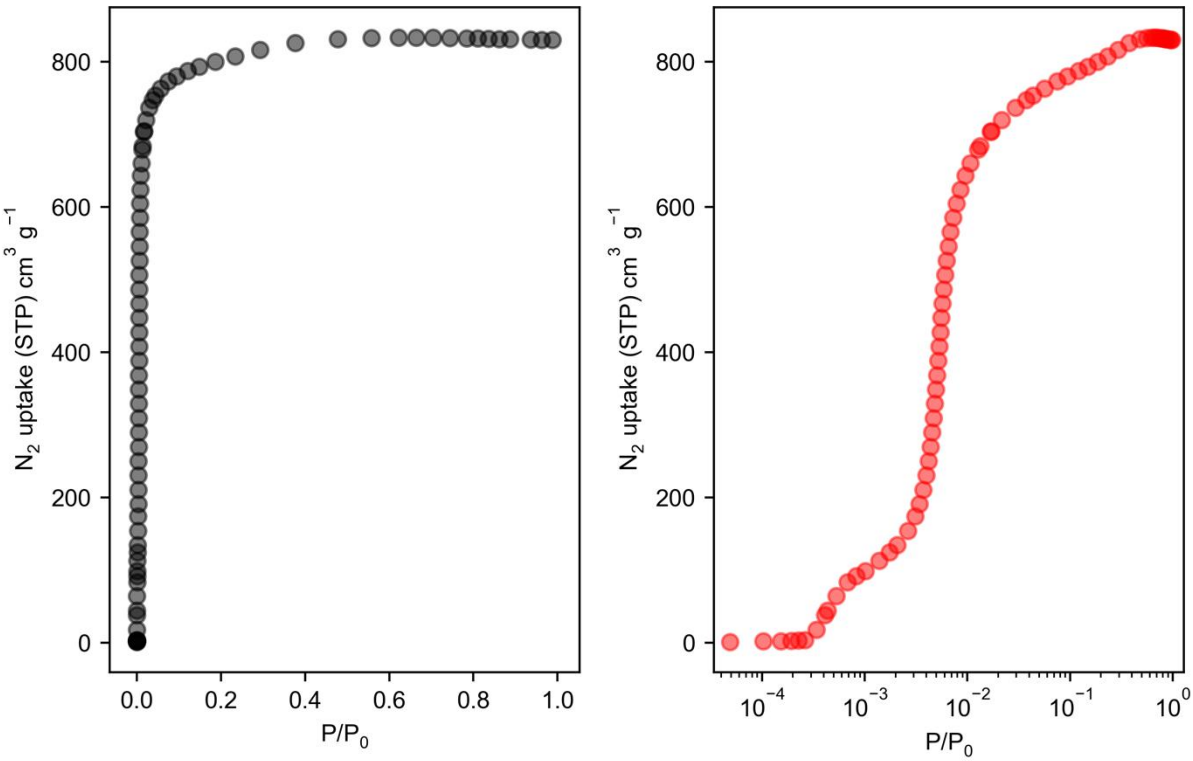

Figure S12 – VII | MOF-5 isotherm in linear representation (black) and semilog (red)

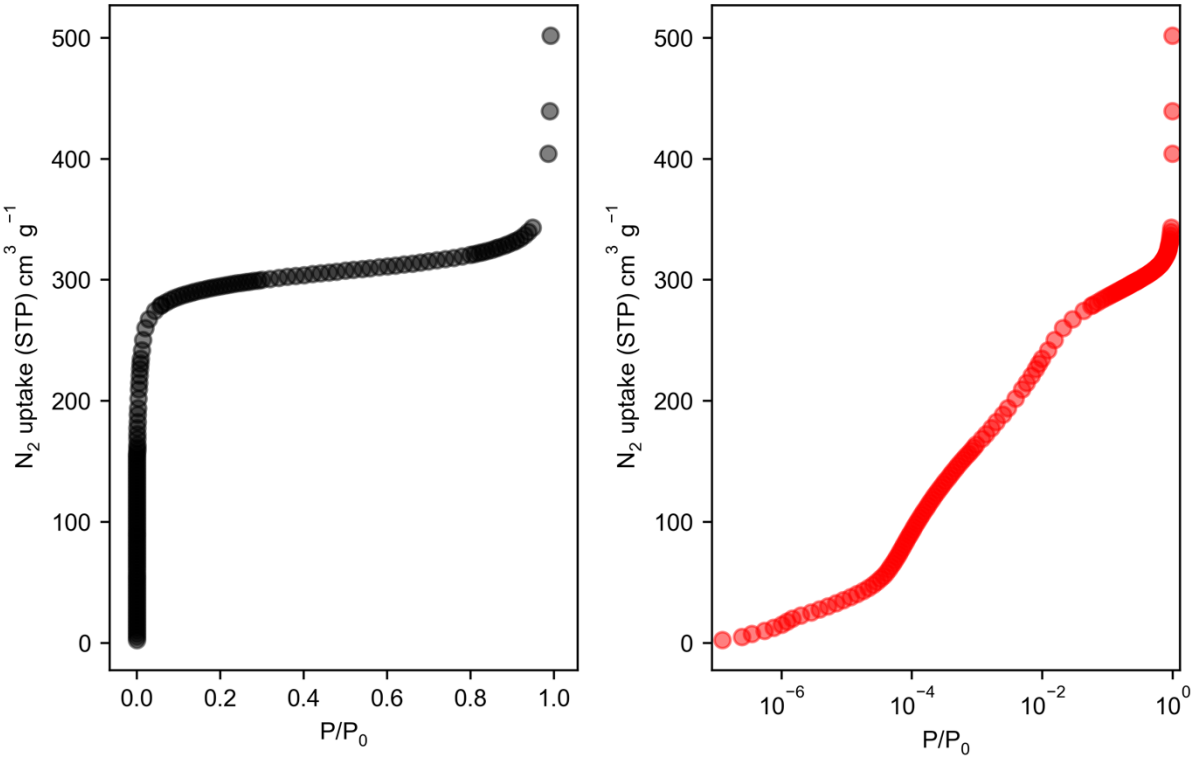

Figure S12 – VIII | UiO-66 isotherm in linear representation (black) and semilog (red)

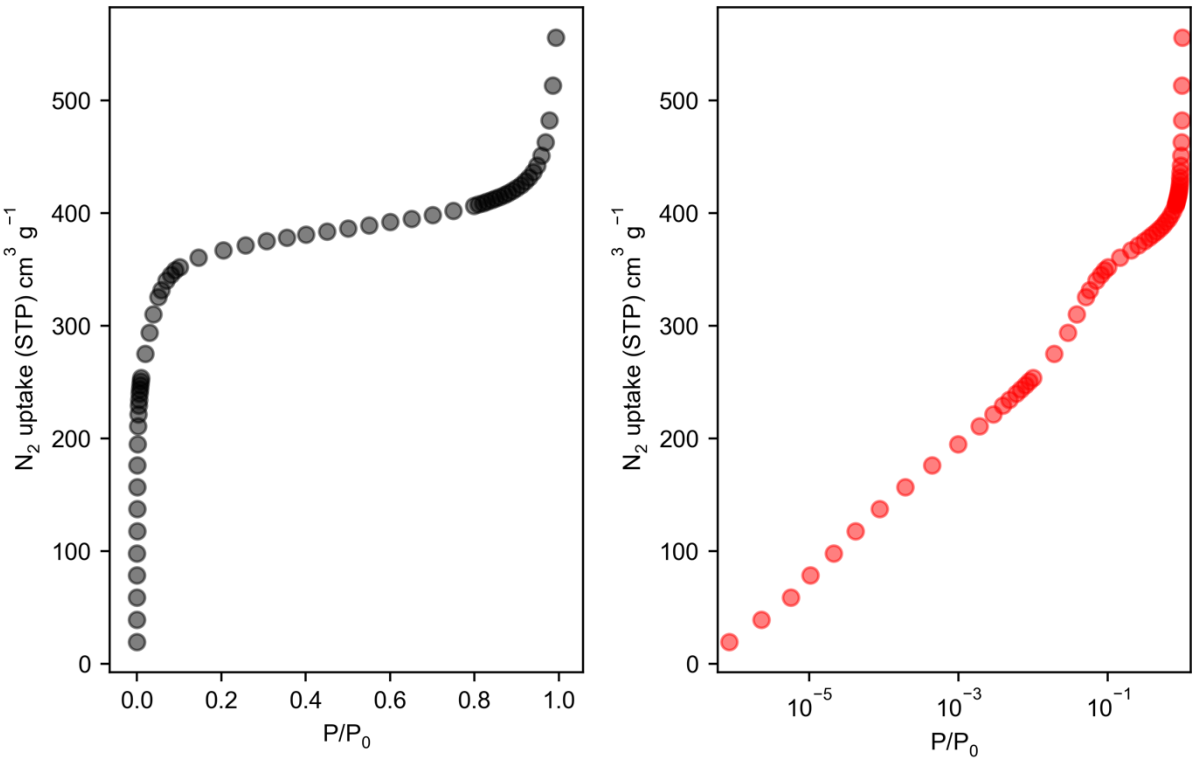

Figure S12 – IX | UiO-66-NH_2 isotherm in linear representation (black) and semilog (red)

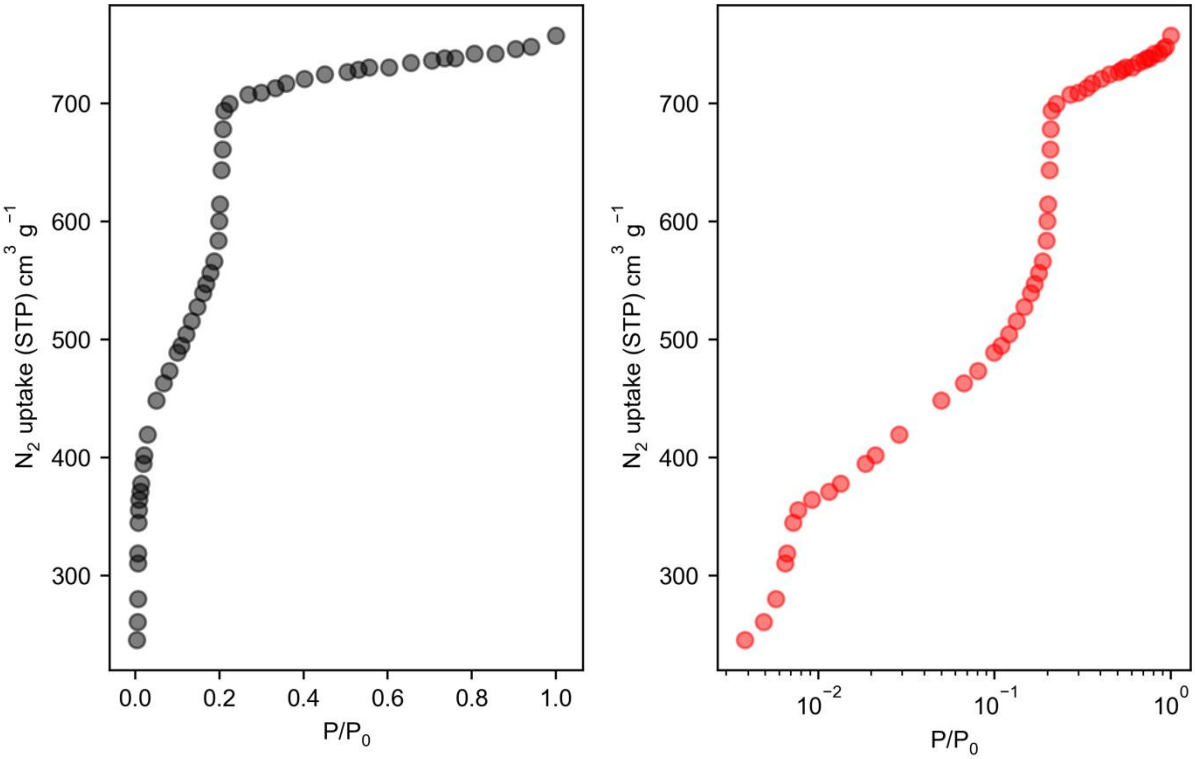

Figure S12 – X | NU-1000 isotherm in linear representation (black) and semilog (red)

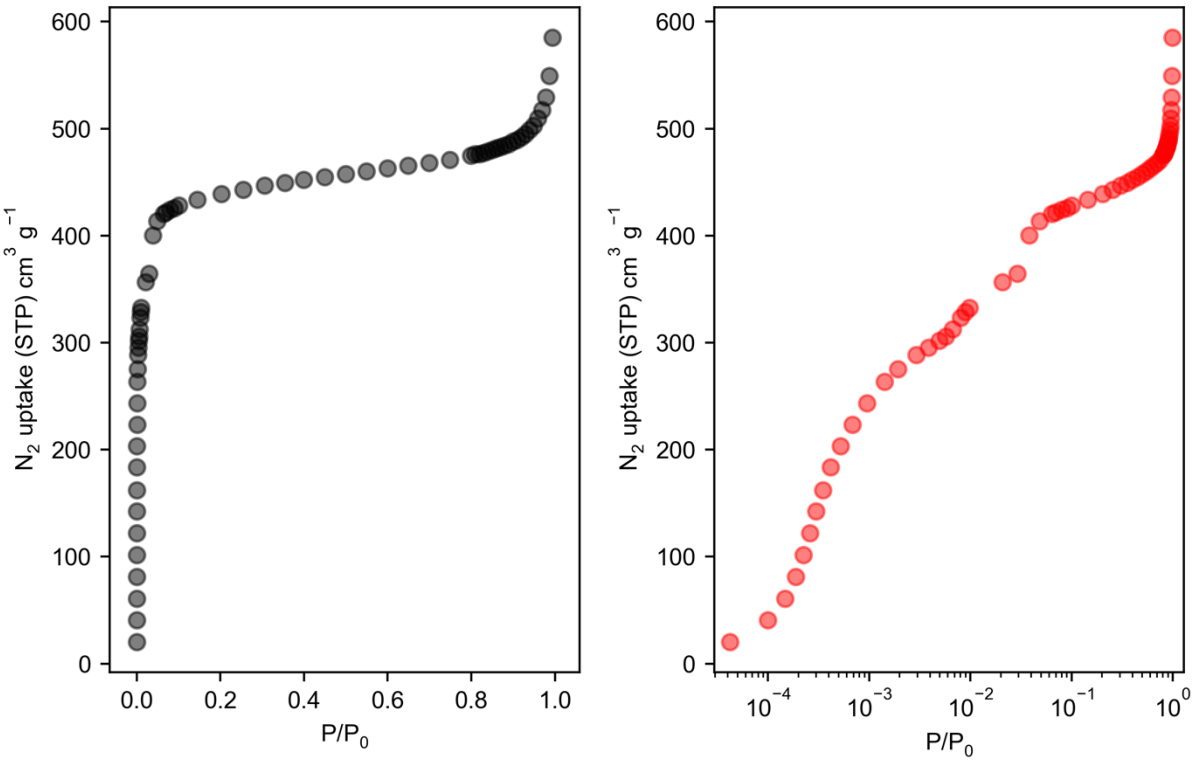

Figure S12 – XI | ZIF-8 isotherm in linear representation (black) and semilog (red)

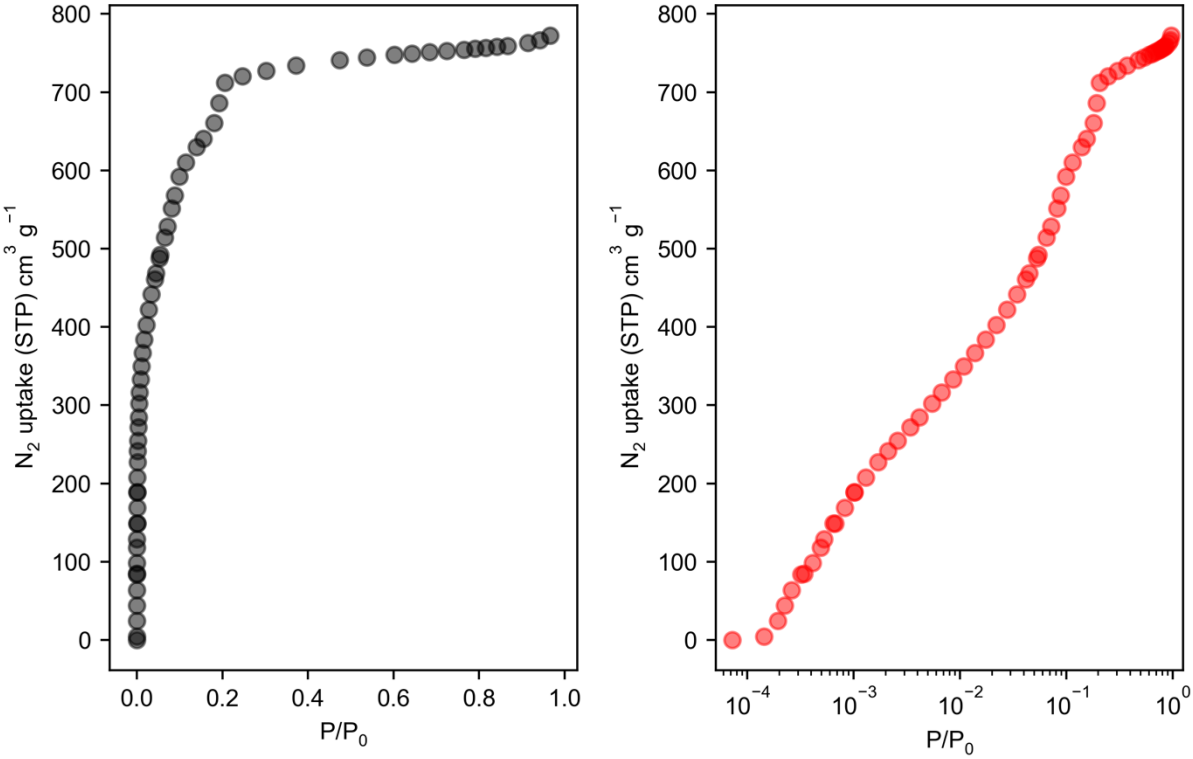

Figure S12 – XII | MIL-101 isotherm in linear representation (black) and semilog (red)

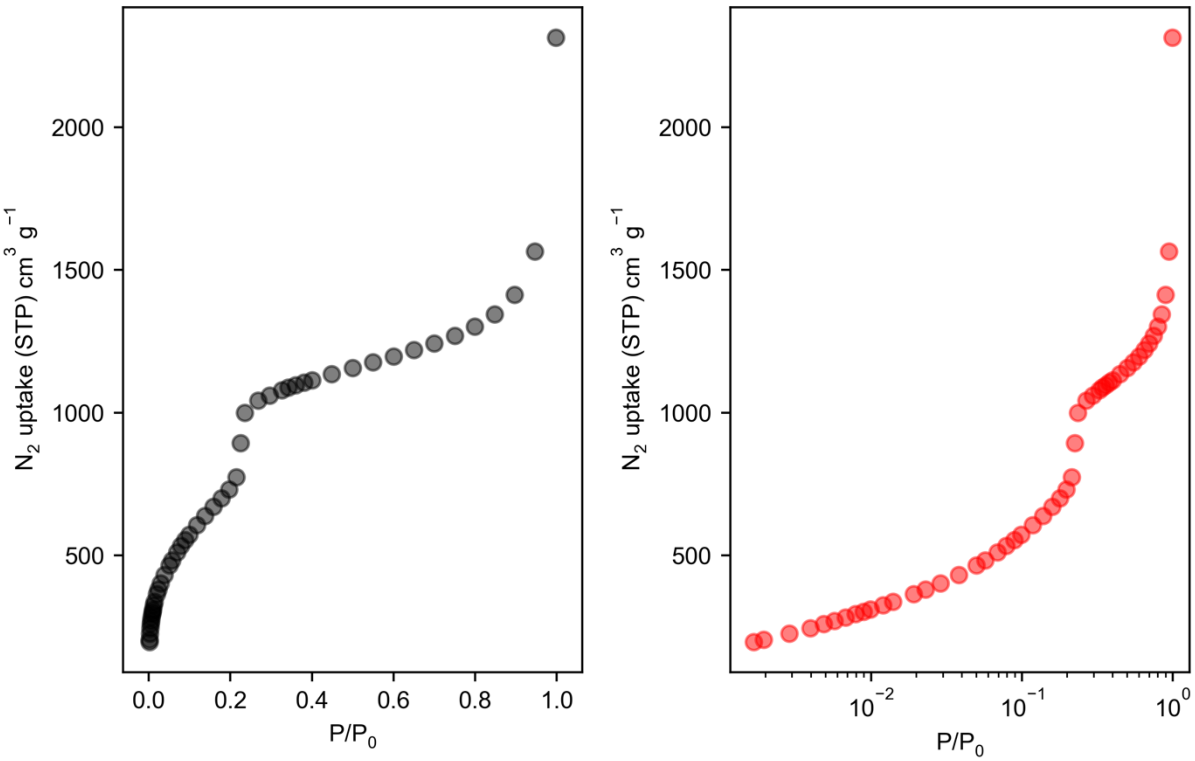

Figure S12 – XIII | TPB-DMTP-COF isotherm in linear representation (black) and semilog (red)

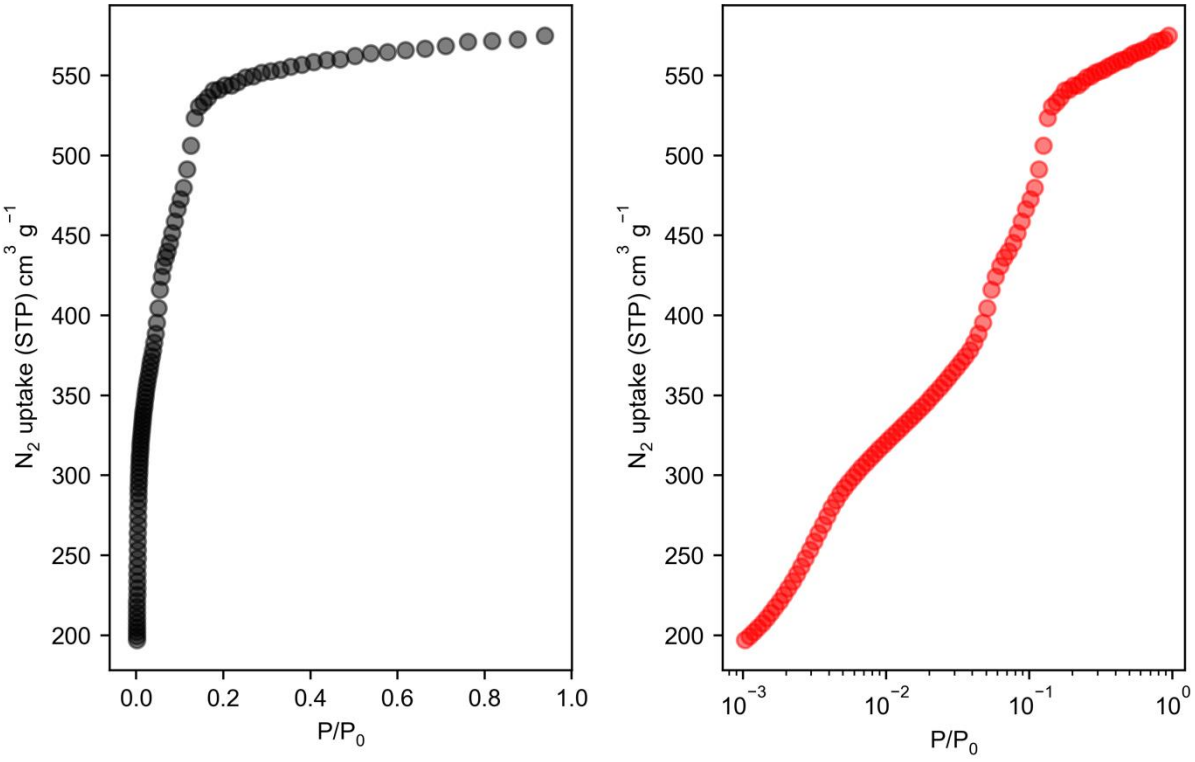

Figure S12 – XIV| MIL-100 isotherm in linear representation (black) and semilog (red)

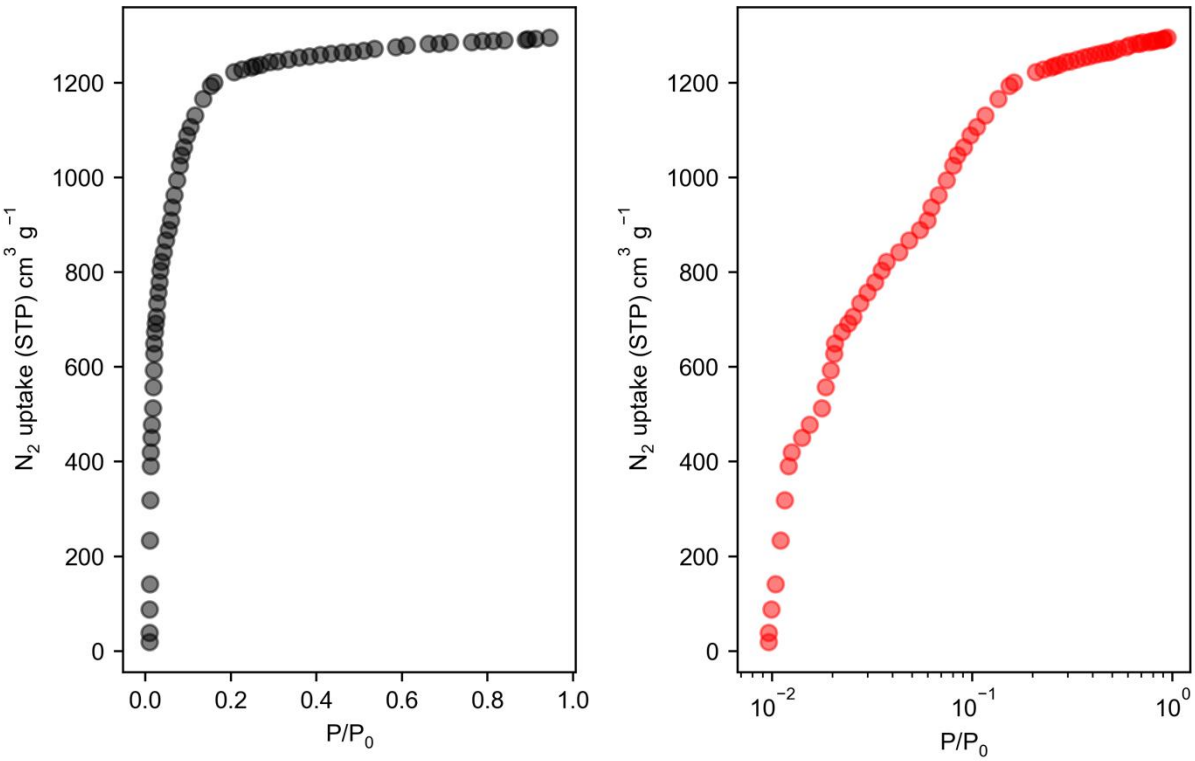

Figure S12 – XV | NU-1102 isotherm in linear representation (black) and semilog (red)

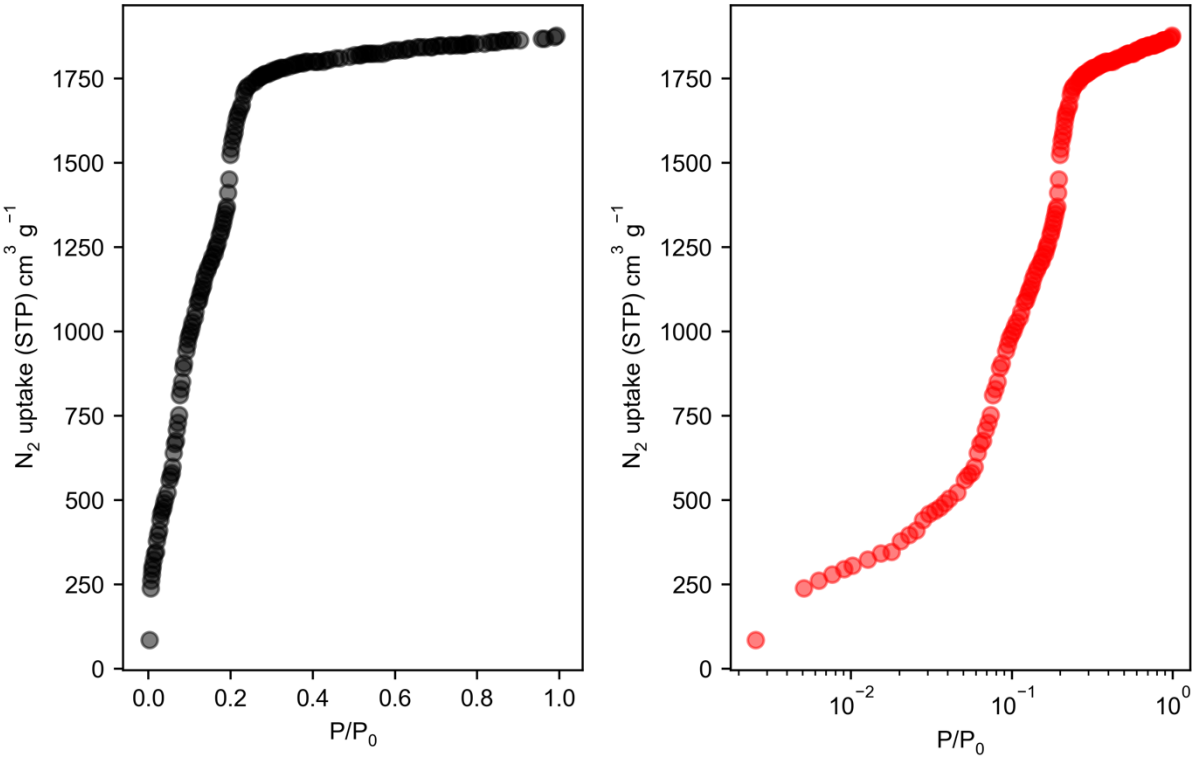

Figure S12 – XVI NU-1104 isotherm in linear representation (black) and semilog (red)

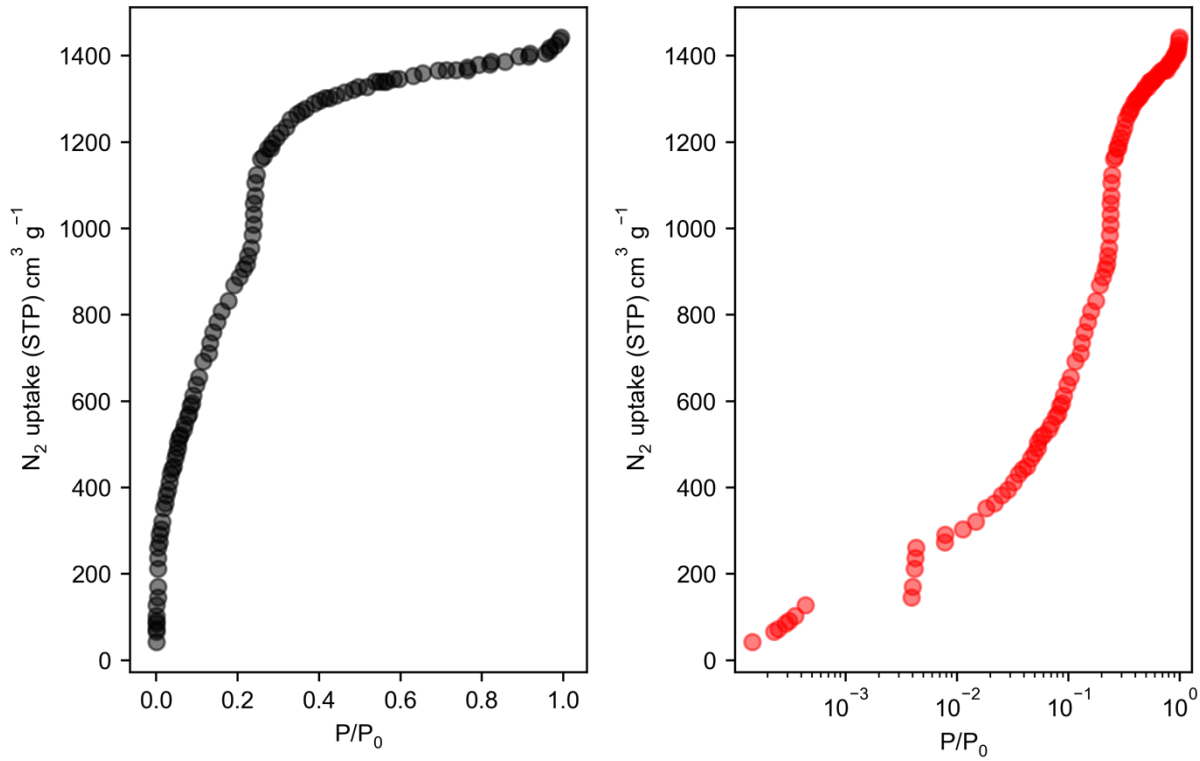

Figure S12 – XVII | NU-1105 isotherm in linear representation (black) and semilog (red)

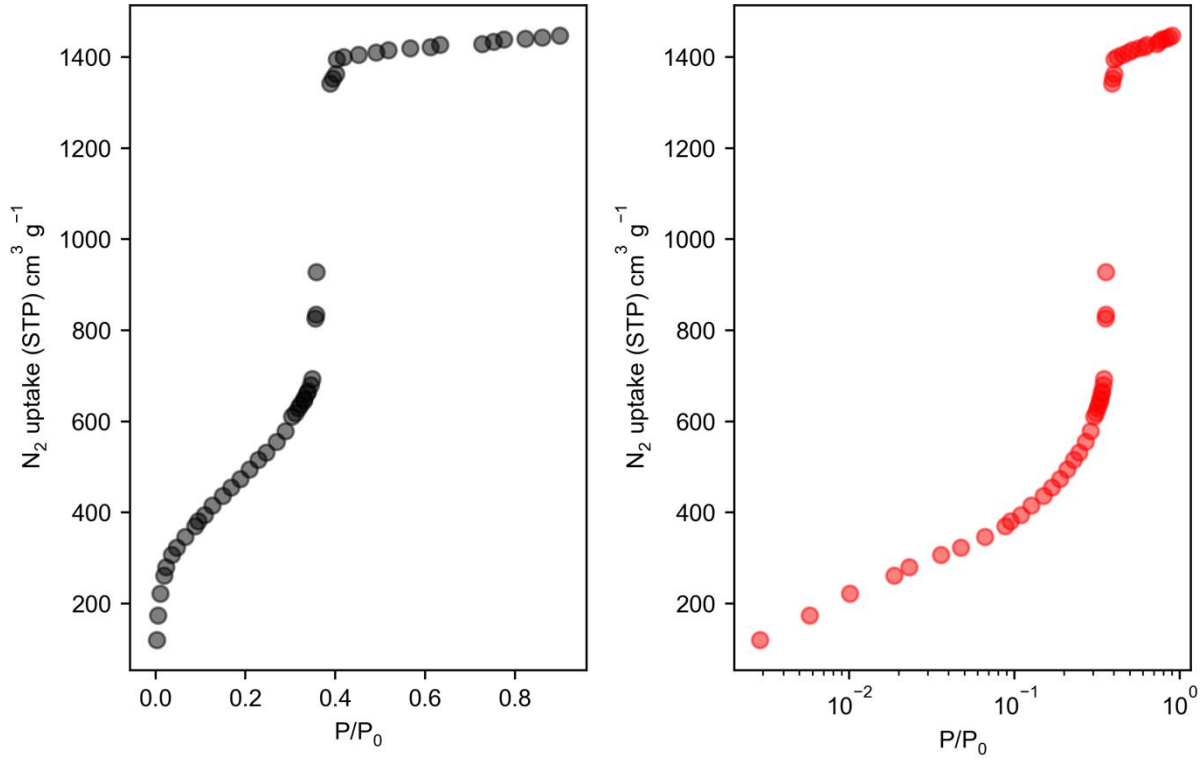

Figure S12 – XVIII | PCN-777 isotherm in linear representation (black) and semilog (red)

Section S13 – Round-robin evaluation individual results

Method: (Give a short description of your method here. If a commercial software was used to calculate the BET areas, please state this here. Please cite any papers or protocols used)

Model calculation: (Please give a model calculation of your method for sample R. Where commercial software was used, screenshots are welcome)

Lab 1

References:

[1] ISO, Determination of the specific surface area of solids by gas adsorption. BET method, ISO 9277. (2010) 1–24. doi:10.3403/30180119.

[2] M. Thommes, K. Kaneko, A. V. Neimark, J.P. Olivier, F. Rodriguez-Reinoso, J. Rouquerol, K.S.W. Sing, Physisorption of gases, with special reference to the evaluation of surface area and pore size distribution (IUPAC Technical Report), 2015. doi:10.1515/pac-2014-1117.

Method:

Fitting of the BET equation was undertaken using the native analysis software of the 3Flex gas sorption analyser (3Flex version 5.02, Micromeritics). To determine BET surface area 5 points were selected within the BET range. The limit of the BET range was identified as the maximum of the Rouquerol plot ($n_a(1-p/p_o)$ vs p/p_o) according to the criterion: $n_a(1-p/p_o)$ must continually increase with p/p_o. The points were then manually selected to ensure the C-value and y-intercept were positive and to maximise the correlation coefficient. For Sample R, the data immediately preceding the Rouquerol maxima (p/p_o ~ 0.40*)* was not valid (the C-value and BET area were negative). Consequently, the BET range was determined from the second inflection (p/p_o ~ 0.35) and correlation coefficient maximised.

Model Calculation (Sample R):

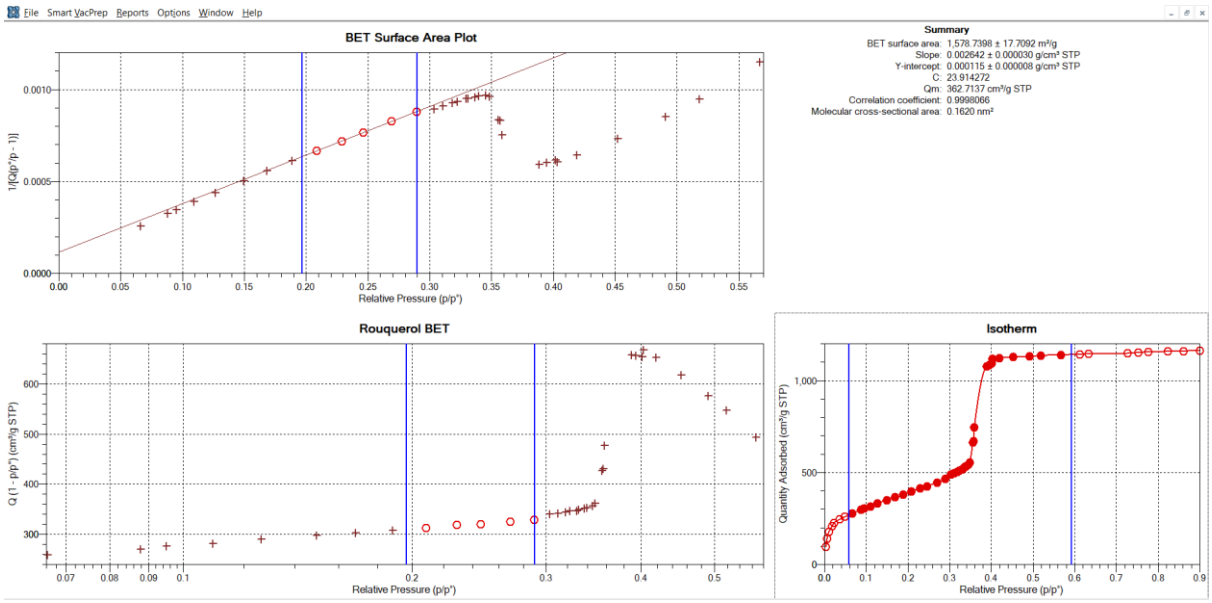

Lab 2

To calculate the surface areas we applied following approach/Rouquerol criteria:

1. Linear fit should be obtained, minimum 5 points should be used for linear fit, the more the better.

$$\frac{\frac{p}{p_0}}{V(1-\frac{p}{p_0})} = \frac{C-1}{V_m C}\left(\frac{p}{p_0}\right) + \frac{1}{V_m C} \quad ; \quad y = aX + b \quad \text{(Linearized BET equation)}$$

2. From the linear fit we would obtain the Vm (Volume adsorbed in a monolayer) as well as the C value.
3. BET "C" constant must be >0
4. Rouquerol transform $V(1-p/p_0)$ plotted against p/p_0 should be increasing with p/p_0.
5. Monolayer capacity (Vm) should be within the limits used to fit BET parameters.
6. The value of $1/(\sqrt{C}+1) \approx p/p_0$ at Vm

Lab 3

Method:

Firstly, according eq-1, linear fitting $1/V(1/(p/p_0)-1)$ (y-axis) vs. p/p_0 (x-axis) when $0.05 < p/p_0 < 0.35$ and ensuring $C > 0$. If $C < 0$ after the linear fitting, p/p_0 for fitting should decreases until $C > 0$.[1,2]

$$\frac{1}{V(\frac{1}{p/p_0}-1)} = \frac{1}{V_m C} + \frac{C-1}{V_m C} p/p_0 \qquad \text{eq-1}$$

where V is adsorption capacity ($cm^3\ g^{-1}$), V_m is monolayer saturation adsorption capacity, C is constant. Thus, $V_m = 1/(1/V_m C+(C-1)/V_m C) = 1/(\text{slope} + \text{intercept})$

Brunauer–Emmett–Teller (BET) surface area (S, $m^2\ g^{-1}$) can be obtained by

$$S = A_m L V_m / 22400 \qquad \text{eq-2}$$

where A_m (m^2) is the cross-sectional area of adsorbent (0.162 nm^2 for N_2 at 77 K), L is Avogadro's constant (6.023×10^{23}/mol).[1]

Model calculation for sample R:

	p/p_0	V_m ($cm^3\ g^{-1}$)	C	BET surface area ($m^2\ g^{-1}$)
R	0.06621-0.34543	374	24	1629

References:

[1] K. S. W. Sing, D. H. Everett, R. A. W. Haul, L. Moscou, R. A. Pierotti, J. Rouquerol, T. Siemieniewska, Reporting physisorption data for gas/solid systems with special reference to the determination of surface area and porosity. *Pure Appl. Chem.* **1985**, *57*, 603-619.

[2] K. S. Walton, R. Q. Snurr. Applicability of the BET method for demining surface areas of microporous metal-organic frameworks. *J. Am. Chem. Soc.* **2007**, *129*, 8552-8556.

Lab 4 – The fitting was undertaken manually in MS Excel.

1 – A Rouquerol criteria plot is produced to establish the P/P° bounds (Figure 1).

- A maximum P/P° of 0.403 was determined, with no minimum.

2 – A BET transform plot is produced over the whole range and a linear regression applied for visual inspection of the data (Figure 2).

3 – The data range is gradually reduced from both directions until a good linear fit is obtained while meeting the following objectives: intercept > 0, maximise number of points for fitting, maximise R^2.

- Data points from the upper end were initially removed as they were clearly unsuitable.
- Points from the lower end were removed individually until the value of R^2 reached a maximum (Figure 3). A calculation range of $0.0878 \leq P/P° \leq 0.337$ is obtained.

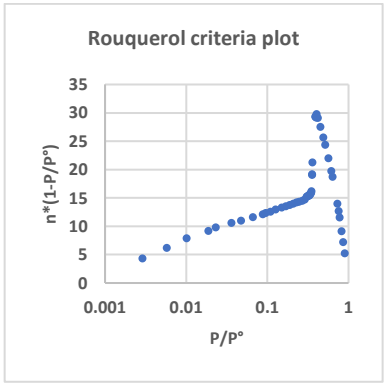

Figure 1

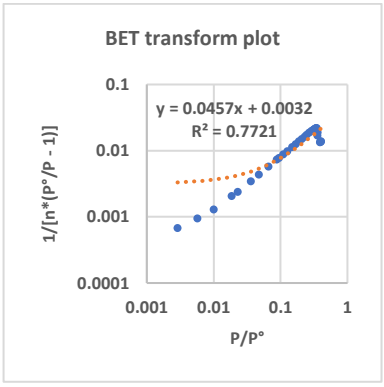

Figure 2

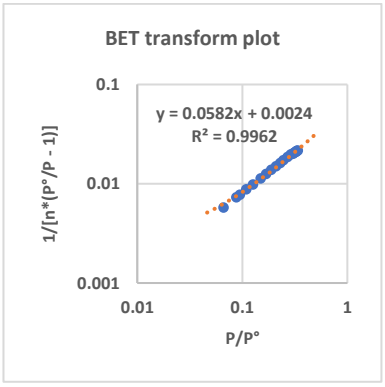

Figure 3

4 – The LINEST tool in Excel is then used to obtain the linear regression.

Parameter	Gradient (m)	Intercept (c)	R^2	DoF
Value	0.057529569	0.002614794	0.996194886	17
Standard error (SE)	0.00086234	0.000213927	N/A	N/A

5 – The BET surface area is calculated in the traditional fashion. A cross-sectional area of 0.162 nm^2/molecule was used for N_2, and a value of $6.02214086 \times 10^{23}$ for Avogadro's constant.

- A monolayer capacity (n_m) of 16.63 mol/kg is obtained, and confirmed to lie within the P/P° range selected for the calculation – as per the Rouquerol criteria.
- A BET constant (C_{BET}) of 23.00 is obtained.
- A BET surface area of 1622 m^2/g is obtained.

6 – The margin of error can be obtained as follows:

- Select desired confidence interval (e.g. 95%), and determine t-value for the DoF, t = 2.10982.
- Determine margin of error (MOE) of fit parameters: $MOE_m = SE_m \times t = \delta_m$, and $MOE_c = SE_c \times t = \delta_c$
- The margin of error in n_m can be calculated with the following, based on error propagation rules:

$$\delta n_m = n_m \times \frac{\sqrt{\delta_m^2 + \delta_c^2}}{m + c} = 0.51821$$

- The margin of error in the BET surface area is calculated by substituting δn_m for n_m in the standard equation, as all other parameters in the BET equation are constants.

$$\delta_{SA} = \delta n_m \times N_A \times A_{N_2}$$

- A margin of error corresponding to a 95% confidence interval of 50.6 m^2/g is obtained.

Therefore, the final reported BET surface area is 1622±51 m^2/g, over the range $0.0878 \leq P/P° \leq 0.337$.

Lab 5

To calculate the BET area of materials, we used an Excel spreadsheet. The isotherm data points, relative pressure and adsorbed volume amount, were pasted into the columns and then the isotherm was plot both in linear and logarithm scale in order to see any irregularities. We used the following BET equation:

Brunauer, Emmett and Teller (BET) adsorption isotherm equation:

$$\frac{1}{\left[V_a\left(\frac{P_o}{P}-1\right)\right]}=\frac{C-1}{V_m C}\times\frac{P}{P_o}+\frac{1}{V_m C} \qquad (1)$$

P = partial vapor pressure of adsorbate gas in equilibrium with the surface at 77.4 K (b.p. of liquid nitrogen), in Pa,
P_o = saturated pressure of adsorbate gas, in Pa,
V_a = volume of gas adsorbed at standard temperature and pressure (STP) [273.15 K and atmospheric pressure (1.013×10^5 Pa)], in mL,
V_m = volume of gas adsorbed at STP to produce an apparent monolayer on the sample surface, in mL,
C = dimensionless constant that is related to the enthalpy of adsorption of the adsorbate gas on the powder sample.

Here, $1/(V(P_0/P-1))$ was plotted against P/P_0. The slope was $(C-1)/V_mC$ and the intercept was $1/V_mC$. Ones V_m was calculated from the slope and the intercept, the BET surface area (S) was calculated using the following equation:

$$S=\frac{V_m N a}{m\times 22\ 400} \qquad (2)$$

N = Avogadro constant (6.023×10^{23} mol^{-1}),
a = effective cross-sectional area of one adsorbate molecule, in square meters (0.162 nm^2 for nitrogen and 0.195 nm^2 for krypton),
m = mass of test powder, in g,
22400 = volume, in mL, occupied by one mole of the adsorbate gas at STP allowing for minor departures from the ideal.

Here, a cross-sectional area of 0.162 nm^2/molecule (a) was used for N_2 with a sample mass (m) of 1 gram and a value of 6.023×10^{23} was used for the Avogadro's constant (N). During these calculations, we aimed to manually fit the data to a range which is linear, we tried to obtain positive C values, and set the maximum value of P/P_0 as 0.3. However, there were some special cases that we did not necessarily follow all these to get a better fit with a higher R^2. For example, we gradually reduced the number of data points (P/P_0) in both directions to catch a good fit but at the same time we aimed to maximize the number of data points used in fitting.

Relative Pressure (P/Po)	Quantity Adsorbed (cm³/g STP)	Po/P	V(Po/P-1)	1/V(Po/P-1)
9,79E-03	1,07E+02	1,02E+02	1,08E+04	9,27E-05
1,30E-02	1,11E+02	7,69E+01	8,41E+03	1,19E-04
1,70E-02	1,16E+02	5,89E+01	6,69E+03	1,49E-04
2,20E-02	1,22E+02	4,55E+01	5,41E+03	1,85E-04
3,00E-02	1,30E+02	3,33E+01	4,21E+03	2,38E-04
3,97E-02	1,38E+02	2,52E+01	3,35E+03	2,99E-04
5,60E-02	1,48E+02	1,78E+01	2,50E+03	4,00E-04
7,13E-02	1,56E+02	1,40E+01	2,03E+03	4,94E-04
1,05E-01	1,69E+02	9,53E+00	1,44E+03	6,93E-04
1,30E-01	1,78E+02	7,71E+00	1,19E+03	8,38E-04
1,60E-01	1,88E+02	6,25E+00	9,85E+02	1,02E-03
1,92E-01	1,97E+02	5,22E+00	8,31E+02	1,20E-03
2,23E-01	2,07E+02	4,49E+00	7,22E+02	1,39E-03
2,53E-01	2,16E+02	3,95E+00	6,39E+02	1,57E-03
2,84E-01	2,28E+02	3,52E+00	5,75E+02	1,74E-03
3,05E-01	2,41E+02	3,28E+00	5,48E+02	1,82E-03
3,16E-01	2,51E+02	3,16E+00	5,43E+02	1,84E-03
3,34E-01	2,95E+02	3,00E+00	5,89E+02	1,70E-03
3,44E-01	3,16E+02	2,91E+00	6,03E+02	1,66E-03
3,73E-01	3,45E+02	2,68E+00	5,80E+02	1,72E-03
4,28E-01	3,71E+02	2,34E+00	4,97E+02	2,01E-03
4,48E-01	3,72E+02	2,23E+00	4,59E+02	2,18E-03
4,77E-01	3,74E+02	2,10E+00	4,10E+02	2,44E-03
5,00E-01	3,75E+02	2,00E+00	3,75E+02	2,67E-03
5,30E-01	3,76E+02	1,89E+00	3,33E+02	3,00E-03
5,61E-01	3,77E+02	1,78E+00	2,96E+02	3,38E-03
5,91E-01	3,78E+02	1,69E+00	2,61E+02	3,83E-03
6,22E-01	3,79E+02	1,61E+00	2,30E+02	4,34E-03
6,53E-01	3,80E+02	1,53E+00	2,02E+02	4,95E-03
6,83E-01	3,81E+02	1,46E+00	1,77E+02	5,66E-03
7,14E-01	3,82E+02	1,40E+00	1,53E+02	6,54E-03
7,45E-01	3,83E+02	1,34E+00	1,31E+02	7,62E-03
7,75E-01	3,84E+02	1,29E+00	1,11E+02	8,98E-03
8,07E-01	3,85E+02	1,24E+00	9,21E+01	1,09E-02
8,37E-01	3,86E+02	1,20E+00	7,54E+01	1,33E-02
8,67E-01	3,87E+02	1,15E+00	5,93E+01	1,69E-02
8,97E-01	3,88E+02	1,11E+00	4,45E+01	2,25E-02
9,38E-01	3,92E+02	1,07E+00	2,59E+01	3,85E-02

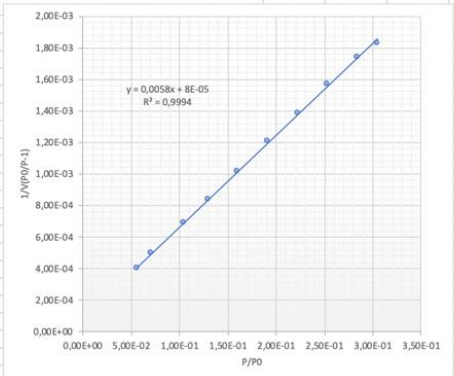

		slope	0,0058
Vm	1,70E+02	intercept	8,00E-05
N	6,02E+23 mol−1		
a (effective cross-sectional area of one adsorbate molecule)	1,62E-19 m2		
m (mass of test powder)	1 g		
	740,80 m2/g		

Lab 6

Method: We have an excel spreadsheet which I cut paste values into. We first look at the normal, then the semi-log isotherm. We then ensure that n(1-X) is increasing: as soon as it becomes negative, or if the value is above p/p° = 0.35, we automatically eliminate these points.
We then look for linearity which can be a bit subjective and then check that:

- C is positive
- n^a_m point should be within the p/p° range under consideration,
- the 1/ÖC+1 value should be 'close' (<5%) to the value of p/p° where n^a_m is taken.

The above verifications are checked in our spredsheet calculation. We then check for irregularities, as noted for individual cases. This last check comes from experience 😊
The calculations are from experiment, so there should be possible leeway – so we did not search for a specific BET range, although some were provided. We often recover the p/p° range which gives the highest BET value if all else seems correct (especially if there enough points). This suggests that we are closest the the knee or point 'B' in the isotherm.

Model calculation for sample R:

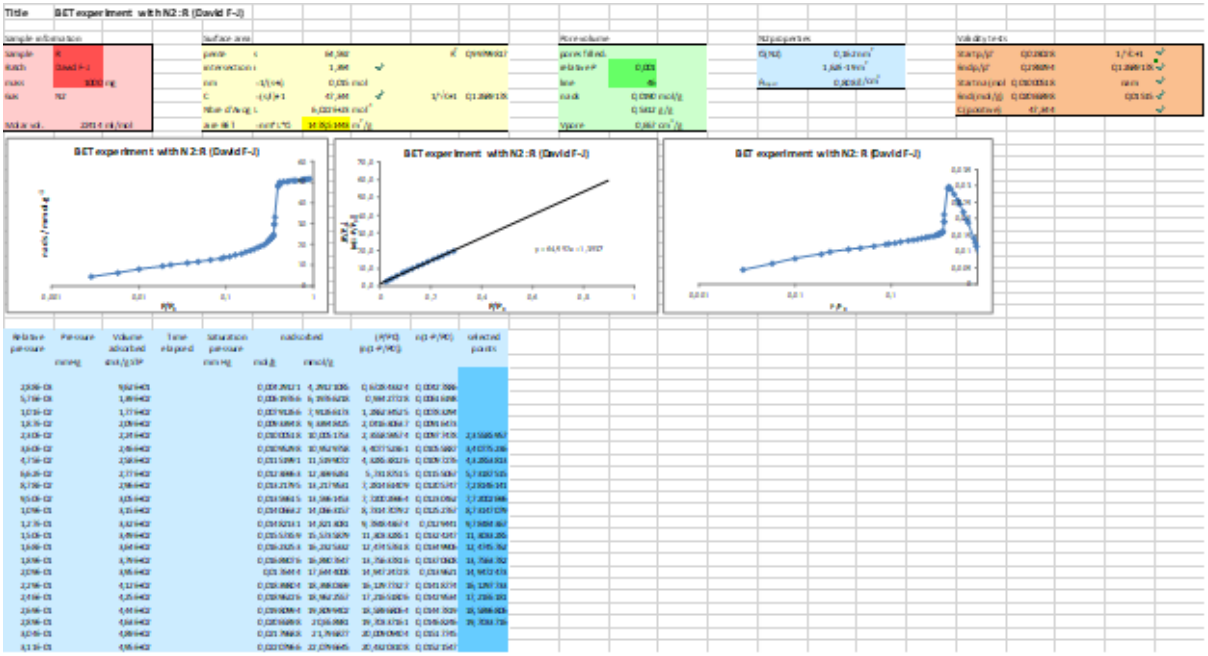

References:
Is the BET equation applicable to microporous adsorbents, J Rouquerol, Philip Llewellyn, F Rouquerol, In Stud. Surf. Sci. Catal., **2007**, 160(49), 1016-.

Lab 7

BET surface areas were determined from analysis of the Rouquerol plots of the isotherm data, using ~10 data points each. The guidelines set forth by Rouquerol use four criteria to obtain the most accurate BET surface area values for microporous materials such as MOFs.

1. The value $V(1-P/P_0)$ must increase with increasing p/p_0 for all points chosen
2. BET constant C must be positive
3. Total monolayer loading should correspond to a relative pressure (P/P_0) within the selected linear region
4. The relative pressure corresponding to the monolayer loading calculated from BET theory should be within 20% of the pressure determined in (3).

To fulfill criterion 1, $V(1-P/P_0)$ was plotted and the maximum point was found *(a)*. Data at higher P/P_0 values was ignored.

a)

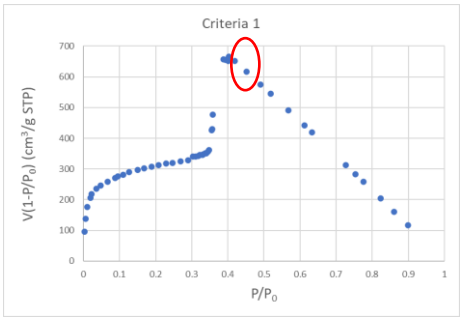

b)

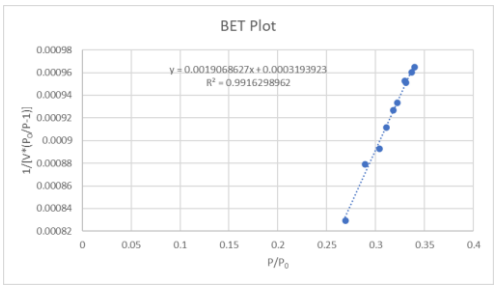

b)

Slope	0.0019068627
Intercept	0.0003193923
C	6.97
Qm	449.18
P/P_0 @ Qm	0.2747155
BET SA	1955.39

d)

P/P_0	$1/[V(P_0/P-1)]$
2.46E-01	7.68E-04
2.69E-01	8.29E-04
2.89E-01	8.79E-04
3.04E-01	8.93E-04
3.11E-01	9.12E-04
3.18E-01	9.27E-04
3.22E-01	9.33E-04
3.30E-01	9.53E-04
3.31E-01	9.51E-04
3.37E-01	9.60E-04
3.40E-01	9.65E-04
3.45E-01	9.71E-04
3.48E-01	9.64E-04

e)

Relative Pressure (P/Po)	Quantity Adsorbed (cm3/g STP)
0.246116	425.02
0.269145	444.02
0.289294	463.0504
0.303687	488.5552
0.310883	494.8936
0.318079	503.3704
0.322398	509.7392
0.329594	516.0768
0.331034	520.3384
0.33679	528.8296
0.339669	533.0752
0.345426	543.7056
0.348305	554.3656

P/P_0 values below this point were then plotted as $1/[V(P_0/P-1)]$ *(b)* and a linear region was found such that the R^2 value (linearity) was maximized and all other criteria were fulfilled *(d)*. Slope and intercept values from the BET plot *(c)* were used to calculate C, which was found to be positive (criterion 2). Total monolayer loading (Q_m) was also calculated. The value was found to correspond to a P/P_0 value in the linear region used *(e)*, fulfilling criterion 3. The relative pressure corresponding to the monolayer loading calculated from the BET equation ($P/P_0@Q_m$) was calculated and found to be within 20% of the experimental value *(c)*.

$C = 1 + \text{slope/intercept}$ $Q_m = 1/(\text{slope+intercept})$ $P/P_0 @ Q_m = 1/(\text{sqrt}(C)+1)$

BET SA = $(Q_m*N*s)/V$, where $N=6.022\times10^{23}$ (Avogadro's number) s=0.162 (cross-sectional area of N_2) and $V = 2.24\times10^{22}$).

References:

(1) Rouquerol, J., Llewellyn, P. & Rouquerol, F. in *Studies in surface science and catalysis* Vol. 160, 49-56 (Elsevier, 2007). (2) Gómez-Gualdrón, D. A. *et al. J. Am. Chem. Soc.* **138,** 215-224 (2016).

Lab 8

Method: The BET surface area was determined manually by employing Excel Software and the Rouquerol criteria, namely:

1. The value $V(1-P/P_0)$ must continuously increase with p/p_0 for all selected points.
2. BET constant C must be positive.
3. The relative pressure corresponding to the monolayer capacity must belong to the pressure range used to fit the BET equation.
4. The regression coefficient R^2 must be > 0.995.
5. The above criteria are checked. If irregularities occur, they are solved individually (often based on experience).

Model calculation for sample R:

Rel. Pressure (P/Po)	Quantity Ads. (cm^3/g STP)	po/p	W	For BET plot
0,002879	96,1832	347,342827	120,211406	0,02401862
0,005757	138,9144	173,701581	173,617590	0,03335108
0,010075	177,3544	99,255583	221,660558	0,04591497
0,018711	209,3352	53,444498	261,630708	0,0728805
0,023028	224,256	43,425395	280,278979	0,0840976
0,035982	245,5	27,791674	306,830093	0,12164722
0,047496	258,2072	21,054405	322,711768	0,1545167
0,066207	277,2528	15,104143	346,515285	0,20461191
0,087796	296,2672	11,390041	370,279806	0,2599278
0,094992	304,744	10,527202	380,874256	0,27558336
0,109385	315,2824	9,142021	394,045328	0,31168908
0,126656	332,2048	7,895402	415,195233	0,34929154
0,149684	349,0664	6,680741	436,269148	0,4034972
0,168395	363,836	5,938419	454,728447	0,44530747
0,188546	378,5896	5,303746	473,167748	0,49106421
0,208695	395,4816	4,791682	494,279658	0,53357491
0,228845	412,3736	4,369770	515,391568	0,57578778
0,246116	425,02	4,063125	531,197255	0,61458152
0,269145	444,02	3,715469	554,943779	0,66359959
0,289294	463,0504	3,456691	578,728298	0,70335524
0,303687	488,5552	3,292864	610,604633	0,71426867
0,310883	494,8936	3,216644	618,526473	0,72936634
0,318079	503,3704	3,143873	629,120923	0,74142428
0,322398	509,7392	3,101756	637,080758	0,74683244
0,329594	516,0768	3,034036	645,001599	0,76222048
0,331034	520,3384	3,020838	650,327819	0,76091514
0,33679	528,8296	2,969209	660,940266	0,76832667
0,339669	533,0752	2,944043	666,246489	0,77207465
0,345426	543,7056	2,894976	679,532545	0,77657966
0,348305	554,3656	2,871047	692,855595	0,77138749
0,355501	661,1936	2,812932	826,371054	0,66748803
0,356941	667,5928	2,801583	834,368883	0,66525403
0,358379	742,4104	2,790342	927,877197	0,60196811
0,388605	1073,496	2,573307	1341,673635	0,47373952
0,394362	1081,984	2,535741	1352,282082	0,48152035
0,401558	1090,464	2,490300	1362,880531	0,49234375

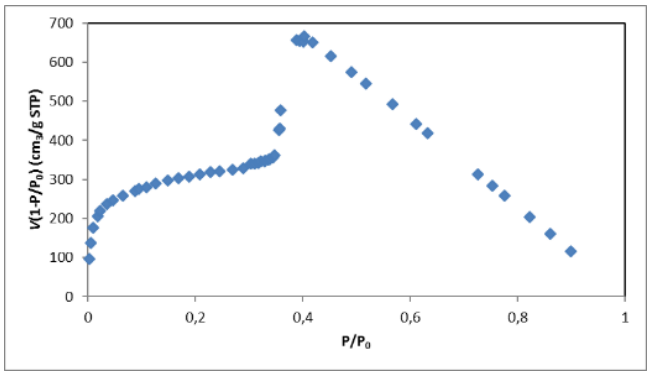

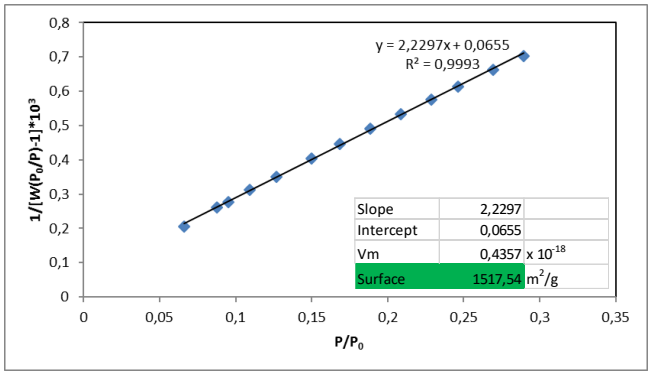

From the slope (S) and intercept (I) of the linear region, V_m and the BET surface area are calculated:

$$S = \frac{(C-1)}{(V_m \times C)} \qquad I = \frac{1}{V_m \times C} \qquad V_m = \frac{1}{S+I} \qquad C = \frac{S}{I} + 1$$

Constants used:
$N_a = 6.022 \cdot 10^{23}$ (Avogadro's number)
$s = 0.162$ nm^2 (cross-sectional area of N_2)
$M(N_2) = 28.0135$ g/mol

References:

Rouquerol J., Llewellyn P., Rouquerol F.: *Is the BET equation applicable to microporous adsorbents?*, Stud. Surf. Sci. Catal., **2007**, 160, 49-56.

Lab 9

Brunauer-Emmett-Teller (BET) equation was applied to calculate the surface area of the samples.

$$\frac{1}{W\left(\left(P_0/P\right)-1\right)} = \frac{1}{W_m C} + \frac{C-1}{W_m C}\left(\frac{P}{P_0}\right)$$

W= weight of gas adsorbed

P/P_0 =relative pressure

Wm = weight of adsorbate as monolayer

C = BET constant

1. Plot $1/(W(P_0/P)-1)$ against (P/P_0).
2. Select 5 points from the plot and conduct linear fitting to obtain the slope and intercept.

Following criteria should be met when choosing the data for linear fitting:
(i) $W(P_0/P-1)$ increases monotonically with P/P_0
(ii) Intercept >0
(iii) R^2 >0.995

3. Calculate W_m from the slope and intercept, W_m=1/(slop+intercept).
4. Calculate S_t from W_m using the equation below:

$$S_t = \frac{W_m \; N \; A_{cs}}{M}$$

N = Avogadro's number (6.023×10^{23})

M = Molecular weight of Adsorbate

A_{cs} = Adsorbate cross sectional area (16.2Å^2 for Nitrogen)

5. Repeat step 2-4 with another two sets of 5 points to obtain error of this calculation.

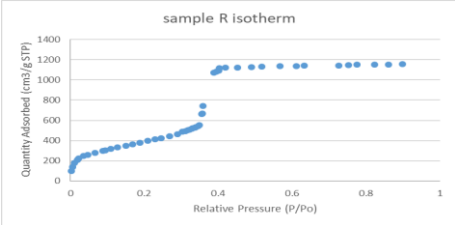

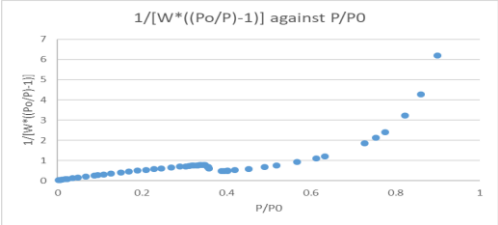

data set 1	
P/P0	1/[W*((Po/P)-1)]
0.06621	0.20458
0.0878	0.25989
0.09499	0.27554
0.10939	0.31164
0.12666	0.34924

data set 2	
P/P0	1/[W*((Po/P)-1)]
0.14968	0.40344
0.16839	0.44524
0.18855	0.49099
0.20869	0.5335
0.22884	0.5757

data set 3	
P/P0	1/[W*((Po/P)-1)]
0.20869	0.5335
0.22884	0.5757
0.24612	0.61449
0.26915	0.6635
0.28929	0.70325

	intercept	slope	intercept error	slope error	R2	C	Wm	m2/g	error
data set 1	0.0476	2.3972	0.0046	0.0468	0.9989	51.3199	0.4090	1424.6596	29.9965
data set 2	0.0784	2.1786	0.0044	0.0230	0.9997	28.7913	0.4431	1543.2312	18.6894
data set 3	0.0915	2.1198	0.0060	0.0239	0.9996	24.1663	0.4522	1575.1219	21.3008
							averaged BET	**1514.3375**	23.8244
							error	**88.5590**	

References:

Gómez-Gualdrón, D. A., Moghadam, P. Z., Hupp, J. T., Farha, O. K., Snurr, R. Q. Application of Consistency Criteria To Calculate BET Areas of Micro- And Mesoporous Metal–Organic Frameworks *J. Am. Chem. Soc.* **2016**, 138, 1, 215–224

Lab 10

Method: The BET surface area was determined manually by applying Rouquerol analysis[1] to the N_2 isotherm according to the guidelines outlined by Walton and Snurr[2] for microporous MOF materials. All calculations were performed using the OriginPro 2016 software. The BET surface area was calculated according to the following procedure:

- After inspection of the initial isotherm, $v(1\text{-}p/p^o)$ *vs*. p/p^o (Figure 1a) was plotted to determine the appropriate range of data points from which the BET surface area could be calculated according to Rouquerol's criteria.
- The chosen data points for the BET fit satisfied the Rouquerol criterion of an increasing $v(1\text{-}p/p^o)$ and an intercept > 0. Data points below $p/p^o = 0.6$ and above 0.27 were excluded to correspond to the optimal BET fitting range of $0.05 < p/p^o < 0.3$ and to maximise the correlation coefficient ($R^2 = 0.9994$).
- Fitting the data (Figure 1b) yielded a BET constant of 37 and a monolayer capacity of $v_m = 346$ mmol g^{-1}. The value of the monolayer capacity corresponded to the pressure range used to fit the BET equation as required by Rouquerol's criteria.
- The BET surface area was then calculated using the formula $A_{BET} = \frac{v_m \sigma_0 N_A}{22400}$ where v_m is the monolayer capacity ($cm^3\ g^{-1}$), σ_0 is the cross-sectional area of an N_2 molecule (1.62×10^{-19} m^2) and N_A is Avogadro's constant (6.022×10^{23} mol^{-1}). The final BET surface area of R was calculated as 1507 $m^2\ g^{-1}$

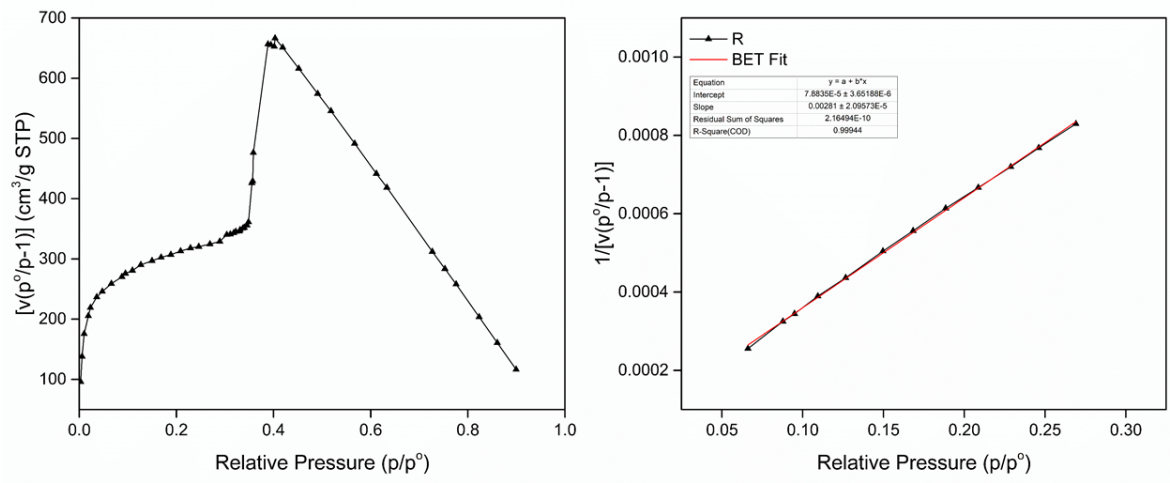

Figure 1. a) Rouquerol BET plot of R and b) surface area plot showing the BET fit and associated parameters.

References:

1. Rouquerol, J.; Llewellyn, P.; Rouquerol, F. *Stud. Surf. Sci. Catal.* **2007**, *160*, 49-56.
2. Walton, K. S.; Snurr, R. Q. *J. Am. Chem. Soc.* **2007**, *129*, 8552-8556.

Lab 11

BET calculations for sample R were carried out according to the following procedure:

1. The uptake (v) and relative pressure (p/p_o) were plotted to obtain the nitrogen isotherm (**Fig. 1**).
2. $v(P_o-P)$ was calculated and plotted against p/p_o (**Fig. 2**) to obtain the suitable p/p_o range for BET analysis (0.094992-0.289294).
3. $1/(v((p_o/p)-1))$ was calculated and plotted against p/p_o to obtain the BET plot. The range specified above was used to calculated BET area while maximizing R^2 (**Fig. 3**).
4. The BET equation was used to obtain c and v_m from the BET plot,

$$\frac{1}{\left[V_a\left(\frac{P_0}{P}-1\right)\right]}=\frac{C-1}{V_mC}\times\frac{P}{P_0}+\frac{1}{V_mC}$$

and the BET surface area equation was used to obtain 1532 m^2/g.

$$S=\frac{V_mN_a}{m\times 22400}$$

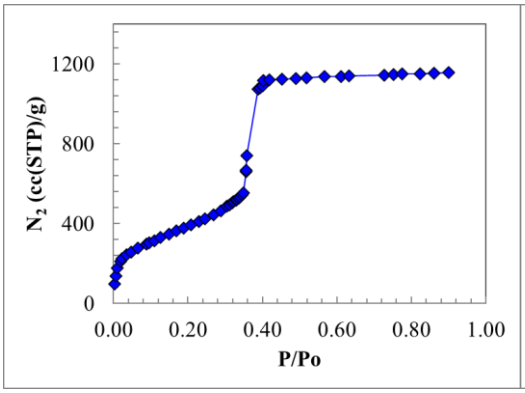

Figure 1. plot of uptake vs. p/p_o.

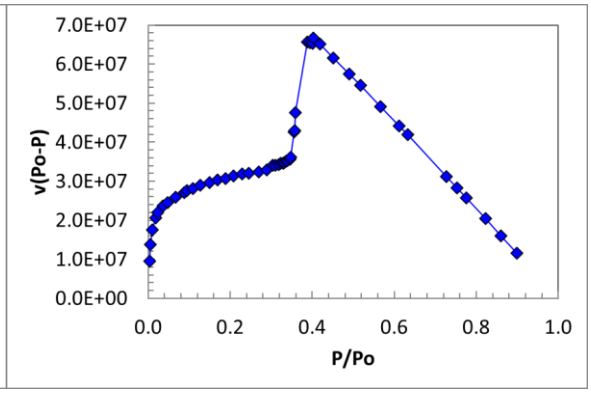

Figure 2. plot of $v(P_o-P)$ vs. p/p_o.

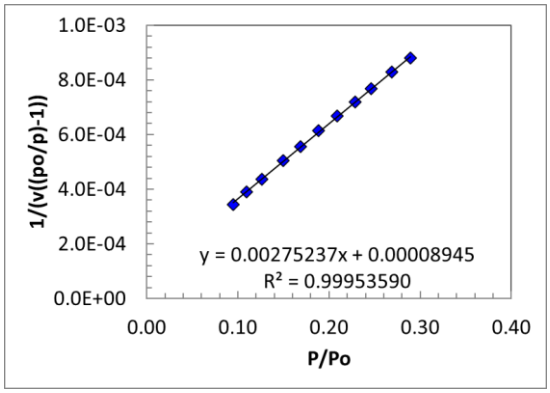

Figure 3. BET plot.

Lab 12

Method: BET areas were calculated manually on Excel following the Rouquerol criteria.

Relative Pressure	Quantity Adsorbed (cm3/g STP)	(P/Po)	N(1-P/Po)	(P/Po)/N(1-P/Po)	
0.002879	96.1832	0.002879	95.91	3.00E-05	
0.005757	138.9144	0.005757	138.11	4.17E-05	
0.010075	177.3544	0.010075	175.57	5.74E-05	
0.018711	209.3352	0.018711	205.42	9.11E-05	
0.023028	224.256	0.023028	219.09	1.05E-04	
0.035982	245.5	0.035982	236.67	1.52E-04	
0.047496	258.2072	0.047496	245.94	1.93E-04	
0.066207	277.2528	0.066207	258.90	2.56E-04	
0.087796	296.2672	0.087796	270.26	3.25E-04	
0.094992	304.744	0.094992	275.80	3.44E-04	
0.109385	315.2824	0.109385	280.80	3.90E-04	
0.126656	332.2048	0.126656	290.13	4.37E-04	
0.149684	349.0664	0.149684	296.82	5.04E-04	
0.168395	363.836	0.168395	302.57	5.57E-04	
0.188546	378.5896	0.188546	307.21	6.14E-04	
0.208695	395.4816	0.208695	312.95	6.67E-04	
0.228845	412.3736	0.228845	318.00	7.20E-04	
0.246116	425.02	0.246116	320.42	7.68E-04	
0.269145	444.02	0.269145	324.51	8.29E-04	
0.289294	463.0504	0.289294	329.09	8.79E-04	
0.303687	488.5552	0.303687	340.19	8.93E-04	
0.310883	494.8936	0.310883	341.04	9.12E-04	
0.318079	503.3704	0.318079	343.26	9.27E-04	
0.322398	509.7392	0.322398	345.40	9.33E-04	
0.329594	516.0768	0.329594	345.98	9.53E-04	
0.331034	520.3384	0.331034	348.09	9.51E-04	
0.33679	528.8296	0.33679	350.73	9.60E-04	
0.339669	533.0752	0.339669	352.01	9.65E-04	
0.345426	543.7056	0.345426	355.90	9.71E-04	
0.348305	554.3656	0.348305	361.28	9.64E-04	
0.355501	661.1936	0.355501	426.14	8.34E-04	
0.356941	667.5928	0.356941	429.30	8.31E-04	
0.358379	742.4104	0.358379	476.35	7.52E-04	
0.388605	1073.496	0.388605	656.33	5.92E-04	Cutoff (1st criteria)
0.394362	1081.984	0.394362	655.29	6.02E-04	
0.401558	1090.464	0.401558	652.58	6.15E-04	
0.402997	1116.104	0.402997	666.32	6.05E-04	
0.418829	1120.216	0.418829	651.04	6.43E-04	
0.451933	1124.144	0.451933	616.11	7.34E-04	
0.490793	1128.008	0.490793	574.39	8.54E-04	
0.51814	1131.992	0.51814	545.46	9.50E-04	
0.567074	1135.752	0.567074	491.70	1.15E-03	
0.611692	1137.424	0.611692	441.67	1.38E-03	
0.633281	1141.472	0.633281	418.60	1.51E-03	
0.726835	1142.624	0.726835	312.12	2.33E-03	
0.752741	1146.624	0.752741	283.51	2.66E-03	
0.77577	1150.656	0.77577	258.01	3.01E-03	
0.823266	1152.296	0.823266	203.65	4.04E-03	
0.860687	1154.04	0.860687	160.77	5.35E-03	
0.899547	1157.904	0.899547	116.31	7.73E-03	

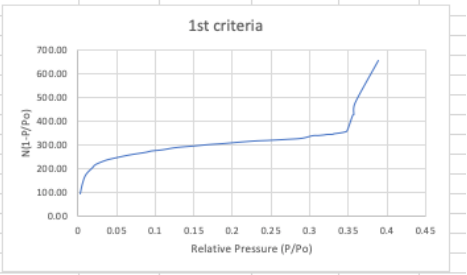

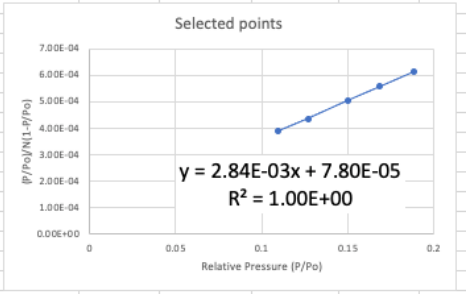

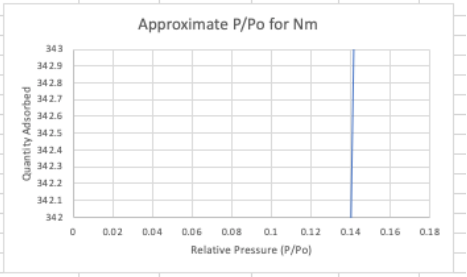

R2	1			
1/NmC	7.80E-05	y-int		
(c-1)/NmC	2.84E-03	slope		
C>0				
C	37.4103			
Nm	342.7005	cm3/g	approx. P/Po	0.14
	0.0003	m3/g		
Nav	6.02E+23			
	2.69E+25	particles/m3		
sigma	16.2	A2		
	1.62E-19	m2		
SA	1492.53	m2/g		
BET P/Po	0.1405			
	0.0281	tolerance		
	0.1124	min		
	0.1686	max		

References:

1. Gómez-Gualdrón, D. A.; Moghadam, P. Z.; Hupp, J. T.; Farha, O. K.; Snurr, R. Q., Application of Consistency Criteria To Calculate BET Areas of Micro- And Mesoporous Metal–Organic Frameworks. Journal of the American Chemical Society 2016, 138 (1), 215-224.
2. Walton, K. S.; Snurr, R. Q., Applicability of the BET method for determining surface areas of microporous metal-organic frameworks. Journal of the American Chemical Society 2007, 129 (27), 8552
3. Wang, T. C.; Bury, W.; Gómez-Gualdrón, D. A.; Vermeulen, N. A.; Mondloch, J. E.; Deria, P.; Zhang, K.; Moghadam, P. Z.; Sarjeant, A. A.; Snurr, R. Q.; Stoddart, J. F.; Hupp, J. T.; Farha, O. K., Ultrahigh Surface Area Zirconium MOFs and Insights into the Applicability of the BET Theory. Journal of the American Chemical Society 2015, 137 (10), 3585-3591.-8556.

Lab 13

Model calculation for sample R

Relative Pressure (P/P_0)	Quantity Adsorbed (cm^3/g STP)	$1/[Q(P_0/P-1)]$
0.002879	96.1832	3.00189E-05
0.005757	138.9144	4.16828E-05
0.010075	177.3544	5.73853E-05
0.018711	209.3352	9.10873E-05
0.023028	224.256	0.000105107
0.035982	245.5	0.000152037
0.047496	258.2072	0.000193118
0.066207	277.2528	0.000255727
0.087796	296.2672	0.000324862
0.094992	304.744	0.000344429
0.109385	315.2824	0.000389554
0.126656	332.2048	0.000436551
0.149684	349.0664	0.000504298
0.168395	363.836	0.000556553
0.188546	378.5896	0.00061374
0.208695	395.4816	0.000666871
0.228845	412.3736	0.000719629
0.246116	425.02	0.000768114
0.269145	444.02	0.000829378
0.289294	463.0504	0.000879065
0.303687	488.5552	0.000892705
0.310883	494.8936	0.000911575
0.318079	503.3704	0.000926645
0.322398	509.7392	0.000933404
0.329594	516.0768	0.000952636
0.331034	520.3384	0.000951005
0.33679	528.8296	0.000960268
0.339669	533.0752	0.000964952
0.345426	543.7056	0.000970583
0.348305	554.3656	0.000964093
0.355501	661.1936	0.000834238

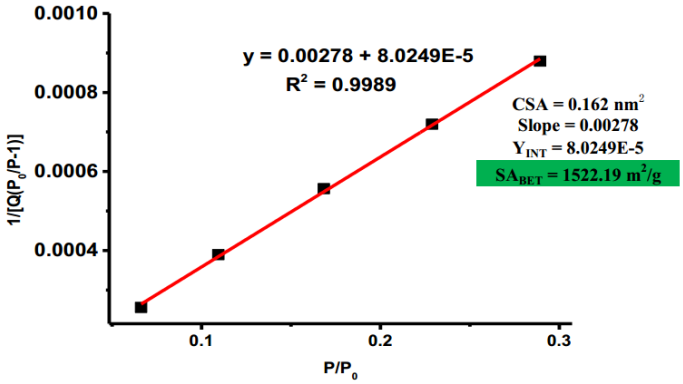

Method

For each point designated for surface area calculations, the BET[2] transformation is calculated as follows:

$$B_1 = \frac{P_{rel_1}}{(1.0 - P_{rel_1}) \times N_{ads_1}}$$

where B_I is in units of g/cm^3 STP.

A least-squares fit is performed on the (P_{relI} ,B_I) designated pairs where P_{relI} is the independent variable and B_I is the dependent variable. The following are calculated:

a. Slope (S g/cm^3 STP)

b. Y-intercept (Y_{INT} g/cm^3 STP)

c. Error of the slope (S_{ERR} g/cm^3 STP)

d. Error of the y-intercept (YI_{ERR} g/cm^3 STP)

e. Correlation coefficient (Cc)

Using the results of the above calculations, the following can be calculated:

BET Surface Area (m^2/g):

$$SA_{BET} = \frac{CSA \times (6.023 \times 10^{23})}{(22414\ cm^3\ STP) \times (10^{18}\ nm^2/m^2) \times (S + Y_{INT})}$$

where

CSA = analysis gas molecular cross-sectional area (nm^2), user-entered on the Adsorptive Properties dialog box

Lab 14

Calculation of the BET surface area for sample R was done in Microsoft Excel following the procedure outlined below:

- The value of $v(1-P/P_0)$ is plotted against P/P_0 in Figure 1 (a). The difference between two consecutive values is calculated. When this difference is < 0, thus $v(1-P/P_0)$ does not increase with P/P_0, the upper limit of the pressure range is selected. Ten data points including the upper limit are used.
- $(v(P_0/P-1))^{-1}$ is plotted against P/P_0 within this range based on the linearized BET equation: $\frac{1}{v\left(\frac{P_0}{P}-1\right)} = \frac{C-1}{V_m \cdot C} \cdot \frac{P}{P_0} + \frac{1}{V_m \cdot C}$
- The intercept of this linear regression must be > 0, so that the C parameter in the BET equation results in a positive value as well.
- The BET surface area is then determined from the intercept and slope assuming a cross-sectional area of a nitrogen molecule of 1.62e-19 m^2 and Avogadro's constant with a value of 6.022e+23 mol^{-1}.

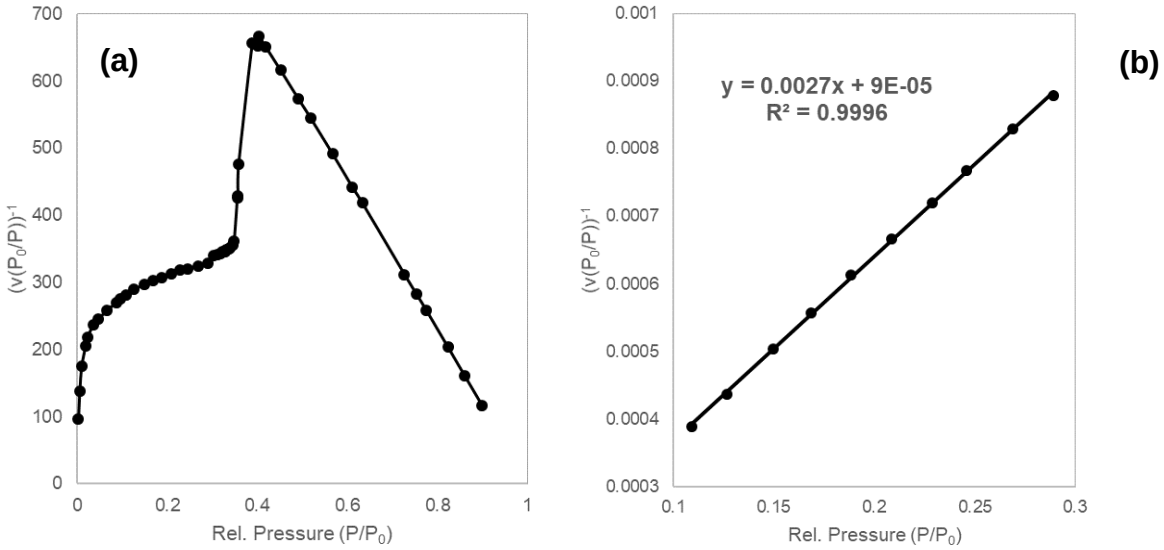

Figure 1. (a) Rouquerol plot and (b) linear regression for linearized BET equation within linear range.

Slope	0.002732081	
Intercept	9.41226E-05	
σ_{N2}	1.62E-19	m^2
V_m	3.54E+02	
C	3.00E+01	
Na	6.022E+23	mol^{-1}
A	1541.01	m^2/g

References:

- Walton, K.S.: Snurr, R.Q.: Applicability of the BET Method for Determining Surface Areas of Microporous Metal-Organic Frameworks. *J. Am. Chem. Soc.* **2007**, 129, 8552-8556
- Rouquerol, J.; Llewellyn, P.; Rouquerol, F.: Is the BET equation applicable to microporous adsorbents? *Stud. Surf. Sci. Catal.* **2007**, 160, 49-56

Lab 15

Method: The BET area was calculated using the Micromeritics Phys ViewCalc© program Attention was paid to the Rouquerol criteria, namely that

(1) The $N(1-P/P_0)$ term monotonically increases with P/P_0
(2) The C constant is positive
(3) The pressure corresponding to the monolayer loading lies in the linear range
(4) The pressure of the monolayer loading as determined by BET theory does not vary by more than 20% from that used in criterion (3)

micromeritics
www.micromeritics.com

Add/Remove Overlays

Minimum/Maximum Analysis	min.	max
Fit Data Limits	0.109385000	0.303687000
Experimental Data Limits	0.005000000	0.500000000

BET Surface Area (m^2/g)	1572.308849	26.86878548 +-
C	26.2021933	
Qm (cm^3/g STP)	361.1847029	
Slope (g/cm^3 STP)	0.002663001	0.000044 +-
Y-Intercept (g/cm^3 STP)	0.000105665	1.62741E-05 +-
Correlation	0.99874994	
Molecular CSA (nm^2)	0.162	*Nitrogen*

BET Data — *Isotherm Data Souce: CARBSV-G*

Relative Pressure (p/p°)	Quantity Adsorbed (cm^3/g STP)	1/[Q(p°/p-1)] (g/cm^3 STP)
0.002879	96.1832	3.00189E-05
0.005757	138.9144	4.16828E-05
0.010075	177.3544	5.73853E-05
0.018711	209.3352	9.10873E-05
0.023028	224.256	0.000105107
0.035982	245.5	0.000152037
0.047496	258.2072	0.000193118
0.066207	277.2528	0.000255727
0.087796	296.2672	0.000324862
0.094992	304.744	0.000344429
0.109385	315.2824	0.000389554
0.126656	332.2048	0.000436551
0.149684	349.0664	0.000504298
0.168395	363.836	0.000556553
0.188546	378.5896	0.00061374
0.208695	395.4816	0.000666871
0.228845	412.3736	0.000719629
0.246116	425.02	0.000768114
0.269145	444.02	0.000829378
0.289294	463.0504	0.000879065
0.303687	488.5552	0.000892705
0.310883	494.8936	0.000911575

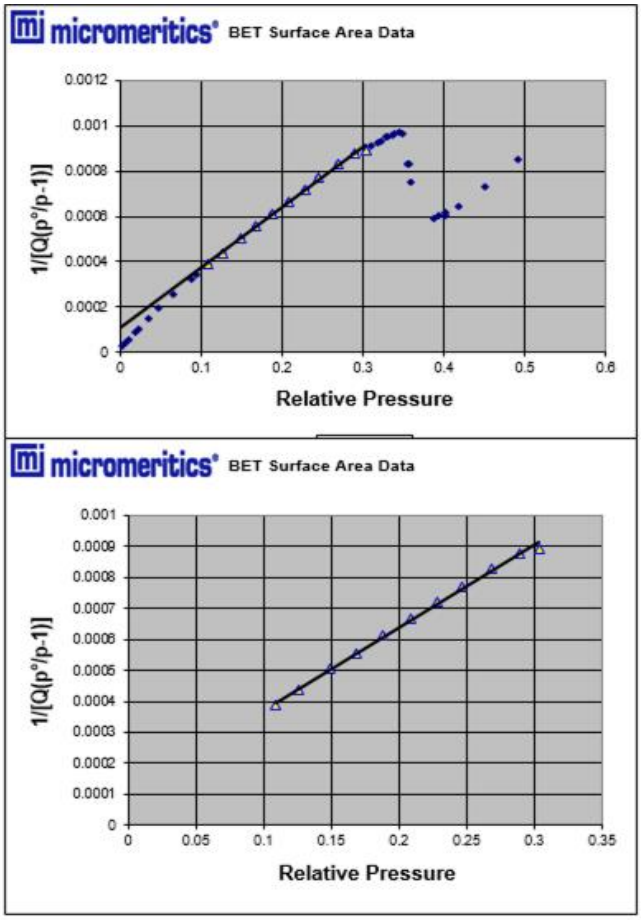

Lab 16

Method. BET equation: $$\frac{1}{V(\frac{1}{P/P_0}-1)} = \frac{1}{V_m C} + \frac{C-1}{V_m C} P/P_0$$

Where the adsorbate loading V with the relative pressure P/P_0, P_0 is the saturation pressure of nitrogen, and C and V_m are constants. C is related to the energetics of adsorption, whereas V_m corresponds to the monolayer loading, which in turn is related to the specific surface area of the material.

The BET calculations were performed following the four BET consistency criteria proposed by Rouquerol et al.,[1] namely:

(1) Only a range where $V(1/(P/P_0) - 1)$ increases monotonically with P/P_0 should be selected.

(2) The value of C resulting from the linear regression should be positive.

(3) The monolayer loading V_m should correspond to a relative pressure P/P_0 falling within the selected linear region.

(4) The relative pressure corresponding to the monolayer loading calculated from BET theory ($1/\sqrt{C} + 1$) should be equal to the pressure determined in criterion 3. (For this criterion, Rouquerol et al. suggested a tolerance of 20%.)

Model calculation for sample R:

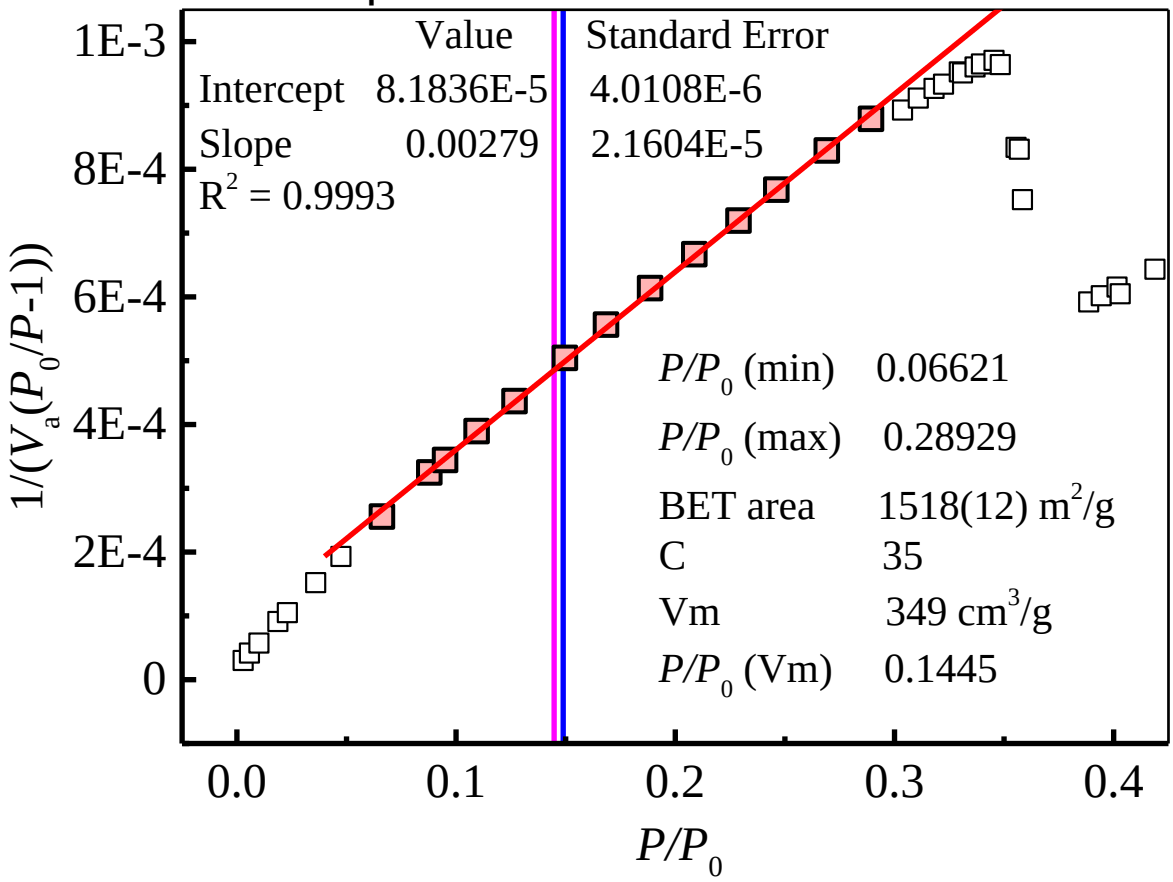

BET area calculation for sample R, that fulfils all consistency criteria. Points are selected based on the first consistency criterion. Blue vertical dashed lines indicate the P/P_0 value that correspond to the BET-predicted monolayer loadings; Pink vertical lines indicate the value of $1/(\sqrt{C}+1)$.

References:

[1] Diego A. Gómez-Gualdrón, Peyman Z. Moghadam, Joseph T. Hupp, Omar K. Farha, and Randall Q. Snurr, *J. Am. Chem. Soc.* **2016**, *138*, 215-224.

Lab 17

Fitting of the BET equation was done importing the raw data to the analysis software MicroActive (version 4.02, e572371, Micromeritics). The limit of the BET range was identified as the maximum of the Rouquerol plot ($n_a(1 - p/p_o)$ vs p/p_o) according to the criteria:
The BET "C" constant must be positive (C > 0)
$n_a(1 - p/p_o)$ must continually increase with p/p_o.
We manually selected a minimum of 5 points in the 0.05 ≤ P/P_0 ≤ 0.30 range to avoid the effect of capillary condensation, maximizing the correlation coefficient R of the line.

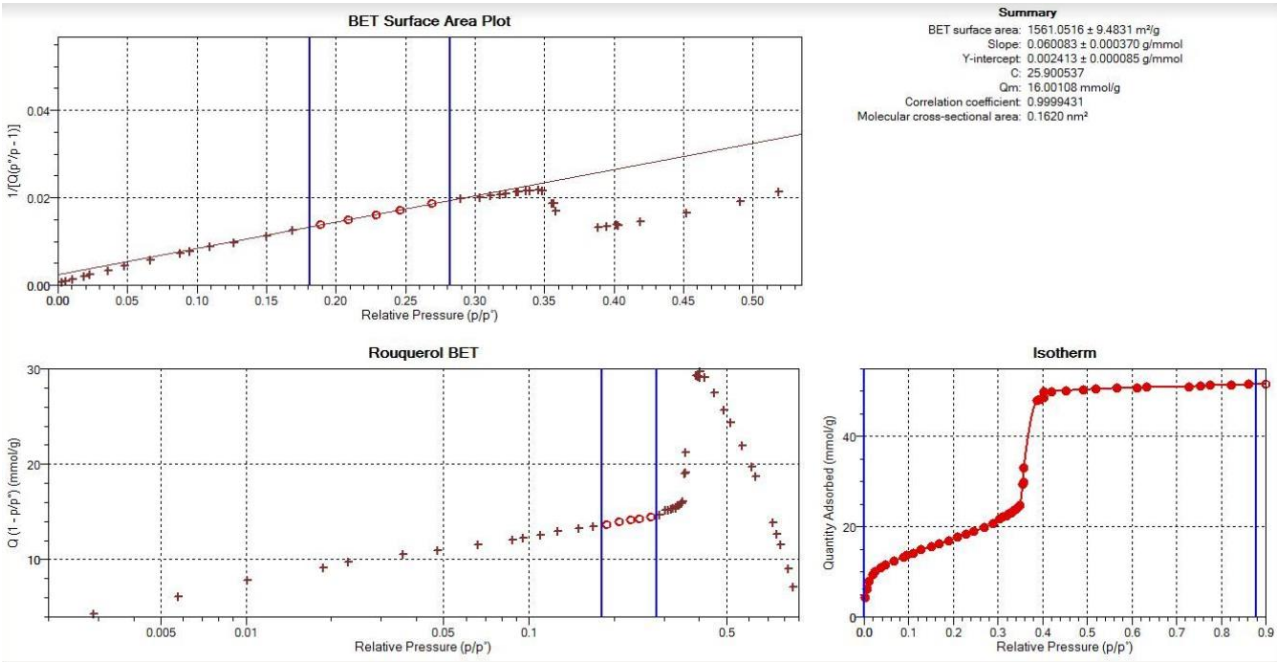

Lab 18

Method:

We determined BET surface areas from the supplied N_2 adsorption isotherm at 77 K (R.csv) according to the following procedures[1]:

1) A section of the adsorption isotherm branch was selected where $v\left(1-\frac{P}{P_0}\right)$ increases versus $\left(\frac{P}{P_0}\right)$, where v is the amount of N_2 adsorbed.

2) Within this section, sequential data points that led to a positive intercept in the plot of $\left[\frac{\left(\frac{P}{P_0}\right)}{v\left(1-\frac{P}{P_0}\right)}\right]$ against (P/P_0), were identified. This plot results in a slope *a*, and a positive intercept *b*. The amount of N_2 adsorbed in the intial monolayer is $v_m = \frac{1}{a+b}$

3) The BET surface area was determined based on the following equation:

$$A_{BET} = v_m\,(cm^3 g^{-1}) \times \frac{1(mol)}{22400(cm^3)} \times s_0\,(\text{Å}^2) \times N_A(mol^{-1}) \times 10^{-20}\ \left(\frac{m^2}{\text{Å}^2}\right)$$

Where N_A is Avogadro's constant (6.023×10^{23} mol^{-1}) and s_0 is the cross-sectional area of a N_2 molecule, which is 16.2 $Å^2$.

Model calculation for sample R:

For the isotherm R.csv, the section 0.003 < $\left(\frac{P}{P_0}\right)$ < 0.345 was selected.

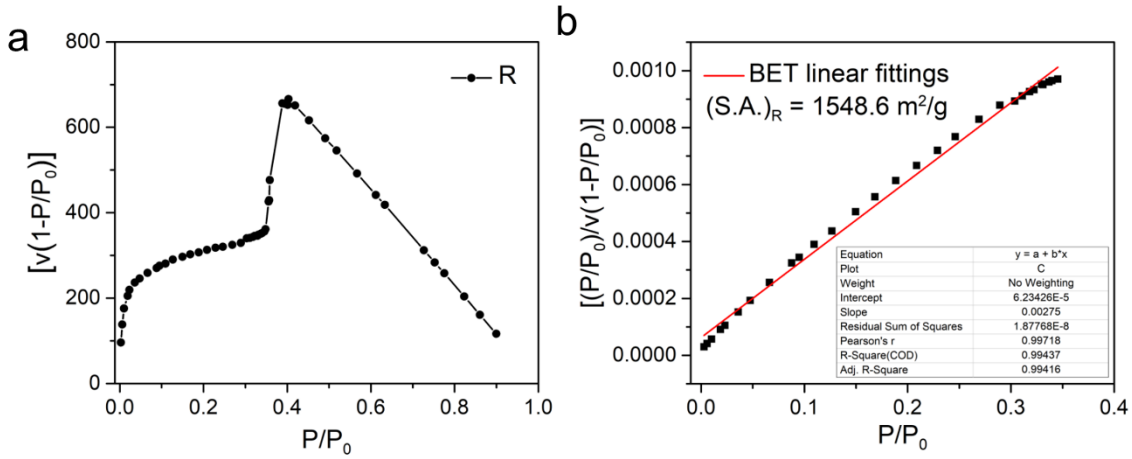

Reference:

[1] K. S. Walton, R. Q. Snurr, *J. Am. Chem. Soc.* **2007**, *129*, 8552-8556.
[2] A. J. Howarth, A. W. Peters, N. A. Vermeulen, T. C. Wang, J. T. Hupp, O. K. Farha, *Chem. Mater.* **2017**, *29*, 26-39.

Lab 19

The method used was:
We calculated the BET SA employing the Micromeritics MicroActive Software (version 4.04) and following the Rouquerol criteria:

- Do a multi-point BET SA determination using the first 5 points (Lowest P/Po) starting at P/Po = .05
- If R2 value is greater than .998, then keep data.
- If R2 value is less than .998, move to higher P/Po point by point until R2 value reaches greater than .998

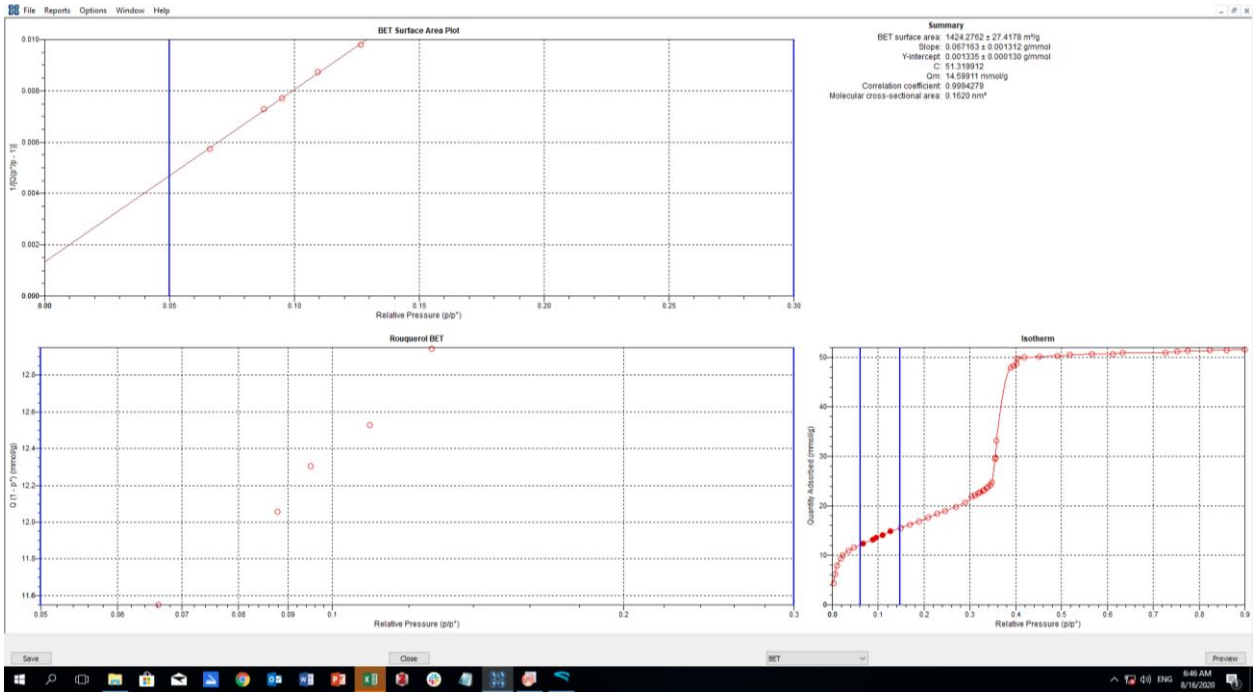

References:

1. Rouquerol, J.; Llewellyn, P.; Rouquerol, F. Is the bet equation applicable to microporous adsorbents? In *Studies in Surface Science and Catalysis*; Elsevier Inc., 2007; Vol. 160, pp. 49–56.

Lab 20

1. We open the isotherm raw data in an excel spreadsheet.
2. We plot the isotherm - Figure 1(a) - to verify its IUPAC classification, behavior or any anomalies.
3. We then plot $\boldsymbol{n(1-P/P_0)}$ against $\boldsymbol{P/P_0}$ - Figure 1(b) - in order to choose the suitable pressure range to be used in the linear plot that calculates BET area – Figure 1 (c). This pressure range must satisfy all Rouquerol criteria [1], as follows.

   Rouquerol criteria:

   a. C should be positive;
   b. Points to be used in BET plot should be within the range where the term $\boldsymbol{n(1-P/P_0)}$ increases with $\boldsymbol{P/P_0}$. Points beyond the maximum in the plot should be discarded;
   c. The pressure corresponding to $\boldsymbol{n_m}$ should be within the pressure range used in BET plot;
   d. The value of $(\boldsymbol{P/P_0})_{\boldsymbol{n_m}}$ should not differ by more than 10% from the value of $\boldsymbol{P/P_0}$corresponding to the $\boldsymbol{n_m}$ from BET plot;

$$\left(\frac{P}{P_0}\right)_{n_m} = \frac{1}{\sqrt{C}+1}$$

Note that sometimes a wide pressure range may satisfy Rouquerol criteria, therefore our points selection is also guided by two additional requirements, i.e., a good linear correlation, ($R^2 \geq 0.998$) and at least four points [2].

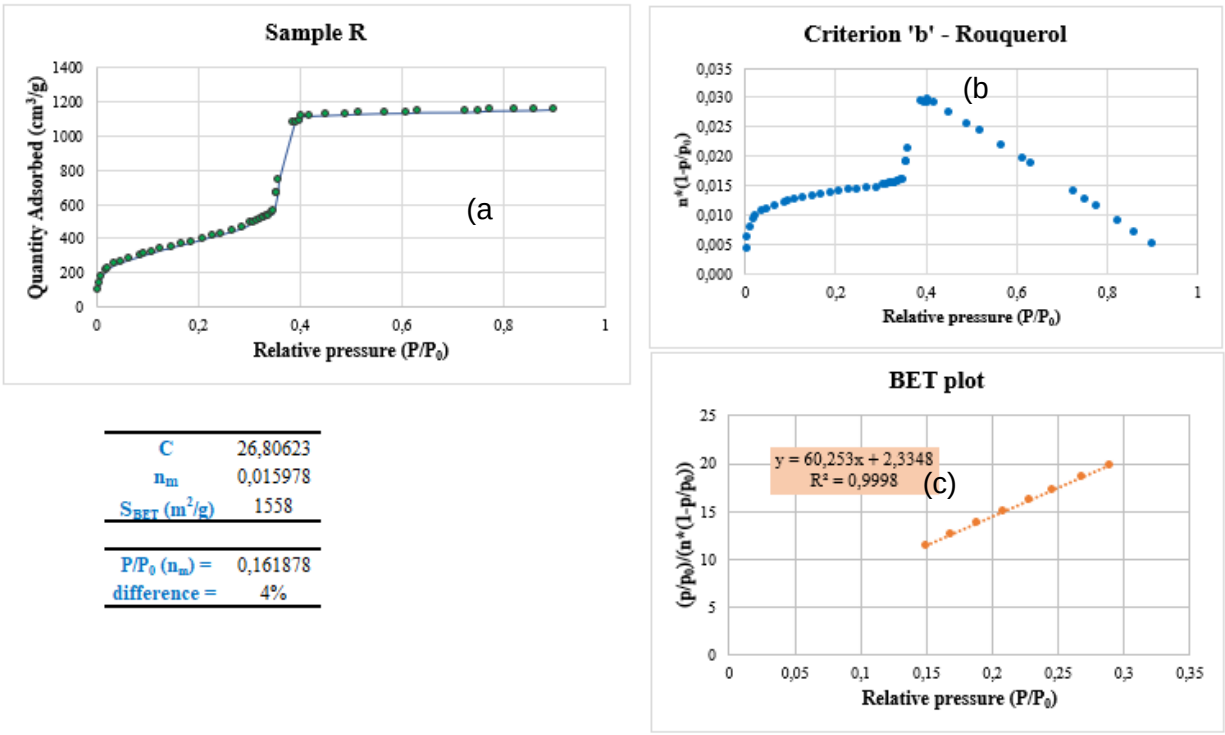

C	26,80623
n_m	0,015978
S_{BET} (m^2/g)	1558
P/P_0 (n_m) =	0,161878
difference =	4%

Figure 1. (a) N_2 adsorption isotherm at 77K for sample R; (b) plot to guide the choice of p/p_0 range to be used in the (c) classical BET linear plot.

[1] ROUQUEROL, Françoise, *et al*. Adsorption by Powders and Porous Solids, 2 ed. France, Elsevier, 2014.

[2] SINHA, Pryia, *et al*. Surface Area Determination of Porous Materials Using the Brunauer Emmett−Teller (BET) Method: Limitations and Improvements. The Journal of Physical Chemistry, 2019, 123, 20195−20209, DOI: 10.1021/acs.jpcc.9b02116.

Lab 21

Method: The BET area was calculated manually in Excel and Origin following the Rouquerol Equation [1]

p/p_0	Q_{ads} (cm^3/g)	Q_{ads} (mmol/g)	$1/(Q_{ads}*((1/p/p_0)-1))$		Ec	y =	0,10075	x +	0,00236
0,00288	96,1832	2,7743	0,00104		nm =	9,69838037	mmol/g		
0,00576	138,9144	4,0068	0,00145		C =	43,690678			
0,01008	177,3544	5,1156	0,00199		BET =	946,139075	m^2/g		
0,01871	209,3352	6,0380	0,00316		Molecular area	0,162	nm^2/molec		
0,02303	224,2560	6,4684	0,00364						
0,03598	245,5000	7,0811	0,00527						
0,0475	258,2072	7,4477	0,0067						
0,06621	277,2528	7,9970	0,00887						
0,0878	296,2672	8,5455	0,01126						
0,09499	304,7440	8,7900	0,01194						
0,10939	315,2824	9,0939	0,01351						
0,12666	332,2048	9,5820	0,01514						
0,14968	349,0664	10,0684	0,01748						
0,16839	363,8360	10,4944	0,0193						
0,18855	378,5896	10,9199	0,02128						
0,20869	395,4816	11,4072	0,02312						
0,22884	412,3736	11,8944	0,02495						
0,24612	425,0200	12,2592	0,02663						
0,26915	444,0200	12,8072	0,02875						
0,28929	463,0504	13,3561	0,03048						
0,30369	488,5552	14,0918	0,03095						
0,31088	494,8936	14,2746	0,0316						
0,31808	503,3704	14,5191	0,03213						
0,3224	509,7392	14,7028	0,03236						
0,32959	516,0768	14,8856	0,03303						
0,33103	520,3384	15,0085	0,03297						
0,33679	528,8296	15,2534	0,03329						
0,33967	533,0752	15,3759	0,03345						
0,34543	543,7056	15,6825	0,03365						
0,3483	554,3656	15,9900	0,03342						
0,3555	661,1936	19,0713	0,02892						
0,35694	667,5928	19,2559	0,02883						
0,35838	742,4104	21,4139	0,02608						
0,3886	1.073,4960	30,9637	0,02053						
0,39436	1.081,9840	31,2085	0,02086						
0,40156	1.090,4640	31,4531	0,02133						
0,403	1.116,1040	32,1926	0,02097						
0,41883	1.120,2160	32,3112	0,0223						
0,45193	1.124,1440	32,4245	0,02543						
0,49079	1.128,0080	32,5360	0,02962						
0,51814	1.131,9920	32,6509	0,03293						
0,56707	1.135,7520	32,7594	0,03998						
0,61169	1.137,4240	32,8076	0,04802						
0,63328	1.141,4720	32,9243	0,05245						
0,72684	1.142,6240	32,9576	0,08073						
0,75274	1.146,6240	33,0729	0,09205						
0,77577	1.150,6560	33,1892	0,10424						
0,82327	1.152,2960	33,2365	0,14015						
0,86069	1.154,0400	33,2868	0,1856						
0,89955	1.157,9040	33,3983	0,26812						

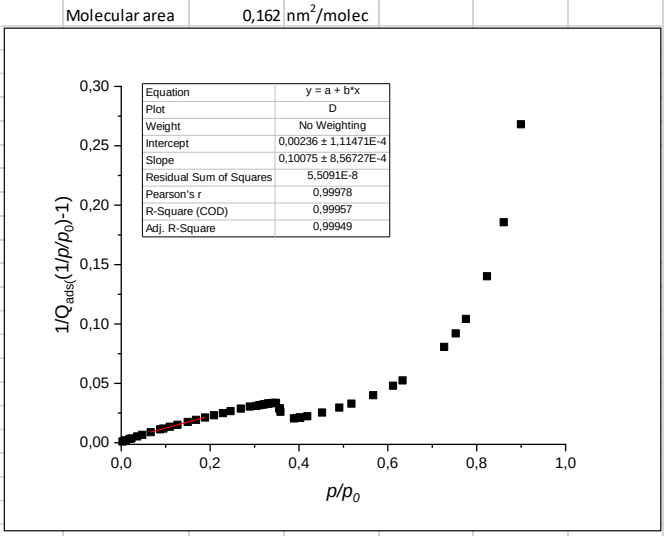

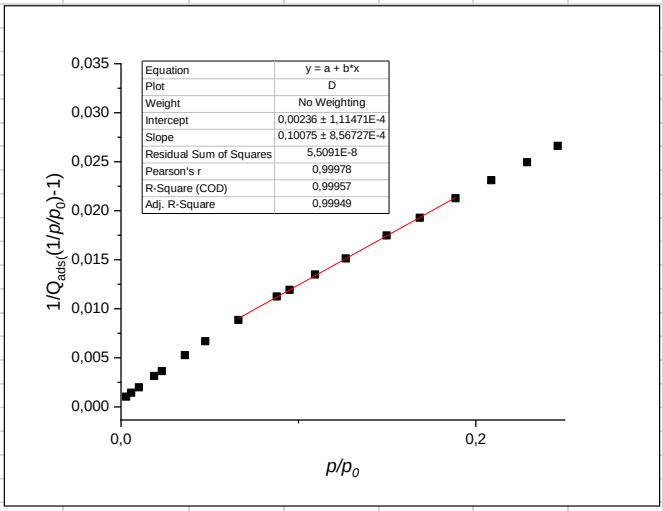

References:

1. Rouquerol, J.; Llewellyn, P.; Rouquerol, F. Is the bet equation applicable to microporous adsorbents? In *Studies in Surface Science and Catalysis*; Elsevier Inc., 2007; Vol. 160, pp. 49–56.

Lab 22

The calculation followed the consistency criteria as set by Roquerol. Namely, N(1-P/P0) increases monotonically in a given range of P/P0, the calculated C value is always positive, the monolayer loading falls in the range of P/P0 selected, and the relative pressure from 1/(sqrt(C) + 1) matches that of the monolayer loading. The figure below shows the data for sample R. The graph shown plots N(1-P/P0) versus the relative pressure for the full range. Then, built-in Microsoft Excel functions are used for the slope and intercept calculations of the desired region. The highlighted cells show the agreement of the monolayer loading and relative pressure.

	A	B	C	D	E	F	G
1	Relative Pressure (P/Po)	Quantity Adsorbed (cm3/g STP)	P	P/(N(Po-P))	N(1-P/Po)		
2	0.002879	96.1832	2.92E-01	3.00E-05	9.59E+01		
3	0.005757	138.9144	5.83E-01	4.17E-05	1.38E+02		
4	0.010075	177.3544	1.02E+00	5.74E-05	1.76E+02		
5	0.018711	209.3352	1.90E+00	9.11E-05	2.05E+02		
6	0.023028	224.256	2.33E+00	1.05E-04	2.19E+02		
7	0.035982	245.5	3.64E+00	1.52E-04	2.37E+02		
8	0.047496	258.2072	4.81E+00	1.93E-04	2.46E+02		
9	0.066207	277.2528	6.71E+00	2.56E-04	2.59E+02		
10	0.087796	296.2672	8.89E+00	3.25E-04	2.70E+02		
11	0.094992	304.744	9.62E+00	3.44E-04	2.76E+02		
12	0.109385	315.2824	1.11E+01	3.90E-04	2.81E+02		
13	0.126656	332.2048	1.28E+01	4.37E-04	2.90E+02		
14	0.149684	349.0664	1.52E+01	5.04E-04	2.97E+02		
15	0.168395	363.836	1.71E+01	5.57E-04	3.03E+02	slope	0.002763464
16	0.188546	378.5896	1.91E+01	6.14E-04	3.07E+02	int	8.69251E-05
17	0.208695	395.4816	2.11E+01	6.67E-04	3.13E+02	N	350.8292759
18	0.228845	412.3736	2.32E+01	7.20E-04	3.18E+02	BETSA	1526.717077
19	0.246116	425.02	2.49E+01	7.68E-04	3.20E+02	C	32.79132224
20	0.269145	444.02	2.73E+01	8.29E-04	3.25E+02	p/p0 nm	0.148668581
21	0.289294	463.0504	2.93E+01	8.79E-04	3.29E+02		
22	0.303687	488.5552	3.08E+01	8.93E-04	3.40E+02		
23	0.310883	494.8936	3.15E+01	9.12E-04	3.41E+02		
24	0.318079	503.3704	3.22E+01	9.27E-04	3.43E+02		
25	0.322398	509.7392	3.27E+01	9.33E-04	3.45E+02		

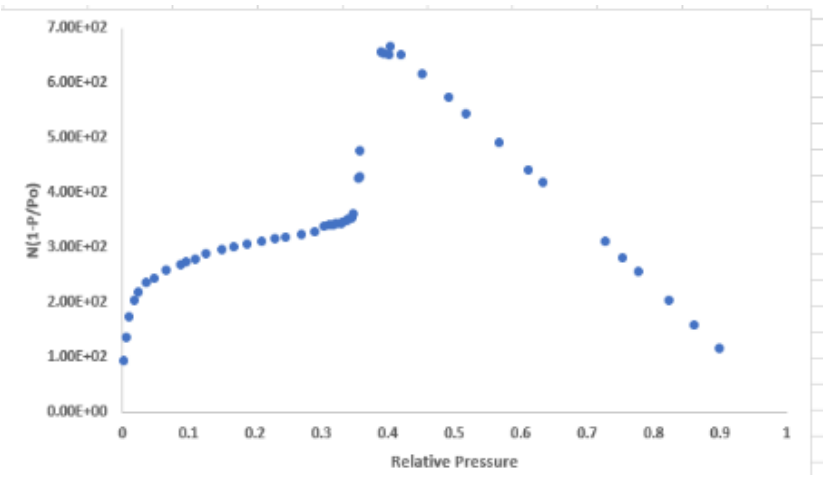

Lab 23

To calculate surface areas we applied the following criteria

1. BET Isotherm fit should be linear over designated range
2. The pressure range selected should monotonically increase with $n(1-P/P_0)$ as a function of P/P_0
3. The parameter C resulting from linear regression should be greater than 0
4. The monolayer loading (i.e. n_m should correspond to a relative pressure (i.e. P/P_0) within the selected linear range
5. The relative pressure corresponding to the calculated value for the monolayer formation (i.e. $[\text{sqrt}(C)+1]^{-1}$) should be equal to the pressure determined in criterion 3 (although a tolerance of 20% is acceptable

Our method, in short was as follows

1. Plot the N_2 physisorption isotherm
2. Calculate $n(1-P/P_0)$ for all points, identifying the range of relative pressure values which satisfied criteria 2 above
3. Plot the BET isotherm for all relative pressures identified in step 2
4. Eliminate any points in the BET isotherm which result in a negative slope of the BET isotherm
5. Starting from the highest relative pressure, plot the linear region of the BET isotherm, and calculate relevant parameters from the slope and intercept of the linear regression
6. Confirm the C parameter is positive (criteria 3 above)
7. Confirm n_m value falls within the range values of quantity adsorbed from the isotherm in the calculated relative pressure range (criteria 4 above)
8. Check Criteria 5 above, confirming we are within 20%
9. In the event multiple linear ranged were found but were bound by values which were eliminated by having negative slopes, both linear regions were considered in the calculation.
10. Round BET surface area values to 2-3 significant digits.

Lab 24

Specific surface area analyses. The Brunauer-Emmett-Teller (BET) surface areas were all assessed from the provided N_2 adsorption isotherms based on the BET equation according to the consistency criteria.[1,2] The original sorption data were converted into .raw files readable by Quantachrome ASiQwin software, version 5.0. P/P_0 region was selected using the micropore BET assistant module based on the first and second consistency criterion. BET plots and linear regression were automatically generated by Multi-point BET plot module. BET surface areas were calculated and rounded for the final report.

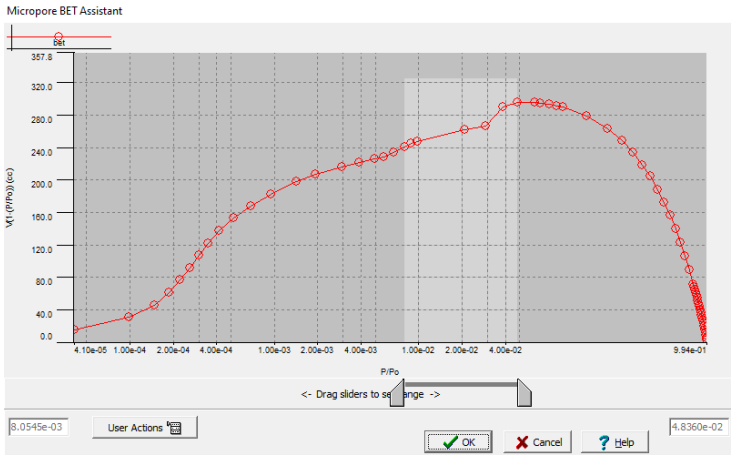

Figure 1. Micropore BET assistant module in Quantachrome ASiQwin was used to determine the P/P_0 region for BET surface area calculation.

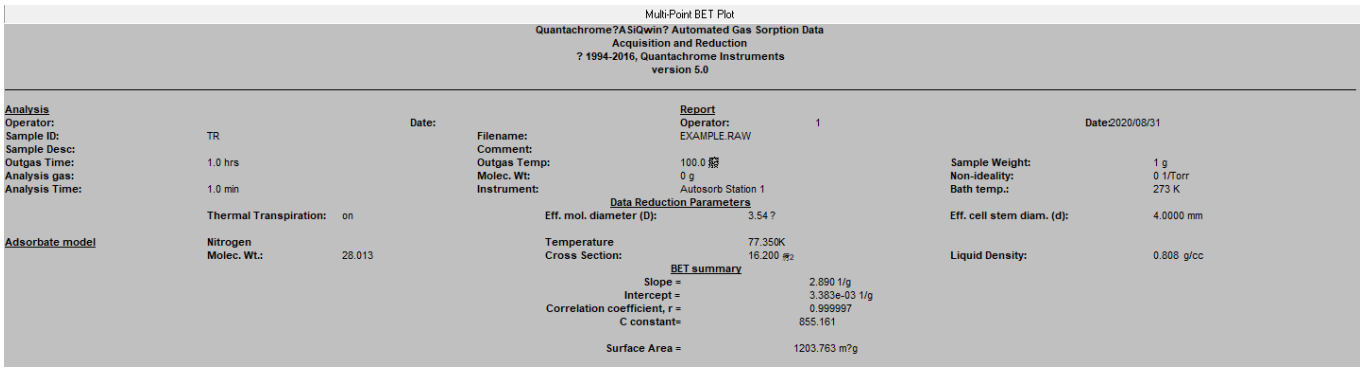

Figure 2. Interface of Quantachrome ASiQwin and BET summary.

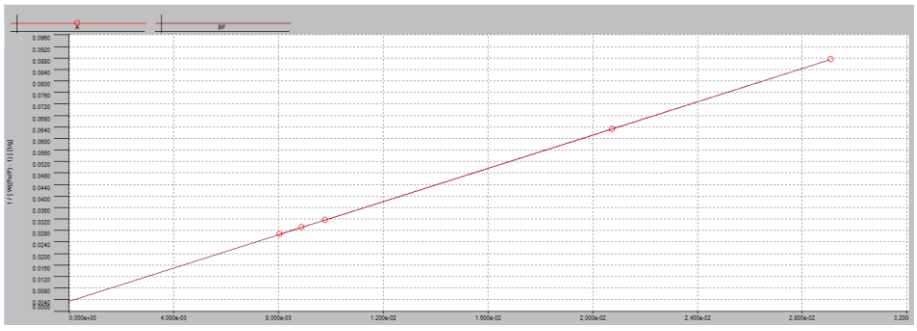

Figure 3. Example of BET plot generated by Quantachrome ASiQwin.

(1) Brunauer, S.; Emmett, P. H.; Teller, E. *Adsorption of Gases in Multimolecular Layers. J. Am. Chem. Soc.* **1938**, *60*, 309–319.
(2) Sing, K. S. W. In *Adsorption by Powders and Porous Solids*, 2nd ed.; Rouquerol, F., Rouquerol, J., Sing, K. S. W., Llewellyn, P., Maurin, G., Eds.; Academic Press: Oxford, **2014**; pp 237.

Lab 25

Method: The BET area was calculated with Excel using Micromeritics Physi ViewCalc© Tool.

Minimum/Maximum Analysis	min.	max
Fit Data Limits	0.149684000	0.246116000
Experimental Data Limits	0.005000000	0.500000000
Real limits	0.005757000	0.490793000

BET Surface Area (m^2/g)	1543.348834	11.47683737 +-
C	28.749842	
Qm (cm^3/g STP)	354.5321203	
Slope (g/cm^3 STP)	0.00272251	0.000019 +-
Y-Intercept (g/cm^3 STP)	0.000098109	8.66924E-06 +-
Correlation	0.999901581	
Molecular CSA (nm^2)	0.162	*Nitrogen*

BET Data	*Isotherm Data Souce: R-1*	
Relative Pressure (p/p)	Quantity Adsorbed (cm^3/g STP)	1/[Q(p°/p-1)] (g/cm^3 STP)
0.005757	138.9144	4.16828E-05
0.010075	177.3544	5.73853E-05
0.018711	209.3352	9.10873E-05
0.023028	224.256	0.000105107
0.035982	245.5	0.000152037
0.047496	258.2072	0.000193118
0.066207	277.2528	0.000255727
0.087796	296.2672	0.000324862
0.094992	304.744	0.000344429
0.109385	315.2824	0.000389554
0.126656	332.2048	0.000436551
0.149684	349.0664	0.000504298
0.168395	363.836	0.000556553
0.188546	378.5896	0.00061374
0.208695	395.4816	0.000666871
0.228845	412.3736	0.000719629
0.246116	425.02	0.000768114
0.269145	444.02	0.000829378
0.289294	463.0504	0.000879065
0.303687	488.5552	0.000892705
0.310883	494.8936	0.000911575
0.318079	503.3704	0.000926645
0.322398	509.7392	0.000933404
0.329594	516.0768	0.000952636
0.331034	520.3384	0.000951005
0.33679	528.8296	0.000960268
0.339669	533.0752	0.000964952
0.345426	543.7056	0.000970583
0.348305	554.3656	0.000964093
0.355501	661.1936	0.000834238
0.356941	667.5928	0.000831446
0.358379	742.4104	0.00075235
0.388605	1073.496	0.000592088
0.394362	1081.984	0.000601812
0.401558	1090.464	0.00061534
0.402997	1116.104	0.000604812
0.418829	1120.216	0.000643326
0.451933	1124.144	0.000733531
0.490793	1128.008	0.00085446

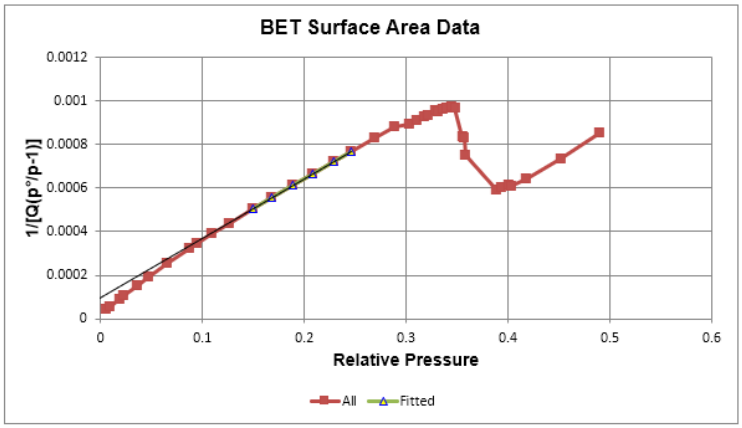

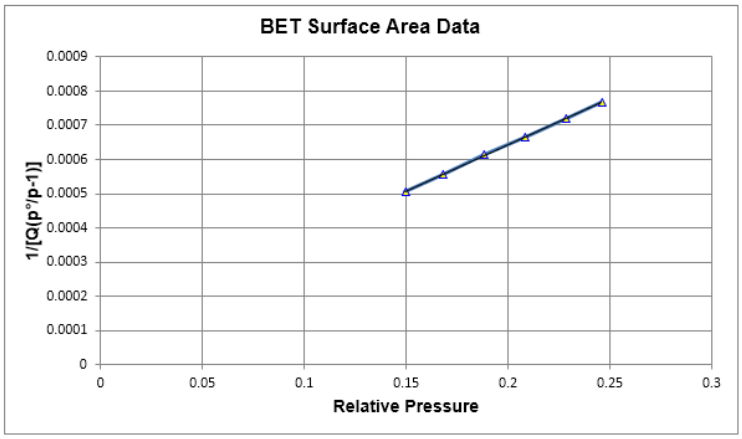

Lab 26

The BET surface areas were calculated manually with BET equation

$$\frac{1}{v[(p_0/p)-1)]} = \frac{c-1}{v_m c}\left(\frac{p}{p_0}\right) + \frac{1}{v_m c} \qquad (1)$$

where p and p_0 are the equilibrium and the saturation pressure of adsorbates at the temperature of adsorption, v is the gravimetric adsorbed gas quantity, and v_m is the gravimetric monolayer adsorbed gas quantity. c is the BET constant.

$\frac{1}{v[(p_0/p)-1)]}$ is plotted against $\frac{p}{p_0}$ with linear fitting. With the slope A and the y-intercept $v_m = \frac{1}{A+I}$ (2)

In the fitting, the following criteria were applied for choosing the fitting $\frac{p}{p_0}$ range:

(1) the plot should be linear in the range.

(2) $v[(p_0/p)-1)]$ increases with $\frac{p}{p_0}$ in the fitting range.

(3) c (or the intercept I) should be positive.

Once determined, the following equation is used for the calculation of BET surface area:

$$S_{BET} = \frac{v_m N s}{V} \qquad (3)$$

$0.05 < \frac{p}{p_0} < 0.30$, and with slope 0.00273 and y-intercept 8.90863E-5, the BET surface area is calculated to be 1543.8 m^2/g.

For all the samples, the BET areas were manually calculated applying the BET equation (1) using a Microsoft Excel® spreadsheet following the Rouquerol criteria, as described in the latest IUPAC technical report (*Pure Appl. Chem.* 87, 1051–1069 (2015)):

1. *c should be positive*
2. *application of the BET equation should be restricted to the range where the term $v(1 - p/p_0)$ continuously increases with p/p_0*
3. *the p/p_0 value corresponding to v_m should be within the selected BET range*

$$\frac{1}{v\left[\left(p_0/p-1\right)\right]} = \frac{c-1}{v_m c}\left(\frac{p}{p_0}\right) + \frac{1}{v_m c} \qquad (1)$$

where p/p_0 and the volume of adsorbed gas were given for every sample (Figure 1a shows the isotherm of sample R). Both v_m (the volume of the monolayer) and *c* (the BET constant) were calculated by plotting $\frac{1}{v\left[\left(p_0/p-1\right)\right]}$ against $\left(\frac{p}{p_0}\right)$ using a region with linear fit ($R^2 > 0.995$), which satisfies the abovementioned criteria. See Figure 1b for the entire plot of sample R and Figure 1c for the selected p/p_0 range.

From the slope (S) and the y-intercept (i) obtained from the fitting, both

$$v_m = \frac{1}{S+i} \qquad (2)$$

$$c = 1 + \frac{S}{i} \qquad (3)$$

From these values, the BET area was obtained using (4). $0.066 < p/p_0 < 0.299$, yielding a value of 1518 m^2/g.

$$S_{BET} = \frac{v_m N \sigma}{V} \qquad (4)$$

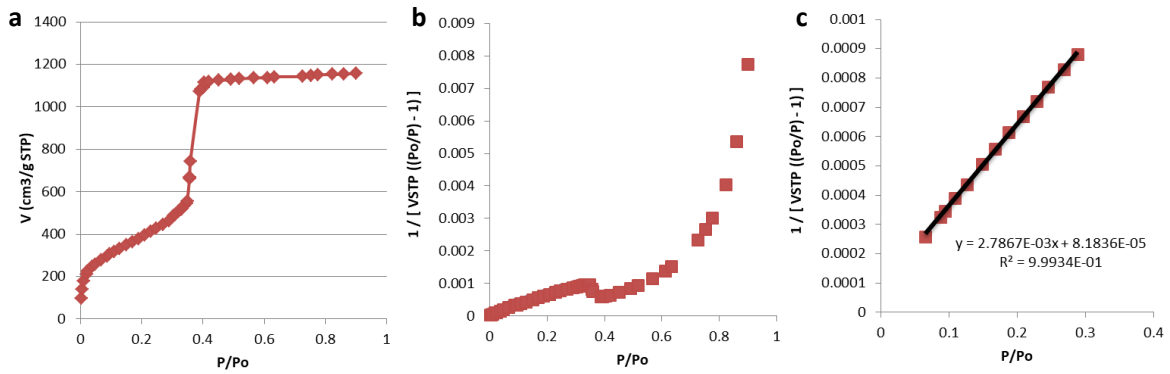

For sample R, the calculation was quite straightforward; however, in other samples (as stated in the paper) the selection of the p/p_0 range was more difficult and required additional steps to satisfy the three aforementioned criteria.

Lab 28

Model Calculation for Material R

We have computed the BET surface areas using the technique outlined in Walton and Snurr.[1] We use the same technique by applying it to experimental N_2 physisorption data. The BET equation for modeling adsorption is given by

$$v = \frac{c v_m (p/p_0)}{(1 - p/p_0)[1 + (c-1)\, p/p_0]}$$

where p/p_0 is relative pressure, v is the volume of adsorbed N_2 per gram of material at STP, c and v_m are the BET parameters to be estimated. Once c and v_m are determined, the BET surface area is computed using $A = v_m \sigma_0 N_{avg}$,where σ_0 is the cross-section area of liquid nitrogen and N_{avg} is the Avogadro constant. The value of σ_0 used in this work is 16.2 $Å^2$.

Figure 1(a) shows the N_2 isotherm at 77 K for material R. We have used the following consistency criteria[1-2] – (i) The isotherm data is restricted to a pressure range where $v(p_0 - p)$ is an increasing function of p/p_0 and (ii) The y-intercept data in the BET linear fit must be positive to obtain a physically meaningful estimate of the c parameter. In Figure 1(b), we have plotted $v(p_0 - p)$ as a function of the relative pressure. On this basis we restricted the isotherm data to $p/p_0 < 0.34$ for the BET analysis. Fig 1(c) shows the restricted isotherm data to which we fit the BET equation, giving a BET surface area for material R of 1578 m^2/g. This fit satisfies criterion (ii).

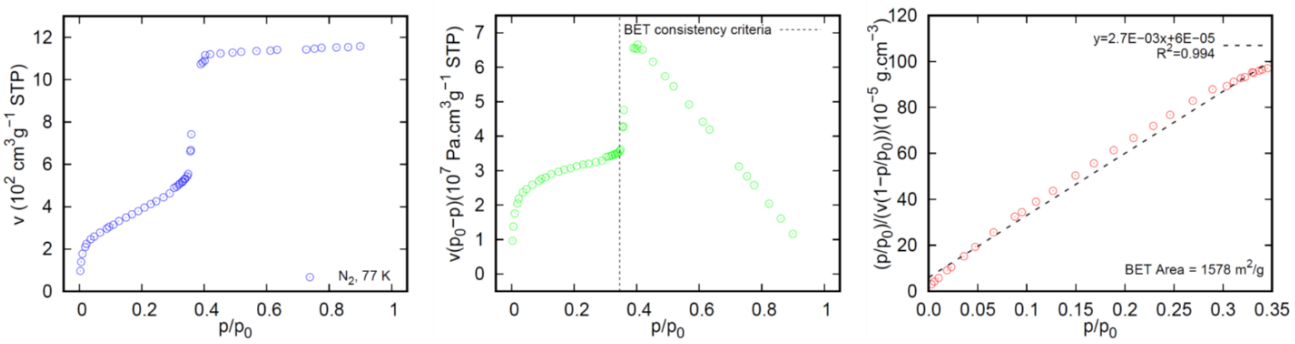

Figure 1: (a) N_2 adsorption isotherm at 77 K for material R (b) BET consistency criteria plot to determine the pressure range for analysis and (c) BET linear fit to the data in the restricted pressure range.

References

1. Walton, K. S.; Snurr, R. Q. Applicability of the BET Method for Determining Surface Areas of Microporous Metal−Organic Frameworks. *J. Am. Chem. Soc.* **2007**, *129*, 8552-8556.
2. Rouquerol, J.; Llewellyn, P.; Rouquerol, F. Is the BET equation applicable to microporous adsorbents? *Stud. Surf. Sci. Catal.* **2007**, 160, 49-56.

Lab 29

The Micromeritics 3Flex software was used to create the .smp files, which were then analysed in the Micromeritics Microactive software package.

Once the .smp file was created, a 'default' set of parameters was applied: for BET surface areas, these are the pressure range used for the calculation. The pressure range was then manually adjusted for each isotherm individually, and the surface area was calculated per the standard BET theory, using the Micromeritics Microactive software package.

Microactive's built-in features were used to help determine the correct pressure range. These include displaying the BET surface area, slope, y-intercept, C-value, the monolayer capacity and the correlation coefficient, which are updated as the pressure range is adjusted. Rouquerol BET plots were used to help determine the maximum capacity. A set of rules for fitting BET surface areas has been defined by IUPAC and Rouquerol et al,[1,2] which was followed here.

References

1. Thommes, M. *et al.* Physisorption of gases, with special reference to the evaluation of surface area and pore size distribution (IUPAC Technical Report). *Pure Appl. Chem.* **87**, 1051–1069 (2015).
2. Rouquerol, J., Llewellyn, P. & Rouquerol, F. Is the BET equation applicable to microporous adsorbents? *Stud. Surf. Sci. Catal.* **160**, 49–56 (2007).

Lab 30

Method:

1) According to BET theory[1], relative pressures near completed monolayers usually occurs at range of $0.05 < P/P_0 < 0.3$. Choose this range as first guess.
2) Plot the left side of eq. (1) versus selected range of relative pressure, do the linear regression data and obtain linear equation from that plot and the value of both *C* and *Nm* as well.
$$\frac{P/P_0}{N(1-P/P_0)} = \frac{1}{N_m C} + \frac{C-1}{N_m C}\left(\frac{P}{P_0}\right) \qquad (1)$$
3) Check the linear equation obtained from step 2. Check if it complies with criteria 1 and 2. If it does not comply, pick another range of relative pressure and back to step 2. If it meets those both criteria continue to step 4.
4) Check whether the selected range from step 1 satisfy criteria 3. If it does not, pick another range of relative pressure and back to step 2. If it meets that criteria continue to step 5.
5) Calculate the value of $(1/\sqrt{C} + 1)$. Check whether the selected range from step 1 satisfy criteria 4[2]. If it does not, pick another range of relative pressure and back to step 2. If it meets that criteria continue to step 6.
6) Calculate the BET surface area using eq. (2)
$$S = N_m . A_{N_2} . N_{AV} . \hat{V}_{N_2} \qquad (2)$$
where: *S* = surface area of MOFs, N_m = nitrogen uptake monolayer in m^3(STP)/g, A_{N2} = cross sectional of nitrogen molecule (1.62×10^{-19} m^2/molecule), N_{AV} = Avogadro number (6.022×10^{23}), $\hat{V}_{N_2}$ = nitrogen molar volume at STP (44.64 mol/m^3).

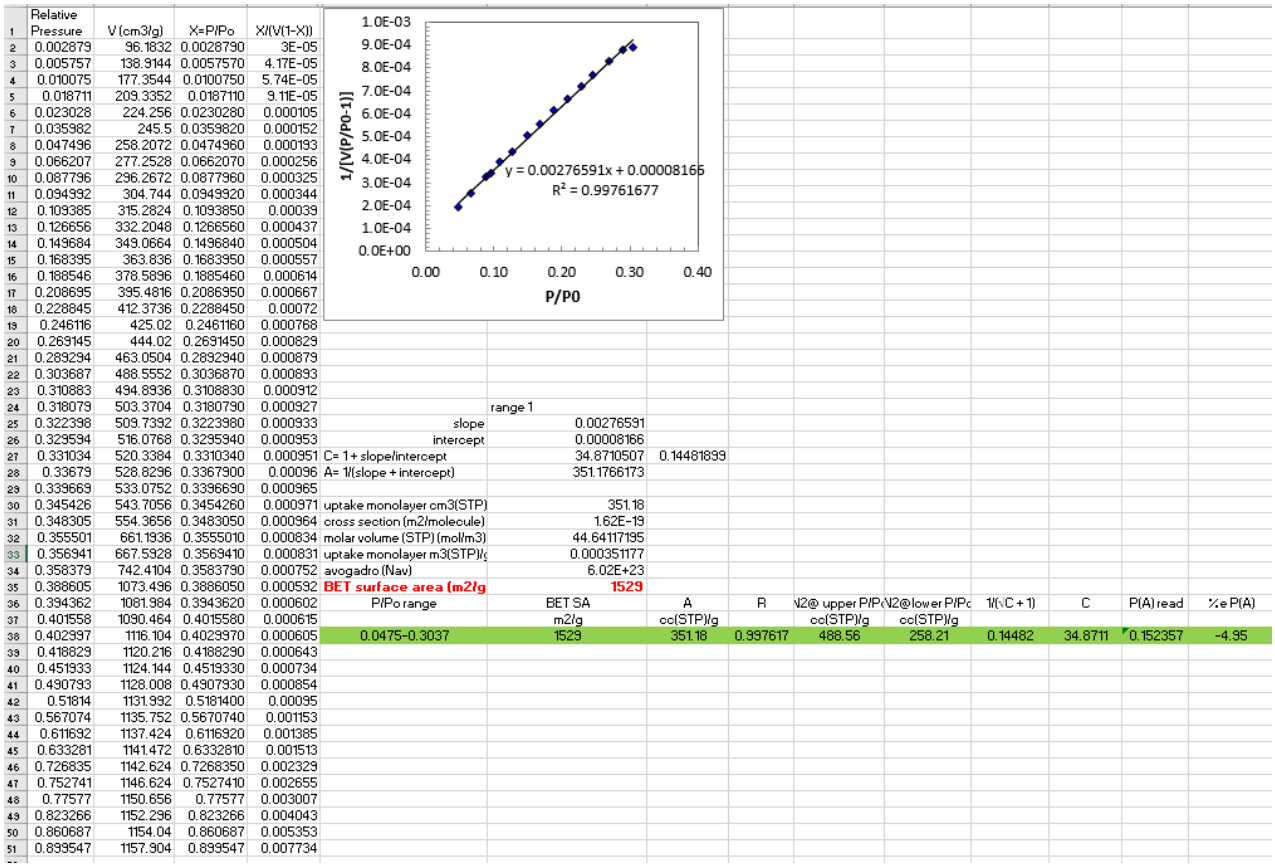

	Relative Pressure	V (cm3/g)	X=P/Po	X/(V(1-X))
2	0.002879	96.1832	0.0028790	3E-05
3	0.005757	138.9144	0.0057570	4.17E-05
4	0.010075	177.3544	0.0100750	5.74E-05
5	0.018711	209.3352	0.0187110	9.11E-05
6	0.023028	224.256	0.0230280	0.000105
7	0.035982	245.5	0.0359820	0.000152
8	0.047496	258.2072	0.0474960	0.000193
9	0.066207	277.2528	0.0662070	0.000256
10	0.087796	296.2672	0.0877960	0.000325
11	0.094992	304.744	0.0949920	0.000344
12	0.109385	315.2824	0.1093850	0.00039
13	0.126656	332.2048	0.1266560	0.000437
14	0.149684	349.0664	0.1496840	0.000504
15	0.168395	363.836	0.1683950	0.000557
16	0.188546	378.5896	0.1885460	0.000614
17	0.208695	395.4816	0.2086950	0.000667
18	0.228845	412.3736	0.2288450	0.00072
19	0.246116	425.02	0.2461160	0.000768
20	0.269145	444.02	0.2691450	0.000829
21	0.289294	463.0504	0.2892940	0.000879
22	0.303687	488.5552	0.3036870	0.000893
23	0.310883	494.8936	0.3108830	0.000912
24	0.318079	503.3704	0.3180790	0.000927
25	0.322398	509.7392	0.3223980	0.000933
26	0.329594	516.0768	0.3295940	0.000953
27	0.331034	520.3384	0.3310340	0.000951
28	0.33679	528.8296	0.3367900	0.00096
29	0.339669	533.0752	0.3396690	0.000965
30	0.345426	543.7056	0.3454260	0.000971
31	0.348305	554.3656	0.3483050	0.000964
32	0.355501	661.1936	0.3555010	0.000834
33	0.356941	667.5928	0.3569410	0.000831
34	0.358379	742.4104	0.3583790	0.000752
35	0.388605	1073.496	0.3886050	0.000532
36	0.394362	1081.984	0.3943620	0.000602
37	0.401558	1090.464	0.4015580	0.000615
38	0.402397	1116.104	0.4023970	0.000605
39	0.418829	1120.216	0.4188290	0.000643
40	0.451933	1124.144	0.4519330	0.000734
41	0.490793	1128.008	0.4907930	0.000854
42	0.51814	1131.932	0.5181400	0.00095
43	0.567074	1135.752	0.5670740	0.001153
44	0.611692	1137.424	0.6116920	0.001385
45	0.633281	1141.472	0.6332810	0.001513
46	0.726835	1142.624	0.7268350	0.002329
47	0.752741	1146.624	0.7527410	0.002655
48	0.77577	1150.656	0.77577	0.003007
49	0.823266	1152.296	0.823266	0.004043
50	0.860687	1154.04	0.860687	0.005353
51	0.899547	1157.904	0.899547	0.007734

		range 1								
slope	0.00276591									
intercept	0.00008166									
C= 1+ slope/intercept	34.8710507	0.14481899								
A= 1/(slope + intercept)	351.1766173									
uptake monolayer cm3(STP)	351.18									
cross section (m2/molecule)	1.62E-19									
molar volume (STP) (mol/m3)	44.64117195									
uptake monolayer m3(STP)/g	0.000351177									
avogadro (Nav)	6.02E+23									
BET surface area (m2/g	**1529**									
P/Po range	BET SA	A	R	N2@ upper P/Po	N2@lower P/Po	1/(√C + 1)	C	P(A) read	%e P(A)	
	m2/g	cc(STP)/g		cc(STP)/g	cc(STP)/g					
0.0475-0.3037	1529	351.18	0.997617	488.56	258.21	0.14482	34.8711	0.152357	-4.95	

References

1. Brunauer, S.; Emmett, P. H.; Teller, E. J. Am. Chem. Soc. 1938, 60, 309.
2. Rouquerol, J.; Llewellyn, P.; Rouquerol, F. In Studies in Surface Science and Catalysis; Llewellyn, P. L., Rodriquez-Reinoso, F., Rouquerol, J., Seaton, N., Eds.; Elsevier: Amsterdam, 2007; Vol. 160, p 49.

Lab 31

The fitting was undertaken using the analysis software Microactive (version 4.03) provided by Micromeritics. Initially the BET transform plot is produced over the range $0<P/P_o<0.35$, the points above $P/P_o>0.35$ are excluded to avoid the interference of the capillary condensation. The P/P_o range is gradually reduced to obtain very good linear fit while the Rouquerol criteria are satisfied. Using the range $0.066<P/P_o<0.269$ the correlation coefficient is $R^2 = 0.9997$, the $n(1- P/P_o)$ of the Rouquerol plot is ascending, C is positive, the monolayer loading, n_m, corresponds to $P/P_o= 0.144$ falling in the middle of the selected region and the monolayer calculated by the BET theory $(1/\sqrt{C+1}) = 0.142$ differs by 2% to the value corresponds to n_m ($P/P_o= 0.145$).

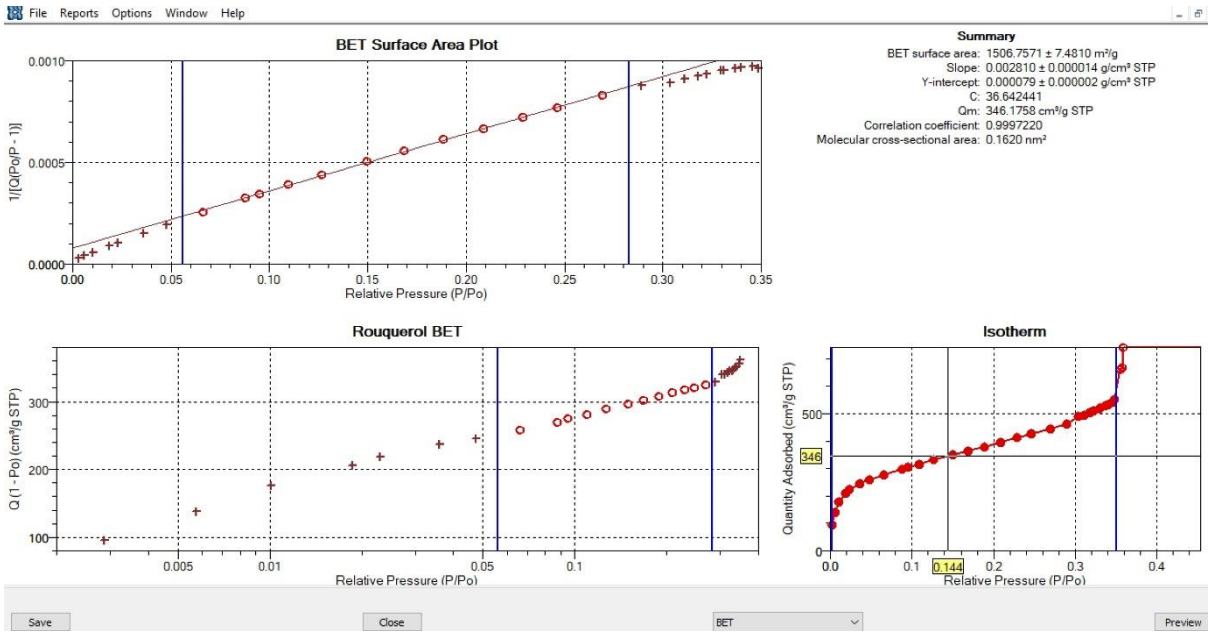

Lab 32

Method: We calculated the BET SA manually employing Excel Software and following the Rouquerol criteria.

Model calculation for sample R.

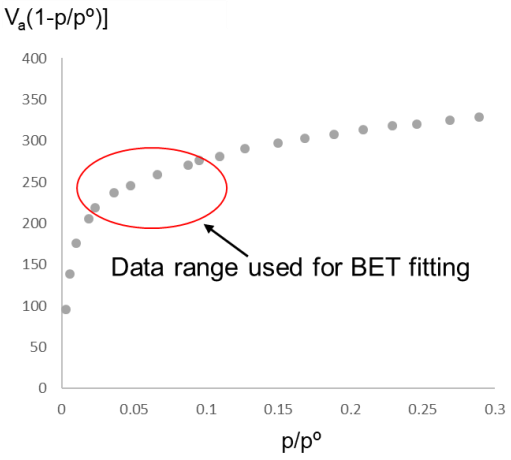

$$\frac{1}{\left[V_a\left(\frac{P_0}{P}-1\right)\right]}=\frac{C-1}{V_mC}\times\frac{P}{P_0}+\frac{1}{V_mC}$$

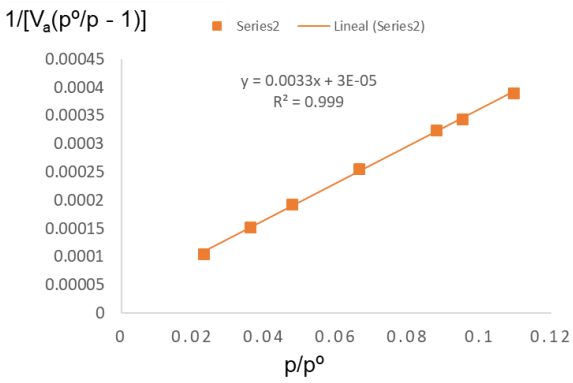

BET Surface Area:	1308.083977	m2g-1
Slope:	0.0033	
Y-Intercept:	3.00E-05	
C:	111	
Qm:	300.3003003	cm3g-1
Correlation Coefficient:	0.999	
Molecular Cross-Sectional Area:	0.1620 nm²	

Lab 33

For the calculation of the BET area we use an Excel spreadsheet, where the points of the isotherm are pasted as (relative pressure and adsorbed volume columns). The isotherm is plot in linear and logarithm scale, to verify its shape, the number of points measured, irregularities, etc. We use the linearization form of BET equation proposed by Parra et al. [1]:
$1/[V(1-x)] = 1/V_m + 1/[(V_m C_{BET})((1-x)/x)]$,
Where V_m is the adsorbed amount needed to fill the monolayer where C_{BET} is the BET constant. x is the relative pressure (p/p_0).
To determine the range where BET equation is fitted, several plots are drawn:
Plot 1: $1/(V(1-x))$ vs $(1-x)/x$
Plot 2: C_{BET} vs V/V_m
Plot 3: V(1-X) vs relative pressure.
We search for the range that complies with the following criteria simultaneously:

i) The chosen range is linear (plot 1)
ii) C_{BET} constant should be positive
iii) fitted relative pressure range is below 0.35
iv) $V/V_m = 1$ is included within the fitted range (plot 2). In the selected range of relative pressures, C_{BET} vs V/V_m should be almost constant (and close to unity).
v) V(1-x) the term V(1-x) increases with p/p_0 (plot 3)
v) (1/□□C+1) value is close to the value of p/p_0 corresponding to V_m.

All these criteria are verified together, particularly for special cases where several linear ranges can be applied and if anomalies are detected (e.g., substeps of adsorption in the range where the equation should be applied).

Example for sample R:

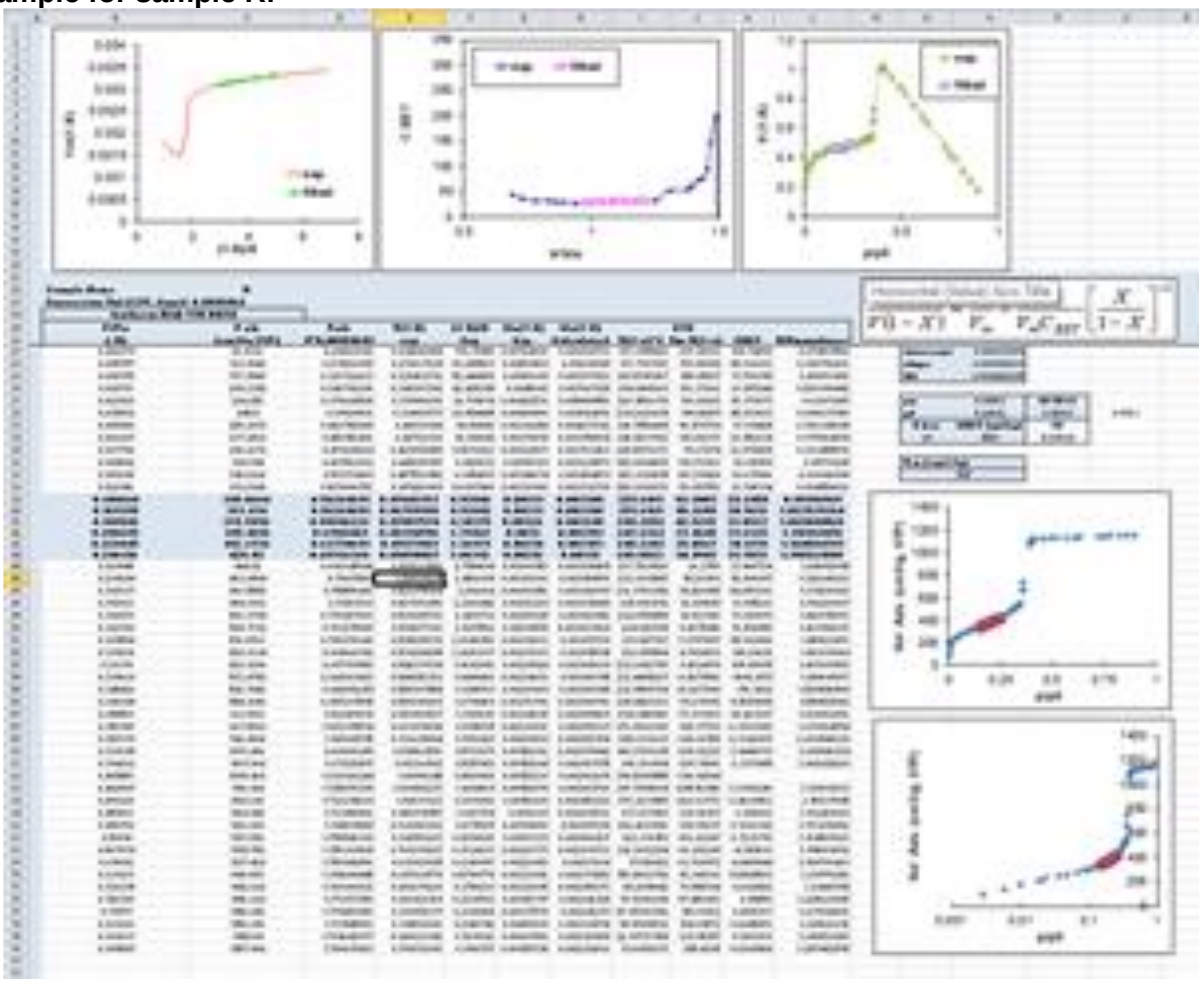

References: [1] Parra et al, Characterization of activated carbons by the BET equation-An alternative approach. Adsorpt. Sci. Technol. 12 (1995) 51.

Lab 34

Method: We calculated the BET SA employing the Micromeritics MicroActive Software (version 4.04) and following the Rouquerol criteria.

To determine BET surface area we selected the range in which the C value is positive. Usually, the upper limit of the BET range is identified as the maximum of the Rouquerol plot. In this case, this maximum corresponds to p/po = 0.403 and was not considered because the C-value was negative. Moreover, a good linear correlation, ($R^2 \geq 0.995$) was taken into consideration for the obtention of the final BET SA.

Model calculation for sample R.

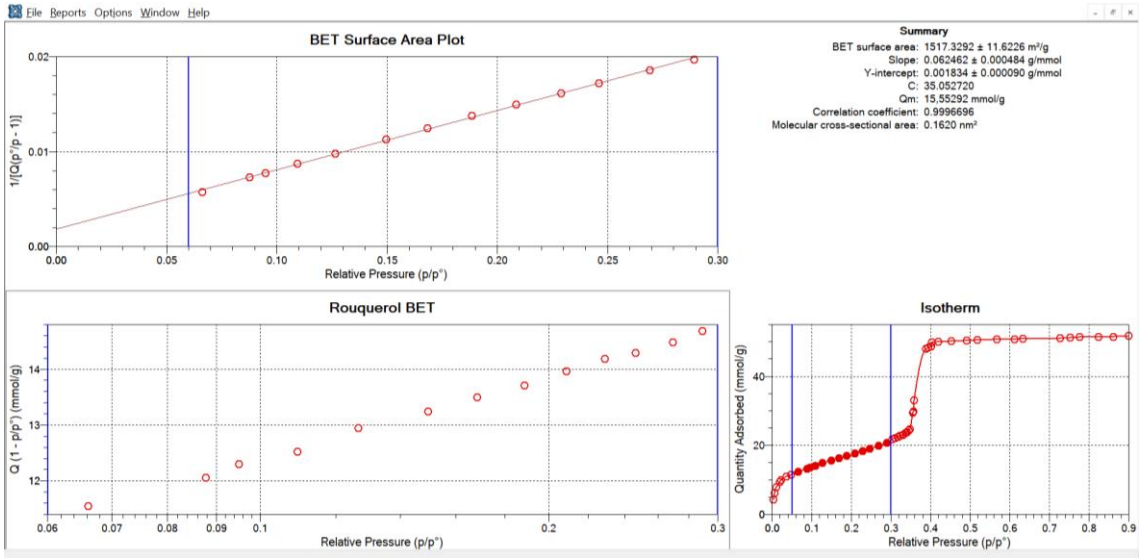

References:

1. Rouquerol, J.; Llewellyn, P.; Rouquerol, F. Is the bet equation applicable to microporous adsorbents? In *Studies in Surface Science and Catalysis*; Elsevier Inc., 2007; Vol. 160, pp. 49–56.

Lab 35

In order to determine the total surface areas of the isotherms, a BET plot of equation (1) was produced, fitting a straight line and calculating the gradient (m) and the y intercept (c). In plotting the BET plot, a minimal number of values were omitted from both ends of the data in order to ensure a high R^2 value and to discount turning points. The plotted values were of a relative pressure between $0.05 < P/P_o < 0.3$.

$$\frac{P}{P_o} \quad vs \quad \frac{1}{\mathrm{v}(\frac{P_o}{P} - 1)} \qquad (1)$$

where v is quantity adsorbed.

From this plot, the monolayer capacity can be solved from the calculated gradient and y intercept, using equation (2)

$$n_m = \frac{1}{m + c} \qquad (2)$$

where n_m is the monolayer capacity, m is the gradient, and c the y intercept.

Using the calculated n_m, the total surface area can be determined using equation (3)

$$S_A = \frac{n_m \times N_A \times s}{V} \qquad (3)$$

where S_A is the total surface area, N_A is Avogadro's constant, s is the adsorption cross section of the adsorbing species (1.62×10^{-19} m^2 for nitrogen) and V is the molar volume of the adsorbate gas (22400 mL).

Relative Pr	Quantity Adsorbed (cm3/g STP)	Po/P	1/V(Po/P-1)
0.002879	96.1832	347.3428	3.00189E-05
0.005757	138.9144	173.7016	4.16828E-05
0.010075	177.3544	99.25558	5.73853E-05
0.018711	209.3352	53.4445	9.10873E-05
0.023028	224.256	43.4254	0.000105107
0.035982	245.5	27.79167	0.000152037
0.047496	258.2072	21.0544	0.000193118
0.066207	277.2528	15.10414	0.000255727
0.087796	296.2672	11.39004	0.000324862
0.094992	304.744	10.5272	0.000344429
0.109385	315.2824	9.142021	0.000389554
0.126656	332.2048	7.895402	0.000436551
0.149684	349.0664	6.680741	0.000504298
0.168395	363.836	5.938419	0.000556553
0.188546	378.5896	5.303746	0.00061374
0.208695	395.4816	4.791682	0.000666871
0.228845	412.3736	4.36977	0.000719629
0.246116	425.02	4.063125	0.000768114
0.269145	444.02	3.715469	0.000829378
0.289294	463.0504	3.456691	0.000879065
0.303687	488.5552	3.292864	0.000892705

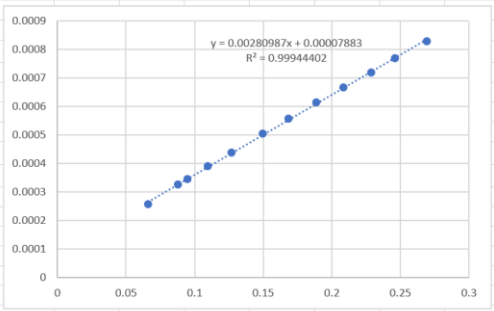

	1/(m+c)	6.02E+23
n_m	346.1765	1.62E-19
		22400
	n_mN_As/V	
S_A	1507.17	

Lab 36

For the calculation of the BET area, we use Micromeritics' Physi Viewcalc Software Tool. The calculation of BET areas was based on the linearized BET isotherm derived from the assumptions made by the BET theory

$$\frac{x}{Q(1-x)} = \frac{1}{Q_m C} + \frac{C-1}{Q_m C}\,x$$

In the equation, x and Q denote the relative pressure (P/P_o) and the adsorbate loading, respectively. C and Q_m are constants, which are related to the energetics of adsorption and the monolayer loading, respectively.[ref 1, 2]

We plot the x/(Q(1-x)) against x using the Physi Viewcalc (Figures a, b) to choose the suitable pressure range to be used for the BET area calculation according to the following consistency criteria:

(1) Only a range where Q(1-x) increases monotonically
(2) The intercept from the plot should be positive.
(3) Q_m should correspond to x falling within the selected linear region.
(4) (1/√C + 1) should be equal to x determined in (3).
(5) R^2 coefficient of the fitting must be > 0.995

To satisfy these criteria, we chose the x range between 0.010075 and 0.188546, that resulting in C = 78.8, (1/□□C+1) = 0.1013, Q_m = 317.4, R^2 = 0.9989. A BET surface area of 1380 ± 20 m^2/g is obtained.

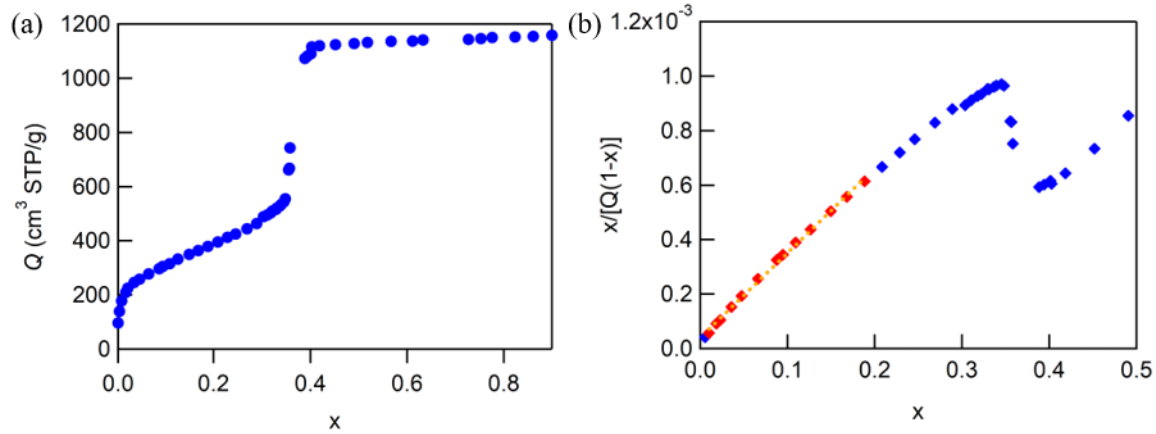

Figure. The plots to estimate the BET surface area (a) Q against x (b) x/(Q(1-x)) against x. The chosen x range was coloured in red.

References: [1] Rouquerol, J.; Llewellyn, P.; Rouquerol, F. *Studies in Surface Science and Catalysis*, Elsevier: Amsterdam **2007**. [2] Gómez-Gualdrón, D. A.; Moghadam, P. Z.; Hupp, J. T.; Farha, O. M.; Snurr, R. Q. *J. Am. Chem. Soc.* **2016**, 138, 215−224

Lab 37

To calculate BET, we normally use Micromeritics Microactive (v4.03.04) employing Rouquerol criteria with an R^2>0.999 (normally). As this was not available at the time, an excel spreadsheet was used to manually measure the BET surface area using Rouquerol protocol. The isotherm data is cut and pasted into the spreadsheet and the isotherm examined.
A Rouquerol BET plot was constructed to establish the maximum value of P/P° (0.403) and this value checked with the isotherm so that the BET calculation area occurs close as possible to the knee of the isotherm. This resulted in the maximum of P/P° being reduced to 0.337 in this case.
A BET transform plot 1/((V(P°/P))-1) v P/P° was constructed and the following criteria are examined to conclude the best fit
1 – C is positive
2 – Quantity of monolayer (Q_m) should be within the data used for the calculation
3 – Value of 1/√C+1 should be within 10% of the value of P/P° where Q_m occurs.
4 – R^2>0.999
5 – minimum number of points is normally 10 (however this is balanced with value of R^2).
A number of permutations are examined and the 'best' fit is selected as the final BET. During this, the data is checked for the spread of BET values obtained while changing the calculation data (small changes infers the final confidence level is high).

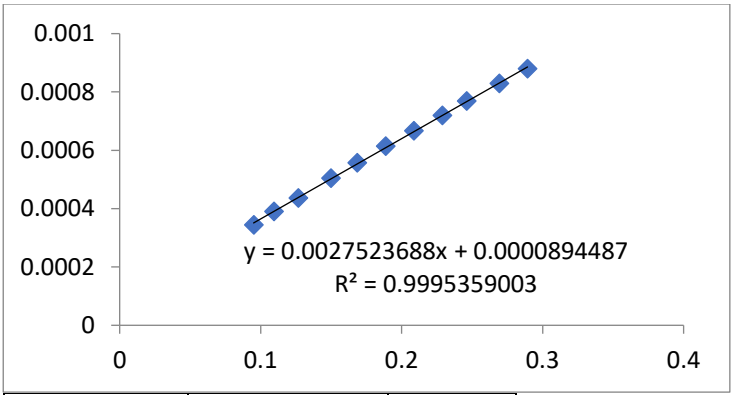

gradient	0.002752369	
intercept	8.94487E-05	
Qm	351.8874805	cm3/g
C	31.77036111	
BET	1531.581859	m2/g
1(√C+1)	0.150681374	

Lab 38

The calculation was performed using Microsoft Excel for data summarization and bulk calculations, and WaveMetrics Igor Pro for curve fitting and graphs, following this procedure:
1) Raw data was copy-pasted into an empty Excel spreadsheet.
2) The Rouquerol (green curve) and the BET curve were calculated according to literature,[1] considering the BET equation:

$$V\left(1-\frac{p}{p_0}\right)=\frac{1}{Q_m C}+\frac{C-1}{Q_m C}\left(\frac{p}{p_0}\right)$$

3) The range of p/p0 was decided using the guidelines from Walton and Snurr,[2] in particular within the p/p0 range between 0.05 and 0.3 that can maximize the correlation coefficient ($R^2 > 0.995$).
4) The obtained data was imported into Igor Pro, and the linear fitting command applied:

CurveFit/NTHR=0 line <*X-axis*>[pcsr(A),pcsr(B)] /X=<*Y-axis*> /D

where <*X-axis*> and <*Y-axis*> refers to the data of p/p0 values and BET curve values, respectively, and pcsr(A),pcsr(B) the upper and lower limits of p/p0 in the 0.05÷0.3 range (highlighted area).

5) From intercept and slope, C value and Q_m were obtained, and thus the BET surface area was calculated using the formula:[1]

$$BET_{SA}=\frac{Q_m\, N_A\, \sigma_{N2}}{V_{mol}}$$

p/p0	Quantity (STP)	V(1-p/p0)	1/V(p0/p-1)	FITTING
0.002879	96.1832	95.90628857	3.00189E-05	9.48811E-05
0.005757	138.9144	138.1146698	4.16828E-05	0.000102834
0.010075	177.3544	175.5675544	5.73853E-05	0.000114767
0.018711	209.3352	205.4183291	9.10873E-05	0.000138633
0.023028	224.256	219.0918328	0.000105107	0.000150563
0.035982	245.5	236.666419	0.000152037	0.000186361
0.047496	258.2072	245.9433908	0.000193118	0.00021818
0.066207	277.2528	258.8967239	0.000255727	0.000269888
0.087796	296.2672	270.2561249	0.000324862	0.000329549
0.094992	304.744	27		
0.109385	315.2824	280		
0.126656	332.2048	290		
0.149684	349.0664	29		
0.168395	363.836	302		
0.188546	378.5896	307		
0.208695	395.4816	312		
0.228845	412.3736	318		
0.246116	425.02	320		
0.269145	444.02	324		
0.289294	463.0504	329		
0.303687	488.5552	34		
0.310883	494.8936	34		
0.318079	503.3704	343		
0.322398	509.7392	345		
0.329594	516.0768	345		
0.331034	520.3384	348		
0.33679	528.8296	35		
0.339669	533.0752	352		
0.345426	543.7056	355.8955494	0.000970583	0.00104151

Parameters	Values
Lowest p/p0	0.087796
Highest p/p0	0.289294
Lowest Q	296.2672
Highest Q	463.0504
A	8.6925E-05
B	2.7635E-03
R^2	0.999549
C	32.79177452
1/(1+√C)	0.148667708
Qm	350.824877
BET Surface Area	2379.709455

Fitting equation: Y = A + B x

Intercept A = 1 / (Qm · C)
Slope B = (C-1) / (Qm · C)

Paramters: C = (B / A) + 1
Qm = 1 / (B + A)

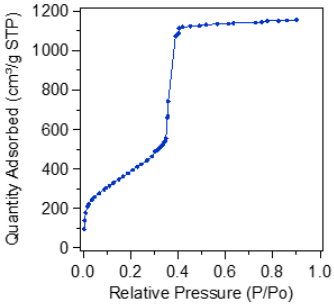

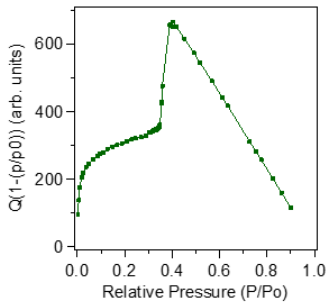

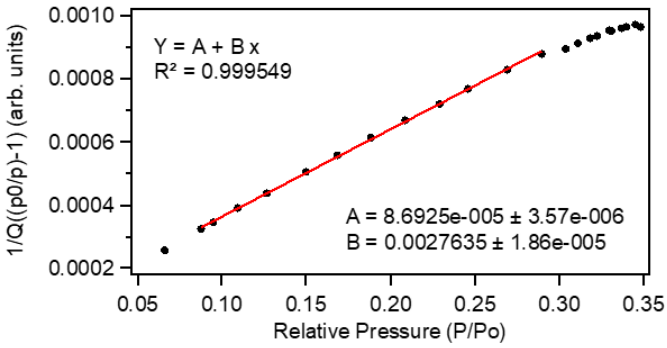

References:

1. Thommes, M. *et al.* Physisorption of gases, with special reference to the evaluation of surface area and pore size distribution (IUPAC Technical Report). *Pure Appl. Chem.* **87**, 3–12 (2015).
2. Walton, K. S. & Snurr, R. Q. Applicability of the BET Method for Determining Surface Areas of Microporous Metal−Organic Frameworks. *J. Am. Chem. Soc.* **129**, 8552–8556 (2007).

Lab 39

The code used for BET fitting in our group is available to all in a Github repository at https://github.com/fxcoudert/BET_isotherms_reproducibility
The code requires Python 3.6 or later, packages numpy, scipy, and matplotlib. The code is stored in a module named **BET.py** and for each isotherm a Jupyter notebook is available showing the parameters chosen and the fit obtained (from **A.ipynb** to **R.ipynb**).
The typical criteria (from Rouquerol et al., *Is the BET Equation Applicable to Microporous Adsorbents?*) for fitting are automatically checked, and the quality of the least-square linear fit (R^2 coefficient) is displayed. Both the BET function and the Rouquerol function are also plotted for visual confirmation of the fit.

```
In [1]: %matplotlib inline
        import BET
        import matplotlib.pyplot as plt

        plt.rcParams['figure.figsize'] = [12, 8]

In [2]: data = BET.readIsothermFromCSVFile("R.csv")
        BET.isothermProperties(data)
        BET.plotIsotherm(data)

        Number of data points: 50
        Minimal value of P/P°: 0.0029
        Maximal value of P/P°: 0.8995
        Minimal value of uptake: 96.2
        Maximal value of uptake: 1157.9

In [4]: BET.plotBET(data, 0.6, 0.002, 0.1)

        ✅ C = 139.36 is positive
        ✅ nmono = 289.49 is within BET range (up to 304.74)
        ✅ Rouquerol plot increasing in fit range
        R^2 = 0.9989

        Surface area = 1260.011 m^2/g
```

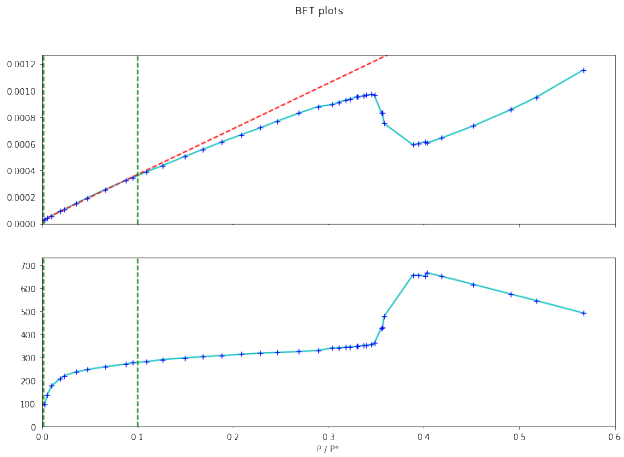

Fig. Fitting procedure and Python code used to estimate the BET surface for sample R.

Lab 40

All BET surfaces were calculated according to the 5 following criteria – which follow more or less exactly the recommendations from Rouquerol et al. [*Is the BET Equation Applicable to Microporous Adsorbents?* Studies in surface science and catalysis, 2007].

(1) The intercept C from BET plot should > 0 (see bottom figure below)

(2) Rouquerol's criterion, which states that the fit should be restricted to the region where $V_a(1 - P/P_0)$ is increasing (middle Figure below)

(3) The pressure P_{ML} corresponding to the monolayer capacity N_0 must belong to the pressure range used to fit the BET equation

(4) The recalculated value $P_{ML}(C)$ by inserting N_0 and C into the BET equation must be small compared to P_{ML} estimated by interpolating the adsorption isotherm at N_0 (typically, this difference D should be smaller than a few %)

(5) The regression coefficient R^2 must be > 0.995

For nearly all adsorption isotherms treated in this paper (except 4), the data could be fitted using the restrictive rule set above. The 4 samples that did not work are those denoted E, N, P, and Q. For these 4 samples, the only failure corresponds to the D criterion which was found to be larger than 10%.

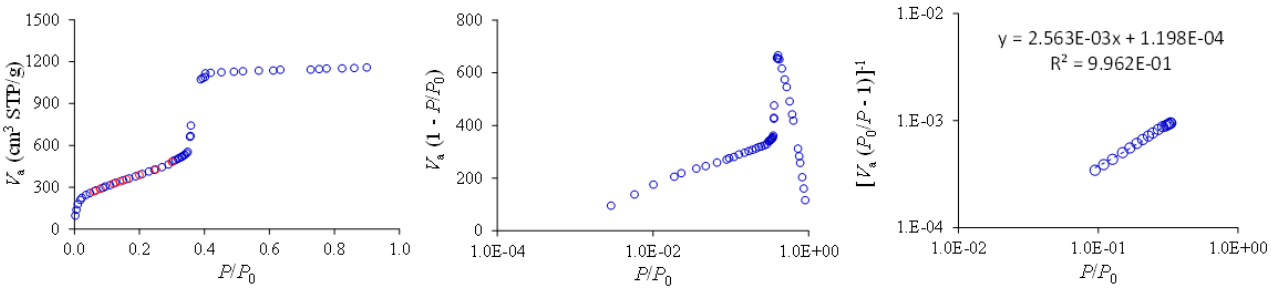

Fig. Illustration of the different criteria used to estimate the BET surface for sample R.

Lab 41

Method:

The native analysis software of the 3Flex gas sorption analyser (MicroActive Version 5.01, Micromeritics) was used to fit the BET equation and determine the corresponding surface area for the different samples. The limit of the BET range was identified as the maximum of the Rouquerol plot ($n_a(1 - p/p_o)$ vs p/p_o) according to the criterion: $n_a(1 - p/p_o)$ must continually increase with p/p_o. The points (at least 3) were then manually selected to ensure the C-value and y-intercept were positive, the Qm (monolayer capacity) is falling within the range of the selected data for the fitting and to maximise the correlation coefficient (> 0.995).

For Sample R, the BET range was determined from the inflection at p/p_o ~ 0.35 because the data immediately preceding the Rouquerol plot maxima (p/p_o ~ 0.40) was not valid (the C-value is negative). The details are given in the screenshot shown below.

Model Calculation (Sample R):

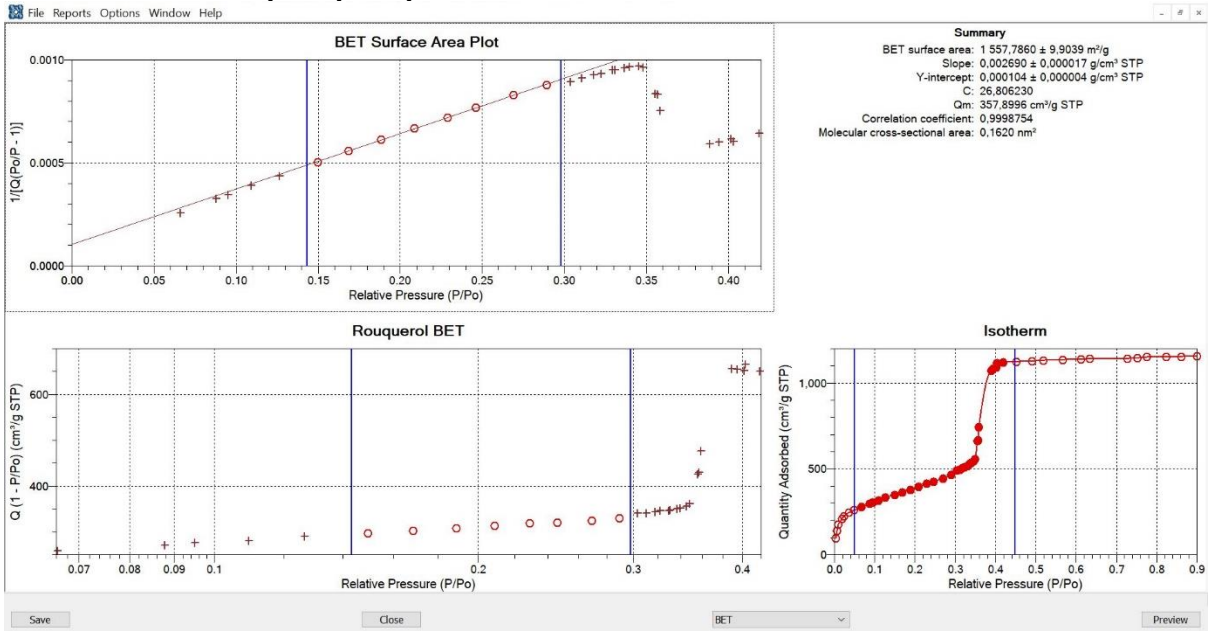

Lab 42

We calculated BET surface area from linear form of BET equation:[1]

$$\frac{1}{V_m(p_0/p-1)} = \frac{1}{V_m C} + \frac{C-1}{V_m C}\left(\frac{p}{p_0}\right)$$

where V_m is a monolayer capacity, while C is a parameter related to the first layer-adsorption energy. After plotting $\{V_m(p_0/p - 1)\}^{-1}$ against the relative pressure (p/p_0) and liner fitting we obtain slope $(slope = C-1/V_m C)$ and intercept $(intercept = 1/V_m C)$ from which we determine the monolayer capacity ($V_m = 1/(slope + intercept)$). The parameter C is expressed as $C = (slope/intercept) + 1$. Following Rouquerol criteria the parameter C must be positive. When fitting the BET equation, we should select the relative pressure range in which the slope and intercept are positive and the R^2 value nearly 1. The figure shows the isotherm and corresponding BET plot. The BET plot shows a step at relative pressure of 0.4. This may be assigned to the structural change of the material during N_2 adsorption. We can divide the BET plot into region I and region II. Region I, before structural change should give more accurate BET surface area.

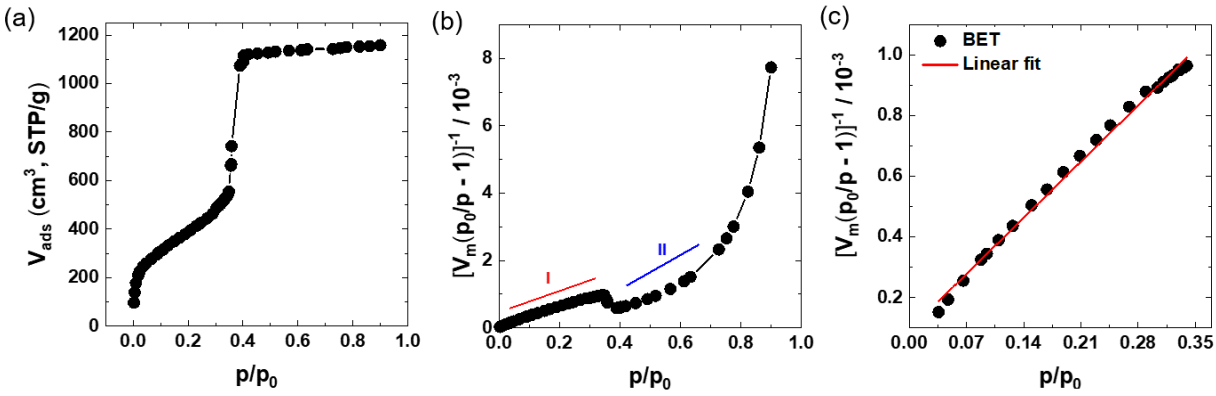

(a) The N_2 adsorption isotherm. (b) The full-scale BET plot. (d) The BET plot and its linear fit in the region I, before structural change.

Thus, we determined the parameters of BET equation for determination of monolayer capacity as given in the following table.

p/p$_0$	S_{BET} (m^2 g^{-1})	R^2	slope	intercept	C	V_m (cm^3 STP g^{-1})
I (0.036 – 0.34)	1588	0.995	$2.6 \cdot 10^{-3}$	$9.3 \cdot 10^{-5}$	28.9	365

Finally, the BET surface area is calculated following $S_{BET} = n_m N_A \sigma$, where n_m is monolayer capacity in *mol/g*, σ is the average area occupied by each molecule, nm^2. Converting n_m to V_m at STP following ideal gas equation and adjusting the units to obtain S_{BET} in $m^2\ g^{-1}$, we have $S_{BET} = 4.35\ V_m$.[1] As shown in Table, the S_{BET} area was determined to be $1588\ m^2\ g^{-1}$.

Reference

1. F. Rouquerol, J. Rouquerol, K.S.W. Sing, P. Llewellyn, G. Maurin. *Adsorption by Powders and Porous Solids: Principles, Methodology and Applications*. 2nd edition. Academic Press, 2014.

Lab 43

To produce a BET area for a given adsorption isotherm, in a semi-automated fashion, this lab uses a python code, which is available to all at the Github repository https://github.com/jackevansadl/super-umbrella.
The code requires Python 3.6 or later and uses the packages numpy, scipy, matplotlib and pandas. The code is stored in the python script **generateBET.py** and an example calculation is demonstrated for the isotherm *R*. The analysis produces graphs of the isotherm, consistency criteria and a comma-separated values (CSV) file of results from the linear regression.
The criteria from Rouquerol et al. [*10.1016/S0167-2991(07)80008-5*] are implemented in the following way:

- The quantity "ads_amount*(1-p/p0)" is evaluated. This is then analysed to find the p/p0 region where this quantity is increasing (simply based from the maximum value).
- The pp0 region of the isotherm is then cropped to the region defined above.
- For each consecutive three points the slope of the BET equation is calculated and recorded only if is linear (based on the r2 value), intercept > 0 and c-value > 0.
- The p/p0 monolayer coverage is then compared to the p/p0 region used to calculate the BET area.

When there are many points where the p/p0 monolayer coverage is within p/p0 region the greater surface area is taken. If the Rouquerol criteria is not fulfilled by any points, usually because the p/p0 monolayer coverage is not within the pp0 region, then the closest region is taken with greatest surface area. The final BET area value should be compared to the variation of BET area for all the p/p0 regions, to ensure it does not correspond to an outlier. Applying this methodology to isotherm *R* we find 3 points between 0.188546 and 0.228845 pp0 result in a p/p0 monolayer coverage that marginally differs from this p/p0 region. This leads to a BET area of 1586 $m^2\ g^{-1}$, assuming that the isotherm represents a N_2 adsorption isotherm with units of relative pressure and $cm^3\ g^{-1}$.

Lab 44

The surface area of sample R was determined based on N_2 adsorption isotherm at 77K according to the following procedure:

1. Plot the isotherm from the obtained data (Figure A).
2. Plot $v(1-p/p_0)$ against p/p_0 (Figure B) to choose the suitable p/p_0 range for the BET plot (within the 0.05-0.35 range in that $v(1-p/p_0)$ increases with p/p_0)
3. Construct the BET plot ($1/[v(p_0/p-1)]$ vs p_0/p) with the chosen range. Narrow down the BET range to choose the most linear region that has the greatest R^2 (Figure C)
4. The slope and intercept of the plot were then used to calculate the c and v_m values based on BET equation (c = 24.25; v_m = 361.8 cm^3/g):

$$\frac{1}{v[(\frac{p0}{p})-1]} = \frac{c-1}{v_m c}(\frac{p}{p0}) + \frac{1}{v_m c}$$

5. Calculate the BET surface area according to the equation (S = 1575.97 m^2/g):

$$S = \frac{v_m N_A a}{22400}$$

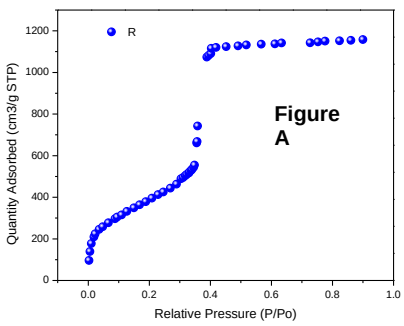

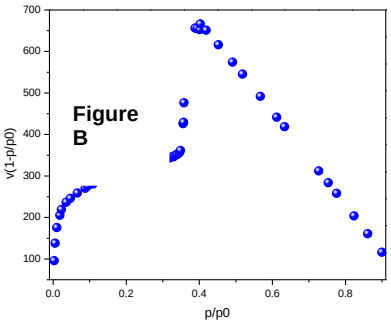

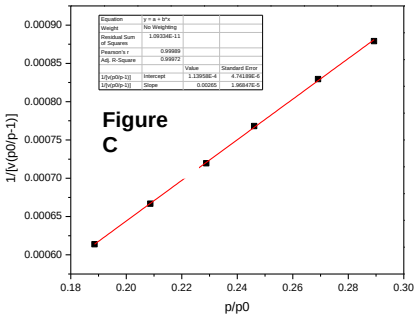

Lab 45

$$\frac{p}{n(p^0-p)} = \frac{1}{n_m C} + \frac{(C-1)}{n_m C}\frac{p}{p^0}$$

Extra parameters:

N_a = 6.023 10^{23}
V_m = 22414 cm^3
N_2 area = 0.162 nm^2

Consistency criteria to select linear BET plot range (ISO, ASTM)

a) C > 0, BET plot intercept should be positive

b) Limited to pressure range where $n(p^0 - p)$, alternatively $n(1 - \frac{p}{p^0})$, continuously increases with $\frac{p}{p^0}$;

c) $(\frac{p}{p^0})_{n_m}$ must be part of the selected calculation range;

d) $0.9\ \frac{1}{\sqrt{C}+1} < (\frac{p}{p^0})_{n_m} < 1.1\ \frac{1}{\sqrt{C}+1}$. $\left(\frac{p}{p^o}\right)_{n_m} = \frac{1}{\sqrt{C}+1}$

1. Isotherm data was plotted
2. $n(1 - \frac{p}{p^0})$ was plotted against p/p^0 in order to identify the pressure range in which criterium b is applicable.
3. $1/(n(p/p^0))$ vs p/p^0 was plotted in the range determined in (2) and a linear regression was used for parametrization of the experimental datapoints.

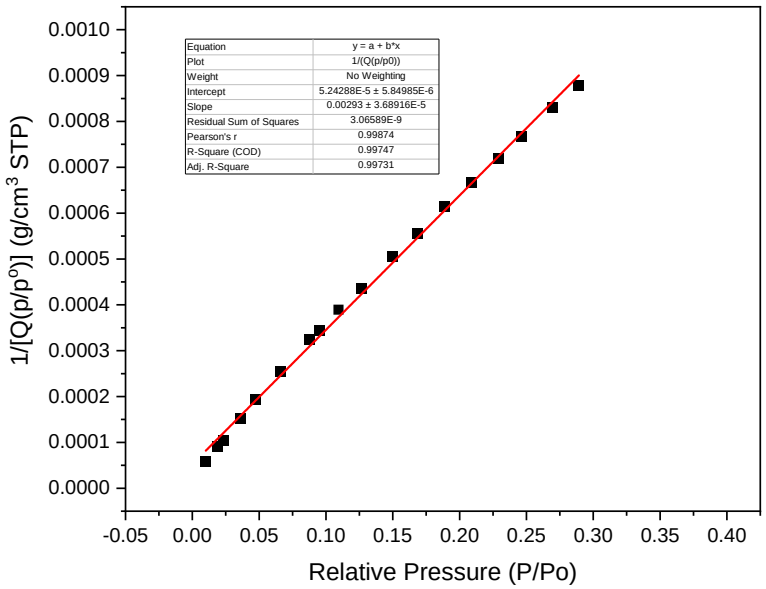

Lower p/p0: 0.01008 Upper p/p0: 0.28929
1/(C^(1/2)+1) = 0.117065376

Linear plot Intercept: 5.24E-05 Slope: 0.00293 C = 56.88531 Qm = 335.29719
BET area = 1459.37302

Lab 46

Method: We performed all data processing, plotting, and fitting in OriginPro 2018b (A). First, the quantity absorbed in $cm^3\ g^{-1}$ is converted into amount absorbed $\boldsymbol{n^a}$ in $mmol\ g^{-1}$ and the isotherm is plotted (B). The terms $\boldsymbol{n}(1-p/p^0)$ and $(p/p^0)/[\boldsymbol{n}(1-p/p^0)]$ are calculated for the Rouquerol (C) and BET plots (D), respectively. The partial pressure range of the BET plot is restricted to the widest possible first linear range, while following three criteria:[1,2]

1. The ordinate and thus C is positive (first Rouquerol criterium);
2. The term $\boldsymbol{n}(1-p/p^0)$ increases continuously with p/p^0 (second Rouquerol criterium);
3. The partial pressure $p/p^0 = 1/(\sqrt{C}+1)$ should be within the selected BET range.

Once we determined a satisfying range for the BET plot, the values are fitted with a linear function using OriginPro. We copied the fitting parameters into an Excel sheet, which was used for all subsequent calculations. The specific monolayer capacity $\boldsymbol{n_m}$ and C are calculated from the slope S and intercept I by

$$\boldsymbol{n}_{\mathrm{m}} = \frac{1}{S+I} = \left(\frac{C-1}{\boldsymbol{n}_{\mathrm{m}}C} + \frac{1}{\boldsymbol{n}_{\mathrm{m}}C}\right)^{-1} \quad \text{and} \quad C = 1 + \frac{S}{I} = 1 + \left(\frac{C-1}{\boldsymbol{n}_{\mathrm{m}}C}\right)\left(\frac{1}{\boldsymbol{n}_{\mathrm{m}}C}\right)^{-1}.$$

Lastly, the BET surface $a_{\mathrm{S}}(\mathrm{BET})$ is calculated by

$$a_{\mathrm{S}}(\mathrm{BET}) = \boldsymbol{n}_{\mathrm{m}} \times L \times \sigma_{\mathrm{m}} = \boldsymbol{n}_{\mathrm{m}} \times 6.02214076 \times 10^{23}\,\frac{1}{\mathrm{mol}} \times 0.162\ \mathrm{nm}^2,$$

where L is the Avogadro constant, and σ_{m} is the molecular cross sectional area of the adsorbate (here 0.162 nm^2 for nitrogen).[3]

Model calculation for sample R:

A: Data processing in OriginPro 2018b

	A(X)	B(Y)	C(Y)	D(Y)	E(Y)	F(Y)
Long Name	Equilibrium relative pressur	Quantity Adsorbed @ STP	Amount absorbed \i(n)\+(a)	\i(n)(1-\i(p)/\i(p)\+(0))	Equilibrium relative pressure \i(p)/\i(p)\+(0)	(\i(p)/\i(p)\+(0))/[\i(n)(1-\i(p)/\i(p)\+(0))]
Units		cm^3g^{-1}	$mmol\ g^{-1}$	$mmol\ g^{-1}$		$g\ mol^{-1}$
Comments	full range		Adsorption		desired BET range	R
F(x)=			wcol(2)/22.4	wcol(3)*(1-wcol(1))		wcol(5)/(wcol(3)/1000)/(1-wcol(5))
Sparklines						
1	0.00288	96.1832	4.29389	4.28153	0.00288	0.67242
2	0.00576	138.9144	6.20154	6.16583	0.00576	0.93369
3	0.01008	177.3544	7.91761	7.83784	0.01008	1.28543
4	0.01871	209.3352	9.34532	9.17046	0.01871	2.04036
5	0.02303	224.256	10.01143	9.78089	0.02303	2.35439
6	0.03598	245.5	10.95982	10.56547	0.03598	3.40562
7	0.0475	258.2072	11.52711	10.97962	0.0475	4.32583

B: Isotherm

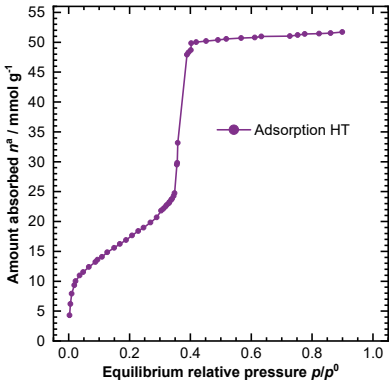

C: Rouquerol plot

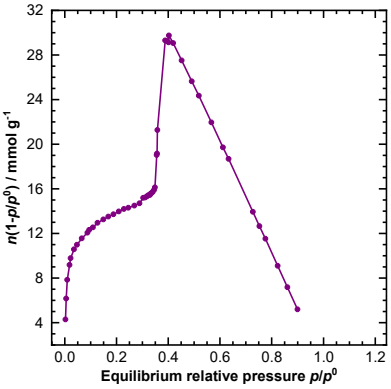

D: BET plot

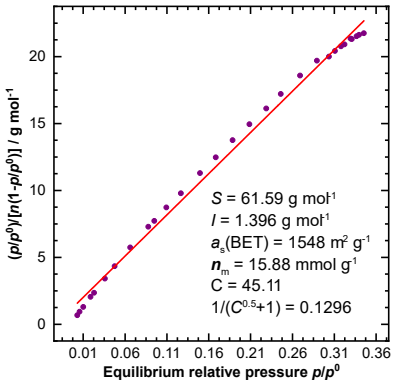

References:

1 J. Rouquerol, P. Llewellyn and F. Rouquerol, *Stud. Surf. Sci. Catal.*, 2007, **160**, 49–56.

2 M. Thommes, K. Kaneko, A. V. Neimark, J. P. Olivier, F. Rodriguez-Reinoso, J. Rouquerol and K. S. W. Sing, *Pure Appl. Chem.*, 2015, **87**, 1051–1069.

3 S. Brunauer, P. H. Emmett and E. Teller, *J. Am. Chem. Soc.*, 1938, **60**, 309–319.

Lab 47

To determine BET surface areas the isotherms (**A**) were plotted and their corresponding Rouquerol plots (***B***) were calculated and analyzed. To find a suitable partial pressure range (~5-10 points)for the BET plot the Rouquerol criteria were followed:[1,2]

1. The ordinate and therefore BET constant C must be positive
2. The term $V(1-p/p^0)$ must increases continuously with p/p^0
3. The partial pressure $p/p^0 = 1/(\sqrt{C}+1)$ should be within the selected linear BET range

After an appropriate, linear range for the BET plot was chosen, the values were plotted as $(p/p^0)/[n(1-p/p^0)]$, with n as the amount absorbed in mmol g^{-1}, and fitted with a linear function (**C**). The obtained fitting parameters for the slope *S* and intercept *I* were then used to calculate the specific monolayer capacity n_m, C and the BET surface area A_{BET}:

$$n_{\mathrm{m}} = \frac{1}{S+I} \quad \text{and} \quad C = 1 + \frac{S}{I}$$

$$A_{BET} = n_{\mathrm{m}} \times N \times \sigma_{\mathrm{m}}$$

where $N = 6.022 * 10^{23}$ (Avogadro's constant), and $\sigma_{\mathrm{m}} = 0.162\ nm^2$ (molecular cross sectional area of nitrogen).

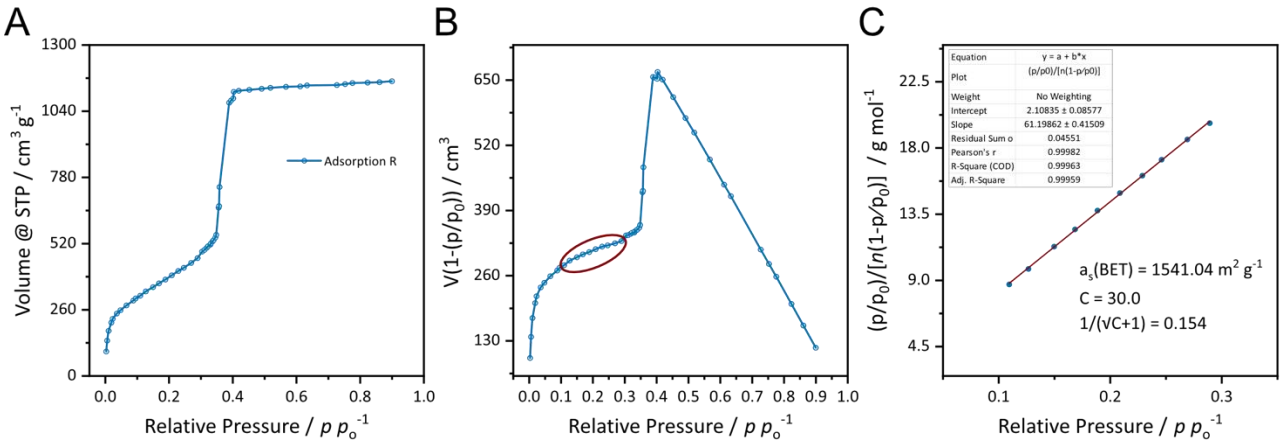

References:

(1) J. Rouquerol, P. Llewellyn and F. Rouquerol, Stud. Surf. Sci. Catal., 2007, 160, 49–56.
(2) M. Thommes, K. Kaneko, A. V. Neimark, J. P. Olivier, F. Rodriguez-Reinoso, J. Rouquerol and K. S. W. Sing, Pure Appl. Chem., 2015, 87, 1051–1069.

Lab 48

The calculation of BET surface areas was performed semi-automatically using BELmaster (version 6.3.1.0, BEL-Japan, Inc) analyzer. For the analysis in BELmaster analyzer, 10 data points were randomly selected from the region $P/P_0 \leq 0.2$ of the isotherm (highlighted in Figure 1) and we manually converted the given values of relative pressure (P/P_0) to absolute pressure P, assuming P_0 = 100.77 kPa. The obtained plot of $P/V_a(P_0-P)$ against P/P_0 for the 10 data points of sample R is shown in Figure 2 (V_a is the amount of adsorbed volume). The BET surface area was automatically calculated to be 1.13×10^3 m^2g^{-1} from the slope and the intercept; we determined the straight line between the origin and the sixth point was the best fitting.

	A	B
1	Relative P	Quantity Adsorbed (cm3/g STP)
2	0.002879	96.1832
3	0.005757	138.9144
4	0.010075	177.3544
5	0.018711	209.3352
6	0.023028	224.256
7	0.035982	245.5
8	0.047496	258.2072
9	0.066207	277.2528
10	0.087796	296.2672
11	0.094992	304.744
12	0.109385	315.2824
13	0.126656	332.2048
14	0.149684	349.0664
15	0.168395	363.836
16	0.188546	378.5896
17	0.208695	395.4816
18	0.228845	412.3736
19	0.246116	425.02
20	0.269145	444.02
21	0.289294	463.0504
22	0.303687	488.5552
23	0.310883	494.8936
24	0.318079	503.3704
25	0.322398	509.7392
26	0.329594	516.0768
27	0.331034	520.3384
28	0.33679	528.8296
29	0.339669	533.0752

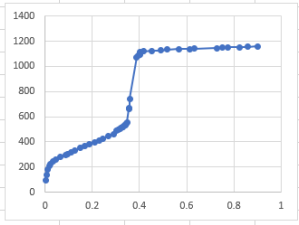

Figure 1

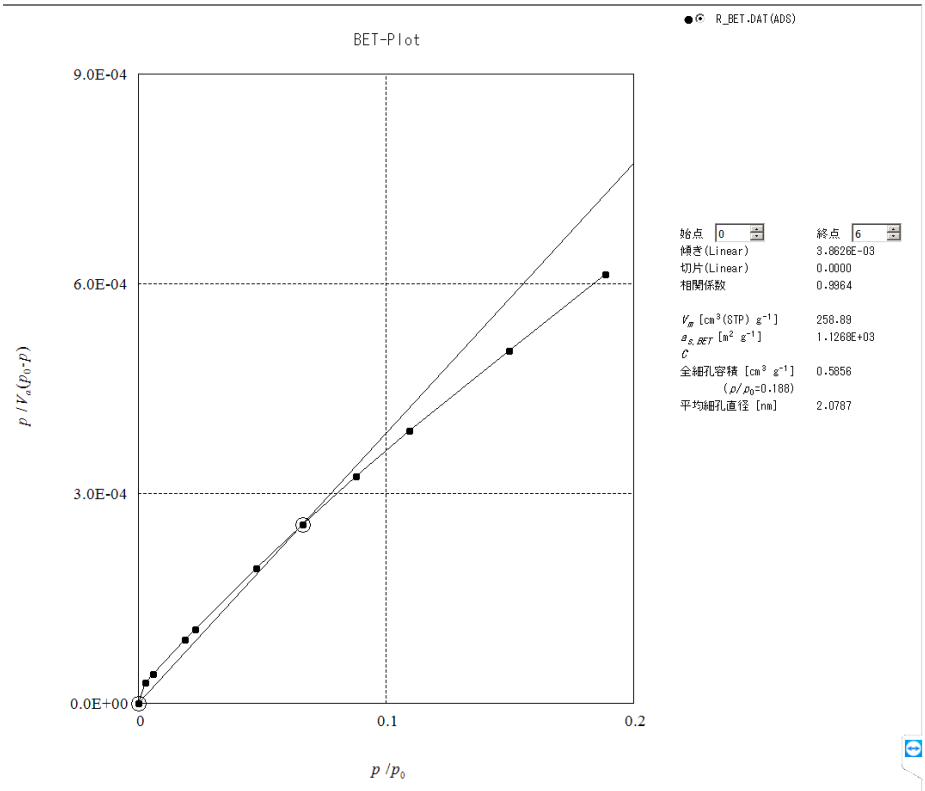

Figure 2

Lab 49

Method: We calculated the BET area using an in-house Python script that selects the best linear fit satisfying the Rouquerol criteria and having a predefined minimum number of data points.

The implemented fitting protocol consists of a three-step process. First, the maximum relative pressure is determined such that all hypothetical fits below this pressure satisfy the first Rouquerol criterion. Second, the minimum relative pressure is determined such that the BET equation above this pressure is monotonically increasing. Finally, in the third step, the final fitting interval is determined as that subset of the pressure interval defined in steps 1 and 2 that:

i. has at least a predefined minimum length (here 2/3 of the total data points)
ii. predicts a positive BET constant (second Rouquerol criterion)
iii. predicts a monolayer loading with a relative pressure within the selected pressure range (third Rouquerol criterion)
iv. satisfies the fourth Rouquerol criterion with a tolerance of 20%

From all intervals determined in this way, the program outputs the fit to that interval that has the smallest root mean squared deviation with respect to the original isotherm.

Model calculation:

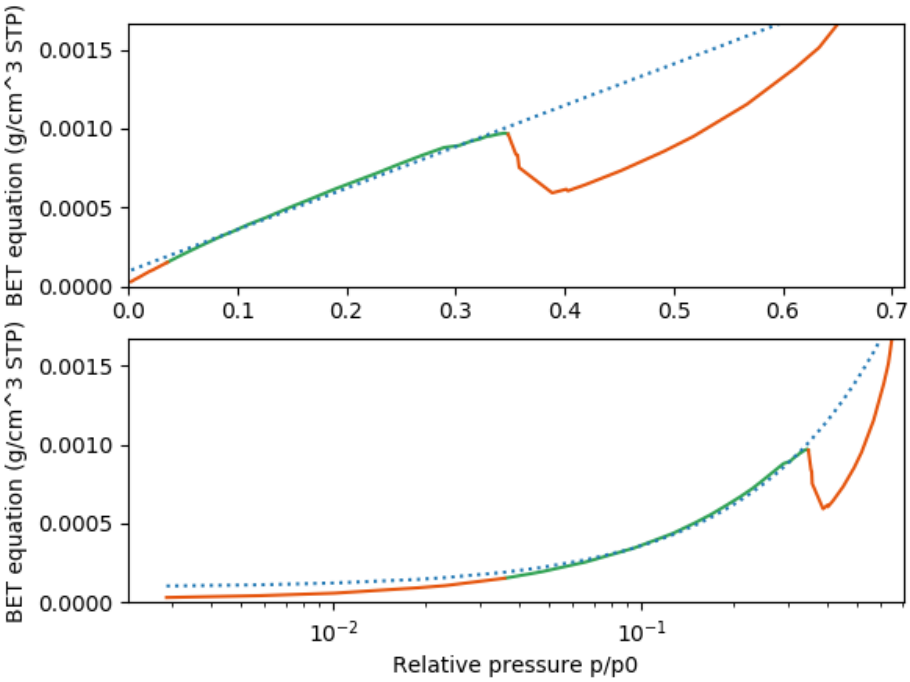

BET surface area (m^2 g^{-1})	fitting range (p/p0)	C	monolayer adsorption capacity (cm^3 g^{-1})	deviation Rouquerol criterium 4
1577	[0.036, 0.348]	28.55	367.2	8.88 %

Figure (top) Linear and (middle) semi-log plots of the BET equation for isotherm R (orange), showing the fitting region (green) and the resulting BET fit (dotted blue line). (bottom) BET parameters extracted from the fit and fitting range.

Lab 50

Evaluation of BET Surface Area of Sample R - Lab 50

We based the calculation of BET areas on the linearized BET isotherm:

$$\frac{p}{n_a(p_0 - p)} s_{total} = \frac{1}{n_m C} + \frac{(C-1)}{n_m C} \cdot \frac{p}{p_0}$$

To apply this theory to the given data, an Excel spreadsheet was used.

In order to correctly extrapolate BET values from the isotherm plot of a given material, there are various criteria that must be considered[1]:

(1) Only a range where $n_a(1 - p/p_o)$ increases monotonically with p/p_o should be selected.

(2) The value of C resulting from the linear regression should be positive.

(3) The monolayer loading n_m should correspond to a relative pressure p/p_o falling within the selected linear region.

(4) The relative pressure corresponding to the monolayer loading calculated from BET theory ($1/\sqrt{C} + 1$) should be equal to the pressure determined in criterion 3.

In our calculations only point (1) is always guaranteed. As the plots were arbitrary scaled (not necessarily in a linear manner) along the y axis, we cannot assume that the slope and intercept of the BET line is the same as the original one. This leads to a loss of physical meaning of n_m and C, as they are calculated as the reciprocal of the slope minus the intercept, and one plus the gradient over the intercept, respectively.

Taking into account these limitations, we calculated the BET area of the given set of data by scanning the BET region of the isotherm (between 0.015 and 0.3 p/p_o) and extrapolating the curve with the best correlation (over 0.999) over the largest number of points.

Sample R:

BET Surface Area (m^2/g): **1491.992931 ± 16.35900005**
C: **42.39192831**
Slope (g/cm^3): **0.00284888 ± 0.000031**
Y-Intercept (g/cm^3): **0.000068827 ± 9.21748E-06**
Correlation: **0.99924924**

[1] Diego A. Gómez-Gualdrón, Peyman Z. Moghadam, Joseph T. Hupp, Omar K. Farha, and Randall Q. Snurr, Journal of the American Chemical Society, **2016** *138* (1), 215-224

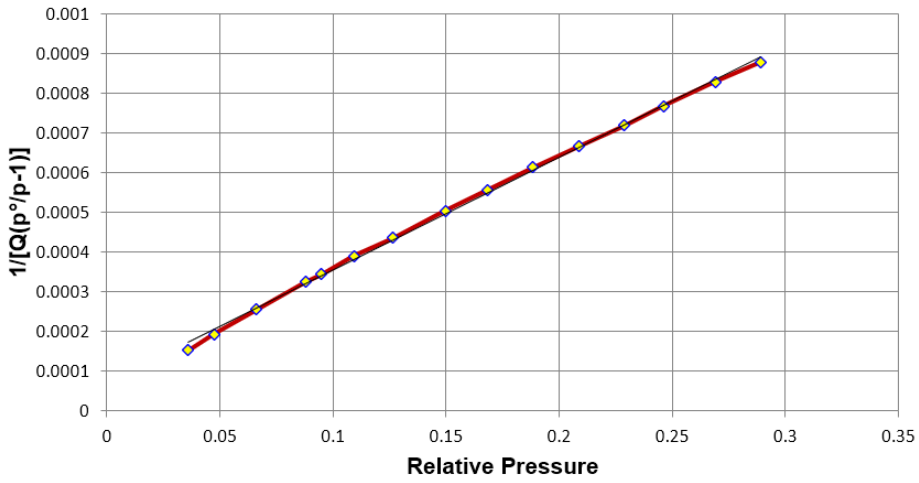

Lab 51

General Procedure Description:

Our lab uses an adapted form of the Rouquerol BET Criteria, implemented in a custom-written Python script:

1) Plot [$N(p)(1-p/p_{sat})$ vs. p/p_{sat}] and select the upper and lower pressure bounds, p_{min} and p_{max}, such that the y-value of the plot is monotonically increasing. (Rouquerol Criteria 2)
2) Given p_{min} and p_{max}, generate every possible series of measurements bounded by p_{low} and p_{high}, such that $p_{high} \leq p_{max}$ and $p_{high} \geq p_{min}$. Compute the linear regression of the BET linearization and collect all solutions such that:
    a. C_{BET} constant is positive. (Rouquerol Criteria 1)
    b. Monolayer capacity (N_m), falls in the pressure range for the BET solution (Rouquerol Criteria 3)
    c. The difference between the monolayer pressure from the regression and measurements is less than 5 %. (Adapted from Rouquerol Criteria 4)
    d. The data series for the regression includes at least eight measurements
3) The selected solution from which the BET area is computed is the solution meeting the above criteria with the largest R^2 correlation coefficient for the linear regression.

Our Python script using the following constants:
Avogadro Constant: $6.02214076 \times 10^{23}$ molecule/mol
Nitrogen molecule area: 0.162 nm^2/molecule
STP Molar Volume: 22 400 cm^3(STP)/mol

Details for computation of BET Area for Sample R:

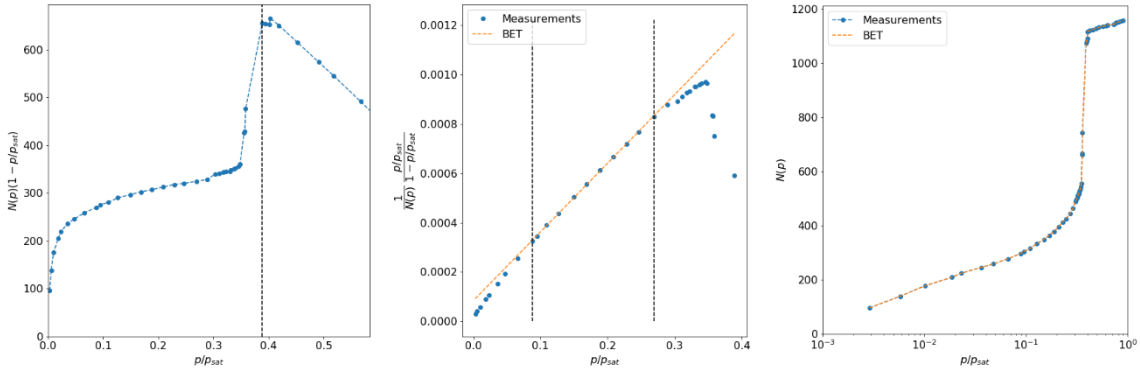

The algorithm selected p_{min}/p_{sat} = 0.002879 and p_{max}/p_{sat} = 0.388605. Step 2 yielded 124 possible solutions, the largest R2 was for p_{low}/p_{sat} = 0.087796 and p_{high}/p_{sat} = 0.269145, encompassing 11 measured data points. The selected fit yielded N_m = 348.510 cm^3(STP)/g, with C_{BET} = 34.2321. The computed BET area is then 1517.86 m^2/g.

Lab 52

The Rouquerol plots of $1/(Q(p_0/p - 1))$ against p/p_0 were fitted in Origin. A linear regression was applied to determine the slope and intercept to be used to calculate the BET surface area, with the selection of data points optimised to fulfil the following criteria:

1. Both the slope and intercept must have positive values.
2. A minimum of 3 points are used in every plot.
3. Points deviating significantly from linearity are excluded and the R^2 value must be ≥ 0.995.

Ideally each plot used data in the p/p_0 range 0.05 - 0.35. However, for samples which displayed Type I character (steep adsorption at low pressure), the points required to obtain a positive intercept and a linear fit were below the typical range of p/p_0 values recommended for BET surface area calculations.

Model calculation for sample R

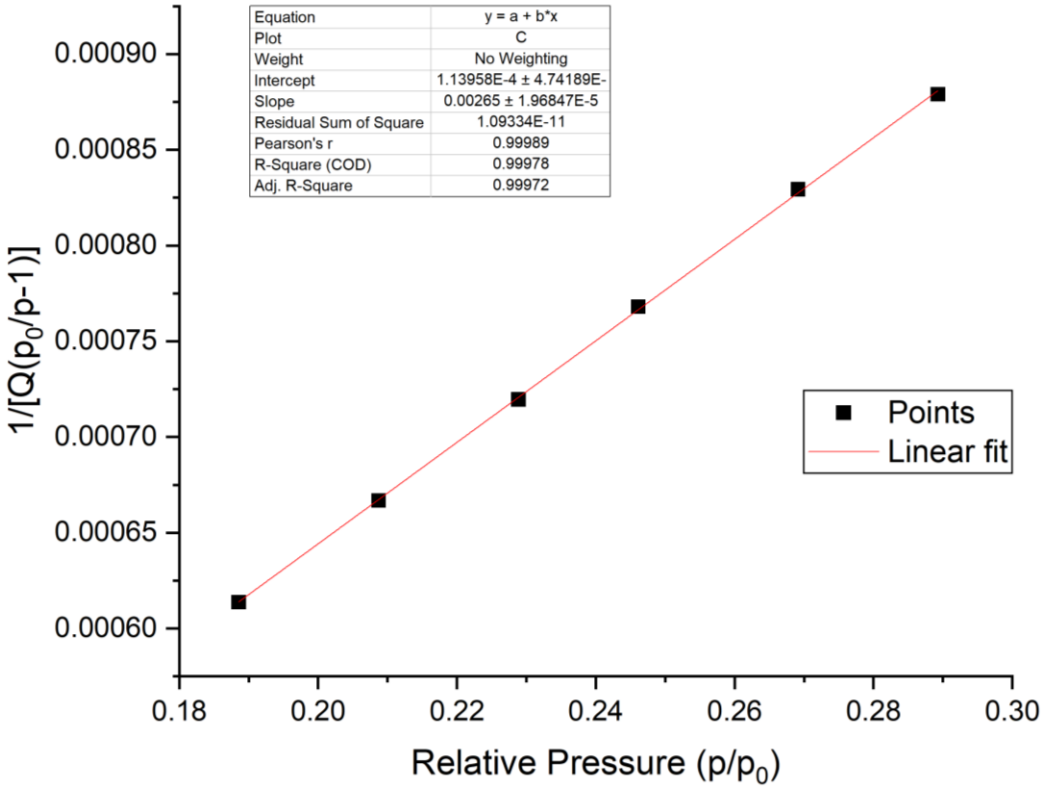

No. of points fitted	p/po range for fit	Slope	Intercept	BET surface area ($m^2\ g^{-1}$)	C
6	0.18855 - 0.28929	0.00265	1.14E-04	1575.64	24.25

Lab 53

The BET surface area was calculated manually using a spreadsheet. Two plots were generated, $\frac{\frac{P}{P_0}}{N\left(1-\frac{P}{P_0}\right)}$ vs $\frac{P}{P_0}$ and $N\left(1-\frac{P}{P_0}\right)$ vs $\frac{P}{P_0}$. A linear region of the first plot was chosen so that the Rouquerol consistency criteria were met. (*J. Am. Chem. Soc.* **2016**, *138* (1), 215–224) An example calculation of sample R was presented below.

index	Relative Pres	Quantity Ad	(P/P0)/(N(1-	N(1-P/P0)
2	2.88E-03	96.1832	3.00E-05	9.59E+01
3	5.76E-03	138.9144	4.17E-05	1.38E+02
4	1.01E-02	177.3544	5.74E-05	1.76E+02
5	1.87E-02	209.3352	9.11E-05	2.05E+02
6	2.30E-02	224.256	1.05E-04	2.19E+02
7	3.60E-02	245.5	1.52E-04	2.37E+02
8	4.75E-02	258.2072	1.93E-04	2.46E+02
9	6.62E-02	277.2528	2.56E-04	2.59E+02
10	8.78E-02	296.2672	3.25E-04	2.70E+02
11	9.50E-02	304.744	3.44E-04	2.76E+02
12	1.09E-01	315.2824	3.90E-04	2.81E+02
13	1.27E-01	332.2048	4.37E-04	2.90E+02
14	1.50E-01	349.0664	5.04E-04	2.97E+02
15	0.168395	363.836	5.57E-04	3.03E+02
16	0.188546	378.5896	6.14E-04	3.07E+02
17	0.208695	395.4816	6.67E-04	3.13E+02
18	0.228845	412.3736	7.20E-04	3.18E+02
19	0.246116	425.02	7.68E-04	3.20E+02
20	0.269145	444.02	8.29E-04	3.25E+02
21	0.289294	463.0504	8.79E-04	3.29E+02
22	0.303687	488.5552	8.93E-04	3.40E+02
23	0.310883	494.8936	9.12E-04	3.41E+02
24	0.318079	503.3704	9.27E-04	3.43E+02
25	0.322398	509.7392	9.33E-04	3.45E+02
26	0.329594	516.0768	9.53E-04	3.46E+02
27	0.331034	520.3384	9.51E-04	3.48E+02
28	0.33679	528.8296	9.60E-04	3.51E+02
29	0.339669	533.0752	9.65E-04	3.52E+02
30	0.345426	543.7056	9.71E-04	3.56E+02
31	0.348305	554.3656	9.64E-04	3.61E+02
32	0.355501	661.1936	8.34E-04	4.26E+02
33	0.356941	667.5928	8.31E-04	4.29E+02
34	0.358379	742.4104	7.52E-04	4.76E+02
35	0.388605	1073.496	5.92E-04	6.56E+02
36	0.394362	1081.984	6.02E-04	6.55E+02
37	0.401558	1090.464	6.15E-04	6.53E+02
38	0.402997	1116.104	6.05E-04	6.66E+02
39	0.418829	1120.216	6.43E-04	6.51E+02
40	0.451933	1124.144	7.34E-04	6.16E+02
41	0.490793	1128.008	8.54E-04	5.74E+02
42	0.51814	1131.992	9.50E-04	5.45E+02
43	0.567074	1135.752	1.15E-03	4.92E+02
44	0.611692	1137.424	1.38E-03	4.42E+02
45	0.633281	1141.472	1.51E-03	4.19E+02
46	0.726835	1142.624	2.33E-03	3.12E+02
47	0.752741	1146.624	2.66E-03	2.84E+02
48	0.77577	1150.656	3.01E-03	2.58E+02
49	0.823266	1152.296	4.04E-03	2.04E+02
50	0.860687	1154.04	5.35E-03	1.61E+02
51	0.899547	1157.904	7.73E-03	1.16E+02

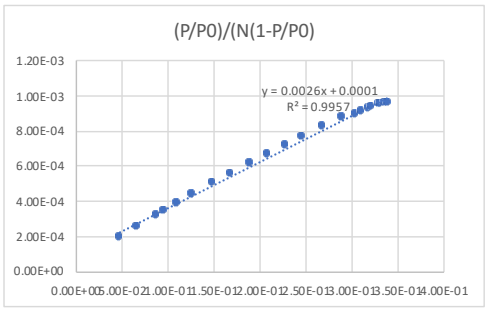

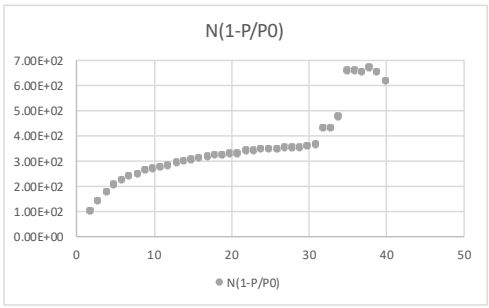

Pmin	Pmax	slope	intercept	R2	C	Nm	(Pmax)	N(Pmax) fror	N(Pmax)
8	29	0.002613533	0.000101742	0.99572994	26.6878128	368.286869	0.339669	519.86196	533.0752

criterion 1 N(1-P/P0) must be increasing in the chosen range
N(1-P/P0)ma 1.28100088
criterion2 C must be positive
C 26.6878128
criterion3 Nm must fall in range of Pmin-Pmax
N(Pmax)-Nm 151.57509 N(Pmax,e)-Nm 164.7883306
criterion4 Calculated monolayer pressure equals experimental
1/(sqrtC+1) 0.16217904 experimental 0.168395 error -3.6912964

surface area 1582.09361

Lab 54

Criteria for the calculation of the BET surface area

In our lab, we typically follow the four criteria proposed by Rouquerol and reported in Chapter 7 of the textbook *Adsorption by Powders and Porous Solids* (http://dx.doi.org/10.1016/B978-0-08-097035-6.00007-3):

a. the quantity C should be positive;

b. the application of the BET equation should be limited to the pressure range where the term $n(p^o-p)$ continuously increases with p/p^o; Fig. 1c, shows $n(p^o-p)$ versus p/p^o for dataset R;

c. the pressure corresponding to n_m should be within the pressure range selected for the calculation;

d. the calculated value of $(p/p^o)n_m$ (given by Equation 7.4) should not differ by more than 10%, from the experimental value of p/p^o corresponding to the BET n_m value obtained by application of Equation (7.1). Otherwise, it is necessary to change the chosen range of relative pressures.

Equation 7.1 is the BET function in its linear form:

$$\frac{p/p^o}{\boldsymbol{n}(1-p/p^o)} = \frac{1}{\boldsymbol{n_m}C} + \frac{C-1}{\boldsymbol{n_m}C}\left(\frac{p}{p^o}\right)$$

While equation 7.4 is:

$$\left(\frac{p}{p^o}\right)_{\boldsymbol{n_m}} = \frac{1}{\sqrt{C}+1}$$

Moreover, we add two additional criteria:

e. some of the first points in the BET plot (Equation (7.1)) are neglected if they overlap or cluster, to avoid distortions in the linear interpolation calculation, since they would weigh more than the more dispersed points at higher relative pressures;

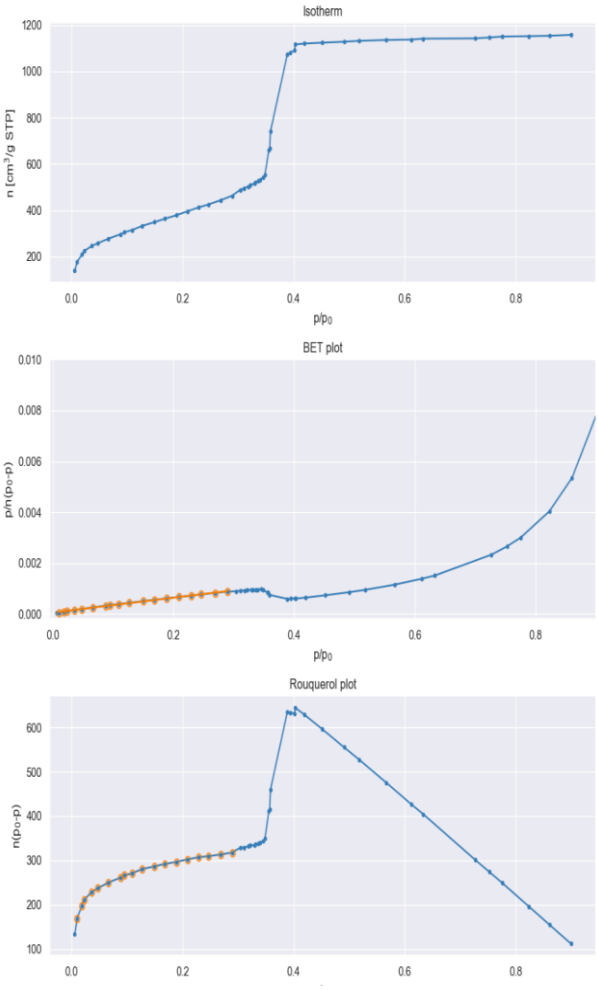

Fig 1. Dataset R: a) provided amount of adsorbed gas versus partial pressure data set, b) BET-plot and c) Rouquerol plot. The data range used for calculation of the BET surface area R is shown in orange.

f. as many points as possible are employed for the calculation, that meet the first five criteria, and show a linear range in the BET plot with $R^2 > 0.99$. For dataset R, the BET-plot is shown in figure 1. b.

In the case of the dataset R, the data range used for determination of the BET surface area is depicted in orange in figure 1.b,c.

Lab 55

Method of calculating the BET area:

The raw data provided was converted to an alternative format (.txt) and then manually imported to the native analysis software available from the 3Flex gas sorption analyser (MicroActive version 4.02, e572371, Micromeritics). Fitting to the BET equation was performed semiautomatically by using 5 to 13 points in the interval $0.05 \leq P/P_0 \leq 0.30$ according to the Rouquerol criteria. We ensured positive values for C and y-intercept by manual selection in all cases.

Model calculation (Sample R):

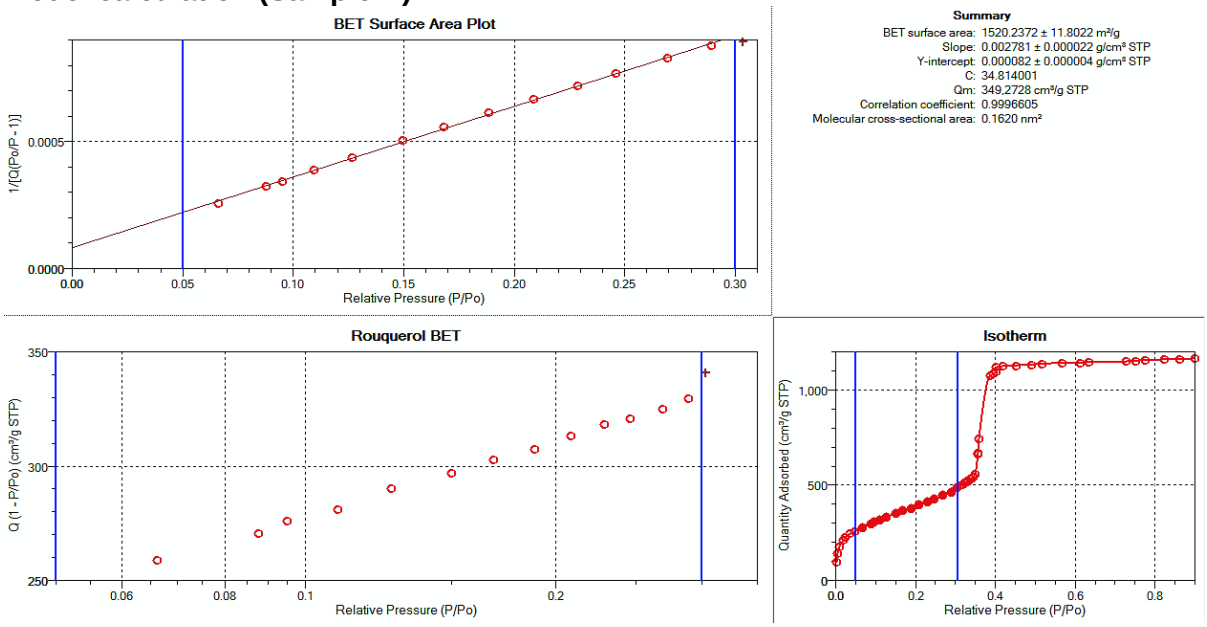

References:

[1] Howarth, A.J., Peters, A.W., Vermeulen, N.A., Wang, T.C., Hupp, J.T., and Farha, O.K. (**2017**). Best Practices for the Synthesis, Activation, and Characterization of Metal–Organic Frameworks. *Chem. Mater. 29*, 26–39.

Lab 56

Sample R Calculation Lab 56

We applied the Rouquerol method [1] to determine the surface area from the data using the Micromeritics surface area calculator 'PhysiViewCalc 2007' which operates through Microsoft Excel. A set of five consecutive data points were selected below 0.04 P/P_0 where BET equation is linear with an increasing value of 1/[Q(p°/p-1)] (see Figure 1 below). This gave rise to a positive C value of 174.

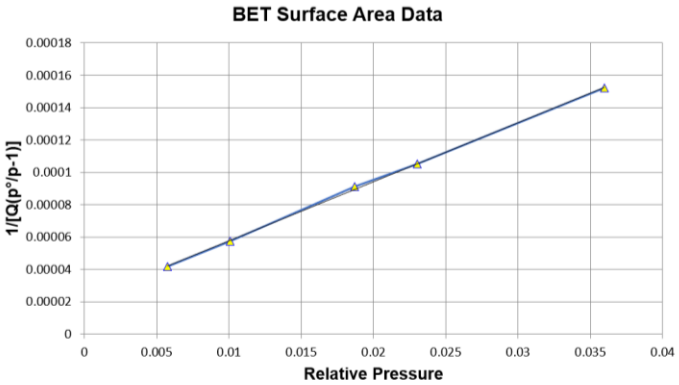

Figure 1. Plot of 1/[Q(p°/p-1)] vs relative pressure for the five consecutive data points selected.

References

1. Rouquerol, F.; Rouquerol, J.; Sing, K.S.W.; Llewellyn P.; Maurin, G.; 1999, *Adsorption by Powders and Porous Solids Principles, Methodology and Applications* Second Edition, Academic Press, London

Lab 57

Method of calculating the BET area:
To calculate the surface area, we applied following approach:

1. Calculate the Rouquerol transform (n*(1-x)) using relative pressure (x) and mmol/g adsorbed (n).
2. Restrict the relative pressure range to a maximum of 0.3.
3. Find the maximum of n*(1-x)
4. Using the relative pressure (x_{max}) at the maximum of n*(1-x), estimate a minimum x from x_{max} / 10. The BET transform and fitting constants via regression require an order of magnitude of relative pressure data and this helps minimize some overweighting of very low relative pressure data.
5. The traditional BET transform is calculated.
6. The slope and intercept of the BET transform are calculated using linear regression, Figure 1.
7. The BET transform and regression are reviewed, any high leverage points are omitted, and the regression is recalculated, Figure 2.
8. The monolayer capacity (n_m) and BET C constant are calculated from the slope and intercept
9. The full recommendation from Rouquerol, Llewelyn, and Rouquerol is then used to evaluate the result:
    a. R^2 as an indication of linearity
    b. $C > 0$
    c. n*(1-x) monotonically increasing with increasing p/po
    d. Monolayer capacity (n_m) and relative pressure at the monolayer (x_m) must be within the range of n and x used for the BET transform calculation.
    e. The value of $1/(C^{0.5} + 1) \approx x_m$

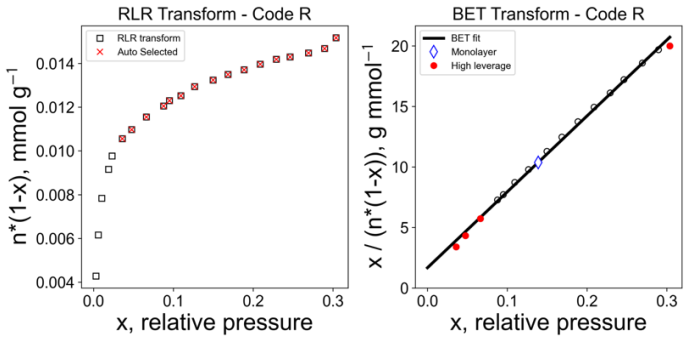

Figure 1 - initial estimate of surface area

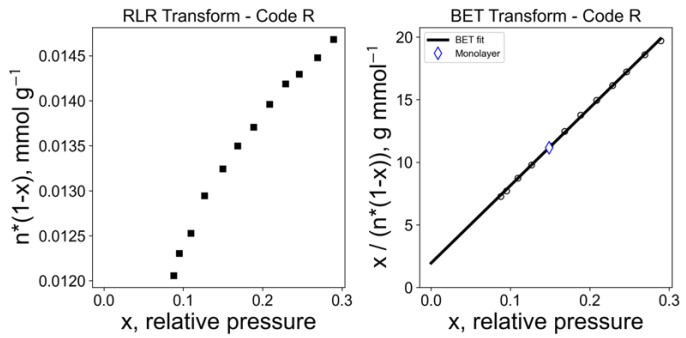

Figure 2 - RLR and BET transform plots for Code R

Lab 58

Multi-point BET Surface Area Calculation Method

BET calculations were performed in Excel, using the Micromeritics Physi ViewCalc Tool (Excel 2007 Version). The following criteria were used to set the range used in the multi-point BET calculation:

- **Determine max P/P_0:** The maximum P/P_0 for the multi-point BET calculation was set to either 0.3 or the value which gives the maximum single-point BET surface area, whichever is lower.

  Single-point BET surface areas (S) were calculated across the isotherm using the equation:

  $$S = \frac{\left(\frac{V_a}{m}\right)\left(1 - \frac{P}{P_o}\right)Na}{22400}$$

  where (V_a/m) is the volume of gas adsorbed per gram (mL/g), P is the partial vapor pressure of adsorbate gas in equilibrium with the surface at 77.4 K (Pa), P_0 is the saturated pressure of adsorbate gas (Pa), N is Avogadro's constant (6.02×10^{23} mol^{-1}), and a is the effective cross-sectional area of the adsorbate molecule (1.62×10^{-19} m^2 for nitrogen).
- **Determine min P/P_0:** The minimum P/P_0 for the multi-point BET calculation was set to either 0.005 or whatever value gives at least 3 data points for the calculation, whichever is lower.
- **Remove non-linearity that is visible at either end of the range:** Observe a plot of $1/[(V_a/m)(P_0/P-1)]$ vs P/P_0, and remove P/P_0 values on either end of the range that deviate from the fit excessively
- **Ensure correlation coefficient is >0.999:** Shrink the P/P_0 range to improve the fit

As an example, consider data set "R":

- The maximum value of single-point BET surface area for the isotherm is found to be 2900 m^2/g at a P/P_0 value of 0.402997. The maximum P/P_0 for the multi-point calculation is thus set to 0.3.
- When the minimum P/P_0 value is set to 0.005, the fit given by the Physi ViewCalc Tool has a correlation coefficient of 0.998
- To improve the fit to the desired correlation coefficient value of >0.999, the minimum P/P_0 is shifted higher as non-linearity is observed in the plot. Removing the first 4 points (setting the minimum P/P_0 to 0.035) increases the correlation coefficient to 0.9992.
- With a linear fit and an acceptable correlation coefficient, the multi-point BET surface area of sample R is found to be 1492 m^2/g using a P/P_0 range of 0.035 to 0.3.

Lab 59

The surface area was estimated using the BET model, following the consistency criteria proposed by Rouquerol *et. al*.[1,2]
i) a '$n(1-P/P_0)$ vs P/P_0' plot was used to determine the partial pressure upper limit (Figure left).
ii) a BET plot was used to estimate the monolayer capacity 'n_m' (0.02747 mol g^{-1}) and 'C' (37.4) parameters (Figure right).
The region selected in a compromise to comply with the consistency criteria and the highest value of 'n_m', 0.38861< P/P_0 < 0.41883 region was selected with a positive 'C' value (37.4) and 'n_m' falls within the selected region. The surface area was then estimated with the following formula:

$$S_{A,BET} = n_m \cdot L \cdot \sigma$$

where 'n_m' is the monolayer capacity (mol g^{-1}), 'L' is the Avogadro's number ($6.02214179 \cdot 10^{23}$ mol^{-1}), and 'σ' is the cross-sectional area of the N_2 (0.162 nm^2). Using the monolayer capacity n_m = 0.02747 mol g^{-1}, the estimated surface area for sample R is $S_{A,BET}$ = 2680.2 m^2 g^{-1} (overestimated value).

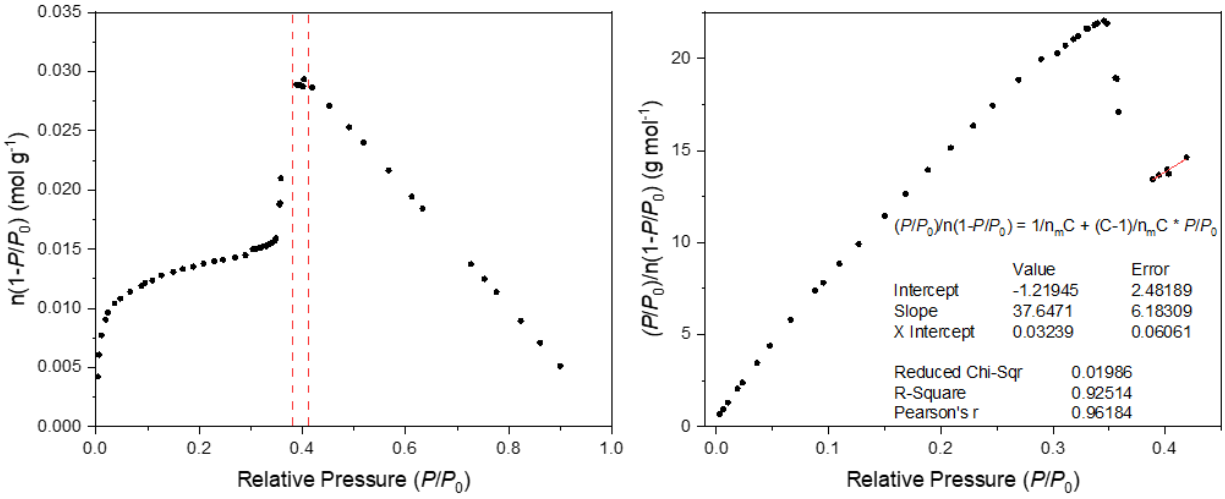

Figure. $n(1-P/P_0)$ vs P/P_0 plot (left) and BET plot (right) for sample R. Range used for surface area estimation is denoted (between red dashed lines).

1. F. Rouquerol, J. Rouquerol, K.S.W. Sing, P. Llewellyn and G. Maurin, *Adsorption by Powders and Porous Solids: Principles, Methodology and Applications*, Academic Press, Oxford, 2nd edn, **2014**, p. 237.
2. K. S. Walton and R. Q. Snurr, *J. Am. Chem. Soc.*, **2007**, 129, 8552.

Lab 60

Procedure: BET surface areas were calculated from the linearized BET isotherm derived from the assumptions made by the BET theory:

$$\frac{\frac{P}{P_o}}{N(1-\frac{P}{P_o})} = \frac{1}{N_m C} + \frac{C-1}{N_m C}\left(\frac{P}{P_o}\right)$$

A plot of $(P/P_0)/(N(1-P/P_0))$ vs (P/P_0) for the N_2 isotherms for sample R. A linear region was selected from the plot to allow for the extraction of the values of C and N_m from linear regression. The linear region with $R^2 > 0.995$ was selected to satisfy the BET consistency criteria proposed by Rouquerol et al.

Linear regression of the data was carried out in excel for a range where $N(1 - P/P_o)$ increases monotonically with P/P_o.

For the BET consistency we then check for (1) Positive value for C, (2) the value of N_m falls within the P/P_o range used for regression (3) The value of $(1/\sqrt{C} + 1)$ should be close (20 %) to P/P_o from where N_m is calculated.

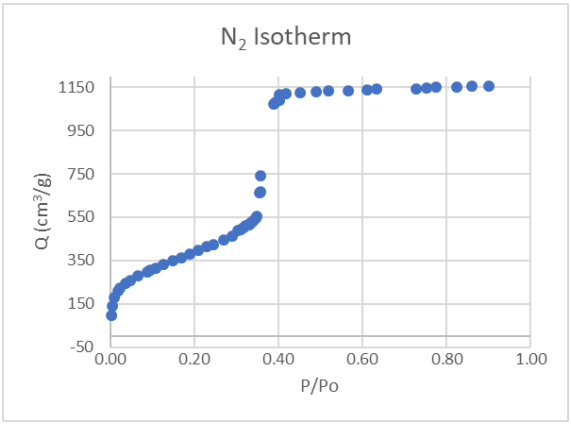

Relative Pressure (P/P_o)	Q (cm^3/g STP)	$1-P/P_0$	$(P/P_0)/(N(1-P/P_0))$
0.002879	96.1832	9.971210E-01	3.001889E-05
0.005757	138.9144	9.942430E-01	4.168276E-05
0.010075	177.3544	9.899250E-01	5.738532E-05
0.018711	209.3352	9.812890E-01	9.108730E-05
0.023028	224.256	9.769720E-01	1.051066E-04
0.035982	245.5	9.640180E-01	1.520368E-04
0.047496	258.2072	9.525040E-01	1.931176E-04
0.066207	277.2528	9.337930E-01	2.557275E-04
0.087796	296.2672	9.122040E-01	3.248622E-04
0.094992	304.744	9.050080E-01	3.444288E-04
0.109385	315.2824	8.906150E-01	3.895543E-04
0.126656	332.2048	8.733440E-01	4.365505E-04
0.149684	349.0664	8.503160E-01	5.042977E-04
0.168395	363.836	8.316050E-01	5.565529E-04
0.188546	378.5896	8.114540E-01	6.137404E-04
0.208695	395.4816	7.913050E-01	6.668710E-04
0.228845	412.3736	7.711550E-01	7.196294E-04
0.246116	425.02	7.538840E-01	7.681145E-04
0.269145	444.02	7.308550E-01	8.293781E-04
0.289294	463.0504	7.107060E-01	8.790654E-04
0.303687	488.5552	6.963130E-01	8.927052E-04
0.310883	494.8936	6.891170E-01	9.115745E-04
0.318079	503.3704	6.819210E-01	9.266447E-04
0.322398	509.7392	6.776020E-01	9.334039E-04
0.329594	516.0768	6.704060E-01	9.526362E-04
0.331034	520.3384	6.689660E-01	9.510047E-04
0.33679	528.8296	6.632100E-01	9.602678E-04
0.339669	533.0752	6.603310E-01	9.649521E-04
0.345426	543.7056	6.545740E-01	9.705825E-04
0.348305	554.3656	6.516950E-01	9.640933E-04
0.355501	661.1936	6.444990E-01	8.342379E-04
0.356941	667.5928	6.430590E-01	8.314459E-04
0.358379	742.4104	6.416210E-01	7.523500E-04
0.388605	1073.496	6.113950E-01	5.920877E-04
0.394362	1081.984	6.056380E-01	6.018124E-04
0.401558	1090.464	5.984420E-01	6.153396E-04
0.402997	1116.104	5.970030E-01	6.048123E-04
0.418829	1120.216	5.811710E-01	6.433259E-04
0.451933	1124.144	5.480670E-01	7.335310E-04
0.490793	1128.008	5.092070E-01	8.544602E-04
0.51814	1131.992	4.818600E-01	9.499109E-04
0.567074	1135.752	4.329260E-01	1.153301E-03
0.611692	1137.424	3.883080E-01	1.384950E-03
0.633281	1141.472	3.667190E-01	1.512857E-03
0.726835	1142.624	2.731650E-01	2.328667E-03
0.752741	1146.624	2.472590E-01	2.655048E-03
0.77577	1150.656	2.242300E-01	3.006725E-03
0.823266	1152.296	1.767340E-01	4.042556E-03
0.860687	1154.04	1.393130E-01	5.353437E-03
0.899547	1157.904	1.004530E-01	7.733719E-03

		BET Consistency Criteria			
Isotherm	**N_m, monolayer loading (mol/g)**	**C, BET Constant (+ve)**	**R^2 (>0.995)**	**P/P_o@C**	**BET SA (m^2/g)**
R	0.01441	60	0.9979666	0.1145306	1405

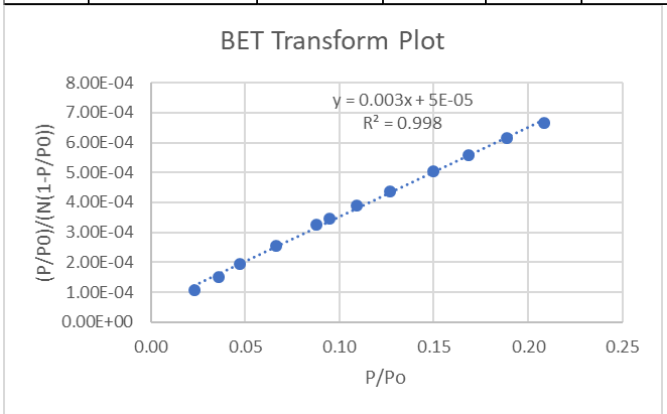

Slope	0.003006441	5.11535E-05	y Intercept
Error	4.29148E-05	5.30057E-06	Error
R^2	0.997966593	8.66241E-06	Standard Deviation

Reference: (1) Rouquerol, J.; Llewellyn, P.; Rouquerol, F. In Studies in Surface Science and Catalysis; Llewellyn, P. L., Rodriquez-Reinoso, F., Rouquerol, J., Seaton, N., Eds.; Elsevier: Amsterdam, 2007; Vol. 160, p 49

Lab 61

BET surface areas were calculated from N_2 adsorption isotherms at 77 K according to the following procedures[1]

1) The uptake ($\boldsymbol{v}$) vs relative pressure ($\boldsymbol{P/P_0}$) was plotted (Fig. a)

2) The isotherm region where $\boldsymbol{v(1-P/P_0)}$ increases versus $\boldsymbol{P/P_0}$, where $\boldsymbol{v}$ is the amount of N_2 adsorbed, was identified (Fig. b).

3) Within this isotherm region (Fig. c), sequential data points that led to a positive intercept in the plot of $\frac{\boldsymbol{P/P_0}}{\boldsymbol{v(1-P/P_0)}}$ against $\boldsymbol{P/P_0}$, were found (Fig. d). This plot yields a slope $\boldsymbol{a}$, and a positive intercept $\boldsymbol{b}$.

4) The BET equation was used to calculate the apparent surface area.

$$\frac{1}{v[(p_0/p)-1]} = \frac{c-1}{v_m c}\left(\frac{p}{p_0}\right) + \frac{1}{v_m c}$$

where

$$v_m = \frac{1}{a+b} \quad \text{and} \quad c = 1 + \frac{a}{b}$$

The BET surface area is

$$S_{BET} = \frac{v_m \cdot N \cdot s}{V \cdot m}$$

Where N is Avogadro's number, s the adsorption cross section of the adsorbing species (0.162 nm2 for N2), V the molar volume

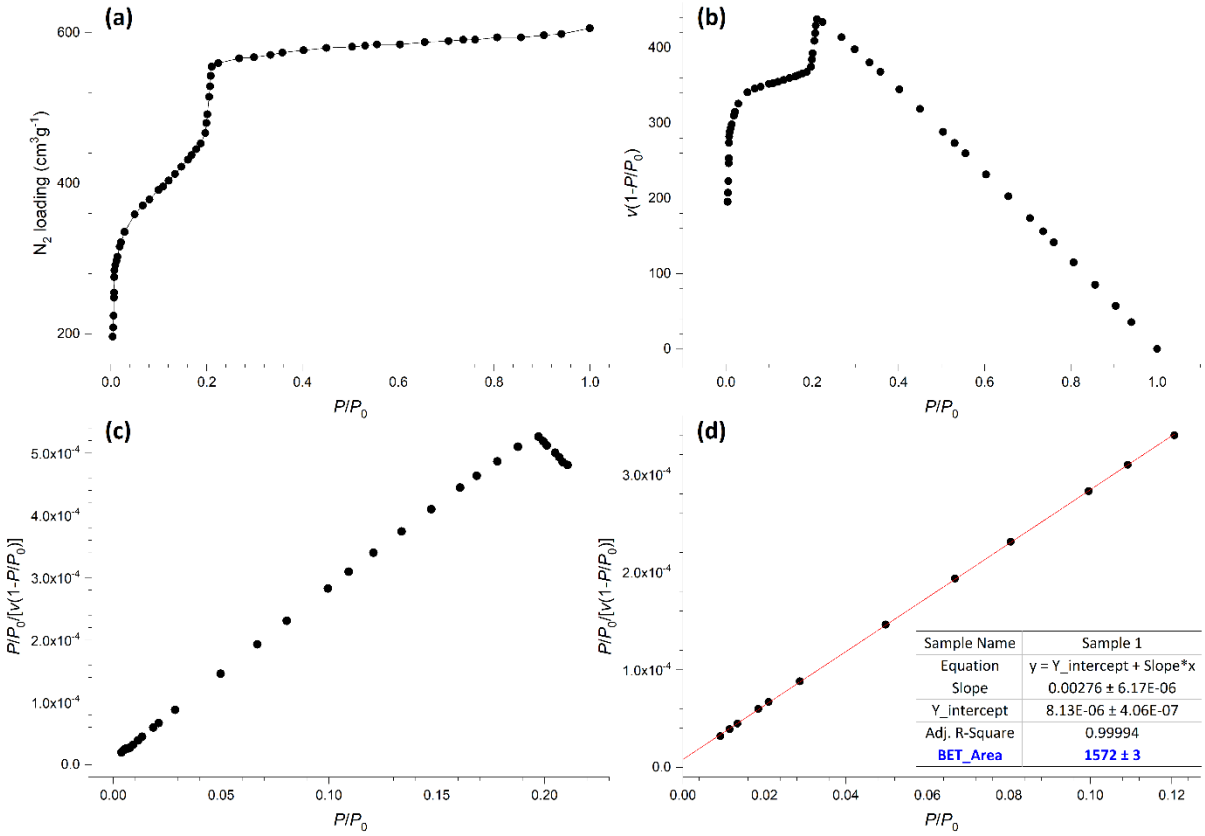

Figure 3. An example set of plots for calculating the BET surface area.

[1] Walton, K. S., & Snurr, R. Q. (2007). Applicability of the BET Method for Determining Surface Areas of Microporous Metal–Organic Frameworks. *Journal of the American Chemical Society, 129*(27), 8552-8556. doi:10.1021/ja071174k

Section S14 – Methods

Round-robin evaluation

N_2 adsorption isotherms of 18 different materials (were sent to international collaborators: HKUST-1, ZIF-8, NU-1000, MIL-101, UiO-66, Al fumarate, Zeolite13X, Mg-MOF-74, UiO-66-NH_2, MOF-5, DMOF-1, MCM-41, TPB-DMTP-COF, MIL-100, NU-1102, NU-1104, NU-1105, and PCN-777; they were anonymised and labelled A-R respectively. Note that this is not the order in which the isotherms appear in the paper. The isotherms were sampled from our own group measurements and from the NIST Adsorption Database. Arbitrary scaling factors were introduced to minimise recollection bias of the isotherms. The isotherms were sent out in .csv format. All colleagues received the same email with the same set of instructions (see email below): To calculate the BET area from the data in the way they saw most fit and to report a rough estimate of how long it took them to calculate them.

For easier data handling, once rescaled, all results were rounded to the next integer. None of the data points have been eliminated. The data is presented as a jitter plot for each material, with a superimposed kernel-density estimation obtained in python.

> Dear XXX,
>
> We are working on a code to systematically calculate BET area from N2 adsorption isotherms (we call this BETSI). As part of that paper, we would like to make a 'social experiment' (round-robin evaluation) where we send a selection of isotherms to labs around the world – working with porous materials – and ask them to calculate a BET area for us from a set of isotherms, to get a feel of a) how large the spread of BET areas that people calculate is, b) how well the BETSI prediction matches this spread and c) how long it takes to calculate it.
>
> To minimise bias, this will be a blind-study: the name of the material corresponding to the isotherm is not given and all isotherms have been scaled-off in some arbitrary manner in y, so it will be more difficult to recognise any isotherms and materials. Our idea is to publish this and to include everybody as co-authors.
>
> Please, let me know if this could interest you. We will only ask to calculate the BET area of 18 materials in any way you consider the most accurate and, if possible, a rough estimate of how much time it took you to calculate them. If you agree, we can share the isotherms with you.

BETSI

The BETSI algorithm is fully published on GitHub https://github.com/fairen-group/betsi-gui. The programme is written in python, and principally uses the numpy library. Looped linear regressions over all consecutive combinations of at least three points, perform full BET analyses and store the fitting parameters in n x n results matrices, where the (j,i)-matrix element denotes a linear regression from the j'th to the i'th point on the isotherm. Binary pass/fail matrices with the same dimensionality are used independently to assess compliance with linearity and fitting criteria. The 'filtering' of BET areas is achieved by element-wise matrix multiplication of the results matrices and the pass/fail

matrices. This allows independent ‘activation’ and ‘deactivation’ of the criteria and observing the effects on the results. The minimum fitting requirement of ten points is coded in a pass/fail matrix to allow for some minimum point flexibility, as is the cut-off value for R^2 of 0.995. To avoid low-leverage non-linearity in the linear region, the first Rouquerol criterion has been extended to also require the linearised BET function to increase monotonically with P/P_0, as well as $N(1-P/P_0)$. The third and fourth Rouquerol criteria are implemented through a 10,000 point Pchip interpolation of the isotherm to reconstruct the N_m (Read). As the third and fourth criteria require the N_m (BET) to be a real value, *i.e.* they require C to be positive, the second criterion cannot be independently deactivated from the third and the fourth. The associated logic has been written into the programme. Following the BETSI filtering by multiplication of results and pass/fail matrices, the isotherm knee is identified as the subset of BET areas whose fitting region end on the highest permissible pressure point. In most cases this will be the highest permissible point under the first Rouquerol criterion. The optimal BETSI prediction is chosen as the fitting region with the lowest percentage error under the fourth criterion and belonging to the isotherm knee subset.

BETSI only requires the adsorption isotherm as input data and returns six plots used to validate the results: the isotherm itself, with the optimal linear region highlighted as well as the BET fit; the ‘Rouquerol representation’ of the isotherm, $N(1-P/P_0)$ plotted against P/P_0; the linearised plot with the OLS regression and the regression parameters; the filtered percentage error vs BET areas plot with the isotherm knee and optimal BET area highlighted; the filtered monolayer-loadings plot showing all permissible monolayer loadings on the isotherm; and the statistical distribution of permissible BET areas with a boxplot. Additionally, BETSI returns four regression diagnostics plots which can be used to assess whether the assumptions of OLS regression have been met: The Residuals vs Fitted values plot can be used to visually inspect whether the residuals are normally distributed around the regression line, and similar information can be obtained from the QQ-plot. Finally, the Scale-Location plot can be used to assess whether the distribution of studentized residuals is homoscedatic or heteroscedatic and the Residuals vs Leverage plot can be used to identify high-leverage points that have an abnormally large influence on the regression line.

Comparison between round-robin evaluation and BETSI results

Statistical analysis of the results was performed in python. The *BETSI variation coefficient* and the *Round-robin variation coefficient* are standard deviations relative to the average of each set. The *pass rate* for each isotherm is the number of permissible BET fits as a fraction of all consecutive combination of points. To account for non-equal spacing of the points on each isotherm, the *pressure-adjusted pass-rate* is obtained by integrating along the pressure axis and dividing the total sum of permissive pressure intervals by the sum of all consecutive pressure intervals. The *hit rate* is the fractional number of BET areas calculated in the round-robin evaluation that lie within the BETSI range.

Section S15 – How to use BETSI

Step 1: Run the file BETSI_gui.py from IDE or executable. Running it from the executable may take some time. Once successfully run, this will prompt:

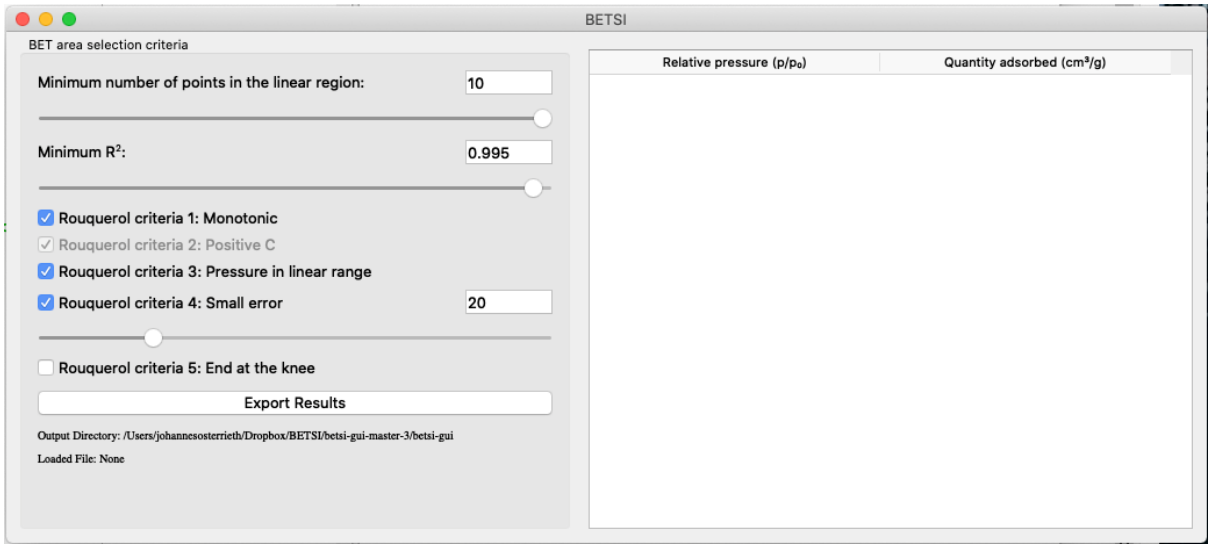

Step 2: Drag the isotherm into BETSI. Please ensure that the isotherm is in the correct format: **It must be a 2-column .csv file with the relative pressure in the first column and the adsorbed quantity in the second. The first row will not be read as this usually contains the header. You must use an adsorption isotherm only, a desorption swing, or discontinuity in the adsorption from pressure equilibration issues will result in an error, with the PChip interpolation method.** Drag the isotherm in the correct format in the empty white space on the right-hand side. The programme will run automatically.

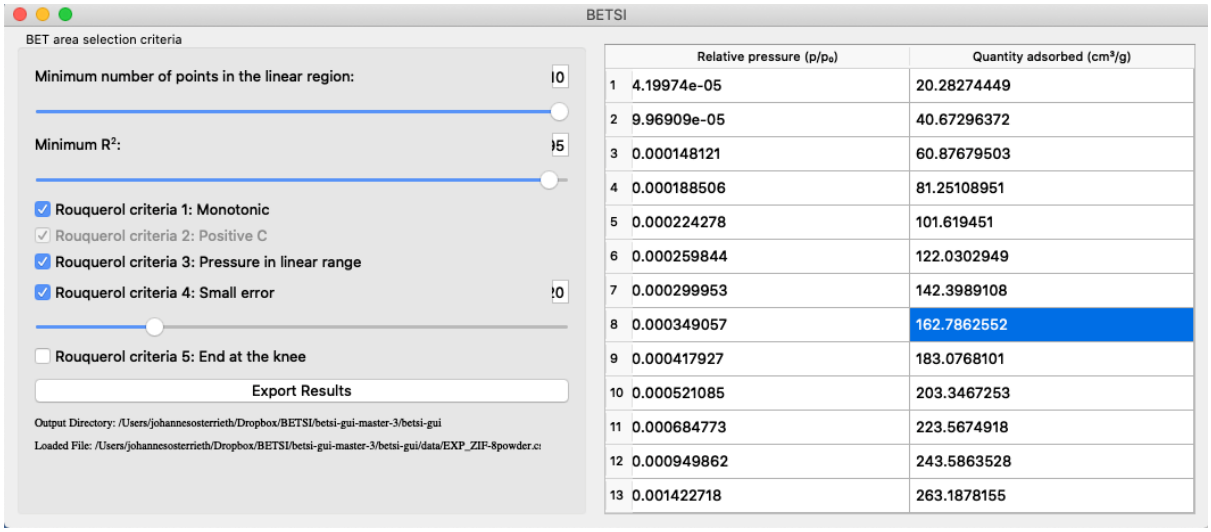

Two windows appear automatically. The first window will be the BETSI report and the second window will show the regression diagnostics for the optimal fitting obtained in BETSI. Full captions for these reports can be found in **Figure S5**.

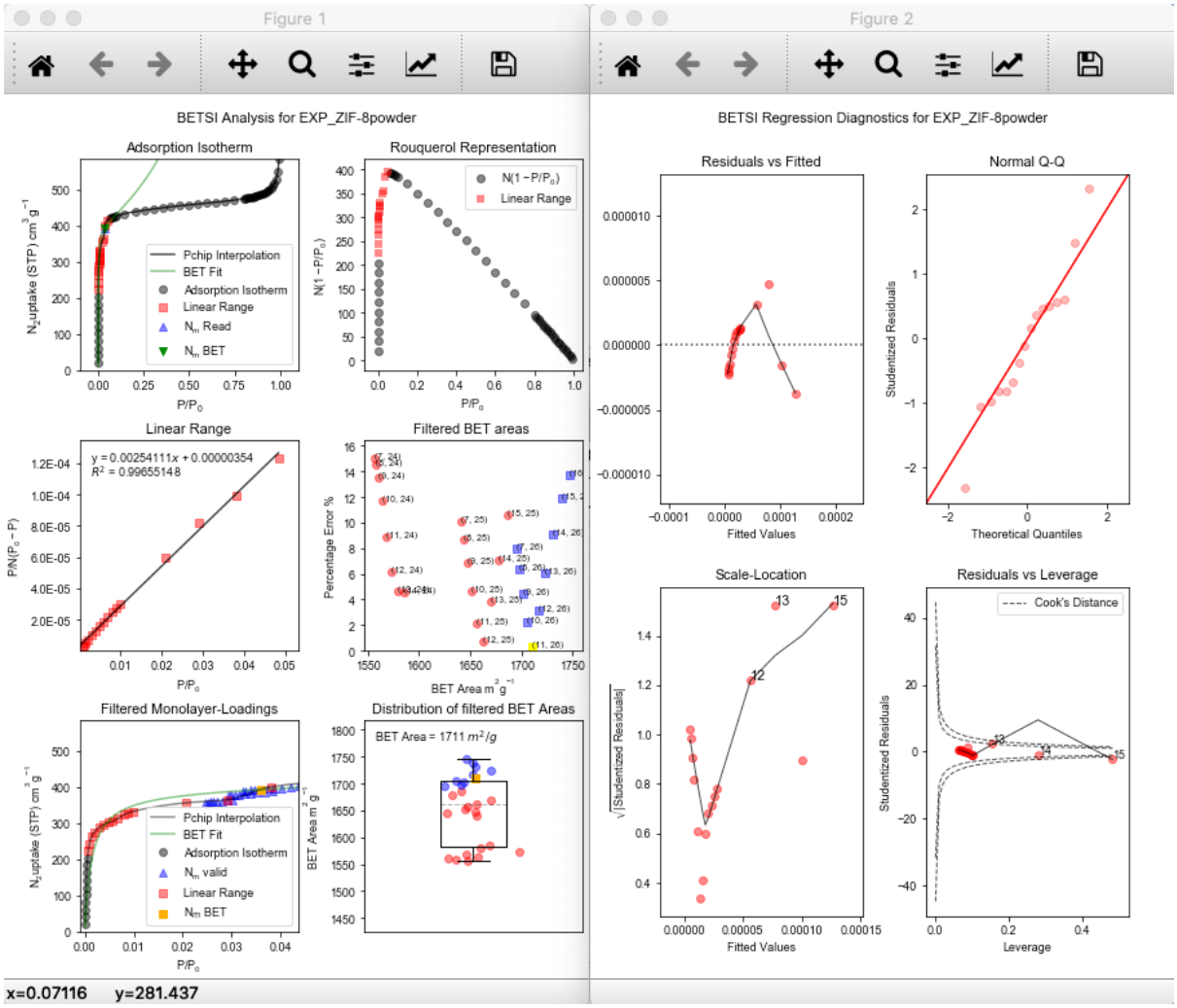

Step 3: Interaction with the GUI allows the user to modify the Rouquerol criteria and see how they filter the BET areas.

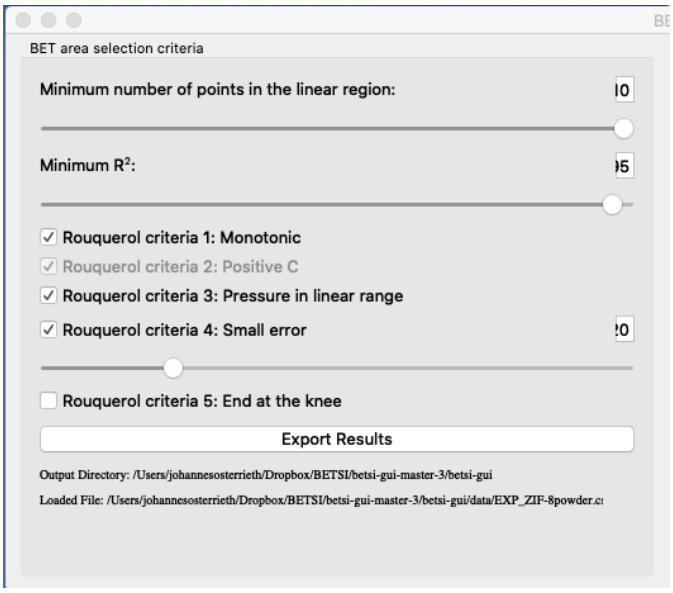

Step 4: All other can be manually selected. In the ‘Filtered BET areas’ plot in the first window, manually click on one of the other points. All other plots will automatically update to the new selected linear region/BET area. The ‘active’ plot will always be shown in yellow.

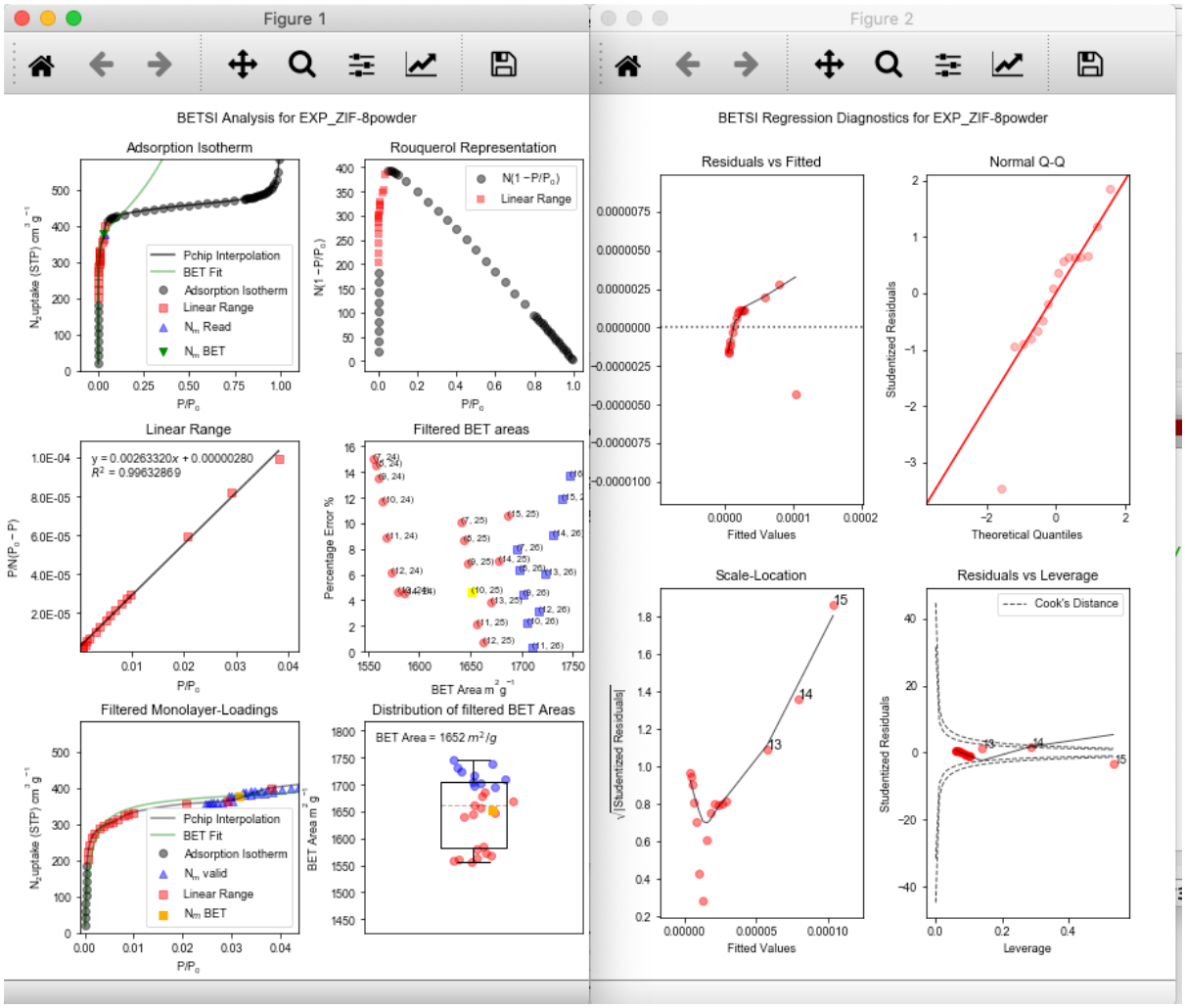

Step 5: To select an output directory, go to File->Set Output Directory and specify the directory you want to export to. The Output directory is specified in the bottom left-side of the GUI.

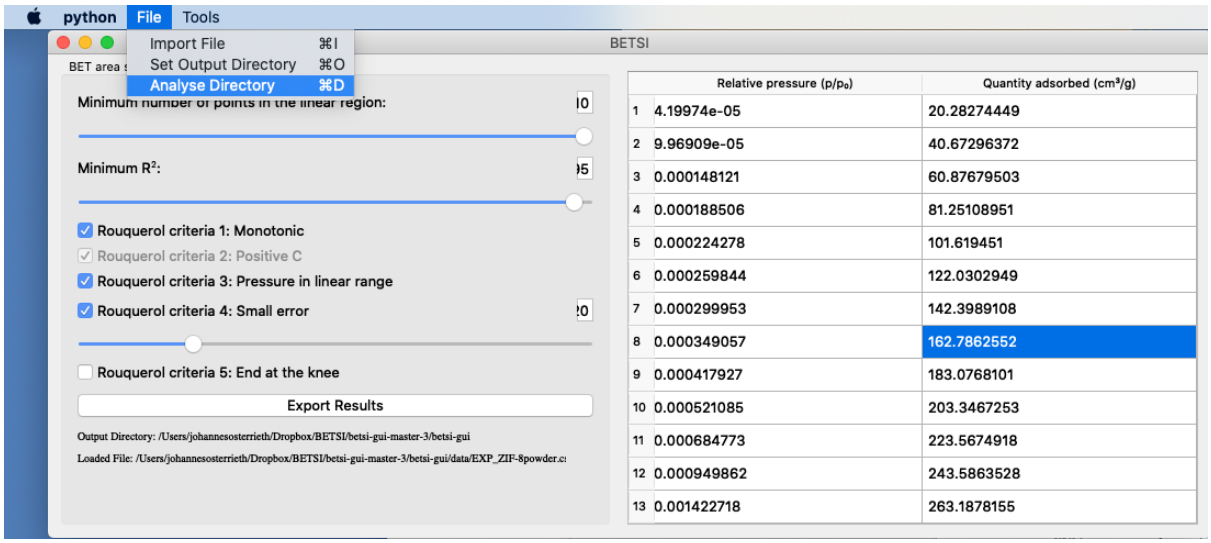

	Relative pressure (p/p₀)	Quantity adsorbed (cm³/g)
1	4.19974e-05	20.28274449
2	9.96909e-05	40.67296372
3	0.000148121	60.87679503
4	0.000188506	81.25108951
5	0.000224278	101.619451
6	0.000259844	122.0302949
7	0.000299953	142.3989108
8	0.000349057	162.7862552
9	0.000417927	183.0768101
10	0.000521085	203.3467253
11	0.000684773	223.5674918
12	0.000949862	243.5863528
13	0.001422718	263.1878155

Step 6: Press Export Results to export the BETSI analysis to the specified directory. The specified directory will contain pdf prints of the two active plots (BETSI analysis and regression diagnostics), a .json file specifying the filter criteria, a .txt file featuring a small summary and a folder containing all matrices that the programme uses.

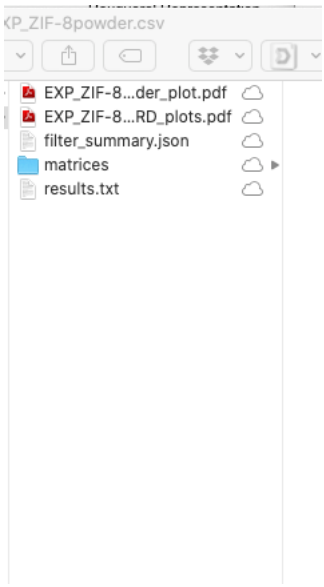

Step 7: To clear and reload a new isotherm, go to Tools -> Clear, or press CMD+C.